Modelling the interactions of Salmonellae with the human host using stem cell-derived intestinal organoids and macrophages

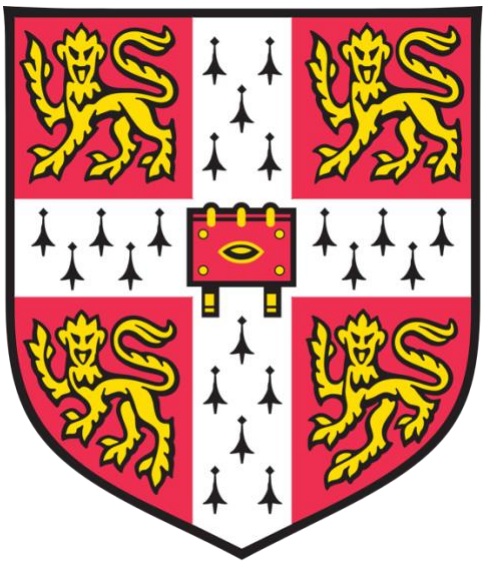

Emily Ann Lees

Wellcome Trust Sanger Institute

Fitzwilliam College, University of Cambridge

This dissertation is submitted for the degree of Doctor of Philosophy

August 2019

Declaration

This dissertation is the result of my own work and includes nothing which is the outcome of work done in collaboration except as declared in the introduction and specified in the text of each chapter.

It is not substantially the same as any work that I have submitted, or, is being concurrently submitted for a degree or diploma or other qualification at the University of Cambridge or any other University or similar institution except as declared in the Preface and specified in the text. I further state that no substantial part of my dissertation has already been submitted, or, is being concurrently submitted for any such degree, diploma or other qualification at the University of Cambridge or any other University or similar institution except as declared in the Preface and specified in the text

It does not exceed the prescribed word limit for the Biology Degree Committee.

Emily Ann Lees

August 2019

Acknowledgements:

"If I have seen further it is only by standing on the shoulders of giants."

This quote, attributed to Sir Isaac Newton was etched into a plaque on the library desk where I wrote much of this thesis. If this work adds anything at all to the score of what we know about Salmonellosis, then this quote absolutely holds true for me. Gordon Dougan has been a fantastic supervisor, allowing me both freedom to investigate ideas and guidance when needed. He has always encouraged me to take opportunities to collaborate and spend time with other people working in this field, and his generosity to other researchers has paid back many fold in the people I've had the opportunity to work with over the past 3 years. Thanks must also go to Arthur Kaser, for the patience and enthusiasm he always brings to scientific discussions, and to Sarah Teichmann both for her advice and her kindness in sharing the expertise of her group with me.

The assistance and friendship of Dougan group members old and new has been a huge asset throughout the course of this PhD, in particular: Jessica Forbester, Sally Forrest, Leanne Kane, Chris Hale, Del Pickard, Sally Kay, David Goulding and Claire Cormie have all offered their skills and advice whenever I have been in need of help, and Sushmita Sridhar has brought cheer and an endless supply of baked goods to our office.

I must also thank Rafal Kolenda, whose collaboration I appreciated whilst working on *S.* Enteritidis, Amber Barton, with whom I enjoyed carrying out cytokine assays, Daniel Kunz for answering my many questions on single cell RNAseq analysis and Artika Nath whose endless time and patience has helped me to bring out some exciting results from bulk RNAseq analysis. Kat Holt has been a brilliant source of advice and guidance on the typhoidal work presented in this thesis. I am also very grateful to Enitan Carrol, who gave me my first research opportunity and has constantly encouraged and championed my ambition to be a clinical academic ever since.

My time in Cambridge has been an unforgettable experience, both for the incredible scientific opportunities that have been available to me, and for the wonderful people I've met during my time here. Fitzwilliam College has been a great community of friends, with particular mention to Sam, Alison and Geoff, adventures with whom have been a highlight of being here. To the inspiring men and women who I have had the pleasure of sharing a basketball court or a boat with over the past 3 years - you have taught me a lot about myself both as an athlete and a person, and I have enjoyed our off court / river discussions as much as the sports themselves.

A huge thank you to my family and friends, who have always supported me in whichever endeavour I've chosen, and for their understanding every time I left an event early to go and 'sort out my cells'.

Lastly, to André for his kindness, patience and confidence in my abilities, his company on evening strolls after days spent in the library, and generosity in sharing his cooking abilities and produce with me. It has been a joy to share my time in Cambridge with you.

Emily Lees

July 2019

Modelling the interactions of Salmonellae with the human host using stem cell-derived intestinal organoids and macrophages

Emily Ann Lees, Wellcome Trust Sanger Institute, Fitzwilliam College, University of Cambridge

Abstract

Salmonellae are Gram-negative, predominantly flagellated, facultative intracellular bacteria, and are an important cause of enteric disease in humans and in animal hosts worldwide. Their transmission is predominantly via the faeco-oral route and members of the *Salmonella enterica* species can be arbitrarily classified into typhoidal and non-typhoidal types based on their pathogenicity in a particular host. *Salmonella enterica* serovar Typhi (*S.* Typhi) and *Salmonella enterica* serovar Paratyphi A (*S.* Paratyphi A) cause typhoid and paratyphoid fevers respectively, which are collectively associated with ~25 million cases and 250,000 deaths per year, predominantly concentrated in regions of Asia and Africa where sanitation and clean water are difficult to access. Non-typhoidal serovars (NTS) (e.g. *S. enterica* serovar Typhimurium (*S.* Typhimurium), *S. enterica* serovar Enteritidis (*S*. Enteritidis)) are responsible for over 93 million infections and ~155,000 deaths worldwide per year, the majority of which are thought to be food-borne infections. NTS infections usually cause self-limiting gastroenteritis, but can progress to invasive disease (iNTS) with bacteraemia and a mortality rate as high as 25% in certain patients. *S.* Typhi and *S*. Paratyphi A are pathogens restricted to humans, meaning that there has been difficulty until recently in producing a valid model with which to study pathogen-mucosal interactions and learn more about the invasion mechanisms of these unique pathogens. Although *S.* Typhimurium is predominantly associated with a localised gastroenteritis in immunocompetent humans; it causes a typhoid-like disease in mice; therefore mouse models have previously been used as surrogates to provide concepts about the interaction between *S.* Typhi and the host mucosa and resultant immune response.

However, in recent years, a new approach to studying pathogen-gut epithelial interactions has been developed; known as “organoids” or human intestinal organoid systems (iHO).

These can be produced from human induced pluripotent stem cells (hiPSCs), or from primary intestinal tissue, and once matured, harbour differentiated enterocytes and secretory cells such as goblet, Paneth and enteroendocrine cells. They have previously proved capable of providing a complementary human model for studying *S.* Typhimurium infection, but their utility has been explored during this project to include the human gut epithelial interaction with other serovars of *Salmonella* (in particular typhoidal strains, which have never been studied in this context) and the transcriptomic/phenotypic response to these enteric pathogens.

In vivo, intestinal epithelial cells (IECs) play a key role in regulating intestinal homeostasis, and can directly inhibit pathogens, although the mechanisms by which this occurs are not well understood. I have demonstrated that the cytokine IL-22 has a role in IEC defence against *S.* Typhimurium in the hiPSC-derived iHO system, with evidence for restriction of intracellular infection of wild type *S*. Typhimurium SL1344 in iHO pre-treated with recombinant human IL-22. I have demonstrated that a mechanism via which this protection occurs is increased phagolysosomal fusion. I have also modelled infections with alternative types of bacteria, including *S*. Enteritidis and enteropathogenic *Escherichia coli* (EPEC); investigating whether luminal killing of bacteria occurs within the iHO system. I have used iHO derived from stem cells with induced mutations to explore genes of interest in epithelial defence. Lastly, I have demonstrated that typhoid-causing Salmonellae (*S*. Typhi and *S*. Paratyphi A) are able to invade both the iHO epithelium and hiPSC-derived macrophages from the same cell line. I investigated these interactions using imaging and bulk RNA-Seq to identify differences in response to the bacteria in the epithelial and immune cell compartments. Strikingly, genes differentially expressed in IECs showed most similarities in response to infection with non-encapsulated serovars (*S*. Paratyphi A and *S*. Typhimurium versus *S*. Typhi), whereas genes differentially expressed in macrophages demonstrated most overlap in response to typhoid-causing strains (*S*. Typhi and *S*. Paratyphi A versus *S*. Typhimurium), raising important questions about the immunomodulatory role of the Vi capsule and the apparent ability of *S*. Paratyphi to behave differently in the epithelial and macrophage environments. It was also possible to demonstrate that H58 serovars of *S*. Typhi caused distinct transcriptional signatures in the macrophage model, versus their non-H58 counterparts. I present this novel data and discuss how this complements what is currently known about the host-pathogen interactions of typhoid-causing Salmonellae.

Table of contents: Page number:

1: Introduction

1.1 Classification of Salmonellae and global burden of disease

Salmonellae are Gram-negative, predominantly flagellated, facultative intracellular bacteria that are an important cause of enteric disease in humans and animal hosts worldwide. They are members of the Enterobacteriaceae family, thought to have diverged from *Escherichia coli* between 100-150 million years ago[1] and are genetically diverse, having adapted to colonise numerous animal hosts and are even able to exist freely in the environment.[2] Transmission is largely via the faeco-oral route. Classification and nomenclature methods have led to some confusion about the number of species of the genus *Salmonella*, but molecular work determined that there are two *Salmonella* species which have the ability to infect humans: *Salmonella enterica* and *Salmonella bongori*.[3,4] Isolates from the *S. enterica* species are the predominant cause of disease in humans, therefore this species will be the main focus of the remainder of this introduction. *S. enterica* is subdivided into six subspecies: *S. enterica* subsp. *enterica*, *S. enterica* subsp. *salamae*, *S. enterica* subsp. *arizonae*, *S. enterica* subsp. *diarizonae*, *S. enterica* subsp. *houtenae* and *S. enterica* subsp. *indica*.[5] These subspecies are separated by a number of differential characteristics, modified from the scheme proposed by Kauffmann in 1973,[6] including physiological characteristics and serological identification of: O (lipopolysaccharide - LPS), H (flagella), and K (capsular) surface antigens. For the purposes of this study, we will focus solely on *S. enterica* subsp. *enterica,* as serovars from this subspecies are the predominant cause of human salmonellosis, both typhoidal and non-typhoidal. *S. enterica* subsp. *enterica* itself is antigenically diverse in terms of major surface antigens, incorporating over 1500 serovars of the ~2500 that have been identified as belonging to the *S. enterica* species.[5]

Medically relevant *S. enterica* serovars can be arbitrarily classified into typhoidal and non-typhoidal (NTS) types based on their pathogenicity in a particular host. *S. enterica* serovar Typhi (*S.* Typhi) is a human-restricted serovar which causes typhoid fever, and is responsible for ~21 million cases and 222,000 deaths per year,[7] with peak incidence in the paediatric and elderly populations. Cases are predominantly concentrated in low-income settings

where sanitation facilities and access to clean water are limited. Other risk factors for the development of typhoid fever are influenced by setting but include: consumption of food or drink from street vendors,[8] a close contact or relative with typhoid fever[9] and recent antimicrobial use.[8]

Parts of South Asia, Southeast Asia and sub-Saharan Africa have traditionally had the highest incidence of typhoid disease, followed by China and Oceania (excluding Australia/New Zealand).[10] However, the incidence of typhoid can vary over time and fluctuations in the levels of disease are common. In addition, many endemic countries do not have a well-established national surveillance system for typhoid fever, so incidence may be inaccurately estimated.[11] Similarly, passive surveillance relies on clinical diagnosis with blood culture facilities not being readily available, so areas where health care infrastructure is weak (and disease burden potentially high) may not be able to record incidence definitively, which can certainly limit available data on circulating strains and antibiotic sensitivities. In recent years, initiatives such as the STRATAA study[12] have produced detailed datasets from areas of high incidence, and obtained important anthropological data on population dynamics and healthcare seeking behaviours, which could prove vital to controlling disease.

The estimated burden of paratyphoid fever, (caused by *Salmonella enterica* serovars Paratyphi A, B and C) suggested that there were ~3.75 million cases of paratyphoid fever in 2016,[13] with 25000 deaths from the condition.[14] Paratyphoid fever may generally have a less severe disease course but these data indicate that it also constitutes a significant global health burden. In fact, in some regions, such as Thailand[10] and China,[15] paratyphoid fever incidence appears to be increasing, which is of especial concern given that there is no effective vaccine available for this pathogen, and cross-protection from typhoid vaccines is limited.[16] **Figure 1.1** demonstrates the global incidence of typhoid and paratyphoid fevers.

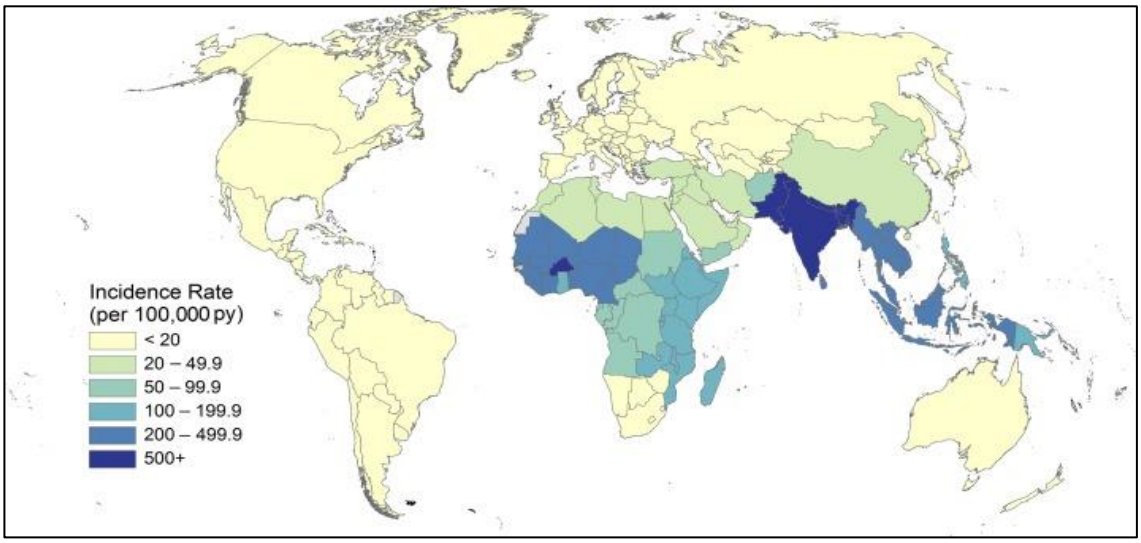

Figure 1.1: Estimated incidence of typhoid and paratyphoid fevers by country per 100,000 population, 2015. (Figure taken from Radhakrishnan, A. *et al*[10])

Non-typhoidal *Salmonella* (NTS) serovars (e.g. *S. enterica* serovar Typhimurium (*S.* Typhimurium), *S. enterica* serovar Enteritidis (*S*. Enteritidis)) are responsible for over 93 million infections and ~155,000 deaths worldwide per year,[17] the majority of which are thought to be food-borne infections. NTS infections impact a range of vertebrate hosts in addition to humans[18] and cause varying disease phenotypes. These pathogens typically cause a self-limiting gastroenteritis in patients in high-income countries, with incidences of complications generally limited to certain patients, such as the elderly or immunocompromised.[19] However, in low-income settings, NTS infections are a common cause of invasive disease (iNTS) involving bacteraemia, with a mortality rate as high as 25%.[20] In adults in these settings, *Salmonella*-associated invasive disease is found predominantly in those co-infected with HIV.[21] In children, malaria,[22] HIV,[23] malnutrition[24] and sickle cell disease[25] are frequently associated with the invasive phenotype. Symptoms of iNTS may be non-specific, but can include persistent fever, pneumonia, enterocolitis and hepatosplenomegaly.[18] Treatment of iNTS infection has also been complicated by the emergence of epidemic-causing MDR strains with distinct genotypes, such as the *S*. Typhimurium ST313 serovar isolated in Sub-Saharan Africa,[26] and the spread of disease is exacerbated by a lack of vaccines directed against iNTS strains.

Given the faeco-oral nature of *Salmonella* transmission, WaSH strategies such as improvements in water supply and sanitation infrastructure and case identification and

treatment have made incidence of typhoidal disease rare in parts of the world where these practices have been put into place. Cases in these areas occur mostly via travellers returning from endemic countries.[27] Much remains to be achieved in countries where disease incidence of typhoid, paratyphoid and iNTS remain high, with antimicrobial resistance becoming an increasing threat to current treatment options.[28]

1.2 Pathogenesis of and host response to *Salmonella* infection

1.2.1 Initial host-epithelial interactions

As implied by the differing disease courses they follow, there are some similarities and some differences between the interactions of typhoidal and non-typhoidal Salmonellae with the host epithelium. This section will explain the generally accepted mechanisms of non-typhoidal *Salmonella* infection and highlight serovar-specific mechanisms where appropriate.

1.2.1.1 From ingestion to the mucosal barrier

Following ingestion in contaminated water or food, *Salmonella* need to reach the small intestine in order to penetrate the intestinal mucosa. This requires the ability to survive the hostile acidic environment experienced within the stomach, with pH reaching as low as 1-2.[29] *Salmonella* have developed acid stress responses, such as the sigma(E) pathway[30] and the PhoPQ regulatory system[31] which enable them to do this. Factors increasing the stomach's pH can increase susceptibility to infection, such as use of proton pump inhibitors,[32] and the infective dose of *Salmonella* is thought to drop if bacteria are ingested with food, due to the temporary increase in stomach pH that food can produce.[29] Other methods by which *Salmonella* can temporarily adapt to a low pH environment, whilst maintaining a constant intracellular pH, include: use of innate proton pumps to extrude protons from the cytoplasm, intracellular conversion of lysine to cadaverine and arginine into agmatine
(reactions which lead to consumption of protons) and alteration in membrane content to increase levels of cyclic fatty acids.[33] Following their journey through the stomach,

Salmonella are further challenged in the duodenum by contact with bile, secreted from the gallbladder. Bile plays an important role in the digestion of lipids and its detergent-like properties make it inherently antimicrobial, allowing it to damage bacterial cell membranes, bacterial DNA and even alter membrane protein composition.[34] Factors affecting susceptibility to iNTS such as malnutrition can decrease the amount of bile produced, increasing the likelihood of bacterial survival in the intestine.[35] *Salmonella* have a number of mechanisms in place to counteract the effects of contact with bile, including bile efflux pumps, LPS expression (with O antigen providing a barrier to entry of external compounds) and again, the PhoPQ transcriptional regulatory system; overexpression of which enhances bile resistance.[36] This ability to tolerate high levels of bile salts is of particular importance for *S*. Typhi, given that chronic carriage of the pathogen is thought to occur within the gallbladder.[37] The PhoPQ system is also involved in controlling genes of the type III secretory systems (T3SS). High levels of bile salts induce *Salmonella* to transcriptionally repress genes of their Salmonella Pathogenicity Island 1 (SPI-1) T3SS, reducing epithelial invasion; suggesting that Salmonella are able to sense bile concentration, allowing them to determine their location in the intestinal lumen and utilise appropriate gene sets. The SPI-1 T3SS is likely then upregulated once *Salmonella* pass through the mucus layer towards the epithelium, as exposure to bile salts is diminished and invasion-related proteins are required.[38]

Having reached the small intestine, the next obstacle to *Salmonella* invasion is the colonisation resistance presented by immunological (e.g. T cell profile), microbiotal and metabolic (e.g. short chain fatty acid predominance) factors in the intestinal lumen,[39] alongside secretory Immunoglobulin A (sIgA), which is able to reduce adhesion and invasion of *Salmonella* into epithelial cells. Non-typhoidal Salmonella are able to overcome colonisation resistance by inducing an inflammatory response from the intestinal epithelium, which they are able to survive and then outcompete the host microbiota.[40,41]

Lastly, in order to adhere to and invade the intestinal epithelium, *Salmonella* need to penetrate the mucus layer lining the gut. Goblet cells in the intestinal epithelium secrete glycosylated proteins called mucins at their apical surface, which form a gelatinous layer preventing contact between the epithelial surface and inflammatory particles such as bacteria.[42] This layer is essential for keeping the intestinal epithelium in a quiescent state, with mice deficient in MUC2 (the major secretory mucin in mice and humans) developing

spontaneous colitis[43] and being significantly more susceptible to *S*. Typhimurium infection with a higher mortality rate.[44] It is not clear exactly how *Salmonella* penetrate the mucus layer; a recent study demonstrated 'near surface swimming' of *S*. Typhimurium in the colonic mucous layer, apparently sensing for sites of mucus heterogeneity which may provide an easier path down to the epithelium.[45] Other research suggests that non-fimbrial adhesins such as SiiE play an important role in invasion as they allow *Salmonella* to bind to glycosylated structures on the apical surface of the epithelial cells.[46,47] Indeed for *S*. Typhi, which has genes encoding a number of fimbrial operons not present in the *S*. Typhimurium genome, fimbrial structures also appear to be important for adhesion to and invasion of host cells.[48] Additionally, flagella are important both for chemotaxis towards the epithelium and subsequent colonisation of cells and induction of inflammation, but it is a matter of debate as to whether these structures facilitate invasion or merely provide proximity to the target epithelium to allow the SPI-1 T3SS to act.[49]

1.2.1.2 Penetration of the intestinal mucosa

If they survive the range of challenging conditions they encounter prior to reaching the small intestinal mucosa, *Salmonella* have the potential to penetrate the epithelial layer via enterocytes, microfold cells (M cells) or migrating dendritic cells. Some of these processes remain obscure given that much of what we know about *Salmonella* interactions with the epithelium, particularly those of the human-specific typhoid-causing serovars, have been extrapolated from mouse or 2-D cell culture models. Entry to enterocytes will be discussed below, but alternate routes of entry may play an important role in *Salmonella* invasion.
M cells are the specialised epithelial cells overlying Peyer's patches in the intestine, which sample antigens from the epithelial surface, initiating immune responses where required. However, many enteric bacteria actively interact with these cells as part of their invasion strategy, as M cells could represent a direct route to the gut-associated lymphoid tissue and potentially into the systemic circulation. Both *S*. Typhi[50] and *S*. Typhimurium[51] appear to selectively invade M cells in mouse models of infection, although *S*. Typhi do this at a lower frequency than *S*. Typhimurium.[52] It may be that this is the case in human disease also, with hyperplasia and ulceration noted at Peyer's patches during typhoid infection.[53] However, *in vitro* studies using both explanted intestinal biopsies and organoid-derived monolayers,

which contained M cells, were only able to demonstrate invasion into enterocytes.[54] In mouse models, it has been established that *S*. Typhimurium is efficient both at entering M cells and causing large structural changes of the cell (membrane ruffles) shortly after invasion. Within 30-60 minutes of *S*. Typhimurium entry, M cells can become necrotic and die.[55] *S*. Typhi are also able to induce large changes in M cell membrane structure, but do not induce cell death as efficiently and are cleared from Peyer's patches, rather than replicating inside them as does *S*. Typhimurium.[52] Interestingly, the T3SS is not required for entry of M cells, with SPI-1 mutants still able to invade M cells and colonise Peyer's patches.[56]

Another SPI-1-independent mechanism of entry for *Salmonella* to the lamina propria is via uptake by CD18+ dendritic cells (DCs), which are migratory phagocytic cells that sample antigens in mucosal tissues; performing a sentinel function similar to M cells. DCs also express some tight junction proteins, allowing them to open tight junctions between epithelial cells, send dendrites to the epithelium to sample bacteria and then re-instate the intestinal barrier's integrity.[57,58] Lastly, the T3SS of SPI-1 and SPI-2 have been shown to contribute to colitis and disruption of tight junctions in mouse models, allowing luminal *S.* Typhimurium to enter the lamina propria between rather than through the epithelial cells.[59]

1.2.1.3 Entry into epithelial cells

Intracellular pathogens such as *Salmonella* enter enterocytes via at least two mechanisms which are differentiated by the morphology induced by membrane re-modelling. The 'trigger' mechanism involves radical cytoskeletal arrangements called membrane ruffles (as described above for uptake by M cells), whereas the 'zipper' mechanism (also known as receptor-mediated entry) requires only limited cytoskeletal change, as the invading bacteria are avidly bound to the host cell membrane.[60] The trigger mechanism requires injection of bacterial effector proteins via T3SSs, whereas the zipper mechanism is induced by activation of host cell receptors and bacterial ligands such as invasin. *Salmonella* are unusual in being able to invade cells via both of these mechanisms,[61] although invasion is primarily thought to occur via the SPI-1 T3SS with the zipper mechanism being less well defined (**Figure 1.2**).

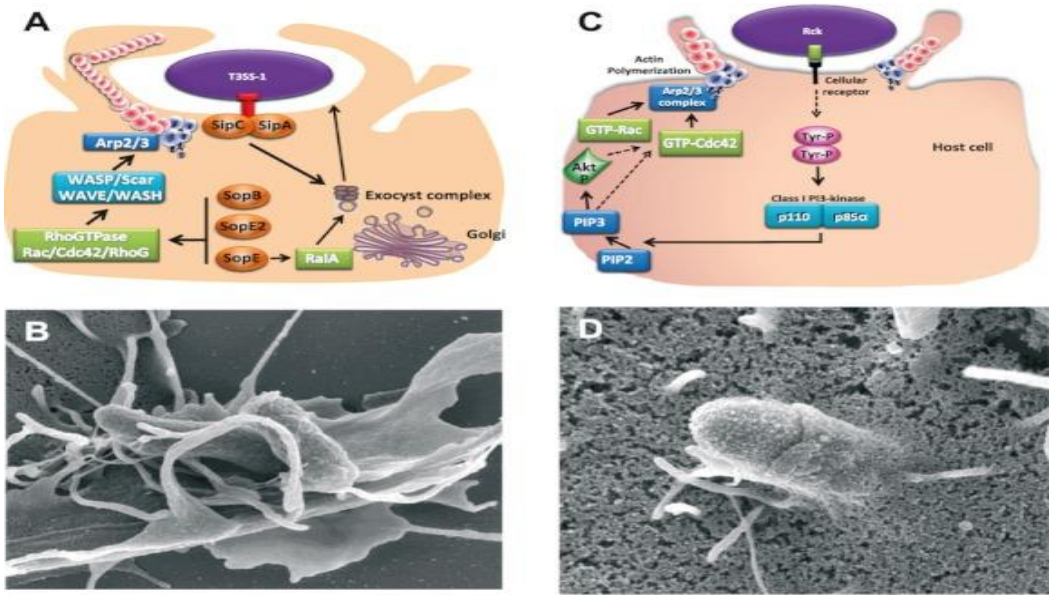

Figure 1.2: Schematic of 'trigger' and 'zipper' mechanisms of *Salmonella* cell entry. (**A**) Trigger mechanism – using T3SS; effector proteins (sipA, SipC, SopB, SopE, SopE2) are injected into host cells. SipA and SipC bind directly to actin. SopB, SopE, SopE2 active RhoGTPases to allow actin remodelling via WASP/Scar/WAVE/WASH proteins which activate Arp2/3 complex. SipC and SopE act on Ras-related protein RalA to recruit exocyst complex and allow bacterial internalisation. (**B**) Scanning EM image of *Salmonella* entering cell via the trigger mechanism with large membrane ruffles at bacterial entry site. (**C**) Zipper mechanism – the Rck invasins expressed on the *Salmonella* membrane interact with host cell membrane receptor, leading to tyrosine kinase phosphorylation. This activates class I PI 3-kinase, inducing PI (3,4,5)P3 formation, activating Akt. This leads to activation of GTPases Rac and Cdc42, triggering actin polymerisation via the Arp2/3 complex. This pathway is less well defined, with dotted lines indicating possible signalling events. (**D**) Scanning EM image of *Salmonella* entering cell via the zipper mechanism, with less defined membrane alterations. (Figure taken from Velge et al 2012[60])

Up to 21 different pathogenicity islands have been annotated in the genome of *S*. enterica,[62] but only 12 have been identified as having a clear role in *Salmonella* pathogenesis.[63] The T3SS encoded by the SPI-1 locus is one of the best characterised *Salmonella* virulence-associated factors, inducing *Salmonella* entry into eukaryotic cells. The T3SS is a protein complex sometimes described as a 'molecular syringe' as it is able to inject effector proteins directly from the bacterial cytoplasm into the host cell cytosol. These effector proteins modify cellular processes in a manner which benefits the bacterium injecting them.[60] Expression of T3SS genes and construction of the T3SS apparatus at the bacterial membrane is modified by environmental factors such as osmolarity, pH, Ca^{2+} availability and growth phase of the bacteria.[64] In a similar manner, genes encoding the Vi capsule in *S*. Typhi are affected by osmolarity; for example, the gene *TviA* which positively regulates the Vi capsule is repressed in high-osmolarity environments and induced in low-osmolarity environments.[65]

As *Salmonella* binds to the host cell surface, bacterial proteins are injected into the host cell via the T3SS needle complex in a specific order,[66] beginning with translocase proteins such as SipB, SipC and SipD. SipA and SipC induce cytoskeletal actin rearrangement, causing membrane ruffles and micropinocytosis of *Salmonella* into the cell; internalising bacteria inside membranous vacuoles (*Salmonella*-containing vacuoles, SCVs).[67] Effector proteins SopE, SopE2 and SopB target and activate Rho GTPases CDC42 and Rac, triggering signal transduction events, which also lead to actin rearrangement and release of pro-inflammatory cytokines via activation of MAP kinases JNK and p38.[68] These effectors can induce activation of the WASP/Scar/WAVE/WASH proteins, which activate Arp2/Arp3 complexes, triggering actin remodelling.[69] Membrane ruffles are transient and tend to occur within 10-30 minutes of contact with bacteria; rearrangements are usually reversed by 2-3 hours after bacterial entry. This reversal is mediated by SptP, an effector protein with a longer half-life than the other effectors, which downregulates CDC42 and Rac1, allowing cell membranes to return to a normal appearance.[70] It was also noted that SipC and SopE-dependent activation of RalA both induce exocyst recruitment, with the exocyst delivering vesicles to sites of bacterial entry to provide extra membrane material to enable ruffling and invasion to occur.[71]

Alternative *Salmonella* genes have also been identified as having a role in invasiveness, for example, *invA*. *S*. Typhimurium with mutations in this gene were less able to invade epithelial cells, in spite of being able to attach to them. The exact mechanisms underlying this invasion deficiency are ill-defined, but mutants appeared unable to alter the distribution of actin microfilaments in infected cells.[72]

1.2.1.4 Intracellular survival

Bacterial internalisation induces changes in host cell signalling, influencing numerous cellular processes, such as cell division, apoptosis, cytokine production, membrane trafficking and antigen presentation.[73] SPI-1 T3SS effectors can play a role in influencing these factors; for example SopB plays a role in SCV genesis and trafficking,[60]

but once invasion into the cell has occurred, *Salmonella* pathogenicity island 2 (SPI-2) T3SS effectors are upregulated and take on the task of promoting *Salmonella* survival within the cell. The SCV initially acquires early endosome markers, which are sequentially replaced by

late endosome and lysosome markers, such as the lysosomal glycoprotein Lamp1.[74] The SCV migrates from the cell periphery towards the nucleus within 1-2 hours of invasion,[75] under control of SPI-1 T3SS (SopB, SopA) and SPI-2 T3SS (SseF, SseG, SifA).[73]

As well as being involved in the early stages of SCV formation and movement, SopB is able to induce dissociation of a number of Rab proteins from the SCV, which delays SCV-lysosome fusion and prolongs bacterial survival.[76] In addition, this protein induces sorting nexin 3 (SNX3) activity, delivering Lamp1 and Rab7 to the SCV, allowing maturation.[77]

Salmonella replication normally occurs 4-6 hours post-invasion and coincides with extension of Lamp1 containing membrane tubules (Sifs) from the surface of the SCV,[74] under the influence of SPI-2 T3SS effectors, which allow the SCV both to remain in its juxtanuclear position and extend tubules towards the cell peripheries.[78] SCVs and Sifs are enriched in cholesterol, due to action of the SPI-2 T3SS effector SseJ.[79] Interestingly, in *S*. Typhi, SseJ is a pseudogene, and when *S*. Typhi are complemented with the *S*. Typhimurium SseJ gene, *S*. Typhi are significantly less toxic to epithelial cells, perhaps suggesting a mechanism by which *S*. Typhi are adapted to causing systemic disease.[80]

SifA, acting in conjunction with SipA, induces actin accumulation around the SCV, essential for intravacuolar replication.[81] One challenge that the SCV does face is a progressive acidification, caused by fusion with endolysosomes. *Salmonella* use mechanisms such as the PhoPQ regulatory system, which is activated by low pH to modify intravacuolar pH.[31] In addition, SifA and PipB2 proteins can manipulate the course of phagosomal maturation, preventing vacuolar lysis and ensuring replication of *Salmonella* within the vacuole.[82]

Having replicated within cells, *Salmonella* are able to induce host cell apoptosis, usually occurring 12-18 hours after bacterial invasion and mediated by TNFα and nitric oxide. Apoptosis may function to remove damaged and infected cells, in order to restore epithelial integrity to the host, but this delay in onset of apoptosis also has the benefit of allowing *Salmonella* to adapt to the intracellular environment before moving deeper into the mucosa.[83] In addition to apoptosis, inflammatory cell death (pyroptosis) can also be induced by the presence of *Salmonella* within the cell. Flagellin, SipB and SopE can all induce activation of caspase-1 and inflammasome construction, which in turn activates IL-1β and IL-18.[84,85] Additionally, LPS is a potent agonist of TLR4, triggering DCs to produce IL-23 in response to *Salmonella* infection.[86] Induction of pyroptosis may be advantageous for

Salmonella, with destruction of the epithelial barrier allowing further bacterial invasion into the lamina propria and exposing cells directly to intestinal luminal contents. This inflammation can also induce host immune response and recruitment of immune cells to the infection site.[87]

Interestingly, although persistence within the macrophage cytosol is potentially fatal for *Salmonella*, they are capable of surviving and replicating within the epithelial cell cytoplasm, at an even higher rate than when inside of the SCV. Once *Salmonella* escape into the cytoplasm (controlled in part by host cell autophagy[88]), they upregulate SPI-1 T3SS and flagellar genes, and as the host cell triggers inflammatory cell death and is extruded from the epithelial layer; this allows the release of numerous invasive and motile *Salmonella* to infect further cells.[89]

1.2.1.5 Invasion factors specific to typhoidal strains

The above pathogenic mechanisms for cellular entry and replication are active largely for non-typhoidal *Salmonella* strains lacking the Vi capsule expressed by *S*. Typhi, which can significantly modify interactions with host cells. Invasion (e.g. via SPI-1 T3SS), survival and replication in the epithelium (e.g. via SPI-2 T3SS) and recognition of bacterial pathogen-associated molecular patterns (PAMPs) by the mucosa all contribute to the inflammatory picture and neutrophil influx induced by non-typhoidal *Salmonella* infection. This neutrophil influx is largely absent in *S*. Typhi infection. *S*. Typhi is able to use SPI-1 T3SS to invade epithelial cells, SPI-2 T3SS to survive intracellularly, expresses PAMPs such as flagellin and LPS, and yet this serovar stealthily evades the inflammatory immune response.[90] Until recently, we lacked the ability to study this human restricted serovar in 3-D cellular models, therefore 2-D tissue culture models were used in attempts to clarify these differences between the serovars. Macrophage stimulation by *S*. Typhi induces much less IL-8 production compared with *S*. Typhimurium.[91] *S*. Typhimurium, but not *S*. Typhi, is able to induce migration of neutrophils across a monolayer of polarised colonic epithelial cells,[92] and *S*. Typhi does not induce a similarly pro-inflammatory transcriptional profile in epithelial cells.[93] These differences could be due, at least in part, to the shielding of flagellin and LPS by the Vi capsule, as *S*. Typhimurium mutants deficient in flagellin produced a similar inflammatory picture to *S*. Typhi, yet with flagellin intact and knocking out of the SPI-1 T3SS,

S. Typhimurium remained strongly pro-inflammatory.[93] Similarly, the presence of the Vi capsular antigen could explain the ability of *S*. Typhi to downregulate the Toll-like receptor (TLR)-mediated host response reducing inflammation and neutrophil influx into the gut epithelium.[94] Transcriptomic studies of *S*. Typhimurium have shown that SPI-1 and flagellin genes were upregulated for longer within epithelial cells than macrophages, potentially contributing to this inflammatory picture.[95] The outcome of differences in these interactions is the differing clinical picture associated with typhoidal and non-typhoidal *Salmonella* disease. The inflammatory response induced by S. Typhimurium for example, induces a diarrhoeal illness, whereas the early stages of *S*. Typhi infection are relatively undetectable, with symptoms only occurring once systemic bacteraemia occurs.

The Vi antigen does have a role in virulence of *S*. Typhi, with isolates lacking in Vi being 10,000 times less virulent than encapsulated *S*. Typhi in intraperitoneal murine infections.[96] Although unencapsulated *S*. Typhi were still able to cause typhoid disease in human challenge studies, they were associated with half the number of cases of Vi encapsulated *S*. Typhi, unless a 100-fold higher inoculum was used.[97] Interestingly, loss of the typhoid toxin gene does not appear to cause any attenuation in ability to induce disease in volunteers, although it did lead to an altered cytokine response suggesting that whilst not necessary for disease induction, toxin is able to modify host responses.[98]

The genes required to produce the Vi capsular antigen are encoded by the *viaB* locus, located on SPI-7, a genetic element which is lacking in *S*. Typhimurium.[99] We know that this antigen is expressed in human infection given the low but significant levels of Vi antigen in recovering typhoid patients and the immunogenicity of typhoid vaccines incorporating the Vi antigen.[100] The SPI-7 element is inherently unstable and Vi expression can be lost during laboratory passage over time. It is also influenced by factors such as osmolarity. For example, TviA (a gene necessary for capsular expression) positively regulates the Vi capsule genes whilst negatively regulating flagellar and SPI-1 T3SS genes.[101] At high osmolarity (as in the intestinal lumen), TviA is repressed, allowing *S*. Typhi to be non-encapsulated and flagellated to increase invasiveness, but then at low osmolarity (in the intestinal mucosa) TviA is induced, allowing *S*. Typhi to be encapsulated with downregulated flagellar and SPI-1 T3SS proteins to reduce host inflammatory response.[102] Supporting this hypothesis is a study of calf ileal loop infection, showing that TviB (another gene necessary for capsular

production) was upregulated after cells entered the epithelium, with Vi capsule being visualised on fluorescence microscopy within cells.[103]

S. Paratyphi A and B cause a similar clinical picture to *S*. Typhi, yet in the absence of SPI-7 and a capsule (in comparison to *S*. Paratyphi C, which harbours SPI-7). *S*. Paratyphi A has been shown to express lower levels of SPI-1 effector proteins compared to *S*. Typhimurium, especially when grown aerobically (as would be the case inside intestinal epithelial cells). When *HilA*, an SPI-1 activator was overexpressed in *S*. Paratyphi A, increases in host cell invasion, pro-inflammatory cytokine release and disruption of epithelial integrity were reported, suggesting that suppression of the SPI-1 components at higher oxygen tension may be a mechanism employed by *S*. Paratyphi A to reduce inflammatory response and evade detection.[65]

There are many gaps in our knowledge of the mechanisms behind the ability of *S*. Typhi and *S*. Paratyphi A to cause invasive disease with a dampening of host immune response. Novel 3-D human cell culture technologies such as the intestinal organoid system may help us to address this.

1.2.2 Innate immune response to *Salmonella* infection

Following epithelial invasion, *Salmonella* reach the lamina propria, where bacteria are phagocytosed by neutrophils or mononuclear cells such as macrophages. The host immune system is able to differentiate luminal commensal bacteria from pathogens such as *Salmonella* by expression of pathogen recognition receptor TLR5 on their basolateral surface.[104] Phagocytes within the lamina propria express numerous pathogen recognition receptors (TLRs 1, 2 and 4-6) on their surface, which are specialised in detecting PAMPs such as flagellin (detected by TLR5)[105] and LPS (detected by TLR4).[106] Detection of *Salmonella* in the lamina propria through TLRs on macrophages and epithelial cells induces a pro-inflammatory transcriptomic change in these cells, inducing expression of neutrophil chemoattractants such as interleukin 8 (IL-8) via NFκB activation[107] and leading to the neutrophil influx into the intestinal mucosa observed in *Salmonella*-induced gastroenteritis. **Figure 1.3** outlines elements of the innate immune response to *S*. Typhimurium infection.

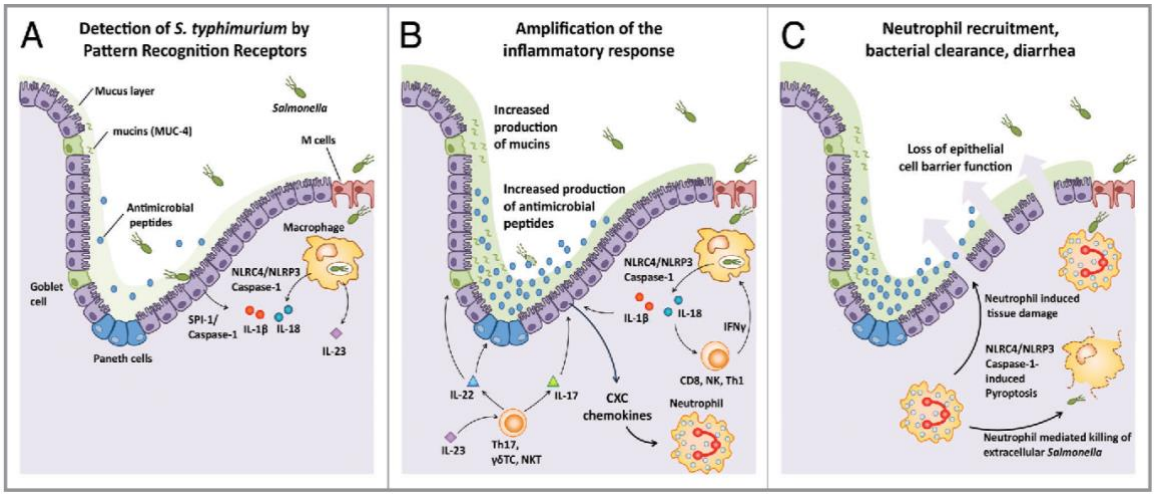

Figure 1.3: Illustration of the innate immune response to *S.* Typhimurium infection. (**A**) After invading the mucosa, *Salmonella* is detected by pattern recognition receptors, or in the case of extracellular *Salmonella*, TLRs, inducing a transcriptional response causing production of pro-inflammatory cytokines such as IL-23. Intracellular *Salmonella* activate NOD-like receptors that also promote IL-23 secretion, and assemble the NLRC4/NLRP3 inflammasomes that activate caspase-1, inducing secretion of IL-1β and IL-18. SPI-1 mediated activation of caspase-1 also contributes to IL-18 secretion. (**B**) IL-18 and IL-23 amplify the inflammatory response via paracrine signalling, causing induction of IFNγ and IL-22/IL-17 respectively. These cytokines increase production and secretion of AMP, mucins, and promote release of CXC cytokines (e.g. IL-8), causing an influx of neutrophils into the mucosa. (**C**) Infiltrating neutrophils kill extracellular *Salmonella*. *Salmonella* may be extracellular following transcytosis via M cells or pyroptosis and host cell lysis. Neutrophils can also cause inflammatory damage to intestinal tissue, causing loss of epithelial barrier integrity and inducing diarrhoea. (Figure taken from Broz et al, 2012[108])

As outlined in the previous segment, interaction of the host epithelium with *Salmonella* induces activation of the inflammasome and production of pro-inflammatory cytokines such as IL-8 and immune cell influx. In addition, antimicrobial peptides (AMPs) are produced by epithelial cells, as are factors such as Lipocalin2, which is an iron sequesterer, thought to limit bacterial growth. Contact between *Salmonella* and the host epithelium also induces expression of the IL-23/IL-22 axis, leading to secretion of AMPs, such as the c-type lectins RegIIIβ and RegIIIγ by Paneth cells.[109] Counterintuitively this may be of benefit to *Salmonella,* as RegIIIβ is able to kill a number of Gram positive and Gram negative pathogens in vitro, but not *Salmonella,* suggesting that this is one way which *Salmonella* overcomes colonisation resistance.[110] *Salmonella* also have defences against other AMPs, expressed via influence of the PhoPQ system, which is able to bind and inactivate cationic AMPs and reduce the immunogenicity of LPS by modifying its lipid A portion.[111]

Another factor *Salmonella* needs to overcome in order to survive in the inflamed gut is limited iron availability. Bacteria produce siderophores; iron chelating compounds, which

transport available iron into the pathogen. Lipocalin2, secreted into the gut lumen, is able to block this iron acquisition by binding a siderophore called enterochelin, produced by *Salmonella.*[112] However, most *Salmonella* can express the *iroBCDEN* gene cluster, which encodes production of salmochelin (a derivative of enterochelin) which is not bound by lipocalin2, allowing *Salmonella* to continue to scavenge iron and resist the action of this AMP.[113]

Production by the epithelium of reactive oxygen species is another defensive mechanism; NADPH oxidase (Nox) and Dual oxidase (Duox) have a role to play in gene expression, apoptosis and the respiratory burst. Production of superoxide (O^-_2) by Nox1 is known to activate NFκB, TNFα and IL-8 production, enhancing the pro-inflammatory response.[114] Paneth cells (producers of AMPs) are thought to proliferate following *Salmonella* infection in order to enhance antimicrobial response.[115] This proliferative response appears to come solely from the transit-amplifying cells, as the study noted no increase in LGR5, and murine organoids have been observed to downregulate iPSC markers (LGR5 and Bmi1) during *Salmonella* infection.[116] Lastly, increased mucus production by goblet cells in the epithelium is a defensive mechanism to increase barrier function, but may also benefit *Salmonella*, as it has been demonstrated that *S*. Typhimurium adjust to lack of nutrients in the inflamed gut by using mucus carbohydrates as a source of energy.[117]

As described above, there are two distinct clinical phenotypes for non-typhoidal *Salmonella* infection, with an inflammatory gastroenteritis caused in most cases, but with invasive systemic infection being possible in those with impaired immunity.[18] iNTS disease is also different to the clinical picture of typhoid disease, with much earlier onset of fever and systemic illness versus the 8-14 day wait normally observed between ingestion of *S*. Typhi and symptom onset. Host factors increasing the likelihood of invasive disease would include mutations in genes involved in the IL-23 axis, which is activated in response to *Salmonella* detection by DCs. IL-23 in turn acts on T cells to induce the IL-22 and IL-17A responses, which are required for maintenance of T_H17 cells, important in the immune response to *Salmonella*.[118] Similarly, the IFNγ response is key to preventing disseminated disease. IL-12 is produced by antigen presenting cells in response to *Salmonella* antigens and stimulates T cells to produce IFNγ, which activates the STAT-1 system in macrophages in order to

eliminate intracellular pathogens. These responses, along with activation of the inflammasome, are key to restricting the spread of NTS infection, with mutations in any pathway increasing susceptibility to iNTS.[119,120] Similarly, individuals with chronic granulomatous disease, characterised by an inability to produce NADPH oxidase and thus reduced bacterial killing within phagocytes, are more susceptible to systemic *Salmonella* infection,[121] as are children with *Plasmodium falciparum* malaria; with haemoglobin breakdown inhibiting phagocytosis.[122] Macrophage defects in those with sickle cell disease may also predispose to invasive disease.[123]

1.2.3 *Salmonella* within the macrophage

Having reached the lamina propria or Peyer's patches, *Salmonella* can be phagocytosed by macrophages, dendritic cells or neutrophils. Uptake by DCs and neutrophils is generally disadvantageous to the bacteria, however, *Salmonella* have developed the ability to survive and replicate inside of macrophages. In macrophages, much like within epithelial cells, *Salmonella* are contained within an SCV, which progressively acidifies, as it sequentially fuses with endosomes. Again SPI-2 T3SS come into play in delaying maturation of the SCV and optimising intravacuolar conditions.[124,125] Originally thought only to occur in epithelial cells, Sifs have also been noted in *Salmonella*-infected macrophages.[120] The PhoPQ system and T3SS effector protein SpiC play key roles in limiting endosome/lysosome fusion with the SCV.[126,127] SPI-2 T3SS are also key in avoiding damage from the NADPH oxidase dependent respiratory burst within the macrophages.[128,129]

In murine studies, the cation transporter natural resistance-associated macrophage protein 1 (Nramp1), located in the phagolysosomal membrane of macrophages, also appears to play a role in host cell resistance to *Salmonella,* both by withholding the availability of cations such as Fe^{2+} and Mg^{2+},[130] and increasing expression of lipocalin2.[131] SPI-2 also acts to exclude damaging reactive nitrogen intermediates, produced by inducible nitric oxide synthase (iNOS) from co-localising with SCVs in the macrophage.[132]

Salmonella are able to induce cell death in macrophages; in comparison to the predominant form of cell death induced in epithelial cells, this is via pyroptosis rather than apoptosis. Pyroptosis is caused by two mechanisms, either by early SPI-1 T3SS induced killing, via SipB mediated caspase-1 activation,[133] or by SPI-2 T3SS mechanisms, involving the spv and PhoPQ systems.[134,135]

S. Typhimurium behaviour inside the macrophage is relatively well studied, but there are a number of unknowns about the actions of *S*. Typhi within the macrophage. Transcriptomic studies of *S*. Typhi within macrophages demonstrated that SPI-1 and SPI-2-encoded T3SS were down- and up-regulated respectively, as would be expected. *S*. Typhi inside macrophages demonstrated upregulation of genes for resistance to AMPs and fatty acid utilisation and did not induce SOS or oxidative stress responses (whereas *S*. Typhimurium within macrophages invoked the expression of SOS response genes). Flagellar expression, iron transport and chemotaxis-related genes were downregulated, as were pili and Vi capsule related genes on SPI-7. However, a number of *S*. Typhi genes with unknown functions were upregulated, suggesting there is more to be learnt about the interactions of *S*. Typhi with the macrophage.[136] Fascinatingly, *S*. Typhi with knockouts for various components of the SPI-2 T3SS [a translocon mutant (*sseB*), an apparatus mutant (*ssaR*) and a transcriptional regulator mutant (*ssrB*)], all known to be required for *S*. Typhimurium survival within macrophages, were not defective in uptake and survival within macrophages compared to wild type equivalent isolates. Rather than suggesting that SPI-2 is not necessary for *S*. Typhi survival in macrophages, these data suggest some form of host adaptation, as a number of SPI-2 effectors expressed by *S*. Typhimurium and required for long term survival in the mouse, have proven to be pseudogenes in *S*. Typhi.[137]

Other mechanisms demonstrated by the Vi encapsulated *S*. Typhi for modifying the immune response within macrophages include dampening inflammasome activation and decreasing IL-1β secretion by repression of flagellin expression (controlled by TviA). This decreased incidence of inflammatory cell death in *S*. Typhi-infected macrophages and was reproduced when the Vi locus was introduced into *S*. Typhimurium prior to macrophage infection.[138] Another capsular-related resistance mechanism is that Vi may be able to prevent innate immune recognition of *S*. Typhi by complement. Compared with an unencapsulated mutant, a Vi encapsulated *S*. Typhi isolate was able to interfere with complement component 3 (C3) deposition, leading to reduced bacterial binding to complement receptor 3 (CR-3) on the surface of murine macrophages and decreased CR-3 dependent clearance of *S*. Typhi from murine livers and spleens post-infection.[139] An additional defence factor employed by S. Typhi for survival and replication within the macrophage appears to be the use of the SPI-1 T3SS to

block the RAB32-associated pathway, given that knockdown of RAB32 or its nucleotide exchange factor BLOC-3 (biogenesis of lysosome-related organelle complex-3) increased S. Typhi replication in human macrophages.[140]

S. Paratyphi A is relatively poorly studied inside the macrophage. One study looking at bacterial transcripts of *S*. Paratyphi A in blood from three bacteraemic patients noted enhanced expression of transcripts of PhoP and the transcriptional regulator SlyA that influences SPI-1 and SPI-2 expression. However, in this study, the largest category of dysregulated transcripts were associated with proteins of unknown function.[141] Additional work on proteins expressed in *S*. Paratyphi A cultured from bacteraemic patients versus laboratory grown *S*. Paratyphi A noted increased expression of proteins involved in cell adhesion, fimbrial structure, antimicrobial resistance, ion transport, proteolysis and oxidoreductase activity in bacteria isolated from blood.[145]

Analysis of the core proteome of laboratory cultured *S*. Paratyphi A versus *S*. Typhi demonstrated differential enrichment of proteins involved in carbohydrate and polysaccharide synthesis and metabolism between the serovars. Proteomes for these serovars were compared to those for *S*. Typhimurium and *S*. Enteritidis. Typhoidal and non-typhoidal serovars readily separated from each other on analysis. This suggests that other than the influence of the Vi capsule, *S*. Paratyphi A and *S*. Typhi behave relatively similarly in culture, but this does not answer the question of what is happening *in vivo* during infection.[146]

Gene expression analysis of blood from patients infected with *S*. Paratyphi A demonstrated elevations in IFNγ, TNFα, IL-6, 8, 10 and 15 in response to infection, but no increase in IL-12 (which induces IFNγ release in Th1 and NK cells and is elevated in NTS infection[142]).[143] The elevation in this study of IFNγ levels was striking (around 75 times baseline levels), which fits with the IFN overexpression observed in patients with acute typhoid fever in human challenge studies.[144]

The data presently available suggest a differing host response to typhoidal versus NTS serovars. However, it is hard to draw conclusions based on limited evidence, and it is clear that further work is required to define the interactions between both *S*. Typhi and *S*. Paratyphi A and the macrophage.

1.2.4 Systemic spread of *Salmonella*

Having been taken up by and replicated within macrophages, and now residing in Peyer's patches (PP) or the lamina propria, typhoidal *Salmonella* are able to spread to the mesenteric lymph nodes (MLN), where they can enter the lymphatic system, eventually reaching the thoracic duct and bloodstream.[147] CD18+ cells such as monocytes, macrophages or DCs are able to traffic *Salmonella* directly from PP or the lamina propria to these organs via haematogenous spread, and DCs may assist in trafficking *Salmonella* to the MLN either directly from the intestinal lumen or from PP / the lamina propria. After prolonged infection, *Salmonella* can travel from the liver and spleen to other organs via the blood, and in the case of *S*. Typhi, excretion from the liver in bile can result in colonisation of the gall bladder, with bacteria from the gall bladder periodically shedding back into the intestine.[87,148] Thus, after passing through the epithelium, primary bacteraemia occurs with little symptomatology or evidence of intestinal inflammation (certainly in comparison to non-typhoidal infection) (**Figure 1.4**).[148] *S*. Typhi bacteria can reside in the reticuloendothelial system for an extended incubation period (usually 8-14 days); thereafter clinical illness may emerge, frequently linked to a secondary bacteraemia. During this bacteraemia, bacterial counts in the blood are low, averaging 1 cfu/mL,[149] versus 10 cfu/mL in bone marrow.[150] Symptoms of typhoid disease include: prolonged fever, fatigue, abdominal pain, nausea, rash, diarrhoea or constipation and headache. Complications that can occur with extended or untreated disease include intestinal perforation and haemorrhage, hepatitis and cholecystitis. Significantly, up to 4% of those who have had typhoid infection can go on to become chronic carriers, shedding *S*. Typhi in their stool sporadically over long periods (from months to years), putting contacts at risk of infection.[151]

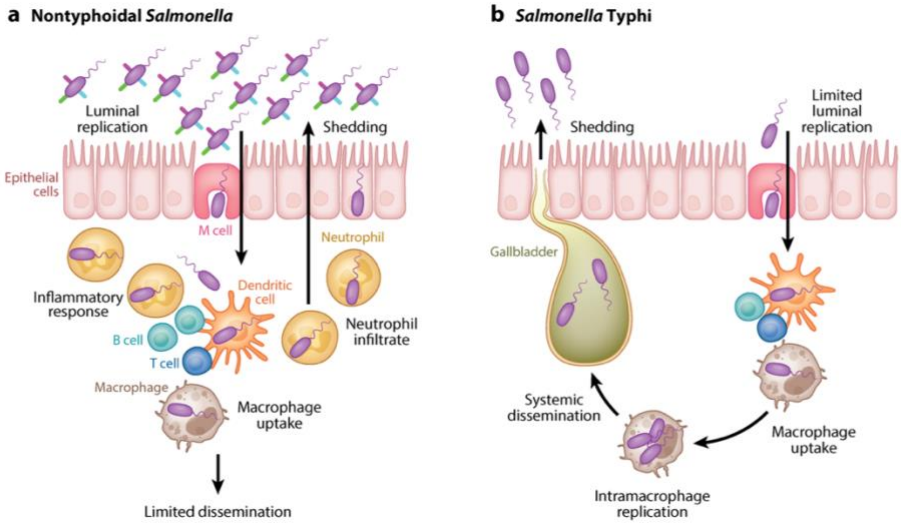

Figure 1.4: Systemic differences between nontyphoidal and *S*. Typhi infections: (**a**) Demonstrates the propensity of nontyphoidal strains to express surface molecules undisguised by Vi capsule, to invade the intestinal epithelium in high numbers, causing an inflammatory response and neutrophil infiltrate, followed by fairly rapid clearance and limited dissemination. (**b**) Demonstrates *S*. Typhi invading in more limited numbers, but uptake, replication and dissemination inside macrophages with a limited inflammatory response. (Figure taken from Dougan & Baker, 2014[148])

In nontyphoidal *Salmonella* infection in healthy individuals, there is limited dissemination of the pathogen, with numerous bacteria being killed by the inflammatory neutrophil response in the gut. Infection is usually restricted to the intestine and mesenteric lymph nodes.[152] Phagocytes in the liver and spleen can rapidly clear *Salmonella* from the blood, should it have disseminated this far. Thus, the clinical picture is one of an inflammatory enterocolitis, with profuse watery diarrhoea, vomiting and abdominal pain, and spontaneous resolution.[153] There is a low rate of secondary bacteraemia (<5%) and this has a mortality rate of 1-5%.[18]

In those with immunodeficiencies as discussed above, iNTS infection can occur, with *Salmonella* able to cause a rapid-onset bacteraemia with fairly diverse symptoms including: fever, enterocolitis (but only in up to 50% cases), pneumonia (may be due to co-infections) and hepatosplenomegaly.[18] Symptoms are difficult to distinguish from other febrile pathologies, such as malaria or lower respiratory tract infection, and even with microbiological confirmation and appropriate treatment, in sub-Saharan Africa this illness has a mortality rate of 22-47%.[20,154]

1.2.5 Adaptive immune response to *Salmonella*

The innate immune response is very effective at controlling the initial aspects of *Salmonella* infection, but is insufficient for achieving protective immunity. Models used in this study will largely focus on cell-mediated (innate) immunity, but here I will briefly discuss the adaptive immune response to *Salmonella* infection. Control and eradication of bacteria during a primary infection and protection from subsequent infections requires the development of a *Salmonella*-specific T-lymphocyte response, in order to recruit these cells to sites of infection,[1] and allow clearance of bacteria.[155] This appears to be in the form of CD4+ TCR-alpha beta cells and associated IFNγ response, with CD8+ cells playing an auxiliary role.[156] Th1 cells also mediate the regulation of *Salmonella*-specific B cell activation and maturation, producing antibodies against bacterial polysaccharide and protein antigens.[157] In mice given oral attenuated vaccines, CD4+, CD8+ and anti-*Salmonella* antibodies all had a role to play in infection resistance.[158] CD4+ cells had a role in cytokine production, particularly IFNγ release, and importantly, mice with deficiencies in CD4+ T cells or IFNγ production experience uncontrolled *Salmonella* growth.[159] This runs in parallel with IFNγ production in the innate response, stimulated by IL-18 release after caspase-1 cleavage in response to flagellins as described earlier in this chapter. CD8+ cells differentiate into cytotoxic T lymphocytes, removing *Salmonella* from infected macrophages.[1]

The expression of certain major histocompatibility complex class II alleles conferred resistance to enteric fever in one genome-wide association study, suggesting that CD4+ T cells have a role both in control of typhoidal and non-typhoidal serovars in humans.[160] Studies on T cells from participants in the *S*. Typhi human challenge model were able to identify antigen-specific T cell responses to three particular antigens: Hlye (a haemolysin with an as yet undetermined role in *Salmonella* pathogenicity), CdtB (a component of the typhoid toxin proposed as a virulence factor for *S*. Typhi and *S*. Paratyphi A[161]) and PhoN (an acid phosphatase induced after PhoPQ system activation). CdtB was able to elicit T cell responses targeting infected cells, and antibody responses neutralising toxin activity. *S*. Typhi CdtB CD4+ responses were not cross-reactive against *S*. Paratyphi A and vice versa, however PhoN-specific T cell responses were active against both typhoidal and

nontyphoidal *Salmonella* strains.[162] Other findings of interest were that *Salmonella* CD4+ responses targeted both constitutively expressed proteins as well as those only expressed after infection, showing that specific T cell repertoire is shaped by the plasticity of the *Salmonella* transcriptome and that T cell response can be tissue specific to the location of the bacteria of interest. In addition, the CD4+ cells studied here (CD4+ CD38+ CCR7- cells) displayed gut homing markers, suggesting that these circulating cells may be able to migrate to the site of bacterial invasion and join tissue resident CD4+ cells in the gut mucosa to prevent re-infection.[162]

Th17 cells are also thought to have a role in control of *Salmonella* infections. These cells express IL-17A, IL-17F, IL-22 and IL-26, with receptors for IL-22 and IL-26 being located on epithelial surfaces;[163] IL-22 receptor complexes are found on the basal surface of intestinal epithelial cells, suggesting a role in the local infection response.[164] IL-17 and IL-22 activate mucosal immune responses, inducing AMP release and chemokine expression. This process will be discussed in more detail later on in this chapter.

Despite their limited role in primary infection, B cells do provide some protection against secondary infection, with sera from Malawian children containing anti-*Salmonella* antibodies able to kill NTS strains,[165] and recent findings in human participants challenged, then re-challenged with *S*. Paratyphi A or *S*. Typhi demonstrating some degree of protection, with baseline anti-O:2 IgG being higher in *S*. Paratyphi A re-challenged patients than in naïve controls.[166]

1.3 Treatment and prevention of *Salmonella* infections

1.3.1 Treatment of *Salmonella* infections and concerns about MDR organisms

Untreated, typhoid fever historically had a mortality rate of up to 15%,[147] but this declined with the introduction of chloramphenicol in the 1940's. With appropriate antimicrobial therapy, mortality can be as low as 1%,[167] although other factors such as age, length of illness before appropriate treatment and ingested dose of the organism also affect disease severity.[147] Other agents used for treatment include trimethoprim/sulphamethoxazole and

ampicillin; however, since the 1990's, multi-drug resistant (MDR) isolates of *S.* Typhi (defined as resistance to chloramphenicol, trimethoprim/sulphamethoxazole and ampicillin) have been isolated with varying frequencies, leading to a higher incidence of severe disease in those infected with drug resistant or intermediately resistant isolates.[167] Current treatment options include fluoroquinolones (e.g. ciprofloxacin), 3rd generation cephalosporins (e.g. ceftriaxone) and azithromycin, but worryingly, resistance to some of these antibiotics has also been recorded, especially as fluoroquinolones have become the predominant treatment used for MDR infections. Whole genome sequencing data allows us to draw associations between antibiotic resistance and *S*. Typhi lineage. For example, in a Vietnamese study, severe typhoid disease was associated with organisms intermediately resistant to ciprofloxacin.[168] This intermediate response has been associated with the H58 MDR haplotype,[169] although such resistance has become common in other *S*. Typhi lineages. A recent study based on the whole genome sequences of over 1800 isolates demonstrated that the H58 lineage has disseminated throughout Asia and into Africa, displacing antibiotic-susceptible lineages and driving disease epidemics.[170] Numerous local typhoid outbreaks have been linked to various H58 sublineages.[171-174]

AMR gene transfer is often facilitated by transposon or plasmid exchange; in the case of *S*. Typhi H58 clades, these genes were initially associated with an IncHI1 plasmid. This type of plasmid has a transposon able to carry multiple resistance genes, including: *dfrA7*, *sul1*, *sul2* (trimethoprim-sulfamethoxazole resistance), $bla_{\text{TEM-1}}$ (ampicillin resistance), *strAB* (streptomycin resistance) and *catA1* (chloramphenicol resistance).[169]
However, this transposon has been integrated into the *S*. Typhi chromosome in some recent H58 lineages and the plasmid has been lost.[170,172] Fluoroquinolone resistance is associated both with acquisition of AMR genes and chromosomal mutations. In H58 clades, mutations in the chromosomal quinolone resistance-determining region (QRDR), which is composed of topoisomerase IV (*parC* and *parE* genes) and DNA gyrase (*gyrA* and *gyrB*) genes are increasingly widespread. Plasmid-mediated resistance (PMQR) genes including *qnr, oqxAB* and *aac(6')Ibcr* can also be acquired and contribute to fluoroquinolone resistance. Ceftriaxone resistance is associated with extended-spectrum β-lactamase (ESBL) gene acquisition.[28] More recently, there has been an outbreak of extensively drug resistant (XDR) *S*. Typhi in Pakistan,[175] resistant to chloramphenicol, trimethoprim/sulphamethoxazole,

ampicillin, fluoroquinolones and 3rd generation cephalosporins. The clade responsible is a H58 clone, with an additional plasmid encoding the *bla*$_{CTX-M-15}$ extended-spectrum β-lactamase and *qnrS* fluoroquinolone resistance gene.[28] Treatment options for such strains are very limited, especially in settings where access to specialist intravenous antibiotics is scarce. These concerning developments have highlighted the need for focused efforts to control typhoid. These efforts could include improved sanitation measures and the licensing and distribution of effective vaccines.

Although less common than *S*. Typhi infection, *S*. Paratyphi A causes up to 40% of cases of enteric fever in certain areas of Asia.[176,177] Fluoroquinolone resistance is the commonest mechanism of drug resistance in *S*. Paratyphi A isolates, recorded in up to 90% of isolates in some studies.[178-180] There is a growing body of evidence on MDR *S*. Paratyphi A infections, as they are becoming an increasingly significant problem across Asia,[176,181-183] although the genetic basis of MDR in many cases is not yet clearly defined.[184]
Studies describing antimicrobial resistance in *S*. Paratyphi A point to plasmids such as IncHI1 as a possible mediator of resistance, although molecular studies are limited thus far.[185-187] Plasmids of varying sizes have been reported as encoding MDR in studies from China, Bangladesh and Calcutta.[184-186] Interestingly, sequencing of an IncHI1 plasmid (pAKU_1), which encoded MDR in an *S*. Paratyphi A isolate from Pakistan, demonstrated that the pAKU_1 plasmid shares a common backbone with the *S*. Typhi plasmid pHCM1 and an S. Typhimurium plasmid pR27; the backbone being thought to have originated from an ancestral IncHI1 replicon. pAKU_1 and pHCM1 share a composite transposon comprising 14 antibiotic resistance genes within mobile elements. The transposons are located in different places on the backbone of each plasmid, suggesting these genes were independently acquired via horizontal transmission. Worryingly, two IncHI1 plasmid types from Vietnamese *S*. Typhi contained features of the pAKU_1 backbone sequence, with the transposon located in exactly the same place as in the pAKU_1 *S*. Paratyphi A plasmid.[184] This is very unlikely to have happened by chance, raising the likelihood that plasmids have been interchanged between these serovars at some point; whether directly or via another pathogen. Other studies have proposed the likelihood of chromosomal recombination between *S*. Typhi and *S*. Paratyphi A, allowing them to adapt to their niche in the human host.[188] These similarities between the pathogens and their mechanisms of antimicrobial

resistance suggest that care needs to be taken when making policy for antimicrobial choices for *S*. Typhi, as this may well simultaneously affect the resistance patterns we see in *S*. Paratyphi A too.

S. Typhimurium is responsible for the majority of cases of iNTS disease in Sub-Saharan Africa, although *S*. Enteritidis is also responsible for many of these infections.[20,21,189] Until recently, extensive iNTS disease had largely been restricted to the African continent, but reports have emerged of iNTS in cohorts of patients in parts of Asia, including: India,[190] Taiwan[191] and Thailand.[192] iNTS in Vietnam has also been documented, with cases associated with the HIV epidemic, as was the case when the disease emerged in sub-Saharan Africa, with the emergence of ST313 lineages I and II each associated with periods of HIV expansion in the early 1980s and 1990s respectively.[193] Acquisition of chloramphenicol resistance has also been associated with increased transmission of this pathogen in Kenya[26] and Malawi[20]

Antimicrobial resistance was common in *S*. Typhimurium associated with iNTS in Vietnam, with over 50% isolates being resistant to ampicillin, amoxicillin, chloramphenicol, trimethoprim/sulfamethoxazole, ciprofloxacin and gentamicin. Multilocus sequence typing on these isolates demonstrated that *S*. Typhimurium STs 34, 19, 1544 and *S*. Enteritidis ST11 were responsible for the majority of cases in this study; of which, all but ST1544 were also resident sequence types seen in African isolates. However, in Africa in recent years, many circulating isolates have been replaced with a newer multidrug resistant *S*. Typhimurium ST313 clone.[26] In this study, sequencing of representative isolates of ST313 lineage I (D23580) and II (A130), showed a unique prophage repertoire and composite genetic element encoding MDR genes, which was situated on a virulence-associated plasmid. Genome degradation had occurred, with a number of invasion related pseudogenes and deleted genes identified which are either absent or known to be pseudogenes in *S*. Typhi and *S*. Paratyphi A. This suggests that ST313 has become adapted to a particular clinical niche or to systemic disease, and continues to microevolve to better suit this environment.

Sequencing has also been performed on another iNTS-causing ST34 clade currently causing the pandemic of iNTS in HIV-infected individuals in Vietnam.[194] In contrast to the ST313 clone, ST34 does not exhibit evidence of genome degradation, and is able to produce both

invasive disease and enterocolitis, unlike ST313 which was primarily associated with invasive disease. Fascinatingly, The Vietnamese ST34 variant derives from the European clone of the monophasic ST34 *S*. Typhimurium variant, *S*. I:4,[5],12:i:−. At some point, these Vietnamese ST34 have re-acquired a phase 2 flagellum, potentially conferring an invasiveness advantage, which would appear to be borne out by studies in murine macrophages (S. Baker, unpublished data). *S*. I:4,[5],12:i:− has also acquired an extensive MDR plasmid, encoding: *oqxAB, blmS, sul1, ⊿aadA2, dfrA12, aph3, sul3, aadA1a, cmlA2, aadA2, floR, sul2, hph, aac(3')-Iva, aac(6')-Ib-cr, blaOXA-1, catB3* and *arr3*. These genes, cause predicted resistance to: fluoroquinolones, bleomycin, sulphonamides, trimethoprim, kanamycin, streptomycin, chloramphenicol, spectinomycin, florfenicol, hygromycin B, apramycin, beta-lactams, and rifampin.[194] It is therefore feasible that this clone would have occupied a niche in HIV-infected individuals, given the frequent use of broad-spectrum antibiotics likely in this population.

Given the very high mortality rates observed with iNTS and their frequent possession of numerous MDR genes, it is important to focus efforts on preventative strategies against these types of pathogen as well as implementing WaSH measures for control of disease.

1.3.2 Status of vaccine development against typhoid, paratyphoid and NTS disease

Given the concerns about the spread of increasingly MDR *S*. Typhi, strategies for vaccination and prevention of cases have been the subject of intensive investigation in recent years. WaSH interventions, such as improved water supply and waste disposal could do much to eradicate infection, as has been the case in Europe and North America. It is clear that the infrastructure required to effect these changes is unlikely to be realised in the short to medium term, therefore, efforts have focused on case prevention and outbreak control. Any vaccine effort ought to be focused on younger children, given that they shoulder a large burden of typhoid disease.[195] However, until recently, available licenced vaccines did not protect this population. The oral live attenuated typhoid vaccine, Ty21a is unsuitable for children under 5, given that it is formulated in large capsules which would be difficult for children to swallow[196] and the parenteral Vi capsular polysaccharide vaccine is not immunogenic in early childhood. Excitingly, there have been recent developments in producing vaccines that would be suitable for use in the paediatric population. Typhoid

conjugate vaccines (TCVs) have been constructed, which combine the Vi polysaccharide capsule with a protein carrier. TCVs can induce enhanced immune responses and appear to be both safe and effective from infancy.[197-200] Rapidly obtained efficacy data for this type of vaccine came from a human challenge study, wherein participants were randomised either to receive a Vi conjugate (Vi-TT; in this case the conjugate was tetanus toxoid), Vi polysaccharide (Vi-PS) or meningococcal vaccine as a control, prior to receiving an oral inoculum of *S*. Typhi sufficient to cause disease.[100] 77% of control participants were diagnosed with typhoid disease, versus 35% in each of the Vi-PS and Vi-TT groups, giving vaccine efficacies of 54.6% for Vi-TT and 53.0% for Vi-PS. The criteria for diagnosis of typhoid disease in this study were rather broad, with a typhoid case being defined as fever of $\geq$ 38 °C for $\geq$ 12 hours, or *S*. Typhi bacteraemia. If a definition of fever of $\geq$ 38 °C followed by *S*. Typhi bacteraemia is used, this vaccine prevented 87% infections versus 52.3% prevented by the Vi-PS vaccine. This latter definition is probably a more realistic representation of diagnostic criteria for reported cases in the field, and has previously been used in field vaccine studies.[201] In addition, protection levels in endemic settings may be higher, as the vaccine is being used in a pre-exposed population, rather than a naïve population as in the challenge study, and in children as well as adults. For example, efficacy of Vi-PS was calculated at 69% within the first year after vaccination during field trials as opposed to the 52.3% found in this study.[196] Seroconversion in the Vi-TT group was 100% and 88.6% in Vi-PS group. One month after vaccination, Vi-TT group participants had significantly higher mean anti-Vi IgG titres.

In addition to the ability to directly prevent cases of typhoid fever, vaccination may also reduce the spread of the disease via reduction of stool shedding during infection. Human challenge studies showed that Vi-PS and Vi-TT both significantly decreased incidence of stool shedding versus unvaccinated controls during typhoid challenge. *S*. Typhi-exposed participants were twice as likely to have stool shedding versus those exposed to *S*. Paratyphi A, with overall shedding rates of 14.5% vs 7.5% including unvaccinated and vaccinated cases.[202] This study, together with evidence from other clinical and immunological studies of TCV vaccines, led in 2017, to the World Health Organisation's (WHO) Strategic Advisory Group of Experts (SAGE) recommending the introduction of TCVs for infants and children > 6 months of age in endemic countries, with priority given to those countries with the highest

disease burden or levels of AMR.[203] It was also recommended to have catch-up campaigns for children up to 15 years of age where feasible / necessary, and that TCVs be used in response to confirmed outbreaks of typhoid fever, as has been the case during the current XDR typhoid outbreak in Pakistan.[204] In January 2018, the WHO pre-qualified its first TCV, Typbar-TCV®, meaning that the vaccine can be procured by UN agencies; also that lower income countries may apply to Gavi, the Vaccine Alliance, for funding assistance to implement vaccine programmes. Initial data from post-licensure phase IV trials, presented at the International Conference on Typhoid and Other Invasive Salmonelloses in April 2019 demonstrated Typbar-TCV® to be both safe and effective at disease prevention, but these studies are not yet published. Overall, there is the potential for TCV vaccines to make a big public health impact on the prevention of typhoid fever over the coming years.

S. Paratyphi A vaccine development is some way behind that of *S*. Typhi. Challenges include the lack of an approved serological correlate of protection, and the host restriction of this pathogen, making the utility of animal models limited. Unfortunately, little cross-protection is seen between *S*. Paratyphi A and *S*. Typhi, either following challenge after previous infection with the other serovar,[166] or for *S*. Paratyphi A following vaccination with either Vi-PS or the oral Ty21a vaccines.[16,205] Some efficacy of Ty21a vaccines against *S*. Paratyphi B has been reported in trials in Chile, with predicted efficacy of 49%.[206] The mechanism for this protection is not entirely clear, with the authors postulating that it may be secondary to some sharing of epitopes amongst the O antigens on the bacteria (although epitopes are shared also with *S*. Paratyphi A, for which there is no cross-protection), or on observing strong T cell responses to the vaccine, a cell-mediated immunity, with as yet undefined shared antigens being a target for the immune response.

To produce safe and effective protection against *S* Paratyphi A, attention is again focused on the development of conjugate vaccines, with phase 1 and 2 immunogenicity trials in Vietnam on O antigen conjugated to tetanus toxoid showing significant increases in mean anti-*S*. Paratyphi A LPS IgG and IgM in both adults and children. These conjugates produced a > 4 fold rise in anti-LPS IgG in $\geq$ 80% participants.[207] The O:2 antigen of *S*. Paratyphi A is known to play a role in virulence and act as an antigen, stimulating the host immune response.[208] Other potential vaccine candidates have been undergoing trials in mice, with

O:2 conjugated to a carrier protein CRM_{197} (a component of diphtheria toxin) also showing promising immugenicity and eliciting a bactericidal serum response.[209] Similarly, *S*. Paratyphi A flagellar protein, FliC has also been shown to enhance phagocytosis and clearance of *S*. Paratyphi A in mice immunised with live attenuated *S*. Paratyphi A strains prior to intraperitoneal challenge.[210] Recent work has improved the O-linked glycosylation method for producing conjugate vaccines, making it more rapid and less expensive.[211]

Efforts have also been made to produce a bivalent vaccine that would protect against *S*. Typhi in addition to *S*. Paratyphi A, by the cloning of the *S*. Typhi *viaB* locus (responsible for Vi capsule biosynthesis) and its insertion into an attenuated *S*. Paratyphi A to produce a candidate oral vaccine. In mice, nasal immunisation with this vaccine induced high levels of *S*. Paratyphi A and Vi-specific antibodies in sera, and total sIgA in the intestine. In addition, the vaccine was significantly protective against *S*. Paratyphi A and *S*. Typhi challenge.[212] Clearly there is some way to go before a clinically implementable vaccine is produced, but given the increase in prevalence of *S*. Paratyphi A across parts of Asia, it is important that these efforts continue, alongside attempts to control spread of disease in endemic areas.

Producing a vaccine for iNTS may prove slightly simpler in principle, given that although these pathogens do not have a published correlate of protection, it is possible to quantify serum bactericidal activity against *S*. Typhimurium and *S*. Enteritidis. Additionally, murine models are very helpful for early work, given that *S*. Typhimurium can cause systemic infection in mice, as well as enterocolitis (following pre-treatment with streptomycin), although differences obviously remain between the human and murine responses to these pathogens *in vivo*. Vaccines for iNTS would need to be safe and immunogenic for infants, as peak disease incidence occurs at 12 months of age, and would need to be safe to use in HIV-infected populations, as these patients are at increased risk of iNTS.

It would make sense to design antibody-inducing vaccines against iNTS serovars, as epidemiological work has shown that incidence of disease decreases with increasing age and acquisition of antibodies. Serum antibodies have also been shown to have *in vitro* bactericidal activity and mediate oxidative killing of iNTS serovars intracellularly.[165,213]

Proposed vaccine targets have included outer membrane proteins (OmpD) purified from whole bacteria, with the idea that if conserved protein antigens, such as OmpC, F or D or flagellin were targeted, the resulting vaccine would achieve broad coverage of clinically relevant serovars.[214] It has been proposed that a multivalent vaccine comprised of 5-6 conjugates could protect against the most prevalent forms of iNTS and gastroenteritis-causing *Salmonella* worldwide.[165,215,216] A bivalent conjugate vaccine linking core and O polysaccharide (COPS) components of *S*. Typhimurium and *S*. Enteritidis LPS to their phase 1 flagellin subunits is under development. Instead of linking the antigens to a protein, such as tetanus toxoid or CRM_{197}, it is hoped that efficacy will be enhanced as both elements of the vaccine will be antibody targets. *S*. Enteritidis COPS-FliC (a flagellin protein) conjugates elicited protective antibody responses in murine trials prior to intraperitoneal challenge.[215] Ongoing work on this project is being done by Bharat Biotech, who produce the recently pre-qualified Typbar-TCV®.

One group has attempted to produce a live attenuated NTS vaccine, derived from a gastroenteritis-associated *S*. Typhimurium strain, with deletions induced in *aroC* and *ssaV* genes. Testing for this vaccine did not go beyond phase 1 trials, as stool shedding occurred in volunteers for up to 23 days post-immunisation.[217] Work on a bivalent live attenuated NTS vaccine is ongoing at the University of Maryland, where attenuated strains of *S*. Typhimurium (CVD 1931, which is derived from an ST313 isolate) and *S*. Enteritidis (CVD 1944, derived from an invasive *S*. Enteritidis) have elicited significant seroconversion in the form of anti-LPS and anti-flagellin antibodies. At the same institute, vaccination with CVD1921, an attenuated ST19 iNTS derivative has proven adequately safe and well tolerated, with limited shedding in simian immunodeficiency virus-infected rhesus macaques.[218]

Other institutes are using the Generalised Modules for Membrane Antigens (GMMA) technique to generate bivalent vaccines for *S*. Typhimurium and *S*. Enteritidis. This involves the introduction of mutations that moderate LPS toxicity into production strains, which also induces the strains to increase production of membrane blebs of immunogenic particles ~50-90nm in diameter. This technology has been used to produce a *Shigella sonnei* vaccine which is currently in phase 1 trials,[219] and immunisation with GMMA has been

demonstrated to be at least as effective as *S*. Enteritidis and *S*. Typhimurium O-antigen-CRM_{197} glycoconjugate vaccines at inducing immunogenicity and reducing bacterial burden in head to head trials in mice.[220]

There are a number of promising avenues then for iNTS vaccines, however at present, there is less political will and funding available for tackling this form of salmonellosis, despite its increasing prevalence and high mortality rates.[221] This needs to be addressed going forwards to accelerate interventions to reduce the global impact of iNTS disease.

1.4 Models for study of host-pathogen interactions and reasons for their use

1.4.1 Current methods of studying host-pathogen interactions for *S*. Typhi, *S*. Paratyphi A and NTS strains

As outlined above, there are numerous gaps in our knowledge about the detailed interactions between host and epithelium for *Salmonella* serovars causing enteric fever, simply because these pathogens have adapted to cause disease in the human host, and are now restricted to this niche. A proxy for a lot of what we know about *S*. Typhi infection comes from studies of *S*. Typhimurium in murine models, since this pathogen causes an invasive disease phenotype in susceptible mice with superficial similarities to that caused by *S*. Typhi in humans. Susceptible target species would include mice that have mutations in genes important for intracellular immunity such as Nramp1. Nramp1 is an intracellular protein recruited to the endosome, where it acts as an Fe^{2+} and Mg^{2+} transporter. Much has been learnt from murine study, such as the actions of the SPI-1 and SPI-2 T3SS during infection,[222] however significant differences remain in the immune response between human and murine hosts and the pathogens it is possible to use in these models. For example, the presence of the Vi capsule of *S*. Typhi, which is absent in *S*. Typhimurium, would cause host-pathogen interactions to differ in humans versus in the murine model. One attempt to bridge this gap has been the study of an *S*. Typhimurium/*S*. Typhi chimera to learn more about the function of the Vi capsule in the murine host.[223] This chimeric derivative is *S*. Typhimurium C5.507 Vi^+, which harbours SPI-7, encoding the genes responsible for producing the Vi capsule. Infection of mice with C5.507 Vi^+, resulted in a decreased recruitment of NK and polymorphonuclear neutrophils, leading to a blunted pro-

inflammatory cytokine response, affecting TNF-α, MIP-2 and perforin, but a large increase in the anti-inflammatory cytokine IL-10. This cytokine was expressed in DCs, macrophages and NK cells in the spleen, and neutralisation of the IL-10 response led to increased migration and activation of splenocytes.

A murine model thought to better mimic the human response to *S*. Typhi involves production of immunodeficient Rag2$^{-/-}$ γc(-/-) mice which have been engrafted with human foetal liver stem and progenitor cells. These mice are able to partially support *S*. Typhi infection, and an *S*. Typhi with a mutation in the PhoPQ system (a gene required for virulence), was unable to replicate in these mice.[224] Human-like innate and adaptive responses were produced by the mice, with *S*. Typhi-specific antibody production occurring and elevated levels of TNFα, IL-8, IL-10, IL-12, IFNγ, MIP-1α and IP-10 being recorded. Similarly, another group used non-obese diabetic (NOD)-scid IL-2Rγ(null) mice engrafted with human haematopoietic stem cells to model typhoid disease, finding that *S*. Typhi were able to replicate and cause lethal infection in these mice, who also produced a cytokine picture similar to that seen in human disease.[225]

Modelling of *S*. Paratyphi A has proven incredibly difficult, given its lack of a proxy for mouse studies, such as *S*. Typhimurium for *S*. Typhi. Some mouse work has been undertaken using attenuated strains and focusing on response to a particular component of the bacterium, such as flagellar proteins.[210]

Models for the study of gastroenteritis-causing NTS strains again include murine hosts; in this case animals are treated with streptomycin prior to *Salmonella* infection in order to deplete the resident microbiota and allow rapid colonisation and expansion of *Salmonella*, which can invade the mucosa and induce an inflammatory colitis as seen in human infections.[226] *S*. Typhimurium, *S*. Enteritidis, *S*. Dublin, *S*. Gallinarium and *S*. Pullorum have all been studied in this fashion.[227] Calf models have also been used for the study of NTS strains, as cows are natural hosts for a number of *Salmonella* serovars, such as *S*. Typhimurium,[228] which causes a gastroenteritis with a secretory and inflammatory response similar to that in humans.[229] Ligated ileal loops from calves have also been used, cells from which display apical membrane ruffling in response to *S*. Typhimurium infection, with bacteria invading M

cells or enterocytes, as may occur in humans.[230,231] Whilst we have learnt a lot from these models, interspecies differences are present in virulence factors, for example, the *spv* operon is required for systemic infection in mice, but not in calves.[232]

Alternatives to animal models have therefore been explored for detailed study of these pathogens. Use of 2-D cell culture models (e.g. HeLa or Caco-2 cells) has enabled us to learn a lot about interactions of numerous serovars of *Salmonella* with the epithelium. Additionally, intestinal samples obtained via biopsy have provided data from differentiated intestinal epithelium.[233,234] Methods used to study these samples are advancing, with tissue explants being maintained in culture, and structurally supported in a way that allows access both to the apical and basal side of the tissue layer.[235] In addition, replication of the intraluminal microbiotal environment has been attempted with the colonic fermentation model of cell culture to recreate colonisation resistance to invasive pathogens.[236] One study co-cultured Caco2 cells with Raji B cells to produce a model containing M-like cells, in order to observe the transcriptional processes of *Salmonella* translocation across the epithelium.[237]

Cell culture models are becoming increasingly more complex, with 3-D organotypic models being developed, such as the use of a rotating wall vessel (RWV) to propagate colonic cell cultures on microbeads; allowing them to create an organised intestinal epithelium more representative of that seen *in vivo*. This also allows reconstitution of some of the chemical and molecular gradients in all dimensions that would occur in the intestine (i.e. apical, basal and lateral interactions).[238] Recently, groups have attempted to take this further and produce models which investigate both the epithelial and immune response to pathogens by setting up organotypic cultures derived from colonic epithelial cells, grown in a RWV, and adding macrophages into the basal aspect of the culture medium to try to recapitulate what would occur in the lamina propria. Macrophages in this study did exhibit phagocytosis and reduce adherence, invasion and survival of a number of *Salmonella* strains versus an epithelial model alone.[239]

Discrete 3-D organoid models which contain an organised, polarised epithelium have been developed from a number of tissues, including mouse intestinal crypts.[240,241] Clearly work

with this particular type of organoid would have some of the same caveats as using a live mouse model, but they are a much more efficient way of looking at the mouse epithelium, as organoids from one animal will self-perpetuate, rather than requiring sacrifice of numerous mice for a set of assays. Organoids have also been generated from human embryonic stem cells (hESC),[233] human intestinal tissue from biopsies (primary organoids),[242] minced intestinal tissue[243] and human induced pluripotent stem cells (hiPSCs) as demonstrated in **Figure 1.5**.[244] As well as self-renewal, organoids are capable of self-organisation, during growth on an extracellular matrix scaffold, and demonstrate similar organ functionality as their tissue of origin.[245] One benefit of the organoid model is the lack of stromal tissue, allowing a reductionist approach for studying the tissue of interest (the epithelium) without confounding influences from the local environment. It is also much more feasible to manipulate signalling pathways or create organoids from different genetic backgrounds than in animal models, particularly in the case of hiPSC-derived organoids (iHO), as CRISPR/Cas9 editing can be used to produce knockout lines alongside the isogenic control line. Some researchers have used organoids as a starting point to produce a more complex model of the gut in vitro, with studies combining differentiating iHO with neural crest cells in culture, and transplanting this into murine kidney capsules, to form an intestinal model featuring epithelium, mesenchyme and neuroglial structures which showed some neuronal activity.[246]

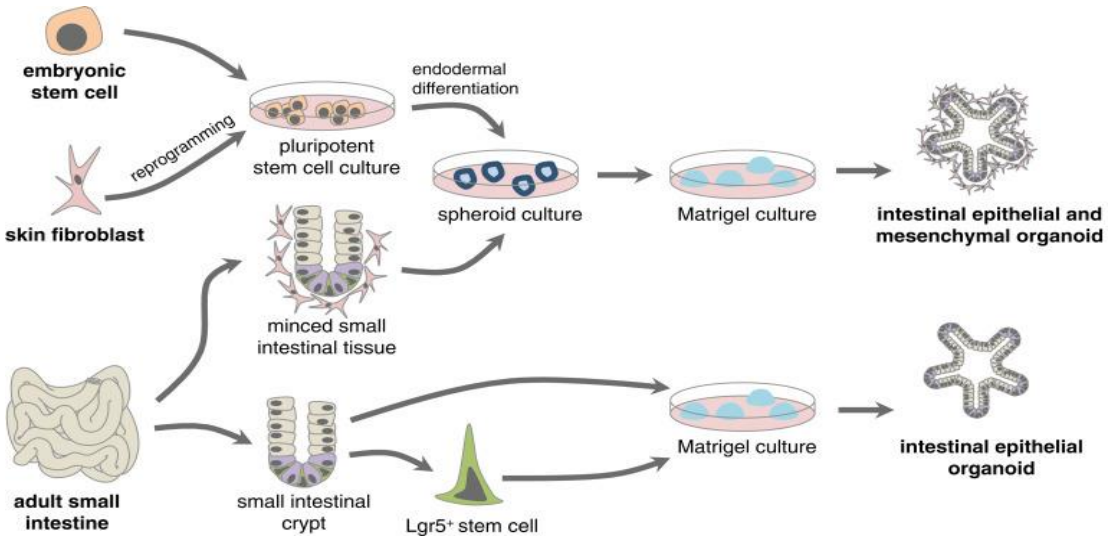

Figure 1.5: Sources of tissue for production of intestinal organoids. (Figure taken from Kretzschmar & Clevers, 2016[247])

Studies of *Salmonella* in human blood, rather than the intestine are rather simpler, given that there is the ability both to make human macrophage-like cells from easily available cell lines, such as THP-1, and the possibility to directly complete assays on blood or serum collected both from healthy volunteers and those who have been exposed to the infection. Nonetheless, hiPSC-derived macrophages are an important development in the study of disease pathogenesis. Not only do these cells phenotypically resemble human macrophages, they also show a more robust killing and cytokine production response versus their THP-1 derived counterparts.[248] In addition; as with the iHO, they can be produced either from iPSC from individuals with disease-causing mutations of interest, or CRISPR/Cas9 could be used to knockout genes of interest. It is possible therefore, to study the host response to *Salmonella* in two different compartments (epithelial and blood) if iHO and macrophages are differentiated from the same donor iPSC, as is the case in this project.

Lastly, the human challenge model, originally used to investigate *S*. Typhi in the 1950-60's,[97] has been revived by the Oxford Vaccine Group to investigate multiple facets of *S*. Typhi and *S*. Paratyphi A infection. Alongside detailed clinical information and blood cytokine, transcriptional and metabolic data, this model has contributed evidence for vaccine efficacy that assisted in the recommendation by Gavi for pre-qualification of the TCV vaccine.[100] This group has since developed a model for *S*. Paratyphi A challenge,[249] and studies are underway to help us discover more about this pathogen in its natural host. One thing that this model cannot offer however, is detailed data on the epithelial response to infection, as gathering these samples would be incredibly invasive and potentially dangerous. Stool samples provide some information by proxy but nothing at the level possible with direct epithelial studies using the iHO model.

1.4.2 Advantages of using the hiPSC-derived iHO model

hiPSC can be generated via reprogramming of cells from somatic tissues such as fibroblasts from skin biopsies, using Sendai vectors (protein factors *OCT4*, *KLF4*, *SOX2* and *MYC*).[250] These hiPSC are then forward programmed using a sequential cocktail of cytokines over 10 days to produce iHO, which are embedded into extracellular matrix and cultured until they reach maturity a few weeks later.[251] The processes for this and embryological rationale behind them will be discussed in more detail later in this chapter. An alternative source of

pluripotent cells, which can be differentiated in this way, are embryonic stem cells (ESC), however, these are much more difficult to obtain and given that their harvest requires the destruction of early embryos, there is ethical debate about use of these cell types. In fact, hiPSC and ESC have been shown to be very similar in gene expression and DNA methylation,[252] with a study looking at hiPSC derived from three different tissue types from individuals and ESCs, finding that inter-individual transcriptional variation in hiPSCs was greater both than variation from somatic tissue of origin or between ESC and hiPSC.[253] There was little evidence of epigenetic 'memory' of previous tissue type, and cell phenotypes within individuals were very reproducible (with three cell lines produced from each tissue). This study suggested that hiPSC should be taken from numerous individuals for experiments, rather than an increasing number of cell lines taken from one individual for replicates, and that hiPSC are a robust and powerful platform for large-scale studies of genetic differences between individuals. Ease of access to numerous cell lines is certainly one advantage that iHO derived from hiSPC have over primary iHO.

Generation of primary iHO from intestinal biopsies containing crypts, requires the availability of donor tissue, usually taken from an individual undergoing investigation for a condition such as inflammatory bowel disease. Biopsies from those who do not have disease are treated as being from 'healthy' samples, however this must be treated with caution if the individual was displaying gastrointestinal symptoms severe enough to warrant a biopsy. Primary iHO are more rapid to manufacture than hiPSC derived iHO, as following isolation and embedding of crypts, LGR5+ cells rapidly divide and reproduce the organoid structure within a matter of days. However, primary cultures require a number of additional growth factors and Wnt conditioned medium, which is tricky to produce consistently. In addition, a number of these growth factors are removed from the culture medium to induce terminal differentiation prior to experimentation, whereas growth conditions for hiPSC-derived iHO remain consistent.[242] Primary iHO are smaller than hiPSC-derived iHO, with their lumen being much more difficult to access via microinjection technology. Response to *Salmonella* infection and rhIL-22 stimulation was demonstrated to be consistent between primary and hiPSC-derived iHO during this project,[254] reinforcing the decision to investigate host-pathogen interactions for *Salmonella* using the hiPSC-derived iHO model.

Finally, it is possible to investigate genetic mutations of interest in primary iHO, using samples from patients with a disease / mutation of interest. In order to have a control line to compare the diseased line to, one could use transcription activator-like effector nucleases (TALENs) or CRISPR/Cas9 to target and repair the mutation in order to restore function and produce a complemented line. This requires time and precision, and could mean that each mutation of interest would be studied in a line with a different genetic background. An efficient way of studying SNPs of interest would be to use CRISPR/Cas9 with single-stranded donor oligonucleotides[255] to induce mutations in hiPSC, then use the original hiPSC line as an isogenic control. Advantages of this would include being able to produce multiple different mutants in the same genetic background, meaning that the control line used would be well characterised, and optimisation of experimental design would not be required every time a new mutant line is produced. It may also be the case that a particular mutation affects more than one target organ. hiPSC derived organoids could be produced for a number of different tissues in order to investigate effects of disease in different compartments, both in organs, and in blood cells such as macrophages, perhaps even simultaneously if it were possible to produce monolayers from iHO and culture them with macrophages from the same iPSC line for infection assays. The beginnings of this type of assay have been trialled by one author with enteroids and PBMCs,[256] and another with murine organoids and intraepithelial lymphocytes.[257] This plasticity of hiSPCs and their ability to differentiate into numerous tissues is one of their advantages as a model for investigating host-pathogen interactions.

1.5 Host defences against enteric pathogens

1.5.1 The role of the intestinal epithelium in defence against enteric pathogens

This chapter has discussed the specific host response to *Salmonella*, but this is better understood by looking at the general role of the intestinal epithelium in defence against enteric pathogens. *In vivo,* intestinal epithelial cells (IECs) play a key role in regulating homeostasis between the epithelial barrier, overlying microbiota and the gastrointestinal immune system. If this homeostasis and the continuity of the epithelium is threatened by attack from a pathogen, the innate immune system rapidly activates; initially with a

generalised response, prior to a slightly more delayed pathogen-specific adaptive immune response.[258] Prior to reaching the epithelial barrier, potential pathogens have to deal with competition for nutrients with the microbiota, or even avoid products which may inhibit pathogen growth, such as bactericidal organic acids produced by *lactobacilli* and *bifidobacteria* which suppress growth of *S*. Typhimurium in vitro.[259]

Secondly, pathogens have to breach the intestinal mucus layer, largely composed of mucin 2. The mucin layer consists of a thinner outer layer which contains components of the microbiota, and a dense inner layer which normally does not contain bacteria, functioning to prevent microbiotal translocation and excessive immune activation.[260] Goblet cells are epithelial cells which produce the mucins making up the mucus layer and also produce trefoil factors, which can increase the viscosity of mucus to increase protection from pathogens. Additionally, trefoil factors enhance mucosal restitution and prevent apoptosis, aiding epithelial repair after damage.[261] Many pathogens have had to acquire virulence-associated factors to overcome this mucus barrier, such as production of flagella and chemotaxis in *S*. Typhimurium and secretion of proteases by Enteropathogenic *Escherichia Coli* (EPEC) once they have adhered to the mucus layer.[262] Goblet cells increase mucus production after stimulation by pathogens, which can expel some pathogens from the lumen, but unfortunately others, such as *Salmonella* can colonise the mucus layer and take advantage of the nutrients and carbohydrates contained within it.[263]

The epithelial layer itself is composed of a number of different cell types, each of which has a role to play in the defence against enteric pathogens. These include enterocytes, M cells, Paneth cells, enteroendocrine cells and goblet cells; the role of which has been outlined above. Enterocytes act as a barrier by forming tight junctions, composed of claudins and zonula occluden proteins, preventing microbes translocating between cells into the lamina propria. Attaching and effacing pathogens (e.g. EPEC) work by inducing tight junction alteration to disrupt the epithelium. Tight junction proteins are partly regulated by cytokines; inflammatory cytokines such as IFNγ and TNFα downregulate junctional proteins.[264] Enterocytes are also able to secrete a number of cytokines and antimicrobial peptides, playing a vital role in the immune response, as illustrated in **Figure 1.6**.

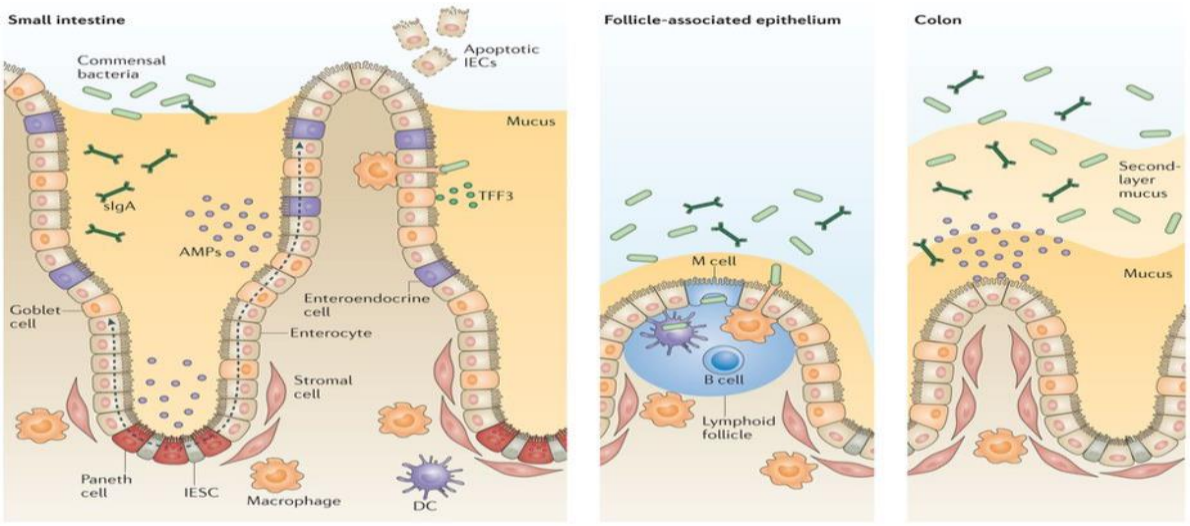

Figure 1.6: Schematic of intestinal epithelial defence mechanisms. The different epithelial cell types and their secretory products are demonstrated here. Paneth cells remain in the crypt, but all other cell types migrate up towards the tip of the villi after production by intestinal epithelial stem cells (IESCs), as shown by dashed arrows. Antimicrobial peptides (AMPs) are secreted by Paneth cells and enterocytes, with mucus and trefoil factor 3 (TFF3) secreted by goblet cells. Secretory IgA (SIgA) is produced by plasma cells in the lamina propria and transcytoses to the lumen. M cells mediate transport of antigens and bacteria across the epithelium to DCs and macrophages. DCs are also able to sample the luminal contents by sending dendrites through epithelial tight junctions. (Figure taken from Peterson & Artis, 2014).[265]

M cells are a part of the follicle-associated epithelium which is located over Peyer's patches. These cells sample and transport pathogens from the lumen to the underlying immune cells, in order for bacteria to be recognised by their antigens and adaptive immune responses initiated.[266] M cells do not have microvilli as do enterocytes, instead having a 'microfold' appearance from whence they get their name. They also largely lack a mucus layer, allowing them to detect antigens and engulf pathogens. On their basolateral surface, M cells have specific invaginations which work as docking sites for DCs, T cells, B cells and macrophages.[267] Whilst M cells are able to initiate the adaptive immune response, they can also be exploited by enteric pathogens, such as *S*. Typhi, *S*. Typhimurium, *Vibrio cholerae* and *Shigella flexneri*, as a method of direct transcytosis into the lamina propria.[268]

Paneth cells are located in the crypts of the small intestine, adjacent to epithelial stem cells. They produce and secrete antimicrobial peptides in response to myeloid differentiation factor (MyD88)-dependent TLR activation on sensing bacteria.[269] These AMPs include α- and β-defensins, which target bacterial membranes that do not contain cholesterol, producing transient pores in these membranes to disrupt their integrity. Defensins also have a chemoattractant property for DCs and T cells. Other compounds secreted by Paneth cells

include lysozyme and phospholipase A2 (sPLA2), which target bacterial cell walls. Paneth cells can also be induced to secrete C-type lectins (RegIIIβ/RegIIIγ), cathelicidins and angiogenin4 after detection of PAMPs.[108] Epithelial cells can also secrete RegIIIγ, calprotectin, β-defensins and RELM-b when PAMP detection occurs.

Lastly, enteroendocrine cells secrete numerous hormones with roles in gastrointestinal motility and digestion. These include: cholecystokinin (gall bladder contraction), somatostatin (an inhibitory hormone for digestive endocrine and exocrine function), glucagon-like peptide 1 (satiety) and serotonin (intestinal motility, secretion and appetite). These cells do not have any direct antimicrobial action, but hormones such as glicentin and glucagon-like peptide 2 promote mucosal enterocyte proliferation, which may be important for repair after pathogen-mediated damage to the epithelial barrier.[270]

Plasma cells in the lamina propria are able to produce secretory IgA (sIgA),[265] which can be antigen specific or non-specific, and is transcytosed across enterocytes to the intestinal lumen. Here, it can bind to surface isotopes on the surface of pathogens to prevent them binding to epithelial cells.[271] In addition, sIgA can cause pathogens to agglutinate in the lumen by binding to antigens on bacterial and viral surfaces.[272] Specific sIgA can be produced as part of the adaptive immune response and has been shown to protect against *Salmonella* infection in mice,[273] alongside reducing bacterial ability to deal with oxidative bursts.[274]

The epithelium also contains a number of pattern recognition receptors (PRRs) which are able to detect PAMPs; for example, LPS or endotoxins expressed by potential invasive pathogens, and are able to activate the innate immune response to try and control this threat. PRRs include Toll-like receptors (TLRs) which are located on the cell surface or inside of lysosomes and endosomes. There are numerous TLRs, but the ones pertinent to the gut are: TLRs 2, 3, 4, 5 and 9. After recognising a pathogen, TLRs recruit adaptor molecules which contain MyD88 and Toll-interleukin 1 receptor to the cytoplasm, initiating transcription of pro-inflammatory genes via activation of NFκB and MAPK.[258] TLRs can also

be triggered by danger-associated molecular patterns (DAMPs) or alarmins, which are released by the host cell in response to tissue injury, stress and necrotic cell death.[108] Other PRRs; nucleotide oligomerization domain (NOD)-like receptors (NLRs) in the cytoplasm detect intracellular microbial molecules. NOD1 and NOD2 are the best studied of this family and are noted to recognise components of peptidoglycans and in response, activate NFκB and induce IL-12 secretion. NLRs are also involved in inflammasome assembly; with the inflammasome composed of pro-caspase-1, an NLR protein and an adaptor molecule such as ASC. The inflammasome induces maturation of pro-caspase-1 into caspase-1 which activates IL-1β and IL-18; cytokines involved in the inflammatory response to infection.[275]

C-type lectins are PRRs which recognise specific carbohydrate structures on pathogen surfaces, and are largely found on macrophages and DCs. An example of one of these proteins would be mannose-binding lectin (MBL), which is able to bind to bacteria, viruses, fungi and protozoa. On binding, MBL changes shape and triggers phagocytosis of the pathogen by immune cells and activation of complement. Lastly, retinoic acid-inducible gene-1 (RIG-1) like receptors (RLRs) are involved in the response to viral pathogens, detecting double stranded RNA in the cytoplasm and inducing IFNα, IFNβ and inflammatory cytokines via activation of NFκB, MAPK and interferon regulatory factors.[276]

IEC have a number of other defence mechanisms to guard against infection, such as the expression of intestinal alkaline phosphatase (IAP) in their apical brush border. IAP removes the phosphate group from LPS, limiting its ability to activate TLR4, and preventing translocation of LPS into the systemic circulation, where it can induce inflammatory cytokine driven septic shock.[277] IEC are also able to produce reactive oxygen species (via expression of Nox and Duox proteins),[114] which have microbicidal effects and help epithelial repair.[278] Autophagy is also a defensive response, aimed at preventing further spread of intracellular bacteria. This process both degrades cellular cytoplasmic contents, but also recognises and degrades intracellular pathogens. Autophagy is mediated by MyD88, in conjunction with the proteins LC3, ATG16L and ATG5 and is activated under cellular stress conditions. *S*. Typhimurium is capable of inducing autophagy in the intestinal epithelium.[279] With increased apoptosis, there is also the need for replacement of apoptosed IEC, requiring an increase in

proliferation by the intestinal stem cells. One pathway which regulates this proliferation is the β-catenin pathway, which can be suppressed by LPS and other bacterial elements.[280] Clearly the intestinal epithelium has many complex regulatory and defence mechanisms that act to maintain homeostasis in both health and disease states. Important to consider also are the mechanisms of pathogen defence which happen once the pathogen has entered the cell.

1.5.2 Phagolysosomal fusion as a mechanism of pathogen destruction

1.5.2.1 Formation of the phagolysosome

Following phagocytosis and entry of the pathogen into the cell, the phagosome undergoes a process of maturation in order to form the microbicidal phagolysosome. Debate has occurred over the mechanism by which lysosomes transfer their contents to the endosomes involved in the maturation process, but imaging studies have shown that this occurs both via lysosomes repeatedly and transiently fusing with endosomes as well as incidents of complete fusion, following which the lysosome reforms from the membrane of the hybrid vesicle.[281] There are three reported stages of phagosome maturation: early, late and phagolysosome, each with different membrane proteins associated.
The early phagosome is defined by the presence of the GTPase Rab5, which regulates fusion events between the phagosome and early endosomes via the membrane recruitment of EEA1 (early endosome antigen 1).[282] Rab 5 is also able to recruit hvPS34 (human vacuolar protein-sorting 34), which is a class III phosphoinositide 3-kinase. This molecule generates phosphatidylinositol 3-phophate, which then recruits other phagosomal maturation proteins such as Rab7, a late endosomal marker.[283] Vacuolar ATPase (V-ATPase) accumulates on the phagosomal membrane and translocates H^+ ions into the phagosome, causing the pH inside the phagosome to acidify (pH 6.1-6.5).[284]

Eventually, Rab5 is lost and replaced by Rab7 on the phagosome membrane. This mediates fusion of the phagosome with late endosomes.[285] Recycling vesicles are formed, which remove proteins to be recycled from the phagosome. Meanwhile, intraluminal vesicles (ILVs) containing proteins for degradation are sent into the lumen of the late phagosome. Accumulation and action of further V-ATPase molecules means that the intraphagosomal pH

drops further (pH 5.5-6.0).[286] Rab7 recruits Rab-interacting lysosomal protein (RILP), which facilitates contact between the phagosome and microtubule and lysosomes. Lysosomal-associated membrane proteins (LAMPs) and proteases such as cathepsins and hydrolases are introduced into the phagosome after fusion with late endosomes. LAMPS regulate membrane fusions and are necessary for phagolysosomal fusion.[287]

Finally, phagolysosomal fusion occurs, producing a very hostile environment for any microbe within the phagolysosome. The pH for the phagolysosome is between 5.0-5.5 following further V-ATPase action,[284] and enzymes such as cathepsins, proteases, lysozymes and lipases are contained within. In addition, NADPH oxidase and other reactive oxygen species are present on the phagolysosomal membrane, and restriction of nutrients such as iron occurs via action of molecules like lactoferrin.[287] **Figure 1.7** demonstrates the phagosomal maturation process.

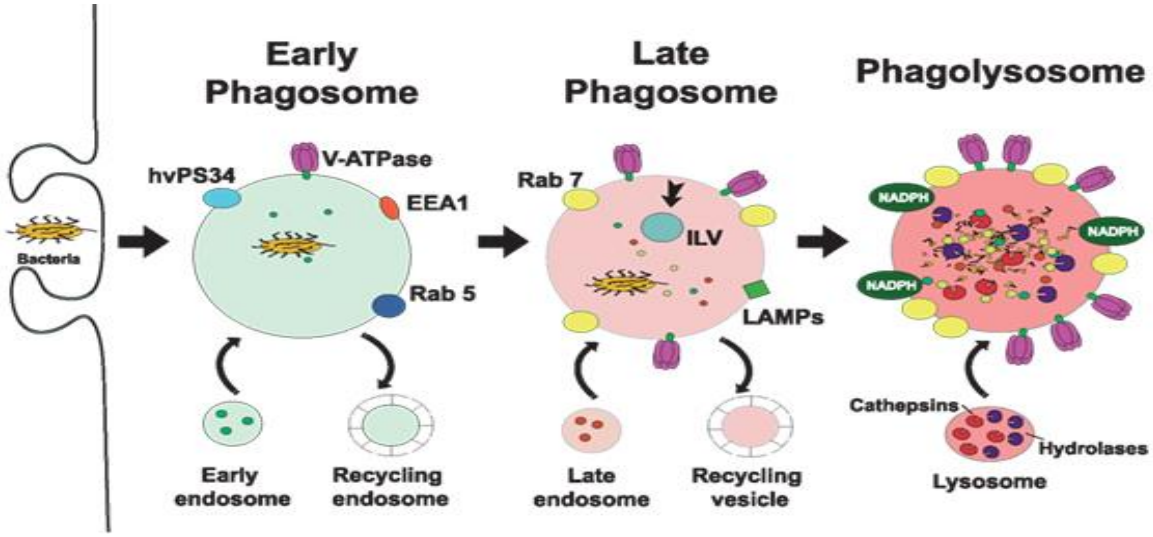

Figure 1.7: Markers involved in phagosomal maturation and phagolysosomal fusion. Presence of Rab5, hvPS34, EEA1 and accumulation of V-ATPase, alongside fusion events with early endosomes mark the early phagosomal stage. This is followed by expression of Rab7, LAMPS, further V-ATPase, fusion with late endosomes and the presence of recycling and intraluminal vesicles (ILVs). Highly acidic phagolysosomes form after fusion of late phagosomes with lysosomes. Enzymes and reactive oxygen species degrade the intraphagosomal pathogen. (Figure taken from Uribe-Querol & Rosales, 2017[287])

1.5.2.2 Avoidance of phagolysosomal fusion

Given the incredibly harsh environment produced inside of the phagolysosome, many intracellular bacteria use inhibition of phagolysosomal fusion as a survival strategy, such as

Mycobacterium tuberculosis, *Brucella* spp., *Legionella pneumophilia*, *Salmonella* and *Listeria monocytogenes*. Some pathogens, such as *Coxiella burnetii* have simply evolved to withstand the low pH inside of the phagolysosome.[288] Others are able to manipulate actions of the Rab GTPases to arrest phagosomal maturation at different stages; for example, *Mycobacteria*-containing phagosomes acquire Rab5a, but maintain their phagosomal compartment at the early endosomal stage, by blocking acquisition of Rab7. In addition, *M*. *tuberculosis* are able to reduce accumulation of vacuolar ATPase, meaning that the phagosome does not fully acidify. Treatment of macrophages with IFNγ restores these processes, allowing phagolysosomal fusion and killing of mycobacterium within the phagolysosome to occur.[289] The mechanisms by which phagolysosomal fusion is inhibited by *M*. *tuberculosis* are not fully established, but interestingly, IL-22 has been found to increase S100A8 and Rab7 expression in *Mycobacterium*-infected macrophages, leading to enhanced phagolysosomal fusion, suggesting that further investigation of the relationship between these effectors may hold clues as to what *Mycobacteria* are inactivating to reduce phagolysosomal fusion *in vivo.*[290]

Studies on *E. coli* K1, which is able to translocate the blood brain barrier after invasion of human brain microvascular endothelial cells (HBMEC) demonstrated that *E. coli*-containing vacuoles (ECV) acquire early endosomal markers in the form of EEA1 and transferrin receptor, along with the late endosomal/lysosomal markers Rab7 and Lamp-1, yet do not undergo phagolysosomal fusion; measured by the lack of cathepsin D, a lysosomal enzyme, and intravacuolar survival of bacteria. An isogenic mutant without the capsule was unable to arrest phagolysosomal fusion and was degraded within the vacuole. The mechanism of action is not yet understood, but it appears that the K1 capsule is somehow able to influence ECV trafficking, in order to avoid phagolysosomal fusion.[291]

Early endosomal markers EEA1 and Rab5a are acquired by phagosomes engulfing *Listeria*, *Legionella* and *Brucella*, but these pathogens have alternative escape mechanisms to avoid phagolysosomal fusion. *Brucella* and *Legionella* enter compartments composed of endoplasmic reticulum membranes, which resemble autophagosomes, in order to evade acquisition of further markers,[289] whereas vacuoles containing *Listeria* acquire late

endosomal markers, but the bacterium then perforates the late endosomal membrane and escapes into the cytosol to replicate therein.[292]

Formation and maturation of the *Salmonella*-containing vacuole (SCV) are discussed in more detail earlier in this chapter, but worth highlighting is the fact that *Salmonella* appear to have cultivated a number of strategies to either avoid phagolysosomal fusion or modify their phagosomal environment to allow improved survival and replication. One study which aimed to investigate methods of phagolysosomal fusion avoidance by *Salmonella* noted that SCVs divide along with *Salmonella*, resulting in many cases in one bacterium per SCV and thus an increased SCV load within the cell, overloading the capabilities of the cell to produce sufficient lysosomes to acidify and deliver enzymes to all of the SCVs.[293] *S*. Typhimurium was found to actively inhibit phagolysosomal fusion in murine macrophages and preferentially divided inside of unfused phagosomes.[294] The exact mechanism by which inhibition occurs is not defined, but one factor which some hosts have to overcome it is the expression of Nramp1. Nramp1 is expressed in lysosomal compartments within macrophages and facilitates killing of intracellular bacteria by increasing phagosomal fusion with lysosomal membrane proteins such as mannose 6-phosphate,[295] and withholding Fe^{2+} and Mg^{2+} from intraphagosomal bacteria.[130]

Similarly to findings with *E. coli*, *S*. Typhimurium within SCVs in HeLa cells acquire EEA1, transferrin receptor, Rab5, Rab7 and Lamp-1 but do not obtain cathepsin D or fuse with lysosomes.[296] This was thought to be due in *Salmonella* to the actions of the SpiC protein, an effector of the SPI-2 T3SS being exported into the cytosol, inhibiting interactions between SCVs and lysosomes, and disrupting vesicular transport, with a SpiC mutant derivative unable to prevent phagolysosomal fusion.[127] Additionally, SifA, an effector protein which is injected into host cells by the SPI-2 T3SS, is required for maintenance of SCV integrity and formation of Sifs in epithelial cells.[297] PipB2 is also thought to prevent vacuolar lysis.[82] The mechanism of action *SifA* is unknown; but thought to be via control of Rab7-dependent recruitment of additional endosomal membranes to the SCV during replication.[298] Lastly, *Salmonella* use determinants such as the PhoPQ regulatory system, which is activated by low pH change to modify intraphagosomal pH and create an optimal environment for replication.[31]

There are many questions still around the mechanisms both driving phagolysosomal fusion and its modification by intracellular pathogens. It would appear that there are numerous effectors exploited by different pathogens alongside multiple methods of avoidance of phagolysosomal fusion, either by breaking out of the vacuole, adapting to life within the phagolysosome or modifying the contents of the phagosome and its maturation to produce a more satisfactory intravacuolar environment. Further detailed study of intracellular bacteria in models such as the iHO model should help to elucidate some of these mechanisms.

1.5.3 The Interleukin-22 (IL-22) pathway

1.5.3.1 Components of the IL-22 pathway and its mechanism of action on the intestinal epithelium

IECs are able both to produce and respond to cytokines as part of their role in maintaining epithelial homeostasis. The cytokine IL-22 is also known to have a role in maintenance of the gut epithelial barrier,[299] is involved in the induction and secretion of antimicrobial peptides and chemokines,[300] epithelial cell proliferation and maintenance of tight junctions[301] in response to infection. It is a part of the IL-10 family of cytokines, made up of: IL-10, IL-19, IL-20, IL-22, IL-24 and IL-26, all of which have differing roles in inflammation and immunity.[302] All but IL-26 have a homolog in mice, meaning that a number of these cytokines are well characterised in part due to murine studies. Common to all of these cytokines is that they require a 2-part receptor complex, with one element of this complex being shared in a number of cases; for example, IL-10R2 (or IL-10Rβ) is a part of the complex for IL-10, IL-22 and IL-26 (**Figure 1.8**). IL-10R2 is fairly ubiquitously expressed across cell types. The other part of the receptor complex for IL-22, is IL-22R1, which is expressed only on epithelial cells lining barrier sites, such as the skin, intestine, liver, lung, kidney and pancreas.[303] IL-22 receptor complexes are located on the basal surface of the polarised intestinal epithelium. Mutations in IL-10R2 can lead to lack of sensitivity to IL-22 and are associated with early-onset inflammatory bowel disease.[304] Functional IL-22 and IL-22R1 protect against dissemination of bacterial infection following *Citrobacter rodentium* infection or DSS-induced colitis in mice.[305,306]

The IL-10 cytokine family are secreted by a number of different cell types, as shown in **Figure 1.8,** with IL-22 being produced by activated T cells, more specifically CD4+ Th17 cells and NK cells and acting on non-haematopoietic cells. More recently, IL-22 has also been discovered to be produced by innate lymphoid cell 3 (ILC3) cells, located in Peyers patches and GALT.[307] Similarly, the other cytokines in the IL-10 family act predominantly on non-haematopoietic cells, with only IL-10 (and possibly IL-19) thought to be able to exert their effects on haematopoietic cells.

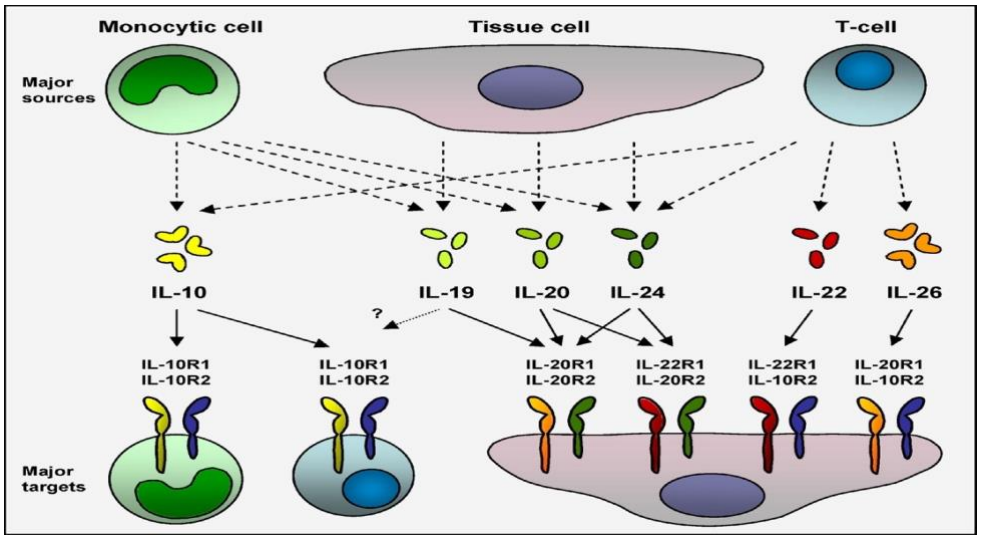

Figure 1.8: Receptor complexes and cells secreting / responding to IL-10 family cytokines. (Figure taken from Sabat, 2010)[302]

IL-22 enhances innate immune response in the intestinal epithelium, as it acts to increase chemokine expression, induce mucus secretion by goblet cells, increase epithelial cell proliferation and induce production of AMPs including RegIIIβ and RegIIIγ,[308] defensins and S100 proteins.[309] It is also able to induce secretion of acute phase reactants in response to liver injury. IL-22 also mediates intestinal epithelial fucosylation, which reduces expression of bacterial virulence genes.[310]

As well as its dimeric receptor complex, a soluble secreted version of the IL-22 receptor exists, IL-22 binding protein (IL-22BP). This is an inhibitory regulator of IL-22, and is highly expressed by DCs in the intestine. It is thought to be involved in maintenance of epithelial homeostasis by ensuring IL-22-induced inflammatory responses are not disproportionate to what is required, as can be seen in diseases associated with increased IL-22 production, such as

Crohn's disease, rheumatoid arthritis, psoriasis and interstitial lung disease.[311] Levels of IL-22 or its transcripts have been shown to correlate with the severity of disease in a number of the above conditions.[302] In addition, these are all T cell mediated diseases, which fits with the preferential production of IL-22 by T cells. IL-22BP appears to act only in response to a sustained increase in IL-22 levels, as the NLRP3 and 6 inflammasomes initially downregulate IL-22BP following acute intestinal epithelial damage[312]

Signalling induced by the binding of IL-22 to its receptor complex largely occurs via the JAK/STAT pathway. IL-22R1 is associated with JAK kinase 1 (JAK1) and IL-10R2 with tyrosine kinase 2 (Tyk2) in particular. JAK kinases phosphorylate tyrosines, and a STAT transcription factor binds to this complex and becomes phosphorylated. STAT molecules exist as dimers in the cytoplasm and change their structure following activation by JAK kinases. STAT3 is the molecule activated most ubiquitously by IL-10 family members, but STAT1 and STAT5 can also be phosphorylated at high IL-22 concentrations. (**Figure 1.9**) Phosphorylated STAT3 migrates into the cell nucleus and binds to promoters, upregulating transcription of certain genes such as suppressor of cytokine signalling (SOCS)3. SOCS3 binds to JAK molecules, inhibiting their activity and completing the feedback loop.[302] Alongside JAK/STAT activation, IL-22 has also been shown to induce phosphorylation and activation of the three major MAP kinase pathways of NFκB via MAPK1/MAPK3, JNK and p38 kinase [313]

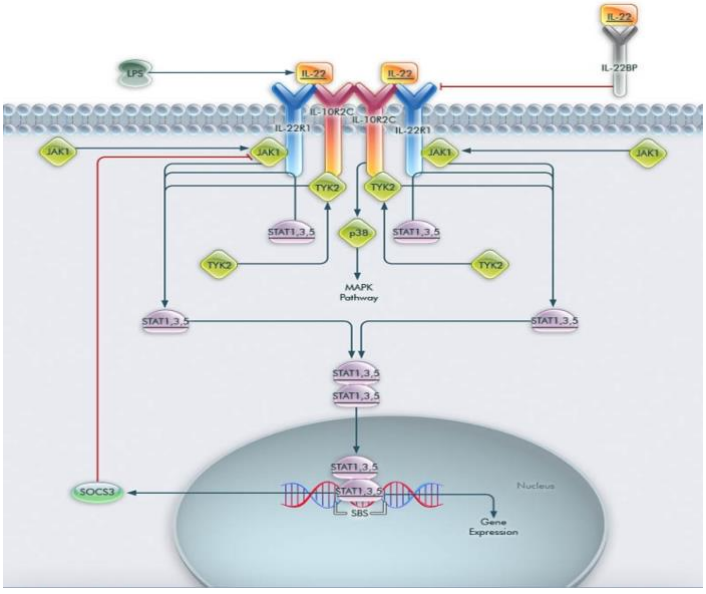

Figure 1.9: Intracellular mechanisms of IL-22 signalling. (Image taken from https://www.thermofisher.com/uk/en/home/life-science/antibodies/antibodies-learning-center/antibodies-resource-library/cell-signaling-pathways/il-22-pathway.html)

1.5.3.2 Sources of IL-22

IL-22 is produced by CD4+ T_H cells (predominantly Th17 cells) in response to IL-6 and TNFα during infection or inflammation. IL-23 is also an important inducer of IL-22 production, enhancing its expression in maturing Th17 cells.[314] This increase in IL-22 expression leads to increased expression of the IL-23 receptor also, and thus increased interactions between IL-23 and its receptor, further increasing IL-22 production. IL-23 itself is produced by DCs and macrophages in response to pathogen invasion of the epithelium. Aryl hydrocarbon receptor (AhR) is activated by cellular stress and Ca^{2+} influx and can induce IL-22 either via direct regulation of IL-22 transcription, or via regulating production and development of Th17 cells and Type 3 innate lymphoid cells (ILC3s). Lastly, IL-1β, which can be produced by macrophages, DCs, neutrophils, T and B cells and epithelial cells, is able to activate NK cells, ILC3s and Th17 cells to produce IL-22 and also promotes NK cell expansion. IL-22 secretion is inhibited by the actions of TGFβ, which is required for Th17 differentiation and is able to influence IL-23R expression in a number of tissues.[315] Sources and actions of IL-22 are illustrated in **Figure 1.10**.

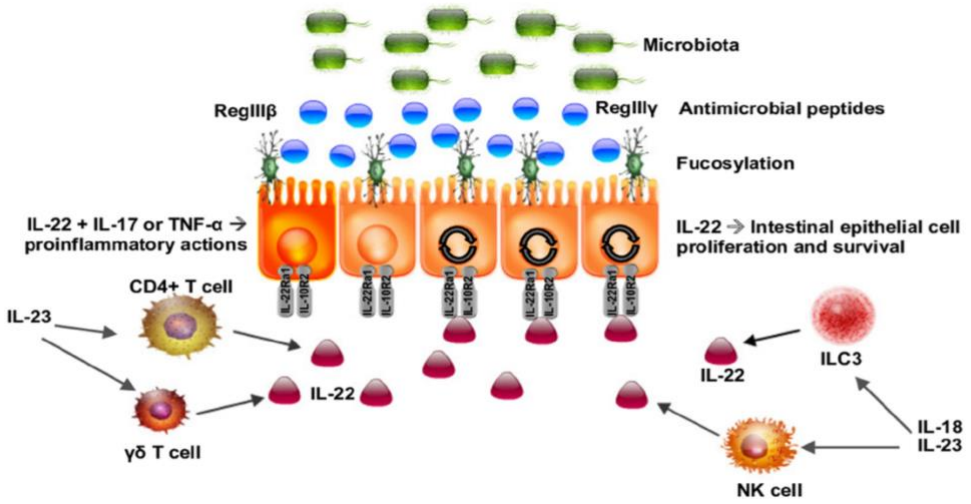

Figure 1.10: Interactions of IL-22 with the intestinal epithelium and immune system. IL-22 is produced by NK cells, T cells and ILC3s. Its actions include fucosylation of epithelial cells, increased mucus production, increased cellular proliferation and AMP release in order to maintain the epithelial barrier. Alongside IL-17 and TNFα, IL-22 can promote a pro-inflammatory response to pathogen invasion. (Figure taken from Parks et al, 2016[309])

The role of IL-22 in pathogen defence is under investigation. Murine intestinal organoids stimulated with IL-22 showed an inflammatory response to pathogens, improved antimicrobial defences and wound healing.[305] IL-22 has been shown to enhance murine survival after exposure to the attaching/effacing organism *C. rodentium* (a murine paralog of EHEC/EPEC),[306] *Klebsiella pneumoniae*[316], *S*. Enteritidis[317], *Candida albicans*[318] and increase the relative growth inhibition of *M. tuberculosis* in human cells.[319]

1.6 hiPSC-derived systems for recapitulating host response to pathogens in vitro

1.6.1 Production of hiPSCs

The simultaneous discovery in 2007 by Takahashi *et al.* and Yu *et al*. that somatic cells could be reprogrammed into a pluripotent state using 4 reprogramming factors (OCT3/4, SOX2, Klf4, c-Myc and OCT4, SOX2, NANOG, LIN28 respectively) brought about an explosion of interest in the possibilities of making patient and disease-specific stem cells and tissues.[320,298] Since that time, alternative means of delivery of these reprogramming factors have been developed, as original methods required retroviral vectors to deliver the factors into cells. Genomic instability and increased risk of tumourgenicity was a problem, as viral vectors integrated permanently into the cellular DNA; especially concerning in the case of c-Myc, which is a potent oncogene.[321] Reprogramming methods have now developed to use either non-viral methods (RNA based delivery or DNA plasmid delivery[322]), or non-integrating viruses such as Adenovirus or Sendai virus.[323] Sendai virus is one of the more widely used methods, as it has proven efficient in a number of different cell types, produces large quantities of protein and following around 10 passages of reprogrammed cells, no trace of viral RNA is detectable in cells. This method is favoured by the HipSci consortium (http://www.hipsci.org) who have produced a large and well-phenotyped bank of hiPSC from both healthy and diseased individuals. The workflow for reprogramming of cells using Sendai virus is depicted in **Figure 1.11**.

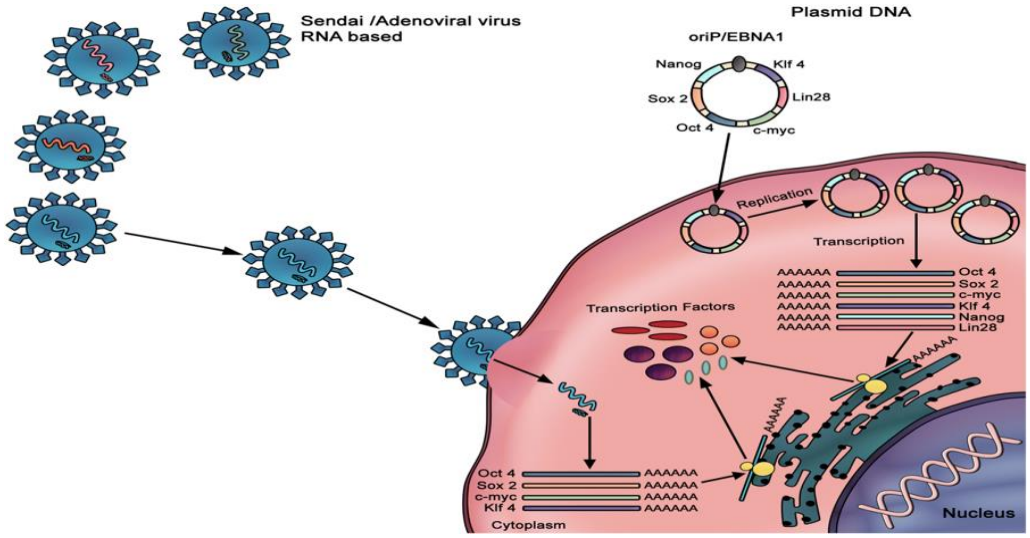

Figure 1.11: Non-integrative methods of delivering reprogramming factors. For RNA-based methods, such as Sendai viral delivery, reprogramming factor mRNA is delivered into the cell without reverse transcriptase and is translated directly into proteins. For plasmid-based methods, DNA is delivered to the cells as a self-replicating plasmid, which does not integrate into the host cell genome. The plasmid is transcribed to RNA and protein produced. (Figure taken from Abou-Saleh et al, 2018[322])

hiPSC have become a popular progenitor cell for the generation of different tissues, as they are easily obtainable, self-renewing and can be genetically manipulated with relative ease, given the recent advent of the CRISPR/Cas9 system. Briefly, this method works via adaptation of a genome editing system that occurs in bacteria. Bacteria capture DNA fragments from invading viruses and create clustered regularly interspaced short palindromic repeats (CRISPR) arrays; storing the viral DNA to allow future recognition of the same or similar pathogens by the bacteria. If this occurs, the relevant CRISPR RNA segment is used to target viral DNA; bacteria attach this RNA to a Cas9 enzyme, which is able to cut the viral DNA at the targeted site, disabling the pathogen. To use this technology for human genome editing, a short guide RNA is produced that targets the DNA sequence of interest. This is attached to a Cas9 enzyme, and the resulting molecule is able to cut the host cell DNA at the targeted region. DNA repair by the cell then takes place either via non-homologous end joining or homology directed repair, either inducing deletions in the targeted gene/sequence, or allowing the researcher to provide a template for DNA repair and make a modification to the existing DNA sequence; by repairing a mutation, for example.[324]

In this way, hiPSC could be produced from patients with disease and repaired to see if cellular functions are restored. Similarly, genes of interest could be knocked out, providing both a mutant cell line and an isogenic control. Wider hiPSC applications currently in progress include high throughput drug screening to reduce need for clinical trials, personalised drug

screening and production of differentiated tissue structures for disease modelling.[325] These applications are discussed in more detail below. Even gene therapy or autologous tissue transplantation could be possibilities, with reports of a patient receiving hiPSC-derived retinal pigment epithelial cells demonstrating arrest of macular degeneration and improved vision and another patient with severe heart failure receiving a scaffold of ESC-derived cardiac progenitor cells and showing improvement in cardiac function post-transplant.[326]

It is possible to differentiate hiPSCs into an increasing number of different cell types or tissues, with protocols being based on studies of embryological development, in order to deduce the correct combination of signals to drive hiPSC to differentiate into the tissue type of choice. These signals can take the form of recombinant growth factors, synthetic small molecules, spontaneous differentiation (e.g. production of embryoid bodies) or co-culture with supporting cell lines.[327] The different cell and tissue types produced using directed differentiation for this study will also be discussed below.

1.6.2 Generation of macrophages from hiPSC

Alongside production of complicated organotypic tissues, cells of haematopoietic lineages such as macrophages can be derived from reprogrammed hiPSC. This has been a particular benefit given that previously, research into infections in which pathogens replicate within macrophages, such as HIV-1, *M. tuberculosis* and *Salmonella* have hit difficulties in producing sufficient and relevant macrophage models for use in studies. Use of blood monocyte-derived macrophages has been the experimental model of choice, however, large amounts of blood are required to obtain sufficient cells to work with. Genetic differences between donors, and the physiological state of the donor on each donation episode will produce variation within data, leading to large amounts of donors and multiple sampling episodes being required to produce representative data.[328] Additionally, terminally differentiated macrophages are not amenable to genetic manipulation, meaning that patient or disease-specific mutations cannot be studied in comparison to isogenic controls. Animal models also cannot completely recapitulate what would be seen in human studies. The other most frequently used representation of macrophages are produced by treatment of THP-1 cells (a monocyte-like immortalised cell line) with Phorbol 12-Myristate 13-acetate

(PMA), however this cell line is karyotypically abnormal and it is not possible to fully differentiate these cells into macrophages. It has been possible to isolate CD34+ haematopoietic stem cells from umbilical cord blood or bone marrow for differentiation and use in experiments. It is possible to genetically manipulate these cells, but they do not self-renew in the way that hiPSC and ESC do.[328] Therefore hiPSC-derived macrophages offer a promising high-throughput, replicable and genetically modifiable system for investigating host-pathogen interactions,[248] as well as having possible applications such as use in cancer therapies,[329,330] modelling of genetic diseases[331,332] and drug screening.[333,334]

Producing terminally differentiated macrophages from hiPSC or ESC requires them to undergo three different steps; firstly, spontaneous differentiation of cultured hiPSC into embryoid bodies (EBs) over 3-4 days. EBs are made up of an ectoderm, mesoderm and endodermal layer. Following this, EBs undergo directed differentiation into myeloid cells, via addition of myelogenic cytokines IL-3 and macrophage colony stimulating factor (M-CSF) to the growth media. This process takes 21 days and produces a population of non-adherent monocytes which can be harvested weekly thereafter from the supernatant around the embryoid bodies. Monocytes are plated and further treated with a higher concentration of M-CSF for 6-7 days to undergo differentiation into macrophages.[328] These matured macrophages have been shown to be comparable to blood monocyte-derived macrophages both phenotypically and in terms of functionality.[335] The process of hiPSC-derived macrophage production is outlined in **Figure 1.12**.

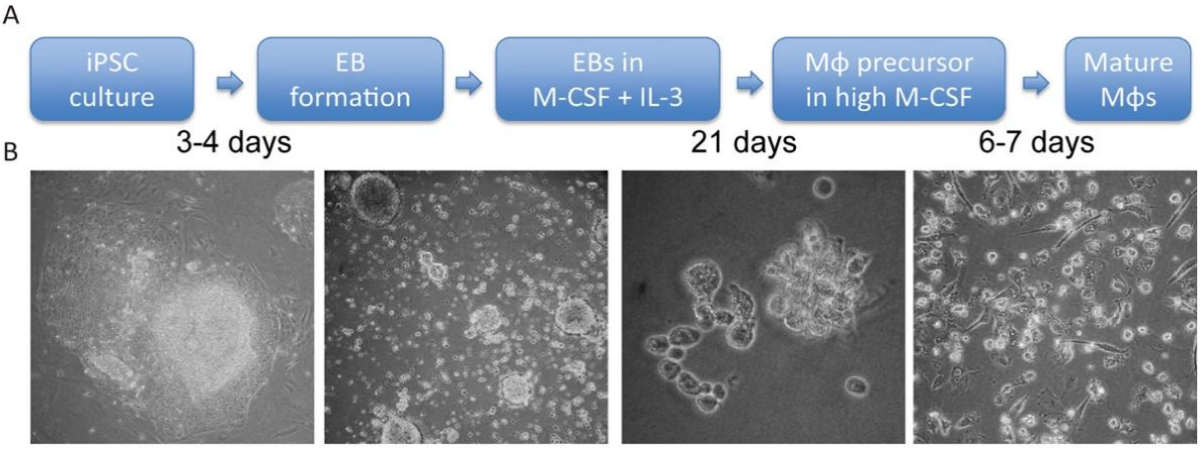

Figure 1.12: Differentiation of iPSC to macrophages. (**A**) Describes culture condition and length of time for each step and (**B**) shows phase contrast micrographs of (L-R): hiPSC, EB, monocytes and macrophages in culture. Mϕ = macrophages (Figure adapted from Hale et al, 2015[248])

1.6.3 Generation of intestinal organoids from hiPSC

One of the first tissue types to be derived from directed differentiation of hiPSCs was intestinal epithelium. This was a hugely exciting development, since as outlined earlier, previous models attempting to reproduce an organised, polarised intestinal epithelium consisting of differentiated cells had proven difficult, or required costly equipment, such as the rotating wall vessel. However, the ability to generate intestinal organoids (iHO) has offered a potential solution, with a consistent and reproducible method of generating self-renewing and expanding models of the intestinal epithelium *in vitro* for relatively long periods of time.[336] Each iHO is a discrete system, consisting of an epithelial monolayer, arranged around a luminal cavity. The monolayer is composed of cells from secretory and absorptive lineages, and these cells are arranged in the manner that they would be in the intestine, with mature organoids demonstrating a 'budded' structure, meaning that they have folds which represent the crypts and villi of the *in vivo* intestine. At the base of these crypts are intestinal stem cells (ISCs) which can be detected by their expression of LGR5, and are responsible for the self-renewing nature of the iHO.[241] iHO are able to expand, since new iHO can develop from each crypt domain when the iHO structure is broken up (**Figure 1.13**).

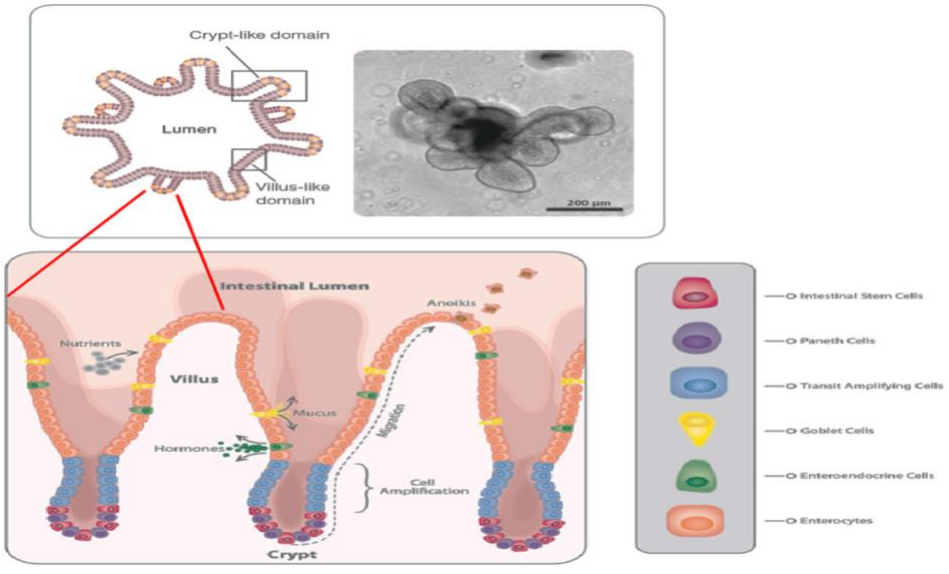

Figure 1.13: Architecture of the iHO and cell types within. iHO retain the crypt/villus structure seen in the intestinal epithelium *in vitro.* Within each crypt are contained: intestinal stem cells, Paneth cells, and after having undergone terminal differentiation, enterocytes, goblet cells and enteroendocrine cells migrate to the tips of villi and are exfoliated into the lumen. (Figures taken from: https://www.stemcell.com/intestinal-organoid-culture-lp.html, https://www.stemcell.com/technical-resources/area-of-interest/organoid-research/intestinal-research/overview.html)

Other cells found in the iHO crypts are Paneth cells, identifiable by their production of lysozyme. These Paneth cells are able to synthesise antimicrobial peptides and secrete them into the iHO lumen. Goblet cells are also present on the villi, detected by their expression of mucin 2. These cells secrete mucus into the lumen, which can be detected as a layer lining the organoid lumen via lectin staining. Enteroendocrine cells are also recapitulated in the iHO, recognisable by expression of chromogranin A and the secretory granules visible in their cytoplasm on TEM. Enterocytes make up the majority of the iHO monolayer, and are able to demonstrate polarisation of the iHO epithelium, with expression of villin on their apical brush border, projecting into the lumen. Having been produced in the crypts, terminally differentiated epithelial cells (with the exception of Paneth cells) migrate up the villous structures and slough off into the iHO lumen within 2-3 days.[336] This exfoliation and collection of cells in the lumen means that iHO have to be passaged via mechanical disruption every 5-7 days to prevent the lumen being filled with dead cells and subsequent death of the iHO. It is possible to passage iHO for long periods, but caution should be exercised with samples older than 6 months, as studies of reprogrammed hiPSC have showed some genetic deletions associated with tumour suppressor genes and duplications of oncogenes at late passage numbers (>12 months).[337]

The process of directed differentiation to produce iHO from hiPSC requires hiPSC to progress down the endodermal lineage to form definitive endoderm, which is then patterned into hindgut. These islands of hindgut are embedded into an extracellular matrix to provide a scaffold (such as Matrigel), that allows progression into iHO to occur.[244]

In order to produce definitive endoderm (DE), Nodal/TGFβ signalling is employed, in the form of Activin A, which is able to mimic the actions of Nodal.[244,338] Wnt signalling enhances endoderm production,[339] and PI3K, a signal transducer, inhibits it. PI3K inhibitors such as LY294002 are therefore used to maximise DE formation.[340] In addition, Wnt inhibitors such as GSK3β are suppressed by the use of CHIR99021.[341] DE can be recognised by elevated expression of the genes: *FOXA2, SOX17* and *CXCR4*. Once DE is produced, it is further differentiated by patterning into hindgut. Two different protocols exist, both leading to formation of islands of hindgut, recognised by expression of *CDX2.* One method uses Wnt3a + FGF[244] and another, (the method used in this study) CHIR99021 + retinoic acid (**Figure 1.14**).[338]

Islands of hindgut are embedded into a pro-intestinal culture system, such as Matrigel, which provides the structure of an extracellular membrane (ECM) to support iHO growth.[244] The presence of this ECM substitute is vital, as without attachment between the epithelium and basal membrane, isolated cells die due to a lack of integrin signalling. The islands of hindgut are overlaid with a growth medium containing supplements and growth factors which both support intestinal stem cell (ISC) development, and the differentiation and proliferation of the ISC into cells from the secretory and absorptive lineages.[245] Those growth factors include R-spondin 1, a Wnt agonist, required for ISC maintenance. Wnt production by Paneth cells following their differentiation is able to produce the budded structure of the iHO. Noggin; a BMP family antagonist and epidermal growth factor (EGF) are necessary in the culture medium to sustain cultures long term and promote iHO growth. Prostaglandin E2 activates the Wnt pathway, blocks anoikis and activates mitogenic signalling,[342] and ROCK inhibitor Y-27632 is added directly following passage to promote cell survival.[343]

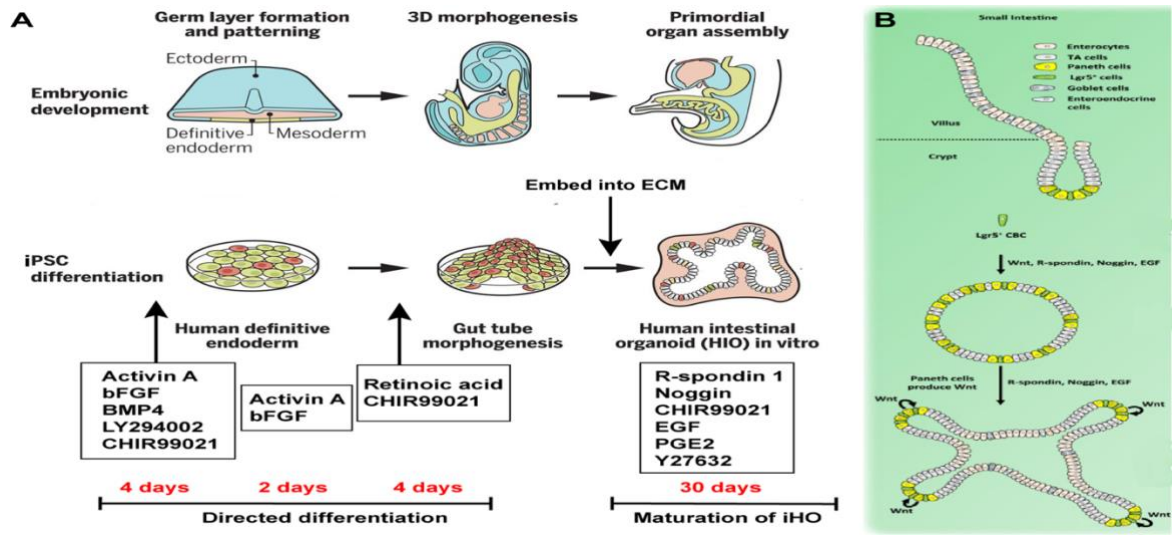

Figure 1.14: Differentiation of hiPSC to iHO. (**A**) Demonstrates growth factors required to drive differentiation from iPSC to definitive endoderm, hindgut and iHO formation/maturation after embedding into ECM (Matrigel). This mimics embryological development seen in the human foetus. (**B**) Demonstrates reformation, differentiation and budding of iHO following splitting, due to presence of LGR5+ ISC in crypts, and Wnt produced by Paneth cells alongside exogenous growth factors. (Figures adapted from: (**A**) Takebe & Wells, 2019[344], (**B**) Merker et al, 2016[345])

Initial investigations into transcriptomic profiles of hiPSC-derived iHO found them to have more similarities to foetal intestinal tissue than to adult intestinal tissue. Genes that are involved in development of the digestive tract were upregulated both in foetal intestinal tissue and iHO, compared to upregulation of genes related to Paneth cell action and digestive

function in adult tissue, and increased expression of *OLM4,* a marker of ISC maturity.[346] Interestingly, after transplantation into murine renal capsules, iHO were transcriptionally more mature and on microscopic examination had developed a more complex structure including the presence of a lamina propria, suggesting that *in vivo* biochemical or structural cues are required to complete maturation.

It has also been demonstrated that some of this maturation can occur *in vitro* for primary foetal iHO. A study comparing iHO derived from primary foetal, paediatric and adult intestinal tissues demonstrated stable epigenetic signatures specific to the gut region of derivation once iHO had been produced, which were retained over prolonged periods in culture. These signatures showed similarities with primary epithelium from the same gut region. Paediatric and adult organoids demonstrated little change in DNA methylation patterns over time, whereas foetal gut-derived organoids underwent dynamic DNA methylation and transcriptional changes, indicating that these cells were maturing *in vitro*.[347]

Other studies suggest that hiPSC-derived iHO are able to demonstrate features of mature tissue; with iHO most closely resembling mature colonic epithelium on transcriptional analysis, but displaying similarities both with mature small and large intestinal tissues, suggesting again that iHO had not reached full maturation and differentiation.[348] This is likely due to the mechanical requirements of the culture model to be dissociated on a regular basis, making continuous uninterrupted culture impossible. However, in spite of their apparent immaturity, hiPSC-derived iHO were able to support stable colonisation by a non-pathogenic strain of *E. coli,* and appeared to make maturational changes as a result of this symbiosis. Innate antimicrobial defence (including NFκB and TLR signalling, and cytokine production) and epithelial barrier function related genes were increased at 24 hours post-colonisation, and then went on to decrease by later time points. Gene sets related to tissue maturation, including those for organ morphogenesis, developmental maturation and regionalisation, differentiation of mesenchymal and muscle cells and nervous system were all upregulated following colonisation.[233]

1.6.4 Applications of organoid technology, including host-pathogen interactions

The use of organoids as models for different tissue types is a rapidly expanding field, with protocols having been developed to produce numerous different tissues from various cell

types with differing degrees of complexity and maturity. Current organs for which organoids have been produced and potential clinical applications are summarised in **Table 1.1**.

Tissue / organ:	**Cellular source:**	**Clinical applications:**
Optic cup / retina	Mouse PSC / Human PSC	Transplantation of retinal organoids for mouse / primate retinal degeneration
Cerebral structures (neocortex, olfactory bulb, hippocampus, hypothalamus, midbrain, choroid plexus, cerebellum)	Mouse PSC / Primate PSC / Human PSC	Model of microcephaly Model of Zika infection on forebrain organoids Drug screening for Zika using forebrain organoids
Stomach (gastric fundus, corpus, pyloric antrum), oesophagus	Mouse PSC / ASC / dissociated tissue / hiPSC / Human dissociated tissue	Gastric organoids from tumour cells to model human gastric cancer Model of Helicobacter pylori infection in gastric organoids to study pathogenesis
Small intestine	Mouse ASC / dissociated tissue Human PSC / Human dissociated tissue	Transplantation of mouse intestinal organoids onto damaged mouse colonic epithelium Modelling of congenital loss of enteroendocrine cells in humans CRISPR/Cas9 correction of *CFTR* in intestinal organoids from patients with cystic fibrosis Development of an *in vitro* readout to evaluate recovery of CFTR function
Colon	Mouse ASC / dissociated tissue / Human PSC / ASC / dissociated tissue	Transplantation of mouse colonic organoids onto damaged mouse colonic epithelium Human colon organoids from tumour cells to model colorectal cancer Use of human organoids with *PHOX2B* mutation to study colon development in Hirschsprung's disease
Liver	Mouse ASC / Human PSC / ASC	Transplantation of mouse liver organoids into mouse model of type I tyrosinaemia Use of patient-derived liver organoids to model α-1 antitrypsin deficiency and Alagille syndrome
Pancreas	Mouse ASC / dissociated tissue / Human dissociated tissue	Use of mouse pancreatic organoids from normal and neoplastic cells has highlighted genes involved in development of pancreatic ductal adenocarcinoma

Trachea / bronchi / alveoli	Mouse ASC / Human PSC / ASC	Use of patient derived bronchial organoids to trial cystic fibrosis drug screening
Thyroid	Mouse PSC	
Prostate	Mouse ASC / dissociated tissue / Human ASC	Genetically engineered murine prostate organoids have been used to model prostate cancer
Fallopian tube	Human ASC	
Kidney	Mouse PSC / Human PSC	Use of human kidney organoids to evaluate nephrotoxicity of compounds CRISPR/Cas9 modified human organoids to model polycystic kidney disease
Mammary gland	Mouse ASC / dissociated tissue / Human ASC	Production of human breast cancer organoid biobank
Salivary gland	Mouse ASC / Human ASC	Mouse organoids have been used to expand gland stem cells that restored salivary function in murine hyposalivation models
Embryonic organoids – pre and post implantation / gastruloids / neural tube	Mouse PSC / Human PSC	

Table 1.1: Tissues from which organoids have been derived and potential clinical applications

(Table adapted from Rossi et al, 2018 – individual studies for each cell type referenced in paper[349])

Key: *ASC = adult stem cell, PSC = pluripotent stem cell (hiPSC / primary tissue), CFTR = cystic fibrosis transmembrane conductance regulator*

It is clear there are many exciting possibilities for what can be done with organoid technology. Regardless of the tissue type generated, these applications can be split up into 5 main categories:[349]

1) Basic research – use of organoids to understand normal tissue development
2) Study of disease mechanisms – this could either be using cells from individuals with genetic diseases, tumour cells, or studying host/pathogen interactions in the tissue that is usually infected
3) Drug screening – use of organoid biobanks would allow large scale screening to identify drugs that are effective against particular disease phenotypes
4) Personalised medicine – organoids from patients could identify which drugs would have the most impact on their particular disease phenotype
5) Regenerative medicine – either using organoids derived from healthy donor cells, or from the patient themselves following correction of a genetic mutation could be transplanted into patients to alleviate disease phenotype

In addition, comparison of what we learn in human organoid models with what is known from animal models of disease may allow us to use organoids over animal models in future, if organoids can prove to be complex and realistic enough models of disease. This type of technology is especially valuable for human restricted diseases or pathogens, as disease can be studied in its natural tissue niche. One example of this would be the use of gastric organoids to study *Helicobacter pylori* infection, for which there is no appropriate animal model. Infection of hiPSC-derived gastric organoids recapitulated histological features of *in vivo* disease; particularly important given the need to understand how this pathogen is associated with development of gastric cancer.[350]

Intestinal organoids are proving a robust model to help us learn about host-pathogen interactions in the gut. Murine primary organoids were initially used for the study of *S*. Typhimurium, and were able to demonstrate bacterial invasion into cells, tight junction disruption, release of pro-inflammatory cytokines and activation of the NFκB pathway. It was also noted that markers of stem cells Lgr5 and Bmi1 were downregulated in infected organoids, which could be a protective mechanism given that *Salmonella* preferentially attacks mitotic cells due to their increased surface cholesterol.[351] Bacteria in this study were however delivered basally, as opposed to apically which would be a more realistic target *in vivo*. Studies have since progressed to the use of microinjection, in order to deliver pathogens directly into the organoid lumen. Studies on murine organoids demonstrated that α-defensins secreted by Paneth cells were able to restrict growth of *S*. Typhimurium in culture, and that *Mmp7*$^{-/-}$ mice, who lack matrix metalloproteinase 7, the enzyme which converts α-defensins into their active form were unable to restrict *S*. Typhimurium growth.[352] Moving into the human model, Forbester *et al* (2015) set up a microinjection infection model for *S*. Typhimurium in hiPSC-derived iHO,[353] which we use as the basis of our investigation into host-epithelial interactions in this project.

In addition to *H. pylori*, and *S*. Typhimurium, hiPSC-derived iHO have proven a useful culture system for other enteric pathogens, including *Cryptosporidium,* a protozoan which is an important cause of diarrhoeal disease and mortality in infants in developing countries. This pathogen is an obligate parasite, needing to complete its entire life cycle inside of its host, meaning that previous attempts to study this pathogen *in vitro* have been relatively

unsuccessful. Excitingly, *Cryptosporidium* were able to propagate and complete their life cycles inside of intestinal and lung organoids, creating opportunities to learn a lot more about the pathophysiology and direct potential drug development for this protozoan.[354]

Another important pathogen for which detailed study is now possible is human norovirus, which is the commonest cause of gastroenteritis worldwide. It was possible to cultivate norovirus in enterocytes in monolayers produced from primary organoids; in this case monolayers were used, given the requirement for bile to be delivered to the apical surface of the epithelial cells for growth of certain strains.[355] Robust studies of human rotavirus were also possible for the first time in human primary organoids; with much of what is previously known about rotavirus having come from use of animal strains in animal models. In this case iHO were disaggregated and rotavirus added to culture medium, before being allowed to re-seal; in this case both apical and basal exposure was occurring. Rotavirus infected enterocytes and enteroendocrine cells, inducing them to produce viroplasms and lipid droplets. Luminal swelling of iHO was also seen following infection, recapitulating the osmotic diarrhoea induced by rotavirus *in vivo*.[356]

In a more complicated model, embryonic stem cell-derived iHO were microinjected with Shiga toxin-producing *E. coli* O157:H7, which induced loss of actin and epithelial integrity. It was possible to show that iHO were demonstrating a defensive response to infection, with increased reactive oxygen species (ROS) production, and on microscopy, O157:H7 were seen growing as filaments, consistent with the bacterial SOS response induced by ROS. In addition, neutrophils were added to the culture medium following infection and were shown to be recruited into the iHO tissue or the lumen.[357]

Lastly, hiPSC-derived iHO were used to study the important nosocomial pathogen *Clostridium difficile*. The iHO epithelial barrier was disrupted following microinjection with a toxin-producing strain of *C. difficile.* This was not the case when a non-toxigenic derivative was used, therefore purified toxins (TcdA and TcdB) were injected into the iHO, demonstrating that TcdA was responsible for damage to the epithelium by the isolate used in this study.[358]

The demonstrated ability of intestinal organoid-derived infection systems to recapitulate *in vivo* features of enteric infection is very encouraging for the possibilities of learning more about direct host-epithelial interactions with these pathogens, and the potential applications of this knowledge to developing and screening treatments or vaccines. It is certainly the

reason for which we chose this model for our studies of the human-restricted pathogens *S*. Typhi and *S*. Paratyphi A which have not previously been closely studied in this fashion.

1.7 Summary

The past 10 years have been an incredibly exciting time for the study of host-pathogen interactions, with the key discoveries of the ability to reprogram somatic cells into hiPSCs, their forward differentiation into numerous tissue models and the ability to rapidly edit the genome of those from whom the tissue models can be made, all combining to allow host and pathogen-specific modelling of human disease in more detail than has ever been possible before. We have already garnered much information on the pathogenic and immunomodulatory qualities of *Salmonella* and other enteric pathogens in different tissues, but the use of iHO technology will allow direct study of the intestinal epithelial response to infection, particularly valuable for human-restricted or difficult to grow pathogens such as typhoidal strains of *Salmonella* and Cryptosporidium. This type of study is becoming increasingly important in the current climate of increasing dissemination of MDR *Salmonella* of multiple serovars, and may aid efforts to discover new vaccine targets or treatments to better prevent disease and control the spread of these pathogens.

1.8 Aims of the thesis

Use of the novel hiPSC-derived iHO system allows non-invasive modelling of the interactions between enteric pathogens and the gut epithelium. This project aims to use this model to investigate further the interactions between *Salmonellae* and the host; commencing by establishing mechanisms of restriction of *S*. Typhimurium invasion by IL-22 both intracellularly and in the iHO lumen. We exploit the ability of the hiPSC-derived iHO system to produce iHO from different genetic backgrounds, using iHO from cell lines with isogenic mutations to model *Salmonella* infections with genes of interest knocked out. This project also examines the possibilities of using the iHO model to study interactions with alternative pathogens and to assess competitiveness of epithelial invasion between different *Salmonella* serovars. Finally, we investigate the interactions of human-restricted pathogens, *S*. Typhi and *S*. Paratyphi A with both iHO and macrophages derived from the same hiPSC

line, learning about early interactions with the epithelium and immune system. This project uses a combination of techniques to investigate these questions, including: infection assays, confocal and electron microscopy imaging, cytokine analysis and transcriptomics, both at the single cell and bulk RNA-Seq levels.

References:

1. Dougan G, John V, Palmer S, Mastroeni P. Immunity to salmonellosis. *Immunol Rev.* 2011;240(1):196-210.
2. Murray CJ. Salmonellae in the environment. *Rev Sci Tech.* 1991;10(3):765-785.
3. Le minor L, Popoff M Y Designation of Salmonella enterica sp. nov., norn. rev., as the Type and Only Species of the Genus Salmonella. *International Journal of Systematic Bacteriology.* 1987;37(4):465-468.
4. Reeves MW, Evins GM, Heiba AA, Plikaytis BD, Farmer JJ, 3rd. Clonal nature of Salmonella typhi and its genetic relatedness to other salmonellae as shown by multilocus enzyme electrophoresis, and proposal of Salmonella bongori comb. nov. *J Clin Microbiol.* 1989;27(2):313-320.
5. Grimont P A D WF-X. Antigenic Formulae of the Salmonella Serovars. In: Salmonella WCCfRaRo, ed. Institut Pasteur2007:166.
6. Kauffmann F. [The classification and nomenclature of salmonella-species]. *Zentralbl Bakteriol Orig A.* 1973;223(4):508-512.
7. WHO. Typhoid - Immunization, Vaccines and Biologicals. 2015; http://www.who.int/immunization/diseases/typhoid/en/. Accessed 18th July, 2016.
8. Luby SP, Faizan MK, Fisher-Hoch SP, et al. Risk factors for typhoid fever in an endemic setting, Karachi, Pakistan. *Epidemiol Infect.* 1998;120(2):129-138.
9. Luxemburger C, Chau MC, Mai NL, et al. Risk factors for typhoid fever in the Mekong delta, southern Viet Nam: a case-control study. *Trans R Soc Trop Med Hyg.* 2001;95(1):19-23.
10. Radhakrishnan A, Als D, Mintz ED, et al. Introductory Article on Global Burden and Epidemiology of Typhoid Fever. *Am J Trop Med Hyg.* 2018;99(3_Suppl):4-9.
11. Crump JA, Ram PK, Gupta SK, Miller MA, Mintz ED. Part I. Analysis of data gaps pertaining to Salmonella enterica serotype Typhi infections in low and medium human development index countries, 1984-2005. *Epidemiol Infect.* 2008;136(4):436-448.
12. Darton TC, Meiring JE, Tonks S, et al. The STRATAA study protocol: a programme to assess the burden of enteric fever in Bangladesh, Malawi and Nepal using

prospective population census, passive surveillance, serological studies and healthcare utilisation surveys. *BMJ Open.* 2017;7(6):e016283.

13. Kassebaum NJ, Smith AGC, Bernabe E, et al. Global, Regional, and National Prevalence, Incidence, and Disability-Adjusted Life Years for Oral Conditions for 195 Countries, 1990-2015: A Systematic Analysis for the Global Burden of Diseases, Injuries, and Risk Factors. *J Dent Res.* 2017;96(4):380-387.
14. Collaborators GBDCoD. Global, regional, and national age-sex specific mortality for 264 causes of death, 1980-2016: a systematic analysis for the Global Burden of Disease Study 2016. *Lancet.* 2017;390(10100):1151-1210.
15. Yan M, Yang B, Wang Z, et al. A Large-Scale Community-Based Outbreak of Paratyphoid Fever Caused by Hospital-Derived Transmission in Southern China. *PLoS Negl Trop Dis.* 2015;9(7):e0003859.
16. McCullagh D, Dobinson HC, Darton T, et al. Understanding paratyphoid infection: study protocol for the development of a human model of Salmonella enterica serovar Paratyphi A challenge in healthy adult volunteers. *BMJ Open.* 2015;5(6):e007481.
17. Majowicz SE, Musto J, Scallan E, et al. The global burden of nontyphoidal Salmonella gastroenteritis. *Clin Infect Dis.* 2010;50(6):882-889.
18. Feasey NA, Dougan G, Kingsley RA, Heyderman RS, Gordon MA. Invasive non-typhoidal salmonella disease: an emerging and neglected tropical disease in Africa. *Lancet.* 2012;379(9835):2489-2499.
19. Gordon MA. Salmonella infections in immunocompromised adults. *J Infect.* 2008;56(6):413-422.
20. Gordon MA, Graham SM, Walsh AL, et al. Epidemics of invasive Salmonella enterica serovar enteritidis and S. enterica Serovar typhimurium infection associated with multidrug resistance among adults and children in Malawi. *Clin Infect Dis.* 2008;46(7):963-969.
21. Reddy EA, Shaw AV, Crump JA. Community-acquired bloodstream infections in Africa: a systematic review and meta-analysis. *Lancet Infect Dis.* 2010;10(6):417-432.
22. Berkley JA, Bejon P, Mwangi T, et al. HIV infection, malnutrition, and invasive bacterial infection among children with severe malaria. *Clin Infect Dis.* 2009;49(3):336-343.

23. Graham SM, Walsh AL, Molyneux EM, Phiri AJ, Molyneux ME. Clinical presentation of non-typhoidal Salmonella bacteraemia in Malawian children. *Trans R Soc Trop Med Hyg.* 2000;94(3):310-314.
24. Graham SM, Molyneux EM, Walsh AL, Cheesbrough JS, Molyneux ME, Hart CA. Nontyphoidal Salmonella infections of children in tropical Africa. *Pediatr Infect Dis J.* 2000;19(12):1189-1196.
25. Williams TN, Uyoga S, Macharia A, et al. Bacteraemia in Kenyan children with sickle-cell anaemia: a retrospective cohort and case-control study. *Lancet.* 2009;374(9698):1364-1370.
26. Kingsley RA, Msefula CL, Thomson NR, et al. Epidemic multiple drug resistant Salmonella Typhimurium causing invasive disease in sub-Saharan Africa have a distinct genotype. *Genome Res.* 2009;19(12):2279-2287.
27. Date KA, Newton AE, Medalla F, et al. Changing Patterns in Enteric Fever Incidence and Increasing Antibiotic Resistance of Enteric Fever Isolates in the United States, 2008-2012. *Clin Infect Dis.* 2016;63(3):322-329.
28. Klemm EJ, Gkrania-Klotsas E, Hadfield J, et al. Emergence of host-adapted Salmonella Enteritidis through rapid evolution in an immunocompromised host. *Nat Microbiol.* 2016;1:15023.
29. Rychlik I, Barrow PA. Salmonella stress management and its relevance to behaviour during intestinal colonisation and infection. *FEMS Microbiol Rev.* 2005;29(5):1021-1040.
30. Muller C, Bang IS, Velayudhan J, et al. Acid stress activation of the sigma(E) stress response in Salmonella enterica serovar Typhimurium. *Mol Microbiol.* 2009;71(5):1228-1238.
31. Bearson BL, Wilson L, Foster JW. A low pH-inducible, PhoPQ-dependent acid tolerance response protects Salmonella typhimurium against inorganic acid stress. *J Bacteriol.* 1998;180(9):2409-2417.
32. Chen Y, Liu B, Glass K, Du W, Banks E, Kirk M. Use of Proton Pump Inhibitors and the Risk of Hospitalization for Infectious Gastroenteritis. *PLoS One.* 2016;11(12):e0168618.
33. Alvarez-Ordonez A, Begley M, Prieto M, et al. Salmonella spp. survival strategies within the host gastrointestinal tract. *Microbiology.* 2011;157(Pt 12):3268-3281.

34. Merritt ME, Donaldson JR. Effect of bile salts on the DNA and membrane integrity of enteric bacteria. *J Med Microbiol.* 2009;58(Pt 12):1533-1541.
35. Opleta K, Butzner JD, Shaffer EA, Gall DG. The effect of protein-calorie malnutrition on the developing liver. *Pediatr Res.* 1988;23(5):505-508.
36. van Velkinburgh JC, Gunn JS. PhoP-PhoQ-regulated loci are required for enhanced bile resistance in Salmonella spp. *Infect Immun.* 1999;67(4):1614-1622.
37. Basnyat B, Baker S. Typhoid carriage in the gallbladder. *Lancet.* 2015;386(9998):1074.
38. Prouty AM, Gunn JS. Salmonella enterica serovar typhimurium invasion is repressed in the presence of bile. *Infect Immun.* 2000;68(12):6763-6769.
39. Lawley TD, Walker AW. Intestinal colonization resistance. *Immunology.* 2013;138(1):1-11.
40. Stecher B, Robbiani R, Walker AW, et al. Salmonella enterica serovar typhimurium exploits inflammation to compete with the intestinal microbiota. *PLoS Biol.* 2007;5(10):2177-2189.
41. Hobbie S, Chen LM, Davis RJ, Galan JE. Involvement of mitogen-activated protein kinase pathways in the nuclear responses and cytokine production induced by Salmonella typhimurium in cultured intestinal epithelial cells. *J Immunol.* 1997;159(11):5550-5559.
42. Hallstrom K, McCormick BA. Salmonella Interaction with and Passage through the Intestinal Mucosa: Through the Lens of the Organism. *Front Microbiol.* 2011;2:88.
43. Van der Sluis M, De Koning BA, De Bruijn AC, et al. Muc2-deficient mice spontaneously develop colitis, indicating that MUC2 is critical for colonic protection. *Gastroenterology.* 2006;131(1):117-129.
44. Zarepour M, Bhullar K, Montero M, et al. The mucin Muc2 limits pathogen burdens and epithelial barrier dysfunction during Salmonella enterica serovar Typhimurium colitis. *Infection and immunity.* 2013;81(10):3672-3683.
45. Furter M, Sellin ME, Hansson GC, Hardt WD. Mucus Architecture and Near-Surface Swimming Affect Distinct Salmonella Typhimurium Infection Patterns along the Murine Intestinal Tract. *Cell Rep.* 2019;27(9):2665-2678 e2663.

46. Gerlach RG, Jackel D, Stecher B, et al. Salmonella Pathogenicity Island 4 encodes a giant non-fimbrial adhesin and the cognate type 1 secretion system. *Cell Microbiol.* 2007;9(7):1834-1850.
47. Wagner C, Barlag B, Gerlach RG, Deiwick J, Hensel M. The Salmonella enterica giant adhesin SiiE binds to polarized epithelial cells in a lectin-like manner. *Cell Microbiol.* 2014;16(6):962-975.
48. Bishop A, House D, Perkins T, Baker S, Kingsley RA, Dougan G. Interaction of Salmonella enterica serovar Typhi with cultured epithelial cells: roles of surface structures in adhesion and invasion. *Microbiology.* 2008;154(Pt 7):1914-1926.
49. Stecher B, Hapfelmeier S, Muller C, Kremer M, Stallmach T, Hardt WD. Flagella and chemotaxis are required for efficient induction of Salmonella enterica serovar Typhimurium colitis in streptomycin-pretreated mice. *Infect Immun.* 2004;72(7):4138-4150.
50. Kohbata S, Yokoyama H, Yabuuchi E. Cytopathogenic effect of Salmonella typhi GIFU 10007 on M cells of murine ileal Peyer's patches in ligated ileal loops: an ultrastructural study. *Microbiol Immunol.* 1986;30(12):1225-1237.
51. Clark MA, Jepson MA, Simmons NL, Hirst BH. Preferential interaction of Salmonella typhimurium with mouse Peyer's patch M cells. *Res Microbiol.* 1994;145(7):543-552.
52. Pascopella L, Raupach B, Ghori N, Monack D, Falkow S, Small PL. Host restriction phenotypes of Salmonella typhi and Salmonella gallinarum. *Infect Immun.* 1995;63(11):4329-4335.
53. Owen RL. M cells--entryways of opportunity for enteropathogens. *J Exp Med.* 1994;180(1):7-9.
54. Nickerson KP, Senger S, Zhang Y, et al. Salmonella Typhi Colonization Provokes Extensive Transcriptional Changes Aimed at Evading Host Mucosal Immune Defense During Early Infection of Human Intestinal Tissue. *EBioMedicine.* 2018;31:92-109.
55. Jensen VB, Harty JT, Jones BD. Interactions of the invasive pathogens Salmonella typhimurium, Listeria monocytogenes, and Shigella flexneri with M cells and murine Peyer's patches. *Infect Immun.* 1998;66(8):3758-3766.
56. Galan JE, Curtiss R, 3rd. Cloning and molecular characterization of genes whose products allow Salmonella typhimurium to penetrate tissue culture cells. *Proc Natl Acad Sci U S A.* 1989;86(16):6383-6387.

57. Rescigno M, Urbano M, Valzasina B, et al. Dendritic cells express tight junction proteins and penetrate gut epithelial monolayers to sample bacteria. *Nat Immunol.* 2001;2(4):361-367.
58. Rescigno M, Rotta G, Valzasina B, Ricciardi-Castagnoli P. Dendritic cells shuttle microbes across gut epithelial monolayers. *Immunobiology.* 2001;204(5):572-581.
59. Hapfelmeier S, Stecher B, Barthel M, et al. The Salmonella pathogenicity island (SPI)-2 and SPI-1 type III secretion systems allow Salmonella serovar typhimurium to trigger colitis via MyD88-dependent and MyD88-independent mechanisms. *J Immunol.* 2005;174(3):1675-1685.
60. Velge P, Wiedemann A, Rosselin M, et al. Multiplicity of Salmonella entry mechanisms, a new paradigm for Salmonella pathogenesis. *Microbiologyopen.* 2012;1(3):243-258.
61. Rosselin M, Virlogeux-Payant I, Roy C, et al. Rck of Salmonella enterica, subspecies enterica serovar enteritidis, mediates zipper-like internalization. *Cell Res.* 2010;20(6):647-664.
62. Blondel CJ, Jimenez JC, Contreras I, Santiviago CA. Comparative genomic analysis uncovers 3 novel loci encoding type six secretion systems differentially distributed in Salmonella serotypes. *BMC Genomics.* 2009;10:354.
63. Siriken B. [Salmonella pathogenicity islands]. *Mikrobiyol Bul.* 2013;47(1):181-188.
64. Galan JE, Collmer A. Type III secretion machines: bacterial devices for protein delivery into host cells. *Science.* 1999;284(5418):1322-1328.
65. Elhadad D, Desai P, Grassl GA, McClelland M, Rahav G, Gal-Mor O. Differences in Host Cell Invasion and Salmonella Pathogenicity Island 1 Expression between Salmonella enterica Serovar Paratyphi A and Nontyphoidal S. Typhimurium. *Infect Immun.* 2016;84(4):1150-1165.
66. Lara-Tejero M, Kato J, Wagner S, Liu X, Galan JE. A sorting platform determines the order of protein secretion in bacterial type III systems. *Science.* 2011;331(6021):1188-1191.
67. Francis CL, Ryan TA, Jones BD, Smith SJ, Falkow S. Ruffles induced by Salmonella and other stimuli direct macropinocytosis of bacteria. *Nature.* 1993;364(6438):639-642.
68. Chen LM, Hobbie S, Galan JE. Requirement of CDC42 for Salmonella-induced cytoskeletal and nuclear responses. *Science.* 1996;274(5295):2115-2118.

69. Blanchoin L, Amann KJ, Higgs HN, Marchand JB, Kaiser DA, Pollard TD. Direct observation of dendritic actin filament networks nucleated by Arp2/3 complex and WASP/Scar proteins. *Nature.* 2000;404(6781):1007-1011.
70. Kubori T, Galan JE. Temporal regulation of salmonella virulence effector function by proteasome-dependent protein degradation. *Cell.* 2003;115(3):333-342.
71. Nichols CD, Casanova JE. Salmonella-directed recruitment of new membrane to invasion foci via the host exocyst complex. *Curr Biol.* 2010;20(14):1316-1320.
72. Galan JE, Ginocchio C, Costeas P. Molecular and functional characterization of the Salmonella invasion gene invA: homology of InvA to members of a new protein family. *J Bacteriol.* 1992;174(13):4338-4349.
73. Malik-Kale P, Jolly CE, Lathrop S, Winfree S, Luterbach C, Steele-Mortimer O. Salmonella - at home in the host cell. *Front Microbiol.* 2011;2:125.
74. Garcia-del Portillo F, Zwick MB, Leung KY, Finlay BB. Salmonella induces the formation of filamentous structures containing lysosomal membrane glycoproteins in epithelial cells. *Proc Natl Acad Sci U S A.* 1993;90(22):10544-10548.
75. Abrahams GL, Muller P, Hensel M. Functional dissection of SseF, a type III effector protein involved in positioning the salmonella-containing vacuole. *Traffic.* 2006;7(8):950-965.
76. Bakowski MA, Braun V, Lam GY, et al. The phosphoinositide phosphatase SopB manipulates membrane surface charge and trafficking of the Salmonella-containing vacuole. *Cell Host Microbe.* 2010;7(6):453-462.
77. Braun V, Wong A, Landekic M, Hong WJ, Grinstein S, Brumell JH. Sorting nexin 3 (SNX3) is a component of a tubular endosomal network induced by Salmonella and involved in maturation of the Salmonella-containing vacuole. *Cell Microbiol.* 2010;12(9):1352-1367.
78. Waterman SR, Holden DW. Functions and effectors of the Salmonella pathogenicity island 2 type III secretion system. *Cell Microbiol.* 2003;5(8):501-511.
79. Nawabi P, Catron DM, Haldar K. Esterification of cholesterol by a type III secretion effector during intracellular Salmonella infection. *Mol Microbiol.* 2008;68(1):173-185.

80. Trombert AN, Berrocal L, Fuentes JA, Mora GC. S. Typhimurium sseJ gene decreases the S. Typhi cytotoxicity toward cultured epithelial cells. *BMC Microbiol.* 2010;10:312.

81. Meresse S, Unsworth KE, Habermann A, et al. Remodelling of the actin cytoskeleton is essential for replication of intravacuolar Salmonella. *Cell Microbiol.* 2001;3(8):567-577.

82. Friedrich N, Hagedorn M, Soldati-Favre D, Soldati T. Prison break: pathogens' strategies to egress from host cells. *Microbiol Mol Biol Rev.* 2012;76(4):707-720.

83. Kim JM, Eckmann L, Savidge TC, Lowe DC, Witthoft T, Kagnoff MF. Apoptosis of human intestinal epithelial cells after bacterial invasion. *J Clin Invest.* 1998;102(10):1815-1823.

84. Franchi L, Amer A, Body-Malapel M, et al. Cytosolic flagellin requires Ipaf for activation of caspase-1 and interleukin 1beta in salmonella-infected macrophages. *Nat Immunol.* 2006;7(6):576-582.

85. Muller AJ, Hoffmann C, Galle M, et al. The S. Typhimurium effector SopE induces caspase-1 activation in stromal cells to initiate gut inflammation. *Cell Host Microbe.* 2009;6(2):125-136.

86. Siegemund S, Schutze N, Freudenberg MA, Lutz MB, Straubinger RK, Alber G. Production of IL-12, IL-23 and IL-27p28 by bone marrow-derived conventional dendritic cells rather than macrophages after LPS/TLR4-dependent induction by Salmonella Enteritidis. *Immunobiology.* 2007;212(9-10):739-750.

87. Watson KG, Holden DW. Dynamics of growth and dissemination of Salmonella in vivo. *Cell Microbiol.* 2010;12(10):1389-1397.

88. Birmingham CL, Brumell JH. Autophagy recognizes intracellular Salmonella enterica serovar Typhimurium in damaged vacuoles. *Autophagy.* 2006;2(3):156-158.

89. Knodler LA, Vallance BA, Celli J, et al. Dissemination of invasive Salmonella via bacterial-induced extrusion of mucosal epithelia. *Proceedings of the National Academy of Sciences of the United States of America.* 2010;107(41):17733-17738.

90. Raffatellu M, Chessa D, Wilson RP, Tukel C, Akcelik M, Baumler AJ. Capsule-mediated immune evasion: a new hypothesis explaining aspects of typhoid fever pathogenesis. *Infect Immun.* 2006;74(1):19-27.

91. Raffatellu M, Chessa D, Wilson RP, Dusold R, Rubino S, Baumler AJ. The Vi capsular antigen of Salmonella enterica serotype Typhi reduces Toll-like receptor-dependent interleukin-8 expression in the intestinal mucosa. *Infect Immun.* 2005;73(6):3367-3374.

92. McCormick BA, Miller SI, Carnes D, Madara JL. Transepithelial signaling to neutrophils by salmonellae: a novel virulence mechanism for gastroenteritis. *Infect Immun.* 1995;63(6):2302-2309.

93. Zeng H, Carlson AQ, Guo Y, et al. Flagellin is the major proinflammatory determinant of enteropathogenic Salmonella. *J Immunol.* 2003;171(7):3668-3674.

94. Wangdi T, Lee CY, Spees AM, et al. The Vi capsular polysaccharide enables Salmonella enterica serovar typhi to evade microbe-guided neutrophil chemotaxis. *PLoS Pathog.* 2014;10(8):e1004306.

95. Hautefort I, Thompson A, Eriksson-Ygberg S, et al. During infection of epithelial cells Salmonella enterica serovar Typhimurium undergoes a time-dependent transcriptional adaptation that results in simultaneous expression of three type 3 secretion systems. *Cell Microbiol.* 2008;10(4):958-984.

96. Hone DM, Attridge SR, Forrest B, et al. A galE via (Vi antigen-negative) mutant of Salmonella typhi Ty2 retains virulence in humans. *Infect Immun.* 1988;56(5):1326-1333.

97. Hornick RB, Greisman SE, Woodward TE, DuPont HL, Dawkins AT, Snyder MJ. Typhoid fever: pathogenesis and immunologic control. *N Engl J Med.* 1970;283(13):686-691.

98. Gibani MM, Jones E, Barton A, et al. Investigation of the role of typhoid toxin in acute typhoid fever in a human challenge model. *Nat Med.* 2019;25(7):1082-1088.

99. Parkhill J, Dougan G, James KD, et al. Complete genome sequence of a multiple drug resistant Salmonella enterica serovar Typhi CT18. *Nature.* 2001;413(6858):848-852.

100. Jin C, Gibani MM, Moore M, et al. Efficacy and immunogenicity of a Vi-tetanus toxoid conjugate vaccine in the prevention of typhoid fever using a controlled human infection model of Salmonella Typhi: a randomised controlled, phase 2b trial. *Lancet.* 2017;390(10111):2472-2480.

101. Winter SE, Winter MG, Thiennimitr P, et al. The TviA auxiliary protein renders the Salmonella enterica serotype Typhi RcsB regulon responsive to changes in osmolarity. *Mol Microbiol.* 2009;74(1):175-193.
102. Winter SE, Winter MG, Godinez I, et al. A rapid change in virulence gene expression during the transition from the intestinal lumen into tissue promotes systemic dissemination of Salmonella. *PLoS Pathog.* 2010;6(8):e1001060.
103. Tran QT, Gomez G, Khare S, et al. The Salmonella enterica serotype Typhi Vi capsular antigen is expressed after the bacterium enters the ileal mucosa. *Infect Immun.* 2010;78(1):527-535.
104. Gewirtz AT, Navas TA, Lyons S, Godowski PJ, Madara JL. Cutting edge: bacterial flagellin activates basolaterally expressed TLR5 to induce epithelial proinflammatory gene expression. *J Immunol.* 2001;167(4):1882-1885.
105. Hayashi F, Smith KD, Ozinsky A, et al. The innate immune response to bacterial flagellin is mediated by Toll-like receptor 5. *Nature.* 2001;410(6832):1099-1103.
106. Shimazu R, Akashi S, Ogata H, et al. MD-2, a molecule that confers lipopolysaccharide responsiveness on Toll-like receptor 4. *J Exp Med.* 1999;189(11):1777-1782.
107. Rosenberger CM, Scott MG, Gold MR, Hancock RE, Finlay BB. Salmonella typhimurium infection and lipopolysaccharide stimulation induce similar changes in macrophage gene expression. *J Immunol.* 2000;164(11):5894-5904.
108. Broz P, Ohlson MB, Monack DM. Innate immune response to Salmonella typhimurium, a model enteric pathogen. *Gut Microbes.* 2012;3(2):62-70.
109. Godinez I, Raffatellu M, Chu H, et al. Interleukin-23 orchestrates mucosal responses to Salmonella enterica serotype Typhimurium in the intestine. *Infect Immun.* 2009;77(1):387-398.
110. Stelter C, Kappeli R, Konig C, et al. Salmonella-induced mucosal lectin RegIIIbeta kills competing gut microbiota. *PLoS One.* 2011;6(6):e20749.
111. Hancock RE, McPhee JB. Salmonella's sensor for host defense molecules. *Cell.* 2005;122(3):320-322.
112. Raffatellu M, George MD, Akiyama Y, et al. Lipocalin-2 resistance confers an advantage to Salmonella enterica serotype Typhimurium for growth and survival in the inflamed intestine. *Cell Host Microbe.* 2009;5(5):476-486.

113. Fischbach MA, Lin H, Zhou L, et al. The pathogen-associated iroA gene cluster mediates bacterial evasion of lipocalin 2. *Proc Natl Acad Sci U S A.* 2006;103(44):16502-16507.
114. Kawahara T, Kuwano Y, Teshima-Kondo S, et al. Role of nicotinamide adenine dinucleotide phosphate oxidase 1 in oxidative burst response to Toll-like receptor 5 signaling in large intestinal epithelial cells. *Journal of immunology.* 2004;172(5):3051-3058.
115. Martinez Rodriguez NR, Eloi MD, Huynh A, et al. Expansion of Paneth cell population in response to enteric Salmonella enterica serovar Typhimurium infection. *Infection and immunity.* 2012;80(1):266-275.
116. Zhang YG, Wu S, Xia Y, Sun J. Salmonella-infected crypt-derived intestinal organoid culture system for host-bacterial interactions. *Physiol Rep.* 2014;2(9).
117. Stecher B, Barthel M, Schlumberger MC, et al. Motility allows S. Typhimurium to benefit from the mucosal defence. *Cell Microbiol.* 2008;10(5):1166-1180.
118. McGeachy MJ, McSorley SJ. Microbial-induced Th17: superhero or supervillain? *J Immunol.* 2012;189(7):3285-3291.
119. Godinez I, Keestra AM, Spees A, Baumler AJ. The IL-23 axis in Salmonella gastroenteritis. *Cell Microbiol.* 2011;13(11):1639-1647.
120. Raupach B, Peuschel SK, Monack DM, Zychlinsky A. Caspase-1-mediated activation of interleukin-1beta (IL-1beta) and IL-18 contributes to innate immune defenses against Salmonella enterica serovar Typhimurium infection. *Infect Immun.* 2006;74(8):4922-4926.
121. Lazarus GM, Neu HC. Agents responsible for infection in chronic granulomatous disease of childhood. *J Pediatr.* 1975;86(3):415-417.
122. Graham SM, Hart CA, Molyneux EM, Walsh AL, Molyneux ME. Malaria and Salmonella infections: cause or coincidence? *Trans R Soc Trop Med Hyg.* 2000;94(2):227.
123. Landesman SH, Rao SP, Ahonkhai VI. Infections in children with sickle cell anemia. Special reference to pneumococcal and salmonella infections. *Am J Pediatr Hematol Oncol.* 1982;4(4):407-418.

124. Kuhle V, Hensel M. SseF and SseG are translocated effectors of the type III secretion system of Salmonella pathogenicity island 2 that modulate aggregation of endosomal compartments. *Cell Microbiol.* 2002;4(12):813-824.
125. Brumell JH, Tang P, Mills SD, Finlay BB. Characterization of Salmonella-induced filaments (Sifs) reveals a delayed interaction between Salmonella-containing vacuoles and late endocytic compartments. *Traffic.* 2001;2(9):643-653.
126. Knodler LA, Vallance BA, Hensel M, Jackel D, Finlay BB, Steele-Mortimer O. Salmonella type III effectors PipB and PipB2 are targeted to detergent-resistant microdomains on internal host cell membranes. *Mol Microbiol.* 2003;49(3):685-704.
127. Uchiya K, Barbieri MA, Funato K, Shah AH, Stahl PD, Groisman EA. A Salmonella virulence protein that inhibits cellular trafficking. *EMBO J.* 1999;18(14):3924-3933.
128. Vazquez-Torres A, Xu Y, Jones-Carson J, et al. Salmonella pathogenicity island 2-dependent evasion of the phagocyte NADPH oxidase. *Science.* 2000;287(5458):1655-1658.
129. Gallois A, Klein JR, Allen LA, Jones BD, Nauseef WM. Salmonella pathogenicity island 2-encoded type III secretion system mediates exclusion of NADPH oxidase assembly from the phagosomal membrane. *J Immunol.* 2001;166(9):5741-5748.
130. Jabado N, Jankowski A, Dougaparsad S, Picard V, Grinstein S, Gros P. Natural resistance to intracellular infections: natural resistance-associated macrophage protein 1 (Nramp1) functions as a pH-dependent manganese transporter at the phagosomal membrane. *J Exp Med.* 2000;192(9):1237-1248.
131. Fritsche G, Nairz M, Libby SJ, Fang FC, Weiss G. Slc11a1 (Nramp1) impairs growth of Salmonella enterica serovar typhimurium in macrophages via stimulation of lipocalin-2 expression. *J Leukoc Biol.* 2012;92(2):353-359.
132. Chakravortty D, Hansen-Wester I, Hensel M. Salmonella pathogenicity island 2 mediates protection of intracellular Salmonella from reactive nitrogen intermediates. *J Exp Med.* 2002;195(9):1155-1166.
133. Hersh D, Monack DM, Smith MR, Ghori N, Falkow S, Zychlinsky A. The Salmonella invasin SipB induces macrophage apoptosis by binding to caspase-1. *Proc Natl Acad Sci U S A.* 1999;96(5):2396-2401.

134. Detweiler CS, Cunanan DB, Falkow S. Host microarray analysis reveals a role for the Salmonella response regulator phoP in human macrophage cell death. *Proc Natl Acad Sci U S A.* 2001;98(10):5850-5855.

135. Browne SH, Lesnick ML, Guiney DG. Genetic requirements for salmonella-induced cytopathology in human monocyte-derived macrophages. *Infect Immun.* 2002;70(12):7126-7135.

136. Faucher SP, Porwollik S, Dozois CM, McClelland M, Daigle F. Transcriptome of Salmonella enterica serovar Typhi within macrophages revealed through the selective capture of transcribed sequences. *Proc Natl Acad Sci U S A.* 2006;103(6):1906-1911.

137. Lawley TD, Chan K, Thompson LJ, Kim CC, Govoni GR, Monack DM. Genome-wide screen for Salmonella genes required for long-term systemic infection of the mouse. *PLoS Pathog.* 2006;2(2):e11.

138. Winter SE, Winter MG, Atluri V, et al. The flagellar regulator TviA reduces pyroptosis by Salmonella enterica serovar Typhi. *Infect Immun.* 2015;83(4):1546-1555.

139. Wilson RP, Winter SE, Spees AM, et al. The Vi capsular polysaccharide prevents complement receptor 3-mediated clearance of Salmonella enterica serotype Typhi. *Infect Immun.* 2011;79(2):830-837.

140. Baldassarre M S-CV, Balci A, Wilson H, Mukhopadhyay S, Dougan G, Spano S. Salmonella Typhi survives in human macrophages by neutralizing the RAB32/BLOC-3 host-defence pathway. *bioRxiv* 2019;570531.

141. Sheikh A, Charles RC, Rollins SM, et al. Analysis of Salmonella enterica serotype paratyphi A gene expression in the blood of bacteremic patients in Bangladesh. *PLoS Negl Trop Dis.* 2010;4(12):e908.

142. Mizuno Y, Takada H, Nomura A, et al. Th1 and Th1-inducing cytokines in Salmonella infection. *Clin Exp Immunol.* 2003;131(1):111-117.

143. Gal-Mor O, Suez J, Elhadad D, et al. Molecular and cellular characterization of a Salmonella enterica serovar Paratyphi a outbreak strain and the human immune response to infection. *Clin Vaccine Immunol.* 2012;19(2):146-156.

144. Blohmke CJ, Darton TC, Jones C, et al. Interferon-driven alterations of the host's amino acid metabolism in the pathogenesis of typhoid fever. *J Exp Med.* 2016;213(6):1061-1077.

145. Alam MM, Tsai LL, Rollins SM, et al. Identification of in vivo-induced bacterial proteins during human infection with Salmonella enterica serotype Paratyphi A. *Clin Vaccine Immunol.* 2013;20(5):712-719.
146. Saleh S, Van Puyvelde S, Staes A, et al. Salmonella Typhi, Paratyphi A, Enteritidis and Typhimurium core proteomes reveal differentially expressed proteins linked to the cell surface and pathogenicity. *PLoS Negl Trop Dis.* 2019;13(5):e0007416.
147. Organisation WH. Background document: The diagnosis, treatment and prevention of typhoid fever. In: Biologicals CDSaRVa, ed. Geneva2003.
148. Dougan G, Baker S. Salmonella enterica serovar Typhi and the pathogenesis of typhoid fever. *Annu Rev Microbiol.* 2014;68:317-336.
149. Wain J, Diep TS, Ho VA, et al. Quantitation of bacteria in blood of typhoid fever patients and relationship between counts and clinical features, transmissibility, and antibiotic resistance. *J Clin Microbiol.* 1998;36(6):1683-1687.
150. Wain J, Pham VB, Ha V, et al. Quantitation of bacteria in bone marrow from patients with typhoid fever: relationship between counts and clinical features. *J Clin Microbiol.* 2001;39(4):1571-1576.
151. Organisation WH. Typhoid Vaccines: WHO Position Paper. 2008; http://www.who.int/wer/2008/wer8306.pdf?ua=1. Accessed 20th May 2017.
152. Zhang S, Kingsley RA, Santos RL, et al. Molecular pathogenesis of Salmonella enterica serotype typhimurium-induced diarrhea. *Infect Immun.* 2003;71(1):1-12.
153. Hohmann EL. Nontyphoidal salmonellosis. *Clin Infect Dis.* 2001;32(2):263-269.
154. Gordon MA, Banda HT, Gondwe M, et al. Non-typhoidal salmonella bacteraemia among HIV-infected Malawian adults: high mortality and frequent recrudescence. *AIDS.* 2002;16(12):1633-1641.
155. Coward C, Restif O, Dybowski R, Grant AJ, Maskell DJ, Mastroeni P. The effects of vaccination and immunity on bacterial infection dynamics in vivo. *PLoS Pathog.* 2014;10(9):e1004359.
156. Hess J, Ladel C, Miko D, Kaufmann SH. Salmonella typhimurium aroA- infection in gene-targeted immunodeficient mice: major role of CD4+ TCR-alpha beta cells and IFN-gamma in bacterial clearance independent of intracellular location. *J Immunol.* 1996;156(9):3321-3326.

157. Sinha K, Mastroeni P, Harrison J, de Hormaeche RD, Hormaeche CE. Salmonella typhimurium aroA, htrA, and aroD htrA mutants cause progressive infections in athymic (nu/nu) BALB/c mice. *Infect Immun.* 1997;65(4):1566-1569.

158. Mastroeni P, Villarreal-Ramos B, Hormaeche CE. Adoptive transfer of immunity to oral challenge with virulent salmonellae in innately susceptible BALB/c mice requires both immune serum and T cells. *Infect Immun.* 1993;61(9):3981-3984.

159. Srinivasan A, Salazar-Gonzalez RM, Jarcho M, Sandau MM, Lefrancois L, McSorley SJ. Innate immune activation of CD4 T cells in salmonella-infected mice is dependent on IL-18. *J Immunol.* 2007;178(10):6342-6349.

160. Dunstan SJ, Hue NT, Han B, et al. Variation at HLA-DRB1 is associated with resistance to enteric fever. *Nat Genet.* 2014;46(12):1333-1336.

161. Song J, Gao X, Galan JE. Structure and function of the Salmonella Typhi chimaeric A(2)B(5) typhoid toxin. *Nature.* 2013;499(7458):350-354.

162. Napolitani G, Kurupati P, Teng KWW, et al. Clonal analysis of Salmonella-specific effector T cells reveals serovar-specific and cross-reactive T cell responses. *Nat Immunol.* 2018;19(7):742-754.

163. Sheikh F, Baurin VV, Lewis-Antes A, et al. Cutting edge: IL-26 signals through a novel receptor complex composed of IL-20 receptor 1 and IL-10 receptor 2. *J Immunol.* 2004;172(4):2006-2010.

164. Xie MH, Aggarwal S, Ho WH, et al. Interleukin (IL)-22, a novel human cytokine that signals through the interferon receptor-related proteins CRF2-4 and IL-22R. *J Biol Chem.* 2000;275(40):31335-31339.

165. MacLennan CA, Gondwe EN, Msefula CL, et al. The neglected role of antibody in protection against bacteremia caused by nontyphoidal strains of Salmonella in African children. *J Clin Invest.* 2008;118(4):1553-1562.

166. Gibani MMJC, Thomaides-Brears H., et al. Investigating Systemic Immunity to Typhoid and Paratyphoid Fever: Characterising the Response to Re-challenge in a Controlled Human Infection Model. OFID; 2017.

167. Parry CM, Hien TT, Dougan G, White NJ, Farrar JJ. Typhoid fever. *N Engl J Med.* 2002;347(22):1770-1782.

168. Parry CM, Thompson C, Vinh H, et al. Risk factors for the development of severe typhoid fever in Vietnam. *BMC Infect Dis.* 2014;14:73.

169. Holt KE, Phan MD, Baker S, et al. Emergence of a globally dominant IncHI1 plasmid type associated with multiple drug resistant typhoid. *PLoS Negl Trop Dis.* 2011;5(7):e1245.
170. Wong VK, Baker S, Pickard DJ, et al. Phylogeographical analysis of the dominant multidrug-resistant H58 clade of Salmonella Typhi identifies inter- and intracontinental transmission events. *Nat Genet.* 2015;47(6):632-639.
171. Feasey NA, Gaskell K, Wong V, et al. Rapid emergence of multidrug resistant, H58-lineage Salmonella typhi in Blantyre, Malawi. *PLoS Negl Trop Dis.* 2015;9(4):e0003748.
172. Hendriksen RS, Leekitcharoenphon P, Lukjancenko O, et al. Genomic signature of multidrug-resistant Salmonella enterica serovar typhi isolates related to a massive outbreak in Zambia between 2010 and 2012. *J Clin Microbiol.* 2015;53(1):262-272.
173. Pham Thanh D, Thompson CN, Rabaa MA, et al. The Molecular and Spatial Epidemiology of Typhoid Fever in Rural Cambodia. *PLoS Negl Trop Dis.* 2016;10(6):e0004785.
174. Pham Thanh D, Karkey A, Dongol S, et al. A novel ciprofloxacin-resistant subclade of H58 Salmonella Typhi is associated with fluoroquinolone treatment failure. *Elife.* 2016;5:e14003.
175. Munir T, Lodhi M, Ansari JK, Andleeb S, Ahmed M. Extended Spectrum Beta Lactamase producing Cephalosporin resistant Salmonella Typhi, reported from Rawalpindi, Pakistan. *J Pak Med Assoc.* 2016;66(8):1035-1036.
176. Ochiai RL, Wang X, von Seidlein L, et al. Salmonella paratyphi A rates, Asia. *Emerg Infect Dis.* 2005;11(11):1764-1766.
177. Hardjo Lugito NP, Cucunawangsih. Antimicrobial Resistance of Salmonella enterica Serovars Typhi and Paratyphi Isolates from a General Hospital in Karawaci, Tangerang, Indonesia: A Five-Year Review. *Int J Microbiol.* 2017;2017:6215136.
178. Woods CW, Murdoch DR, Zimmerman MD, et al. Emergence of Salmonella enterica serotype Paratyphi A as a major cause of enteric fever in Kathmandu, Nepal. *Trans R Soc Trop Med Hyg.* 2006;100(11):1063-1067.
179. Qamar FN, Yousafzai MT, Sultana S, et al. A Retrospective Study of Laboratory-Based Enteric Fever Surveillance, Pakistan, 2012-2014. *J Infect Dis.* 2018;218(suppl_4):S201-S205.

180. Gupta SK, Medalla F, Omondi MW, et al. Laboratory-based surveillance of paratyphoid fever in the United States: travel and antimicrobial resistance. *Clin Infect Dis.* 2008;46(11):1656-1663.

181. Chandel DS, Chaudhry R, Dhawan B, Pandey A, Dey AB. Drug-resistant Salmonella enterica serotype paratyphi A in India. *Emerg Infect Dis.* 2000;6(4):420-421.

182. Maskey AP, Day JN, Phung QT, et al. Salmonella enterica serovar Paratyphi A and S. enterica serovar Typhi cause indistinguishable clinical syndromes in Kathmandu, Nepal. *Clin Infect Dis.* 2006;42(9):1247-1253.

183. Sood S, Kapil A, Dash N, Das BK, Goel V, Seth P. Paratyphoid fever in India: An emerging problem. *Emerg Infect Dis.* 1999;5(3):483-484.

184. Holt KE, Thomson NR, Wain J, et al. Multidrug-resistant Salmonella enterica serovar paratyphi A harbors IncHI1 plasmids similar to those found in serovar typhi. *J Bacteriol.* 2007;189(11):4257-4264.

185. Mandal S, Mandal MD, Pal NK. Antibiotic resistance of Salmonella enterica serovar Paratyphi A in India: emerging and reemerging problem. *J Postgrad Med.* 2006;52(3):163-166.

186. Hasan Z, Rahman KM, Alam MN, et al. Role of a large plasmid in mediation of multiple drug resistance in Salmonella typhi and paratyphi A in Bangladesh. *Bangladesh Med Res Counc Bull.* 1995;21(1):50-54.

187. Zhou Z, McCann A, Weill FX, et al. Transient Darwinian selection in Salmonella enterica serovar Paratyphi A during 450 years of global spread of enteric fever. *Proc Natl Acad Sci U S A.* 2014;111(33):12199-12204.

188. Didelot X, Achtman M, Parkhill J, Thomson NR, Falush D. A bimodal pattern of relatedness between the Salmonella Paratyphi A and Typhi genomes: convergence or divergence by homologous recombination? *Genome Res.* 2007;17(1):61-68.

189. Graham SM. Nontyphoidal salmonellosis in Africa. *Curr Opin Infect Dis.* 2010;23(5):409-414.

190. Menezes GA, Khan MA, Harish BN, et al. Molecular characterization of antimicrobial resistance in non-typhoidal salmonellae associated with systemic manifestations from India. *J Med Microbiol.* 2010;59(Pt 12):1477-1483.

191. Chen PL, Li CY, Hsieh TH, et al. Epidemiology, disease spectrum and economic burden of non-typhoidal Salmonella infections in Taiwan, 2006-2008. *Epidemiol Infect.* 2012;140(12):2256-2263.
192. Kiratisin P. Bacteraemia due to non-typhoidal Salmonella in Thailand: clinical and microbiological analysis. *Trans R Soc Trop Med Hyg.* 2008;102(4):384-388.
193. Phu Huong Lan N, Le Thi Phuong T, Nguyen Huu H, et al. Invasive Non-typhoidal Salmonella Infections in Asia: Clinical Observations, Disease Outcome and Dominant Serovars from an Infectious Disease Hospital in Vietnam. *PLoS Negl Trop Dis.* 2016;10(8):e0004857.
194. Mather AE, Phuong TLT, Gao Y, et al. New Variant of Multidrug-Resistant Salmonella enterica Serovar Typhimurium Associated with Invasive Disease in Immunocompromised Patients in Vietnam. *MBio.* 2018;9(5).
195. Britto C, Pollard AJ, Voysey M, Blohmke CJ. An Appraisal of the Clinical Features of Pediatric Enteric Fever: Systematic Review and Meta-analysis of the Age-Stratified Disease Occurrence. *Clin Infect Dis.* 2017;64(11):1604-1611.
196. Anwar E, Goldberg E, Fraser A, Acosta CJ, Paul M, Leibovici L. Vaccines for preventing typhoid fever. *Cochrane Database Syst Rev.* 2014(1):CD001261.
197. Thiem VD, Lin FY, Canh DG, et al. The Vi conjugate typhoid vaccine is safe, elicits protective levels of IgG anti-Vi, and is compatible with routine infant vaccines. *Clin Vaccine Immunol.* 2011;18(5):730-735.
198. Mohan VK, Varanasi V, Singh A, et al. Safety and immunogenicity of a Vi polysaccharide-tetanus toxoid conjugate vaccine (Typbar-TCV) in healthy infants, children, and adults in typhoid endemic areas: a multicenter, 2-cohort, open-label, double-blind, randomized controlled phase 3 study. *Clin Infect Dis.* 2015;61(3):393-402.
199. Mitra M, Shah N, Ghosh A, et al. Efficacy and safety of vi-tetanus toxoid conjugated typhoid vaccine (PedaTyph) in Indian children: School based cluster randomized study. *Hum Vaccin Immunother.* 2016;12(4):939-945.
200. Lin FY, Ho VA, Khiem HB, et al. The efficacy of a Salmonella typhi Vi conjugate vaccine in two-to-five-year-old children. *N Engl J Med.* 2001;344(17):1263-1269.
201. Darton TC, Jones C, Blohmke CJ, et al. Using a Human Challenge Model of Infection to Measure Vaccine Efficacy: A Randomised, Controlled Trial Comparing the Typhoid

Vaccines M01ZH09 with Placebo and Ty21a. *PLoS Negl Trop Dis.* 2016;10(8):e0004926.

202. Gibani MM, Voysey M, Jin C, et al. The Impact of Vaccination and Prior Exposure on Stool Shedding of Salmonella Typhi and Salmonella Paratyphi in 6 Controlled Human Infection Studies. *Clin Infect Dis.* 2019;68(8):1265-1273.
203. Organization WH. Summary of the October 2017 meeting of the Strategic Advisory Group of Experts on Immunization. 2017.
204. Organization WH. Typhoid fever - Islamic Republic of Pakistan. 2018. Accessed 20th July, 2019.
205. Simanjuntak CH, Paleologo FP, Punjabi NH, et al. Oral immunisation against typhoid fever in Indonesia with Ty21a vaccine. *Lancet.* 1991;338(8774):1055-1059.
206. Levine MM, Ferreccio C, Black RE, Lagos R, San Martin O, Blackwelder WC. Ty21a live oral typhoid vaccine and prevention of paratyphoid fever caused by Salmonella enterica Serovar Paratyphi B. *Clin Infect Dis.* 2007;45 Suppl 1:S24-28.
207. Konadu EY, Lin FY, Ho VA, et al. Phase 1 and phase 2 studies of Salmonella enterica serovar paratyphi A O-specific polysaccharide-tetanus toxoid conjugates in adults, teenagers, and 2- to 4-year-old children in Vietnam. *Infect Immun.* 2000;68(3):1529-1534.
208. Konadu E, Shiloach J, Bryla DA, Robbins JB, Szu SC. Synthesis, characterization, and immunological properties in mice of conjugates composed of detoxified lipopolysaccharide of Salmonella paratyphi A bound to tetanus toxoid with emphasis on the role of O acetyls. *Infect Immun.* 1996;64(7):2709-2715.
209. Micoli F, Rondini S, Gavini M, et al. O:2-CRM(197) conjugates against Salmonella Paratyphi A. *PLoS One.* 2012;7(11):e47039.
210. Gat O, Galen JE, Tennant S, et al. Cell-associated flagella enhance the protection conferred by mucosally-administered attenuated Salmonella Paratyphi A vaccines. *PLoS Negl Trop Dis.* 2011;5(11):e1373.
211. Sun P, Pan C, Zeng M, et al. Design and production of conjugate vaccines against S. Paratyphi A using an O-linked glycosylation system in vivo. *NPJ Vaccines.* 2018;3:4.
212. Xiong K, Zhu C, Chen Z, et al. Vi Capsular Polysaccharide Produced by Recombinant Salmonella enterica Serovar Paratyphi A Confers Immunoprotection against Infection by Salmonella enterica Serovar Typhi. *Front Cell Infect Microbiol.* 2017;7:135.

213. Gondwe EN, Molyneux ME, Goodall M, et al. Importance of antibody and complement for oxidative burst and killing of invasive nontyphoidal Salmonella by blood cells in Africans. *Proc Natl Acad Sci U S A.* 2010;107(7):3070-3075.
214. Gil-Cruz C, Bobat S, Marshall JL, et al. The porin OmpD from nontyphoidal Salmonella is a key target for a protective B1b cell antibody response. *Proc Natl Acad Sci U S A.* 2009;106(24):9803-9808.
215. Simon R, Wang JY, Boyd MA, et al. Sustained protection in mice immunized with fractional doses of Salmonella Enteritidis core and O polysaccharide-flagellin glycoconjugates. *PLoS One.* 2013;8(5):e64680.
216. Boyd MA, Tennant SM, Saague VA, et al. Serum bactericidal assays to evaluate typhoidal and nontyphoidal Salmonella vaccines. *Clin Vaccine Immunol.* 2014;21(5):712-721.
217. Organization WH. *Status of Vaccine Research and Development for Nontyphoidal Salmonelloses Prepared for WHO PD-VAC.* 2014.
218. Ault A, Tennant SM, Gorres JP, et al. Safety and tolerability of a live oral Salmonella typhimurium vaccine candidate in SIV-infected nonhuman primates. *Vaccine.* 2013;31(49):5879-5888.
219. Gerke C, Colucci AM, Giannelli C, et al. Production of a Shigella sonnei Vaccine Based on Generalized Modules for Membrane Antigens (GMMA), 1790GAHB. *PLoS One.* 2015;10(8):e0134478.
220. Micoli F, Rondini S, Alfini R, et al. Comparative immunogenicity and efficacy of equivalent outer membrane vesicle and glycoconjugate vaccines against nontyphoidal Salmonella. *Proc Natl Acad Sci U S A.* 2018;115(41):10428-10433.
221. Balasubramanian R, Im J, Lee JS, et al. The global burden and epidemiology of invasive non-typhoidal Salmonella infections. *Hum Vaccin Immunother.* 2019;15(6):1421-1426.
222. Santos RL, Zhang S, Tsolis RM, Kingsley RA, Adams LG, Baumler AJ. Animal models of Salmonella infections: enteritis versus typhoid fever. *Microbes Infect.* 2001;3(14-15):1335-1344.
223. Jansen AM, Hall LJ, Clare S, et al. A Salmonella Typhimurium-Typhi genomic chimera: a model to study Vi polysaccharide capsule function in vivo. *PLoS Pathog.* 2011;7(7):e1002131.

224. Song J, Willinger T, Rongvaux A, et al. A mouse model for the human pathogen Salmonella typhi. *Cell Host Microbe.* 2010;8(4):369-376.
225. Libby SJ, Brehm MA, Greiner DL, et al. Humanized nonobese diabetic-scid IL2rgammanull mice are susceptible to lethal Salmonella Typhi infection. *Proc Natl Acad Sci U S A.* 2010;107(35):15589-15594.
226. Barthel M, Hapfelmeier S, Quintanilla-Martinez L, et al. Pretreatment of mice with streptomycin provides a Salmonella enterica serovar Typhimurium colitis model that allows analysis of both pathogen and host. *Infect Immun.* 2003;71(5):2839-2858.
227. Suar M, Jantsch J, Hapfelmeier S, et al. Virulence of broad- and narrow-host-range Salmonella enterica serovars in the streptomycin-pretreated mouse model. *Infect Immun.* 2006;74(1):632-644.
228. Richardson A. Outbreaks of bovine salmonellosis caused by serotypes other than S. dublin and S. typhimurium. *J Hyg (Lond).* 1975;74(2):195-203.
229. Smith BP, Habasha F, Reina-Guerra M, Hardy AJ. Bovine salmonellosis: experimental production and characterization of the disease in calves, using oral challenge with Salmonella typhimurium. *Am J Vet Res.* 1979;40(11):1510-1513.
230. Frost AJ, Bland AP, Wallis TS. The early dynamic response of the calf ileal epithelium to Salmonella typhimurium. *Vet Pathol.* 1997;34(5):369-386.
231. Bolton AJ, Osborne MP, Wallis TS, Stephen J. Interaction of Salmonella choleraesuis, Salmonella dublin and Salmonella typhimurium with porcine and bovine terminal ileum in vivo. *Microbiology.* 1999;145 (Pt 9):2431-2441.
232. Tsolis RM, Adams LG, Ficht TA, Baumler AJ. Contribution of Salmonella typhimurium virulence factors to diarrheal disease in calves. *Infect Immun.* 1999;67(9):4879-4885.
233. Hill DR, Huang S, Nagy MS, et al. Bacterial colonization stimulates a complex physiological response in the immature human intestinal epithelium. *Elife.* 2017;6.
234. Haque A, Bowe F, Fitzhenry RJ, et al. Early interactions of Salmonella enterica serovar typhimurium with human small intestinal epithelial explants. *Gut.* 2004;53(10):1424-1430.
235. Tsilingiri K, Barbosa T, Penna G, et al. Probiotic and postbiotic activity in health and disease: comparison on a novel polarised ex-vivo organ culture model. *Gut.* 2012;61(7):1007-1015.

236. Dostal A, Gagnon M, Chassard C, Zimmermann MB, O'Mahony L, Lacroix C. Salmonella adhesion, invasion and cellular immune responses are differentially affected by iron concentrations in a combined in vitro gut fermentation-cell model. *PLoS One.* 2014;9(3):e93549.

237. Martinez-Argudo I, Jepson MA. Salmonella translocates across an in vitro M cell model independently of SPI-1 and SPI-2. *Microbiology.* 2008;154(Pt 12):3887-3894.

238. Honer zu Bentrup K, Ramamurthy R, Ott CM, et al. Three-dimensional organotypic models of human colonic epithelium to study the early stages of enteric salmonellosis. *Microbes Infect.* 2006;8(7):1813-1825.

239. Barrila J, Yang J, Crabbe A, et al. Three-dimensional organotypic co-culture model of intestinal epithelial cells and macrophages to study Salmonella enterica colonization patterns. *NPJ Microgravity.* 2017;3:10.

240. Zhang K, Dupont A, Torow N, et al. Age-dependent enterocyte invasion and microcolony formation by Salmonella. *PLoS Pathog.* 2014;10(9):e1004385.

241. Sato T, Vries RG, Snippert HJ, et al. Single Lgr5 stem cells build crypt-villus structures in vitro without a mesenchymal niche. *Nature.* 2009;459(7244):262-265.

242. Sato T, Stange DE, Ferrante M, et al. Long-term expansion of epithelial organoids from human colon, adenoma, adenocarcinoma, and Barrett's epithelium. *Gastroenterology.* 2011;141(5):1762-1772.

243. Ootani A, Li X, Sangiorgi E, et al. Sustained in vitro intestinal epithelial culture within a Wnt-dependent stem cell niche. *Nat Med.* 2009;15(6):701-706.

244. Spence JR, Mayhew CN, Rankin SA, et al. Directed differentiation of human pluripotent stem cells into intestinal tissue in vitro. *Nature.* 2011;470(7332):105-109.

245. Fatehullah A, Tan SH, Barker N. Organoids as an in vitro model of human development and disease. *Nat Cell Biol.* 2016;18(3):246-254.

246. Workman MJ, Mahe MM, Trisno S, et al. Engineered human pluripotent-stem-cell-derived intestinal tissues with a functional enteric nervous system. *Nat Med.* 2017;23(1):49-59.

247. Kretzschmar K, Clevers H. Organoids: Modeling Development and the Stem Cell Niche in a Dish. *Dev Cell.* 2016;38(6):590-600.

248. Hale C, Yeung A, Goulding D, et al. Induced pluripotent stem cell derived macrophages as a cellular system to study salmonella and other pathogens. *PLoS One.* 2015;10(5):e0124307.
249. Dobinson HC, Gibani MM, Jones C, et al. Evaluation of the Clinical and Microbiological Response to Salmonella Paratyphi A Infection in the First Paratyphoid Human Challenge Model. *Clin Infect Dis.* 2017;64(8):1066-1073.
250. Fusaki N, Ban H, Nishiyama A, Saeki K, Hasegawa M. Efficient induction of transgene-free human pluripotent stem cells using a vector based on Sendai virus, an RNA virus that does not integrate into the host genome. *Proc Jpn Acad Ser B Phys Biol Sci.* 2009;85(8):348-362.
251. Forbester JL, Hannan N, Vallier L, Dougan G. Derivation of Intestinal Organoids from Human Induced Pluripotent Stem Cells for Use as an Infection System. *Methods Mol Biol.* 2016.
252. Bock C, Kiskinis E, Verstappen G, et al. Reference Maps of human ES and iPS cell variation enable high-throughput characterization of pluripotent cell lines. *Cell.* 2011;144(3):439-452.
253. Rouhani F, Kumasaka N, de Brito MC, Bradley A, Vallier L, Gaffney D. Genetic background drives transcriptional variation in human induced pluripotent stem cells. *PLoS Genet.* 2014;10(6):e1004432.
254. Forbester JL, Lees EA, Goulding D, et al. Interleukin-22 promotes phagolysosomal fusion to induce protection against Salmonella enterica Typhimurium in human epithelial cells. *Proc Natl Acad Sci U S A.* 2018;115(40):10118-10123.
255. Okamoto S, Amaishi Y, Maki I, Enoki T, Mineno J. Highly efficient genome editing for single-base substitutions using optimized ssODNs with Cas9-RNPs. *Sci Rep.* 2019;9(1):4811.
256. Noel G, Baetz NW, Staab JF, et al. A primary human macrophage-enteroid co-culture model to investigate mucosal gut physiology and host-pathogen interactions. *Sci Rep.* 2017;7:45270.
257. Nozaki K, Mochizuki W, Matsumoto Y, et al. Co-culture with intestinal epithelial organoids allows efficient expansion and motility analysis of intraepithelial lymphocytes. *J Gastroenterol.* 2016;51(3):206-213.

258. Kinnebrew MA, Pamer EG. Innate immune signaling in defense against intestinal microbes. *Immunol Rev.* 2012;245(1):113-131.
259. Silva AM, Barbosa FH, Duarte R, Vieira LQ, Arantes RM, Nicoli JR. Effect of Bifidobacterium longum ingestion on experimental salmonellosis in mice. *J Appl Microbiol.* 2004;97(1):29-37.
260. Hollingsworth MA, Swanson BJ. Mucins in cancer: protection and control of the cell surface. *Nat Rev Cancer.* 2004;4(1):45-60.
261. Taupin D, Podolsky DK. Trefoil factors: initiators of mucosal healing. *Nat Rev Mol Cell Biol.* 2003;4(9):721-732.
262. Gill N, Wlodarska M, Finlay BB. Roadblocks in the gut: barriers to enteric infection. *Cell Microbiol.* 2011;13(5):660-669.
263. Deplancke B, Gaskins HR. Microbial modulation of innate defense: goblet cells and the intestinal mucus layer. *Am J Clin Nutr.* 2001;73(6):1131s-1141s.
264. Bruewer M, Luegering A, Kucharzik T, et al. Proinflammatory cytokines disrupt epithelial barrier function by apoptosis-independent mechanisms. *J Immunol.* 2003;171(11):6164-6172.
265. Peterson LW, Artis D. Intestinal epithelial cells: regulators of barrier function and immune homeostasis. *Nat Rev Immunol.* 2014;14(3):141-153.
266. Corr SC, Gahan CC, Hill C. M-cells: origin, morphology and role in mucosal immunity and microbial pathogenesis. *FEMS Immunol Med Microbiol.* 2008;52(1):2-12.
267. Neutra MR, Frey A, Kraehenbuhl JP. Epithelial M cells: gateways for mucosal infection and immunization. *Cell.* 1996;86(3):345-348.
268. Sansonetti PJ, Phalipon A. M cells as ports of entry for enteroinvasive pathogens: mechanisms of interaction, consequences for the disease process. *Semin Immunol.* 1999;11(3):193-203.
269. Vaishnava S, Behrendt CL, Ismail AS, Eckmann L, Hooper LV. Paneth cells directly sense gut commensals and maintain homeostasis at the intestinal host-microbial interface. *Proc Natl Acad Sci U S A.* 2008;105(52):20858-20863.
270. Gunawardene AR, Corfe BM, Staton CA. Classification and functions of enteroendocrine cells of the lower gastrointestinal tract. *Int J Exp Pathol.* 2011;92(4):219-231.

271. Mestecky J, Russell MW. Specific antibody activity, glycan heterogeneity and polyreactivity contribute to the protective activity of S-IgA at mucosal surfaces. *Immunol Lett.* 2009;124(2):57-62.
272. Mantis NJ, Forbes SJ. Secretory IgA: arresting microbial pathogens at epithelial borders. *Immunol Invest.* 2010;39(4-5):383-406.
273. Iankov ID, Petrov DP, Mladenov IV, et al. Protective efficacy of IgA monoclonal antibodies to O and H antigens in a mouse model of intranasal challenge with Salmonella enterica serotype Enteritidis. *Microbes Infect.* 2004;6(10):901-910.
274. Peterson DA, McNulty NP, Guruge JL, Gordon JI. IgA response to symbiotic bacteria as a mediator of gut homeostasis. *Cell Host Microbe.* 2007;2(5):328-339.
275. Osawa R, Williams KL, Singh N. The inflammasome regulatory pathway and infections: role in pathophysiology and clinical implications. *J Infect.* 2011;62(2):119-129.
276. Kawai T, Akira S. The roles of TLRs, RLRs and NLRs in pathogen recognition. *Int Immunol.* 2009;21(4):317-337.
277. Shapira L, Soskolne WA, Houri Y, Barak V, Halabi A, Stabholz A. Protection against endotoxic shock and lipopolysaccharide-induced local inflammation by tetracycline: correlation with inhibition of cytokine secretion. *Infect Immun.* 1996;64(3):825-828.
278. Lipinski S, Till A, Sina C, et al. DUOX2-derived reactive oxygen species are effectors of NOD2-mediated antibacterial responses. *J Cell Sci.* 2009;122(Pt 19):3522-3530.
279. Benjamin JL, Sumpter R, Levine B, Hooper LV. Intestinal Epithelial Autophagy Is Essential for Host Defense against Invasive Bacteria. *Cell host & microbe.* 2013;13(6):723-734.
280. Neal MD, Richardson WM, Sodhi CP, Russo A, Hackam DJ. Intestinal Stem Cells and Their Roles During Mucosal Injury and Repair. *J Surg Res.* 2011;167(1):1-8.
281. Bright NA, Gratian MJ, Luzio JP. Endocytic delivery to lysosomes mediated by concurrent fusion and kissing events in living cells. *Curr Biol.* 2005;15(4):360-365.
282. Christoforidis S, McBride HM, Burgoyne RD, Zerial M. The Rab5 effector EEA1 is a core component of endosome docking. *Nature.* 1999;397(6720):621-625.
283. Vieira OV, Bucci C, Harrison RE, et al. Modulation of Rab5 and Rab7 recruitment to phagosomes by phosphatidylinositol 3-kinase. *Mol Cell Biol.* 2003;23(7):2501-2514.

284. Marshansky V, Futai M. The V-type H+-ATPase in vesicular trafficking: targeting, regulation and function. *Curr Opin Cell Biol.* 2008;20(4):415-426.
285. Rink J, Ghigo E, Kalaidzidis Y, Zerial M. Rab conversion as a mechanism of progression from early to late endosomes. *Cell.* 2005;122(5):735-749.
286. Kinchen JM, Ravichandran KS. Phagosome maturation: going through the acid test. *Nat Rev Mol Cell Biol.* 2008;9(10):781-795.
287. Uribe-Querol E, Rosales C. Control of Phagocytosis by Microbial Pathogens. *Front Immunol.* 2017;8:1368.
288. Heinzen RA, Hackstadt T, Samuel JE. Developmental biology of Coxiella burnettii. *Trends Microbiol.* 1999;7(4):149-154.
289. Reece ST, Kaufmann, S.H.E. Host Defenses to Intracellular Bacteria. In: *Clinical Immunology (Fifth Edition).* Elsevier; 2019:375-389.e371.
290. Dhiman R, Venkatasubramanian S, Paidipally P, Barnes PF, Tvinnereim A, Vankayalapati R. Interleukin 22 inhibits intracellular growth of Mycobacterium tuberculosis by enhancing calgranulin A expression. *J Infect Dis.* 2014;209(4):578-587.
291. Kim KJ, Elliott SJ, Di Cello F, Stins MF, Kim KS. The K1 capsule modulates trafficking of E. coli-containing vacuoles and enhances intracellular bacterial survival in human brain microvascular endothelial cells. *Cell Microbiol.* 2003;5(4):245-252.
292. Goebel W, Kuhn M. Bacterial replication in the host cell cytosol. *Curr Opin Microbiol.* 2000;3(1):49-53.
293. Eswarappa SM, Negi VD, Chakraborty S, Chandrasekhar Sagar BK, Chakravortty D. Division of the Salmonella-containing vacuole and depletion of acidic lysosomes in Salmonella-infected host cells are novel strategies of Salmonella enterica to avoid lysosomes. *Infect Immun.* 2010;78(1):68-79.
294. Buchmeier NA, Heffron F. Inhibition of macrophage phagosome-lysosome fusion by Salmonella typhimurium. *Infect Immun.* 1991;59(7):2232-2238.
295. Cuellar-Mata P, Jabado N, Liu J, et al. Nramp1 modifies the fusion of Salmonella typhimurium-containing vacuoles with cellular endomembranes in macrophages. *J Biol Chem.* 2002;277(3):2258-2265.

296. Meresse S, Steele-Mortimer O, Finlay BB, Gorvel JP. The rab7 GTPase controls the maturation of Salmonella typhimurium-containing vacuoles in HeLa cells. *EMBO J.* 1999;18(16):4394-4403.

297. Stein MA, Leung KY, Zwick M, Garcia-del Portillo F, Finlay BB. Identification of a Salmonella virulence gene required for formation of filamentous structures containing lysosomal membrane glycoproteins within epithelial cells. *Mol Microbiol.* 1996;20(1):151-164.

298. Beuzon CR, Meresse S, Unsworth KE, et al. Salmonella maintains the integrity of its intracellular vacuole through the action of SifA. *EMBO J.* 2000;19(13):3235-3249.

299. Schreiber F, Arasteh JM, Lawley TD. Pathogen Resistance Mediated by IL-22 Signaling at the Epithelial-Microbiota Interface. *J Mol Biol.* 2015;427(23):3676-3682.

300. Sabat R, Ouyang W, Wolk K. Therapeutic opportunities of the IL-22-IL-22R1 system. *Nat Rev Drug Discov.* 2014;13(1):21-38.

301. Kim CJ, Nazli A, Rojas OL, et al. A role for mucosal IL-22 production and Th22 cells in HIV-associated mucosal immunopathogenesis. *Mucosal Immunol.* 2012;5(6):670-680.

302. Sabat R. IL-10 family of cytokines. *Cytokine Growth Factor Rev.* 2010;21(5):315-324.

303. Gurney AL. IL-22, a Th1 cytokine that targets the pancreas and select other peripheral tissues. *Int Immunopharmacol.* 2004;4(5):669-677.

304. Glocker EO, Kotlarz D, Boztug K, et al. Inflammatory bowel disease and mutations affecting the interleukin-10 receptor. *N Engl J Med.* 2009;361(21):2033-2045.

305. Pham TA, Clare S, Goulding D, et al. Epithelial IL-22RA1-mediated fucosylation promotes intestinal colonization resistance to an opportunistic pathogen. *Cell Host Microbe.* 2014;16(4):504-516.

306. Zheng Y, Valdez PA, Danilenko DM, et al. Interleukin-22 mediates early host defense against attaching and effacing bacterial pathogens. *Nat Med.* 2008;14(3):282-289.

307. Diefenbach A. Interleukin-22, the guardian of the intestinal stem cell niche? *Immunity.* 2012;37(2):196-198.

308. Rutz S, Eidenschenk C, Ouyang W. IL-22, not simply a Th17 cytokine. *Immunological reviews.* 2013;252(1):116-132.

309. Parks OB, Pociask DA, Hodzic Z, Kolls JK, Good M. Interleukin-22 Signaling in the Regulation of Intestinal Health and Disease. *Front Cell Dev Biol.* 2015;3:85.

310. Pickard JM, Maurice CF, Kinnebrew MA, et al. Rapid fucosylation of intestinal epithelium sustains host-commensal symbiosis in sickness. *Nature.* 2014;514(7524):638-641.
311. Martin JC, Beriou G, Heslan M, et al. Interleukin-22 binding protein (IL-22BP) is constitutively expressed by a subset of conventional dendritic cells and is strongly induced by retinoic acid. *Mucosal immunology.* 2014;7(1):101-113.
312. Huber S, Gagliani N, Zenewicz LA, et al. IL-22BP is regulated by the inflammasome and modulates tumorigenesis in the intestine. *Nature.* 2012;491(7423):259-263.
313. Andoh A, Zhang Z, Inatomi O, et al. Interleukin-22, a member of the IL-10 subfamily, induces inflammatory responses in colonic subepithelial myofibroblasts. *Gastroenterology.* 2005;129(3):969-984.
314. Kastelein RA, Hunter CA, Cua DJ. Discovery and biology of IL-23 and IL-27: related but functionally distinct regulators of inflammation. *Annu Rev Immunol.* 2007;25:221-242.
315. Morishima N, Mizoguchi I, Takeda K, Mizuguchi J, Yoshimoto T. TGF-beta is necessary for induction of IL-23R and Th17 differentiation by IL-6 and IL-23. *Biochem Biophys Res Commun.* 2009;386(1):105-110.
316. Aujla SJ, Chan YR, Zheng M, et al. IL-22 mediates mucosal host defense against Gram-negative bacterial pneumonia. *Nat Med.* 2008;14(3):275-281.
317. Schulz SM, Kohler G, Schutze N, et al. Protective immunity to systemic infection with attenuated Salmonella enterica serovar enteritidis in the absence of IL-12 is associated with IL-23-dependent IL-22, but not IL-17. *J Immunol.* 2008;181(11):7891-7901.
318. De Luca A, Zelante T, D'Angelo C, et al. IL-22 defines a novel immune pathway of antifungal resistance. *Mucosal Immunol.* 2010;3(4):361-373.
319. Dhiman R, Indramohan M, Barnes PF, et al. IL-22 produced by human NK cells inhibits growth of Mycobacterium tuberculosis by enhancing phagolysosomal fusion. *J Immunol.* 2009;183(10):6639-6645.
320. Takahashi K, Tanabe K, Ohnuki M, et al. Induction of pluripotent stem cells from adult human fibroblasts by defined factors. *Cell.* 2007;131(5):861-872.
321. Higuchi A, Ling QD, Kumar SS, et al. Generation of pluripotent stem cells without the use of genetic material. *Lab Invest.* 2015;95(1):26-42.

322. Abou-Saleh H, Zouein FA, El-Yazbi A, et al. The march of pluripotent stem cells in cardiovascular regenerative medicine. *Stem Cell Res Ther.* 2018;9(1):201.
323. Malik N, Rao MS. A review of the methods for human iPSC derivation. *Methods in molecular biology.* 2013;997:23-33.
324. Ran FA, Hsu PD, Wright J, Agarwala V, Scott DA, Zhang F. Genome engineering using the CRISPR-Cas9 system. *Nat Protoc.* 2013;8(11):2281-2308.
325. Singh VK, Kalsan M, Kumar N, Saini A, Chandra R. Induced pluripotent stem cells: applications in regenerative medicine, disease modeling, and drug discovery. *Front Cell Dev Biol.* 2015;3:2.
326. Shi Y, Inoue H, Wu JC, Yamanaka S. Induced pluripotent stem cell technology: a decade of progress. *Nat Rev Drug Discov.* 2017;16(2):115-130.
327. Cohen DE, Melton D. Turning straw into gold: directing cell fate for regenerative medicine. *Nat Rev Genet.* 2011;12(4):243-252.
328. van Wilgenburg B, Browne C, Vowles J, Cowley SA. Efficient, long term production of monocyte-derived macrophages from human pluripotent stem cells under partly-defined and fully-defined conditions. *PLoS One.* 2013;8(8):e71098.
329. Senju S, Koba C, Haruta M, et al. Application of iPS cell-derived macrophages to cancer therapy. *Oncoimmunology.* 2014;3(1):e27927.
330. Bernareggi D, Pouyanfard S, Kaufman DS. Development of innate immune cells from human pluripotent stem cells. *Exp Hematol.* 2019;71:13-23.
331. Jiang Y, Cowley SA, Siler U, et al. Derivation and functional analysis of patient-specific induced pluripotent stem cells as an in vitro model of chronic granulomatous disease. *Stem Cells.* 2012;30(4):599-611.
332. Panicker LM, Miller D, Park TS, et al. Induced pluripotent stem cell model recapitulates pathologic hallmarks of Gaucher disease. *Proc Natl Acad Sci U S A.* 2012;109(44):18054-18059.
333. Aflaki E, Stubblefield BK, Maniwang E, et al. Macrophage models of Gaucher disease for evaluating disease pathogenesis and candidate drugs. *Sci Transl Med.* 2014;6(240):240ra273.
334. Tanaka T, Takahashi K, Yamane M, et al. Induced pluripotent stem cells from CINCA syndrome patients as a model for dissecting somatic mosaicism and drug discovery. *Blood.* 2012;120(6):1299-1308.

335. Karlsson KR, Cowley S, Martinez FO, Shaw M, Minger SL, James W. Homogeneous monocytes and macrophages from human embryonic stem cells following coculture-free differentiation in M-CSF and IL-3. *Exp Hematol.* 2008;36(9):1167-1175.
336. Sato T, Clevers H. Growing self-organizing mini-guts from a single intestinal stem cell: mechanism and applications. *Science.* 2013;340(6137):1190-1194.
337. Laurent LC, Ulitsky I, Slavin I, et al. Dynamic Changes in the Copy Number of Pluripotency and Cell Proliferation Genes in Human ESCs and iPSCs during Reprogramming and Time in Culture. *Cell stem cell.* 2011;8(1):106-118.
338. Hannan NR, Fordham RP, Syed YA, et al. Generation of multipotent foregut stem cells from human pluripotent stem cells. *Stem Cell Reports.* 2013;1(4):293-306.
339. Takeuchi H, Nakatsuji N, Suemori H. Endodermal differentiation of human pluripotent stem cells to insulin-producing cells in 3D culture. *Sci Rep.* 2014;4:4488.
340. McLean AB, D'Amour KA, Jones KL, et al. Activin a efficiently specifies definitive endoderm from human embryonic stem cells only when phosphatidylinositol 3-kinase signaling is suppressed. *Stem cells.* 2007;25(1):29-38.
341. Naujok O, Diekmann U, Lenzen S. The generation of definitive endoderm from human embryonic stem cells is initially independent from activin A but requires canonical Wnt-signaling. *Stem Cell Rev.* 2014;10(4):480-493.
342. Jung P, Sato T, Merlos-Suarez A, et al. Isolation and in vitro expansion of human colonic stem cells. *Nat Med.* 2011;17(10):1225-1227.
343. Date S, Sato T. Mini-gut organoids: reconstitution of the stem cell niche. *Annu Rev Cell Dev Biol.* 2015;31:269-289.
344. Takebe T, Wells JM. Organoids by design. *Science.* 2019;364(6444):956-959.
345. Merker SR, Weitz J, Stange DE. Gastrointestinal organoids: How they gut it out. *Dev Biol.* 2016;420(2):239-250.
346. Finkbeiner SR, Hill DR, Altheim CH, et al. Transcriptome-wide Analysis Reveals Hallmarks of Human Intestine Development and Maturation In Vitro and In Vivo. *Stem Cell Reports.* 2015.
347. Kraiczy J, Nayak KM, Howell KJ, et al. DNA methylation defines regional identity of human intestinal epithelial organoids and undergoes dynamic changes during development. *Gut.* 2019;68(1):49-61.

348. Kraiczy J, Ross ADB, Forbester JL, Dougan G, Vallier L, Zilbauer M. Genome-Wide Epigenetic and Transcriptomic Characterization of Human-Induced Pluripotent Stem Cell-Derived Intestinal Epithelial Organoids. *Cell Mol Gastroenterol Hepatol.* 2019;7(2):285-288.

349. Rossi G, Manfrin A, Lutolf MP. Progress and potential in organoid research. *Nat Rev Genet.* 2018;19(11):671-687.

350. McCracken KW, Howell JC, Wells JM, Spence JR. Generating human intestinal tissue from pluripotent stem cells in vitro. *Nat Protoc.* 2011;6(12):1920-1928.

351. Santos AJ, Meinecke M, Fessler MB, Holden DW, Boucrot E. Preferential invasion of mitotic cells by Salmonella reveals that cell surface cholesterol is maximal during metaphase. *J Cell Sci.* 2013;126(Pt 14):2990-2996.

352. Wilson SS, Tocchi A, Holly MK, Parks WC, Smith JG. A small intestinal organoid model of non-invasive enteric pathogen-epithelial cell interactions. *Mucosal Immunol.* 2015;8(2):352-361.

353. Forbester JL, Goulding D, Vallier L, et al. Interaction of Salmonella enterica Serovar Typhimurium with Intestinal Organoids Derived from Human Induced Pluripotent Stem Cells. *Infect Immun.* 2015;83(7):2926-2934.

354. Heo I, Dutta D, Schaefer DA, et al. Modelling Cryptosporidium infection in human small intestinal and lung organoids. *Nat Microbiol.* 2018;3(7):814-823.

355. Ettayebi K, Crawford SE, Murakami K, et al. Replication of human noroviruses in stem cell-derived human enteroids. *Science.* 2016;353(6306):1387-1393.

356. Saxena K, Blutt SE, Ettayebi K, et al. Human Intestinal Enteroids: a New Model To Study Human Rotavirus Infection, Host Restriction, and Pathophysiology. *J Virol.* 2016;90(1):43-56.

357. Karve SS, Pradhan S, Ward DV, Weiss AA. Intestinal organoids model human responses to infection by commensal and Shiga toxin producing Escherichia coli. *PLoS One.* 2017;12(6):e0178966.

358. Leslie JL, Huang S, Opp JS, et al. Persistence and toxin production by Clostridium difficile within human intestinal organoids result in disruption of epithelial paracellular barrier function. *Infect Immun.* 2015;83(1):138-145.

4: The role of IL-22 in restriction of *Salmonella* invasion of the intestinal epithelium

Collaboration note:

Some of the data in this chapter have been published as: "Interleukin-22 promotes phagolysosomal fusion to induce protection against Salmonella enterica Typhimurium in human epithelial cells" (Forbester et al., 2018) on which I am listed as second author.

4.1 Introduction

In vivo, IECs play a key role in regulating intestinal homeostasis and may directly inhibit pathogens, although the mechanisms by which this occurs are not currently well understood. The cytokine IL-22 is known to have a role in the maintenance of the gut epithelial barrier[1] and is involved in the induction and secretion of antimicrobial peptides and chemokines in response to infection.[2] It is produced by activated T cells (particularly, CD4+ Th17 cells) as well as by natural killer (NK) cells and binds to a heterodimeric receptor composed of the IL-22R1 and IL-10R2 subunits.[3] The receptor for IL-22 is expressed basally on IECs, meaning that in the iHO model, it is possible to pre-treat organoids with rhIL-22 simply by its addition to the culture medium.

Work on the iHO model by Jessica Forbester prior to the commencement of this project, had established via RNA sequencing that stimulation of iHO with rhIL-22 at 100 ng/mL 18 h prior to infection upregulates antimicrobial genes and other genes previously associated with the barrier defense phenotype (**Figure 4.1**). Notable examples include the interferon-regulated genes, IFITM1, IFITM2 and IFITM3, which are known to be involved in antimycobacterial and anti-viral response[4] and DUOXA2; an NADPH-oxidase involved in H_2O_2 production at the epithelial surface, previously noted to have role in defence against enteric Salmonella infection.[5,6] In addition, antimicrobial protein coding genes RegIIIα and RegIβ and mucin-producing genes MUC1 and MUC4 were amongst those most highly

upregulated, suggesting an epithelium primed for pathogen defence. The differential expression of some of these genes was also demonstrated via immunostaining of iHO, highlighting for example, increased MUC4 expression following rhIL-22 stimulation.

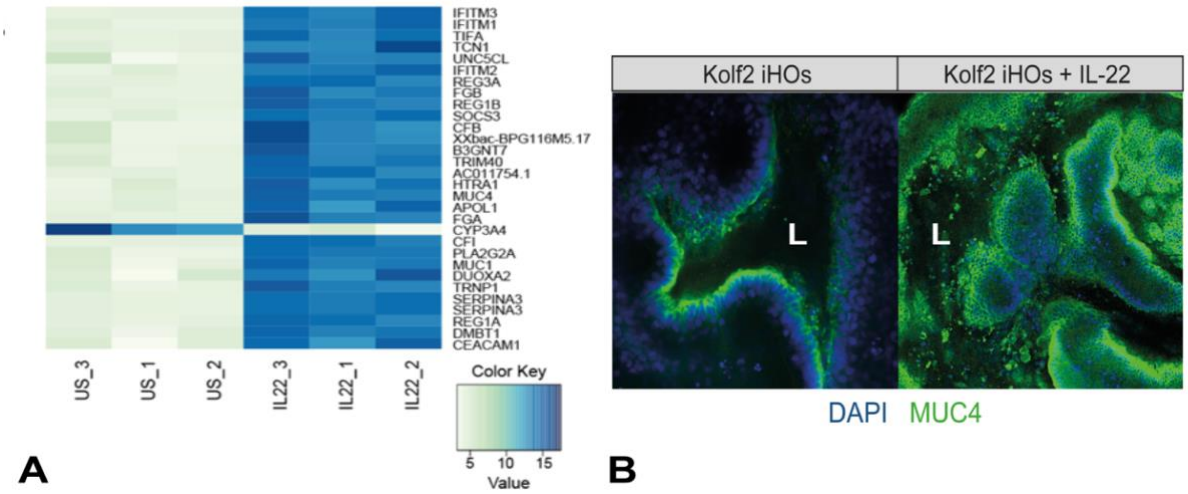

Figure 4.1: IL-22 stimulation induces a barrier phenotype in the iHO (**A**) Heat map of RNA-Seq expression data calculated using DESeq2 for the 30 most significantly differentially expressed genes following stimulation of Kolf2 iHO with rhIL-22. Data presented are from three biological replicates per condition. (**B**) Immunostaining of iHO for MUC4 (green) and DAPI (blue) expression either unstimulated or following rhIL-22 stimulation (L = iHO lumen). Images taken on the on Zeiss LSM 510 Meta confocal microscope at 20x magnification. (Figure adapted from Forbester et al, 2018[7])

Alongside maintaining the epithelial barrier, IECs produce and respond to cytokines; of particular importance in this case are cytokines from the IL-10 family (IL-10, IL-19, IL-20, IL-22, IL-26), which have roles both in the innate response to pathogens and in more chronic states of inflammation, such as in inflammatory bowel disease or psoriasis.[8] The receptor complexes for these cytokines overlap, with the surface receptor complex for IL-22 being formed of two subunits; IL-10R2 and IL-22R1, with loss of either subunit causing loss of response to IL-22.[9] Mutations in IL-10R2 can cause severe early-onset inflammatory bowel disease in humans[10] or colitis in mice.[11] IL-22 or IL-22R1 deficient mice were more susceptible to lethal systemic bacterial infection following infection with *Citrobacter rodentium* or chemically-induced colitis.[12,13] IL-10R2 expression is found across many types of cell, both from the haematopoietic and non-haematopoietic lineages, whereas IL-22R1 expression is more limited, being predominantly located on epithelial cells from the skin, respiratory system, kidney and digestive systems.

iHO produced from hiPSC from a patient with infantile IBD (with a homozygous splice site mutation at the boundary between intron and exon 3 in the IL10R2 gene[14]) did not display upregulation of the IL-22 regulated genes Lipochalin2 (LCN2) or Dual oxidase 2 (DUOX2) upon stimulation with rhIL-22.[15] However, this response was restored in an isogenic control line with this mutation complemented via TALEN-based engineering. iHO from healthy volunteers and the isogenic control line demonstrated restriction of intracellular infection with *S*. Typhimurium SL1344 following pre-treatment with rhIL-22 versus those produced from the patient cell line which showed no difference in invasion level.[7]

Enteric bacteria such as Salmonellae are thought to invade the epithelium through transcytosis via M-cells, or enterocytes.[16] Once inside the epithelial cell, Salmonellae are able to set up an intracellular niche inside the *Salmonella*-containing vacuole (SCV), which eventually fuses with endolysosomes, producing a drop in pH in the vacuole. *Salmonella* uses a T3SS, encoded on SPI-2 to manipulate the course of phagosomal maturation, delaying acidification and allowing intravacuolar replication.[17]

Given the restriction of intracellular *S*. Typhimurium infection in iHO pre-treated with IL-22, we hypothesised that IL-22 was able to enhance intracellular defences against *S*. Typhimurium, most likely by altering the environment within the SCV to induce bacterial killing. This chapter investigates the molecular mechanisms behind this hypothesis.

4.2. Phenotyping iHO derived from healthy volunteer cell lines to demonstrate presence of the IL-22 receptor complex

iHO were produced from hiPSCs derived from the healthy volunteer Kolf2 cell line as outlined in Chapter 2 (2.1.2-2.1.4). Once matured, these were immunostained for the IL-22R1 and IL10R2 elements of the IL-22 receptor complex (2.1.5). iHO demonstrated the presence of both subunits, with IL-22R1 being expressed fairly ubiquitously across the basal surface of the iHO, but IL-10R2 appearing clustered to individual cells. This appeared to co-localise with expression of chromogranin A, a protein produced by enteroendocrine cells (**Figure 4.3**). This basal expression of receptors facilitated the delivery of the cytokine rhIL-22 to the basal surface of the iHO during stimulation assays.

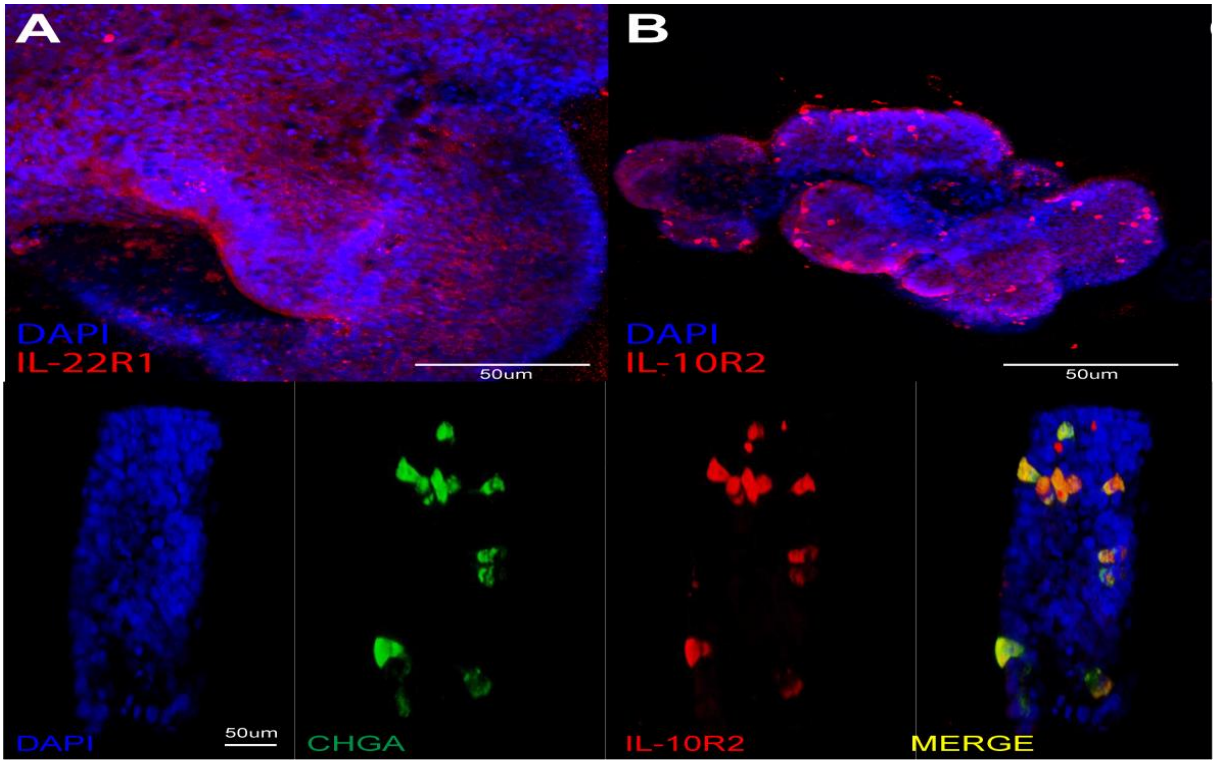

Figure 4.3: IL-22 receptor immunostaining: (**A**) Kolf2 iHO displaying diffuse IL-22R1 expression (red), (**B**) clustered IL-10R2 expression (red) and (**C**) colocalization of chromogranin A (green) and IL-10R2 (red) expression. DAPI (blue) marks cell nuclei in all panels. (Panel **C** adapted from Forbester et al, 2018[7]). Images taken on the on Zeiss LSM 510 Meta confocal microscope at 20x (Panels A&B) or 40x (Panel C) magnification.

RNA was extracted from iHO and iPSC derived from the Kolf2 line and RT-qPCR completed as described in 2.1.5 to check expression of the receptor complex subunits. mRNA was detected for IL-22R1 and IL-10R2 in samples from iPSC and iHO, with significantly increased expression of both receptors in iHO versus iPSC (**Figure 4.4**).

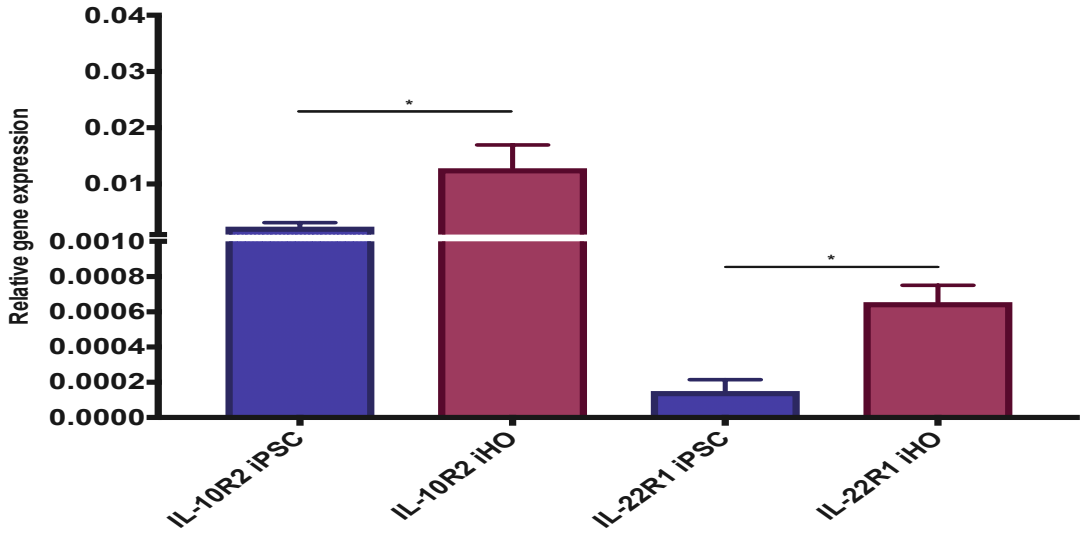

Figure 4.4: Relative gene expression for IL-22R1 and IL-10R2 in iPSC and iHO from Kolf2 cell line. Data presented are from 4 technical replicates, with assays repeated 3 times using paired iPSC/iHO of different batches. Data were analysed using the comparative cycle threshold (C_T) method, with GAPDH as an endogenous control. Unpaired Mann-Whitney test was used to compare results (*$p < 0.05$).

4.3 Response of IL-22-regulated genes in iHO following rhIL-22 stimulation

Given that LCN2 and DUOX2 are known to be upregulated in response to IL-22, these genes were used as markers of the ability of iHO to respond to IL-22. This response was checked in mature iHO designated for use in experiments. rhIL-22 at a concentration of 100 ng/mL was added to culture medium for 18 hours prior to the harvesting of iHO. RNA extraction and RT-qPCR to monitor expression of LCN2 and DUOX2 were completed using methods described in 2.1.5. Transcripts for LCN2 and DUOX2 were significantly upregulated following rhIL-22 stimulation (**Figure 4.5**).

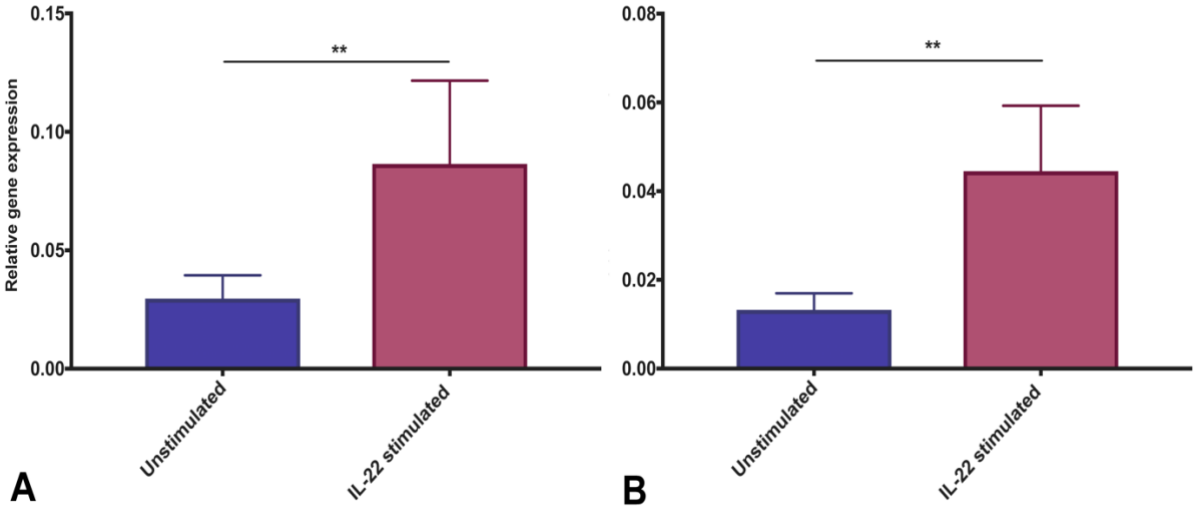

Figure 4.5: Relative gene expression for (A) LCN2 and (B) DUOX2 following rhIL-22 stimulation in Kolf2 cell line. Prior to harvesting, iHO were treated for 18 hours with rhIL-22 at a concentration of 100 ng/mL or left unstimulated. Data presented are from 4 technical replicates, with assays repeated 6 times on separate occasions. Data were analysed using the comparative cycle threshold (C_T) method, with GAPDH as an endogenous control. Unpaired Mann-Whitney test was used to compare results (**$p < 0.001$).

4.4 Effect of IL-22 stimulation on *S.* Typhimurium SL1344 infection of iHO

To establish whether IL-22 stimulation had any effect on the interactions of the iHO with *S.* Typhimurium, Kolf2 iHO were microinjected with *S.* Typhimurium SL1344 (henceforth, SL1344) after they had been treated with rhIL-22 for 18 hours (outlined in 2.3). Following modified gentamicin assays measuring intracellular bacterial survival, there were significant differences in the amount of bacteria recovered from cells in each condition, with fewer bacteria recovered from iHO pre-treated with rhIL-22 (**Figure 4.6**). In order to try to establish where in the infection process this difference was occurring, these invasion assays were also

performed and iHO harvested at 30 minutes to look at early stage invasion. There was a significant reduction in intracellular SL1344 counts in iHO pre-stimulated with rhIL-22, suggesting some inhibition of early invasion. However, in addition to this, infected iHO were incubated for a further 90 minutes following the gentamicin incubation step to investigate longer term intracellular survival, and there was a greater difference in survival seen here, with fewer bacteria recovered from the rhIL-22 treated cells. (**Figure 4.6**). Gentamicin protection assays were repeated in primary human organoids produced from duodenal tissue and again, significantly fewer bacteria were recovered from cells which had been pre-treated with rhIL-22.[7]

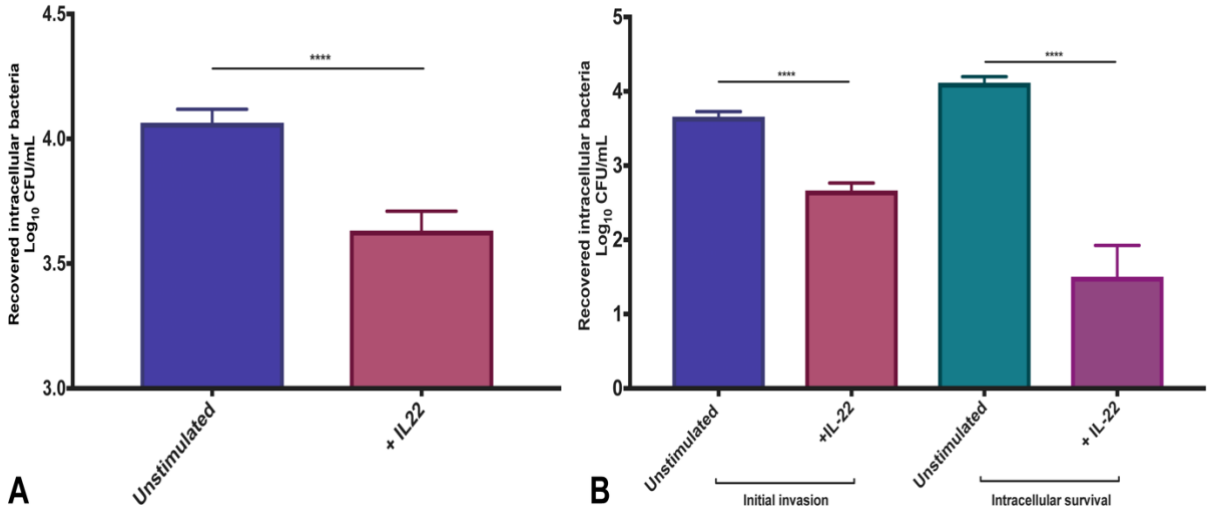

Figure 4.6: Restriction of intracellular SL1344 infection in Kolf2 iHO pre-treated with rhIL-22. (**A**) Modified gentamicin protection assay demonstrates that pre-treatment of Kolf2 iHO with rhIL-22 at 100 ng/mL for 18 hours inhibits SL1344 infection in the iHO at 1.5 hours post-infection. (**B**) Invasion into cells and survival within cells both appear to be affected, with differences in counts of bacteria recovered both at an early timepoint (30 minutes post-infection) and following a prolonged incubation period within cells (an additional 90 minutes post-gentamicin treatment). Data presented are for at least 3 biological replicates (each averaged from 3 technical replicates), with 30 iHO injected per replicate +/- SEM. Unpaired Mann-Whitney tests were used for all assays (**** $p < 0.0001$).

To further investigate this phenotype, intracellular invasion assays were performed with *S.* Typhimurium ST4/74 (the ancestral strain from which the histidine auxotroph SL1344 was derived) and ST4/74 with a double gene deletion knockout in the PhoP/Q system (ST4/74 ΔPhoPQ). PhoP/Q is a virulence-associated regulatory system, activated by mildly acidic pH (such as that found inside the endosomes of neutrophils/macrophages following phagocytosis). The PhoP/Q system negatively regulates invasion associated genes and positively regulates genes required for intracellular survival within the SCV. *Salmonellae* with mutations in the genes regulating this system are more sensitive to defensins, with multiple

components of the PhoP/Q system required to resist defensins. ST4/74 exhibited an indistinguishable phenotype compared to SL1344; when injected into iHO that had been pre-treated with rhIL-22; fewer intracellular bacteria were recovered in the IL-22 treated group. There were significantly higher intracellular counts of ST4/74 than ST4/74 ΔPhoPQ. However, for ST4/74 ΔPhoPQ there was no significant difference in the counts of bacteria recovered intracellularly between the treated and untreated groups (**Figure 4.7**). This data suggested that ST4/74 ΔPhoPQ bacteria were either killed more rapidly in the lumen by their increased susceptibility to antimicrobial peptides, or that bacteria invaded but were unable to survive intracellularly without enhanced survival systems provided by the PhoPQ apparatus. The possibility of luminal bacterial killing is further explored in Chapter 5.

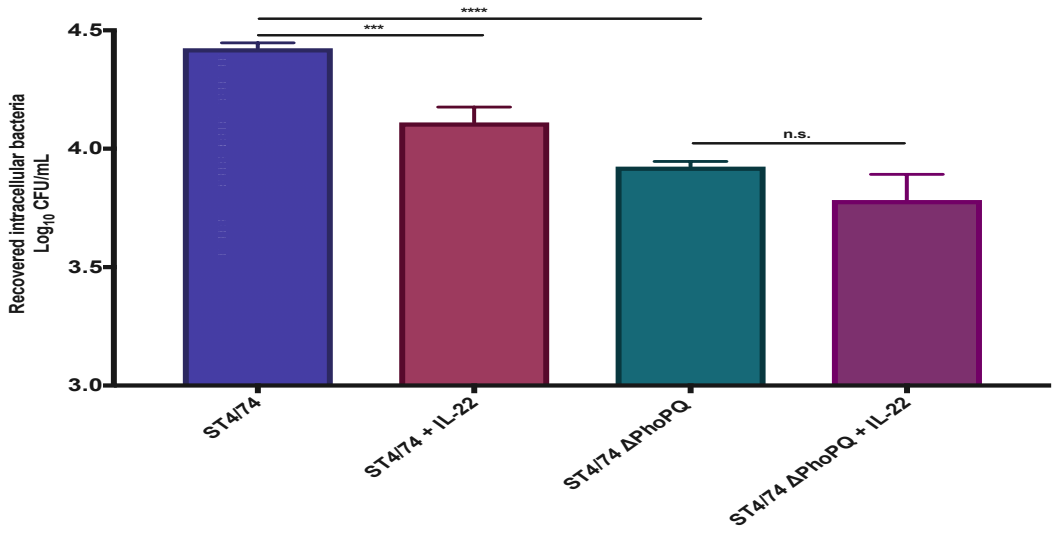

Figure 4.7: Intracellular bacterial counts at timepoints following injection for ST4/74 and ST4/74 ΔPhoPQ in Kolf2 iHO. iHO were pre-treated for 18 hours with rhIL-22 at 100 ng/mL or left unstimulated. Following this, iHO were infected with either ST4/74 or ST4/74 ΔPhoPQ and incubated for 1.5 hours prior to modified gentamicin protection assay and recovery of intracellular bacteria. Data presented are for at least 3 biological replicates (each averaged from 3 technical replicates), with 30 iHO injected per replicate, +/- SEM. Unpaired Mann-Whitney tests were used for all assays (n.s. – not significant, *** < p<0.001, **** p< 0.0001). There were significantly fewer ST4/74 bacteria recovered from cells in iHO pre-treated with rhIL-22. This difference with IL-22 treatment was not seen in ST4/74 ΔPhoPQ, however significantly fewer ST4/74 ΔPhoPQ were recovered intracellularly following infection.

Time course assays for intracellular bacterial invasion were also completed to attempt to further establish the duration of protective effect of rhIL-22 against *Salmonella* infection. Here, assays were completed using ST4/74 or ST4/74 ΔPhoPQ, with iHO harvested at 1.5, 3, 6 and 8 hours. The initial restrictive effect of rhIL-22 pre-treatment on infection only appeared to hold true until the 3 hour timepoint in iHO injected with ST4/74, and there were no

differences in recovered bacterial counts at any timepoint for iHO injected with ST4/74 ΔPhoPQ (**Figure 4.8**). Again, recovered intracellular counts were lower for ST4/74 ΔPhoPQ at all timepoints (p = 0.02). Beyond the 3 hour timepoint, there was visible disruption of iHO integrity when examined under the microscope, suggesting that bacteria were not restricted to the enclosed lumen at this point and could invade the epithelium from either its apical or basal surface with less concentrated exposure to the iHO luminal contents.

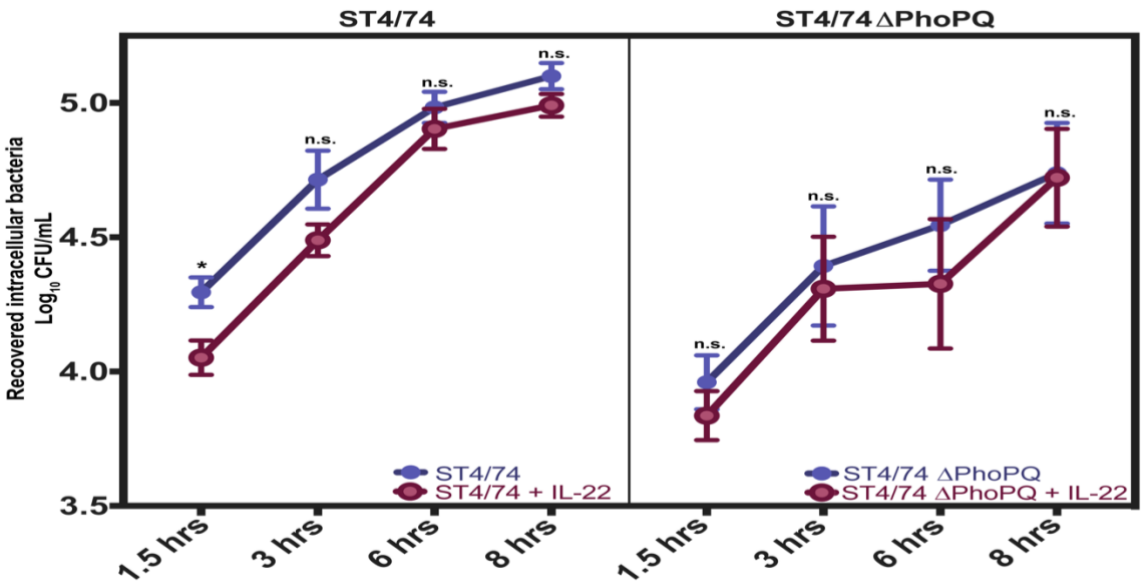

Figure 4.8: Intracellular bacterial counts at timepoints following injection for ST4/74 versus ST4/74 ΔPhoPQ in Kolf2 iHO. iHO were pre-treated for 18 hours with rhIL-22 at 100 ng/mL or left unstimulated. Following this, iHO were infected with either ST4/74 or ST4/74 ΔPhoPQ and incubated for 1.5, 3, 6 or 8 hours prior to modified gentamicin protection assay and recovery of intracellular bacteria. Data presented are for 3 biological replicates (each averaged from 3 technical replicates), with 30 iHO injected per replicate, +/- SEM. Unpaired Mann-Whitney tests were used for all assays (**n.s.** not significant, * < p<0.05). Restrictive effect of rhIL-22 on infection appears to only last up to the 3 hour timepoint for ST4/74, and no protective effect is seen with ST4/74 ΔPhoPQ. Recovered intracellular bacterial counts are lower in untreated ST4/74 ΔPhoPQ than ST4/74.

4.5 Effect of IL-22 stimulation on *S.* Typhimurium SL1344 infection in iMO

In order to ensure that the restrictive effect of IL-22 treatment was not an artefact in the iHO system, murine intestinal organoids (iMO) were produced and phenotyped from mucosal small intestine tissue from 2 wild type (WT) C57/B6 mice and 2 equivalent mice harbouring the *IL-22ra1*$^{-/-}$ mutation, as described in 2.5. Prior to use of iMO for invasion assays, RT-qPCR was completed to check for the presence of the components of the IL-22 receptor complex, and to assess if the IL-22-regulated genes LCN2 and DUOX2 responded to

IL-22 stimulation. Interestingly, whilst IL-10R2 was expressed in both WT and *IL-22ra1*$^{-/-}$ mice, it appeared to be expressed at a lower level in *IL-22ra1*$^{-/-}$ mice. IL-22R1 was expressed at a significantly higher level in WT mice than in *IL-22ra1*$^{-/-}$ mice and recombinant murine (rm)IL-22 stimulation yielded no upregulation of DUOX2 or LCN2 in *IL-22ra1*$^{-/-}$ mice, confirming the expected phenotype of lack of response to IL-22 (**Figure 4.9**).

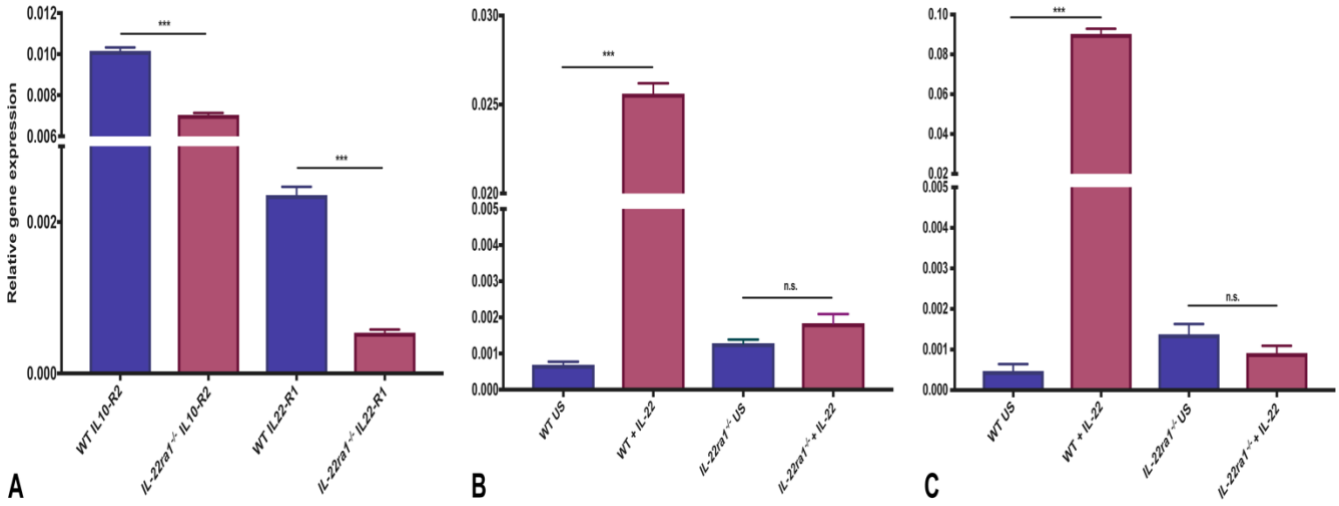

Figure 4.9: Relative gene expression for IL-22 receptor complex and response of IL-22 regulated genes to rmIL-22 stimulation. RNA harvested from iMO generated from both WT and *IL-22ra1*$^{-/-}$ mice underwent RT-qPCR to check for expression of the components of the IL-22 receptor (Panel **A**). iMO from WT and *IL-22ra1*$^{-/-}$ mice were treated with rmIL-22 at 100 ng/mL for 18 hours or left unstimulated. RNA was harvested and RT-qPCR completed to compare expression of IL-22 regulated genes DUOX2 (Panel **B**) and LCN2 (Panel **C**). Data presented are from 4 technical replicates, with assays repeated 3 times per mouse. Data were analysed using the comparative cycle threshold (C_T) method, with GAPDH as an endogenous control. Unpaired Mann-Whitney test was used to compare results (**n.s.** not significant, ***$p < 0.001$). (**A**) IL-10R2 was expressed in both wild type (WT) and *IL-22ra1*$^{-/-}$ mice but at a higher level in WT mice; IL-22R1 was expressed at a significantly lower level in *IL-22ra1*$^{-/-}$ mice. DUOX2 (**B**) and LCN2 (**C**) expression was significantly upregulated after treatment with rmIL-22 in WT mice but not in *IL-22ra1*$^{-/-}$ mice.

Microinjection assays to assess intracellular invasion of SL1344 were then completed (as described in 2.6) in WT and *IL-22ra1*$^{-/-}$ iMO, either unstimulated or following treatment with rmIL-22 at 100 ng/mL for 18 hours. There were significantly fewer bacteria recovered from WT iMO pre-treated with rmIL-22, and no difference in bacterial counts between the treated and untreated *IL-22ra1*$^{-/-}$iMO, indicating that IL-22-induced restriction of infection occurs in the iMO model in addition to the iHO model, and that IL-22R1 mediated signalling is necessary for that protection to occur (**Figure 4.10**).

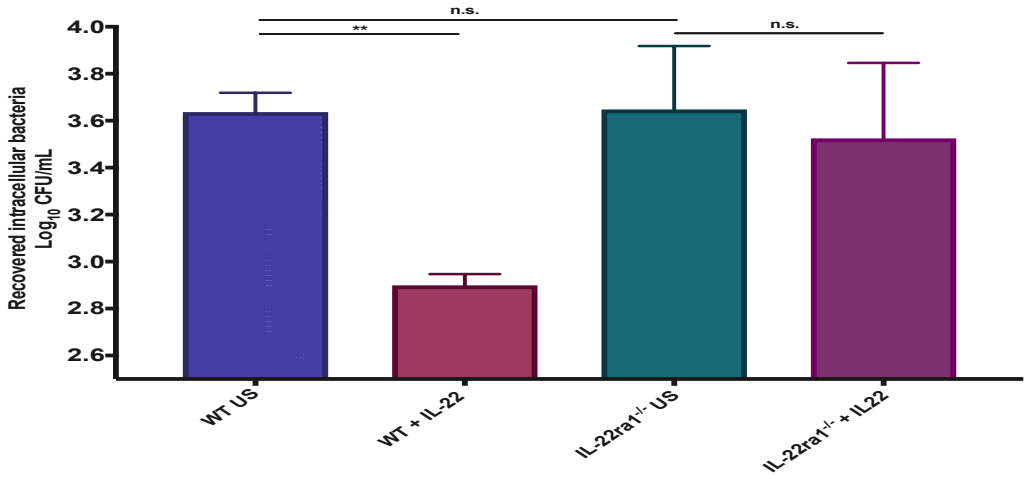

Figure 4.10: Restriction of intracellular SL1344 in WT iMO pre-treated with rmIL-22. iMO from WT and *IL-22ra1*$^{-/-}$ mice were treated with rmIL-22 at 100 ng/mL for 18 hours or left unstimulated. iMO were injected luminally with SL1344 and incubated for 1.5 hours prior to modified gentamicin protection assay and recovery of intracellular bacteria. Data presented are for 6 biological replicates (each averaged from 3 technical replicates), with 50 iMO injected per replicate +/- SEM. Unpaired Mann-Whitney tests were used for all assays (** $p < 0.01$, n.s. - not significant). Pre-treatment of WT iMO with rmIL-22 inhibited intracellular SL1344 infection. This inhibition of infection was not observed in *IL-22ra1*$^{-/-}$ iMO following rmIL-22 treatment.

4.6 Establishing the mechanism of protection mediated by IL-22 treatment in the iHO model

The reduced intracellular bacterial survival in iHO pre-treated with rhIL-22, suggests a difference in intracellular environment induced by IL-22. To further investigate this, TEM images were produced by Jessica Forbester and David Goulding at 90 minutes post-infection for iHO pre-treated with rhIL-22 versus untreated, and intracellular SL1344 populations reviewed at high resolution. Clear differences in the appearance of bacteria were noted between groups, with intracellular bacteria in the rhIL-22 treated group visibly more degraded, and increased numbers of phagolysosomes versus *Salmonella*-containing vacuoles seen in this cohort (**Figure 4.11**). Representative images were taken from 30 iHO injected per condition, using 100 µM sections of 1 mm iHO mucosa, and blinded scoring was used to produce counts for bacterial location as listed in **Table 4.1**. There were more degraded bacteria in Kolf2 iHO pre-treated with rhIL-22 than those untreated (49 vs. 11 respectively), and a significantly higher proportion of phagolysosomes to *Salmonella*-containing vacuoles in the IL-22 treated group.

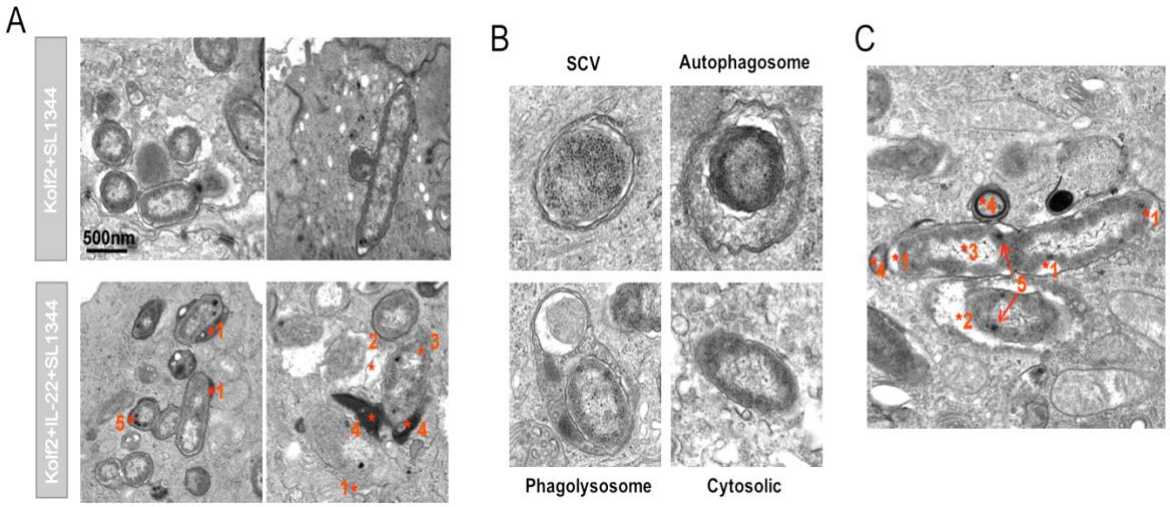

Figure 4.11: IL-22 protection is mediated through enhanced lysosomal fusion with SCVs in rhIL-22 treated Kolf2 iHO. (**A**) TEM images of SL1344 internalised into IECs of Kolf2 iHO pre-treated for 18hr with 100ng/mL IL-22 (bottom panel) or left untreated (top panel), showing healthy bacteria in untreated iHO, and degraded bacteria in rhIL-22 treated iHO 1.5 hours post-infection. (**B**) Visual characteristics used for classification of data displayed in **Table 4.1**. (**C**) Visual characterisation of bacterial cell damage/stress used for scoring: (1) widening of periplasmic space; (2) membrane damage and ragged appearance; (3) decrease in cytosol density; (4) direct contact with lysosomes; (5) volutin granules present (Figure adapted from Forbester et al, 2018[7])

Pathology:	**Kolf2**	**Kolf2 + IL-22**
Salmonella-containing vacuole	65	65
Autophagosome	1	2
Phagolysosome	6	30
Cytosolic	1	5
Fisher's exact test		**P=0.0003**

Table 4.1: Intracellular bacterial localisation in untreated versus rhIL-22 treated Kolf2 iHO.

It has been reported that IL-22 is able to restrict the intracellular growth of *Mycobacterium tuberculosis* in macrophages and that this effect can be negated by pre-treatment of cells with W7, a synthetic compound which inhibits phagolysosomal fusion.[18] Specifically, W7 (N-(6- Aminohexyl)-5-chloro-1-naphthalenesulfonamide hydrochloride, Sigma-Aldrich) inhibits Ca^{2+}/calmodulin interactions with their binding partners, which are part of the signalling pathway required for phagosomal maturation.[19] To investigate whether inhibition of phagolysosomal fusion reversed the protective effect of IL-22 treatment on intracellular infection with SL1344, 50µM W7 was added for 6 hours to Kolf2 iHO pre-treated with rhIL-22, prior to microinjecting with SL1344 and completing gentamicin protection assays for intracellular bacterial counts. These assays showed that in the presence of W7, the

restrictive effect of IL-22 on intracellular infection is lost, and recovered bacterial counts are equivalent to those from untreated iHO. In addition, this phenotype was replicated using pre-treatment with 100nM Concanamycin A (Insight biotechnology); a macrolide antibiotic which acts as a vacuolar ATPase inhibitor and has been shown to inhibit acidification of phagosomes and phagolysosomal fusion.[20,21] In order to show that neither phagolysosomal fusion inhibitor was affecting bacterial invasion via an alternative pathway, intracellular bacterial counts from untreated iHO were compared with W7 and Concanamycin A only treated iHO following injection with SL1344. These assays showed no significant difference in numbers of bacteria recovered between conditions (**Figure 4.12**).

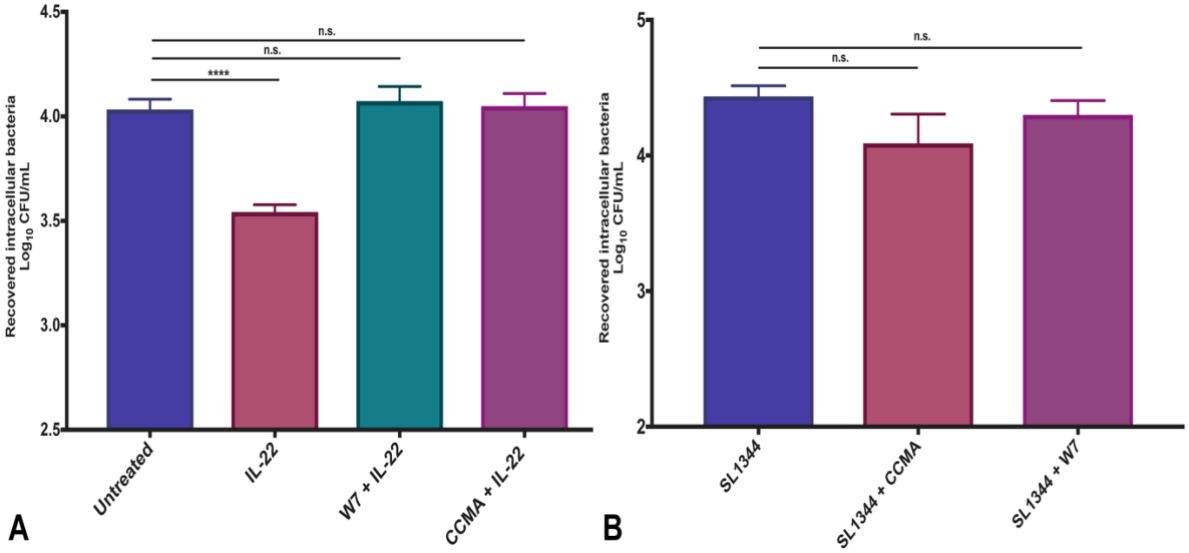

Figure 4.12: Use of phagolysosomal fusion inhibitors negates IL-22 mediated protection from SL1344 in Kolf2 iHO. Unstimulated iHO and iHO that had been pre-treated with rhIL-22 at 100 ng/mL for 18 hours, were additionally treated with 50 μM W7 for 6 hours or 100 nM Concanamycin A (CCMA) for 4 hours, or left untreated prior to injection with SL1344 and incubation for 1.5 hours. Modified gentamicin protection assays were performed and intracellular bacteria recovered. Data presented are for 3 biological replicates (each averaged from 3 technical replicates), with 30 iHO injected per replicate +/- SEM. Unpaired Mann-Whitney tests were used for all assays (**n.s**. not significant, **** p< 0.0001). (**A**) Kolf2 iHO pre-treated with IL-22 alone demonstrated restriction of intracellular SL1344 infection, whereas iHO treated with both IL-22 and W7 or CCMA showed no significant difference to untreated iHO in terms of numbers of intracellular bacteria recovered. (**B**) No significant difference in recovered intracellular bacteria was noted between untreated iHO and those treated with W7 or CCMA alone prior to injection with SL1344.

Rab7, a member of the Rab family of small GTP-ases, acts as a marker of the late endosome and late phagosome.[22,23] To this end, Rab7 immunostaining and RT-qPCR were used to further validate the mechanism of increased phagolysosomal fusion secondary to IL-22 treatment (methods outlined in 2.1.5). Fold change in *RAB7A* was significantly higher in iHO pre-treated with rhIL-22 then infected versus those left untreated and infected (**Figure 4.13**). In addition,

increased Rab7 expression via immunostaining was noted in SL1344-injected iHO pre-treated with rhIL-22, with Rab7 staining co-localising with common *Salmonella* antigen-1 (CSA-1), used to denote the presence of SL1344. Decreased Rab7 staining was observed in iHO which were treated with W7 in addition to rhIL-22. As noted on qPCR, increased Rab7 staining was also seen in uninfected iHO stimulated with rhIL-22 (data not shown).

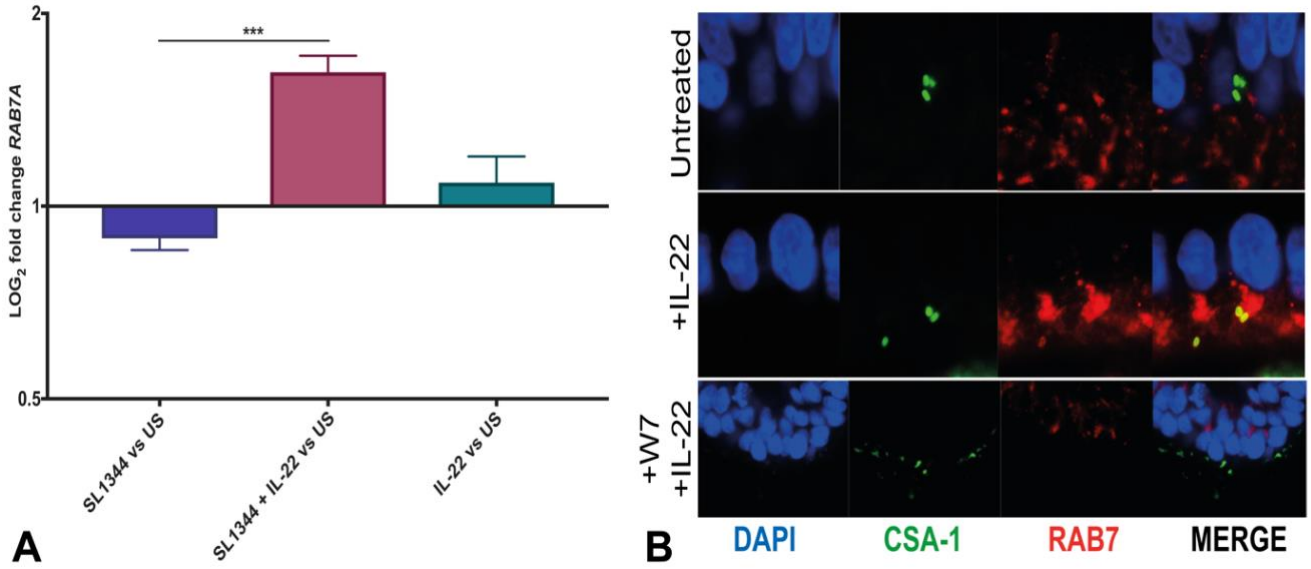

Figure 4.13: Increased expression of RAB7A in iHO pre-treated with rhIL-22. (**A**) iHO were either left unstimulated, or treated for 18 hours with rhIL-22 at 100 ng/mL. iHO were then left uninfected or injected with SL1344 and incubated for 3 hours, followed by harvesting and RNA extraction. RT-qPCR with TaqMan gene expression assay for *RAB7A* was then completed to compare RAB7A expression between treatment groups and unstimulated iHO. Data presented are LOG_2 fold change in expression of *RAB7A*, averaged from 4 technical replicates, with assays repeated 3 times. Data were analysed using the comparative cycle threshold (C_T) method, with GAPDH as an endogenous control. Unpaired student's t-test was used to compare results (***$p < 0.001$). A significant difference in *RAB7A* expression in SL1344-infected iHO pre-treated with rhIL-22 was noted versus those left untreated. (**B**) Kolf2 iHO were either left untreated, treated with rhIL-22 (100 ng/mL for 18 hours), or rhIL-22 + W7 (50 μM for 6 hours) prior to injection with SL1344 and incubation for 3 hours before fixing and staining. Immunostaining highlights DAPI (blue), Rab7 (red) and CSA-1 (green), with increased intensity of staining seen in samples pre-treated with rhIL-22 alone, and co-localisation of Rab7 and CSA-1 staining. Images taken on Zeiss LSM 510 Meta confocal microscope at 63x (Untreated, +IL-22 panels) or 40x (+W7 +IL-22 panel) magnification.

4.7 The role of Calgranulin B in IL-22-induced phagolysosomal fusion

It has been suggested that enhanced calgranulin A (S100A8) expression in response to IL-22 is necessary for enhancement of phagolysosomal fusion and inhibition of mycobacterial growth in macrophages.[24] This was not noted to be the case in this study by RT-qPCR (data not shown), however, increased expression of calgranulin B (S100A9) was induced by pre-

2: Materials and Methods

Collaboration note

Some of the methods described in this chapter have been published as: “Interleukin-22 promotes phagolysosomal fusion to induce protection against *Salmonella enterica* Typhimurium in human epithelial cells” (Forbester et al., 2018) and “Using Human Induced Pluripotent Stem Cell-derived Intestinal Organoids to Study and Modify Epithelial Cell Protection Against Salmonella and Other Pathogens” (Lees et al. 2019).

TEM imaging was performed by David Goulding, and I am grateful for the help of Christine Hale in setting up macrophage cultures, Jessica Forbester for advice on troubleshooting with organoid cultures and Derek Pickard for his assistance in producing the TIMER^{bac} EPEC strain. Bulk RNA-Seq libraries were constructed and sequenced by the DNA pipelines core facility at the Wellcome Trust Sanger Institute, and I thank Artika Nath for her help with the bulk RNA-Seq data analysis and Daniel Kunz for his assistance with the single cell RNA-Seq data analysis. Dr Simon Clare, WTSI, kindly provided the mice used to produce murine organoids.

2.1 Growth and differentiation of hiPSCs into iHO

2.1.1 Culture and passage of induced pluripotent stem cells

Human induced pluripotent stem cells (hiPSCs) were routinely maintained in the Essential 8 Flex™ (Gibco, E8 Flex) medium kit, as per manufacturer’s instructions, to allow weekend-free culture. However, hiPSCs can be adapted from other hiPSC culture systems, such as Essential 8™ (Gibco) and TeSR™-E8™ (Stemcell Technologies) with relative ease. Human intestinal organoids (iHO) were generated using hiPSCs derived from the Kolf2, Rayr2 and Sojd2 lines, as per the protocol published by Forbester et al.[1] These hiPSC were acquired through the Human Induced Pluripotent Stem Cells Initiative Consortium (HipSci; www.hipsci.org), an open-access reference panel of characterised hiPSC lines.[2]

Demographic information for these cell lines is detailed in **Table 2.1**. All lines come from healthy volunteers, with the Kolf2 line having been used extensively in research on host-pathogen interactions by the Dougan group.[3,4] Both this line and the other lines selected as comparators were chosen based on parameters provided during phenotyping by the HipSci consortium; namely high pluritest score, low copy number variations, well characterised assay data and high differentiation potential.

Table 2.1: Demographics of healthy volunteer cell lines used in this study

Cell line:	Donor age (years):	Donor sex:	Donor ethnicity:
Kolf2	55-59	Male	White – British
Sojd2	45-49	Female	White – Other
Rayr2	75-79	Male	White – British

iPSCs were grown until colonies covered approximately 80-90% of the plate surface. Plates for passage were prepared 1 hour prior to use, by adding Vitronectin XF 10 μg/mL (Stemcell Technologies) diluted in Dulbecco's PBS without calcium and magnesium (DPBS; Gibco) to tissue-culture treated plates and E8 Flex medium warmed to room temperature (r.t.). Medium was removed from iPSCs ready for passage and cells washed twice with DPBS (No Ca^{2+} or Mg^{2+}). Versene solution (Life Technologies) was added to plates, and they were incubated at r.t. for 5-8 minutes, until holes started to appear in the centre of the previously confluent iPSC colonies. At this time, Versene was aspirated, discarded, and replaced with E8 Flex. iPSCs were dislodged by washing the plate surface in this medium and cells moved to a 15mL Falcon tube. Vitronectin was aspirated from the pre-coated plates and replaced with E8 Flex, and the appropriate volume of iPSC suspension to give a 1:10 dilution of cells on the new plate. Ratios for splitting can be adjusted dependent on iPSC growth rate of different cell lines. Plates were rocked to disperse the iPSC across their surface, incubated at 37 °C / 5% CO_2 and fed the day following passage.

2.1.2 Differentiation from iPSC to hindgut

The directed differentiation process and cytokines involved are outlined in **Table 2.2.**

Table 2.2: Directed differentiation process for hindgut production from hiPSC

Day:	Activity:
0	iPSCs were split onto a 10cm tissue culture-treated dish, pre-coated with Vitronectin XF as described above, into 10 mL Essential 8 Flex medium supplemented with activin A (10 ng/mL) + basic fibroblast growth factor (bFGF; 12 ng/mL). Growth factors were added to medium directly before use; as was the case in all subsequent steps.
1	Medium was changed to 10 mL Essential 8 Flex medium supplemented with activin A (10 ng/mL) + basic fibroblast growth factor (bFGF; 12 ng/mL).
2	Differentiation was commenced by changing the medium to 10 mL Essential 8 Flex medium supplemented with the growth factors: activin A (100 ng/mL), bFGF (100 ng/mL), Bone morphogenetic protein 4 (BMP-4; 10 ng/mL), phosphoinositol 3-kinase inhibitor LY294002 (10 µM) and GSK3 inhibitor CHIR99021 (3 µM).
3	Medium was changed to 10 mL Essential 8 Flex medium supplemented with activin A (100 ng/mL), bFGF (100 ng/mL), BMP-4 (10 ng/mL) and LY294002 (10 µM). Endoderm specification induced by this medium resulted in visible changes to iPSC colony morphology over the following 24 hours.
4	Medium was changed to 10 mL RPMI/B27 medium supplemented with activin A (100 ng/mL) and bFGF (100 ng/mL). RPMI/B27 medium contains: 500 mL of RPMI Medium 1640 with GlutaMAX supplement, 10 mL B27 Supplement (50X, serum free) and 5 mL non-essential amino acids, with optional addition of 5 mL penicillin–streptomycin (10,000 U/ml).
5	Medium was changed to 10 mL RPMI/B-27 medium supplemented with activin A (50 ng/mL).
6	To begin patterning posterior endoderm to hindgut, medium was changed to 10 mL RPMI/B27 supplemented with CHIR99021 (6 µM) + Retinoic acid (3 µM).
7,8,9	Medium was changed daily with the same composition as for day 6. During these steps visible 3-D structures of hindgut became apparent, covering the surface of the plate.
10	The resulting hindgut was embedded in Matrigel (Corning) (See **Figure 2.1** for outline of process with illustration).

2.1.3 Embedding of hindgut into Matrigel

iHO base growth medium (BGM) was produced (see **Table 2.3** for contents) and filter sterilized before use. Medium was removed from the hindgut plate, which was washed once with DPBS (No Ca^{2+} or Mg^{2+}). 5 mL collagenase solution (see **Table 2.4** for contents) was added to the plate and incubated at 37 °C for 5 minutes. The collagenase was inactivated by addition of 5 mL BGM to plate, hindgut structures were dislodged using a cell scraper, and the resulting

suspension collected into a 15 mL falcon tube. The suspension was centrifuged at 1200 rpm for 1 minute. Supernatant was removed and replaced with 10 mL BGM, and hindgut gently pipetted to break it up into smaller pieces. This solution was centrifuged at 750 rpm for 1 minute and washed twice with BGM by repeating this step. Cells were re-suspended in a small volume of BGM (~300-500 µL) and around 100 µL of this solution was added to 1.5 mL Matrigel. 60 µL of this solution was added to one well of a 24 well plate (set up on a plate heater at 37 °C) and allowed to set. Density was checked under a microscope, and if required, further hindgut solution was added until the desired density of seeding was achieved. Matrigel was then spotted out into the remaining wells on the plate. After incubation of the plate at 37 °C for 10 minutes, 800µL BGM containing growth factors (see **Table 2.5**) was added to each well.

Medium was changed every 2-3 days, or immediately if medium was discoloured; on these occasions, Y-27632 was omitted as it is only required when splitting/seeding. After initial seeding into Matrigel, iHO were allowed around 7 days to develop before splitting. By day 3–4 post-embedding, distinct spheres were visible in the culture.

2.1.4 Maintenance and passage of iHO

iHO require at least 1 month of routine passaging after seeding to facilitate maturation, with splitting required every 4–7 days. Note that there will be some variation in iHO development depending on iPSC line used and the density of the initial culture. During the first few passages there will be visible contaminating cells which are not iHO. These will eventually die, leaving a clean culture of spherical and, after approximately 4 weeks, budded organoids (as demonstrated in **Figure 2.1**). In addition, use of an in-hood imaging system can be used to select and passage only iHO with the desired morphology. As iHO mature, they will require splitting every 6-7 days, dependent on growth rate and density. If any of the following are true, iHO should be split prior to this point:

- The luminal cavities of the iHO start to fill up with dead cells
- The Matrigel starts to disintegrate
- iHO start to grow out of the Matrigel
- The culture is too dense and the medium starts to go yellow rapidly

Splitting process:

Medium was removed from iHO and replaced with 500 µL Cell Recovery Solution (BD) per well. The plate was then incubated at 4 °C for 40-50 minutes, at which point iHO were floating in solution. This solution was then gently pipetted into 15 mL falcon tubes (trying not to break up iHO) and allowed to settle for 3-5 minutes before removing supernatant and single cells. iHO were re-suspended in 5 mL BGM and pipetted gently to wash, then centrifuged at 750 pm for 2 minutes. Supernatant was removed, iHO re-suspended in ~300-500 µL BGM and a P1000 was used to break up iHO into smaller chunks. Around 100 µL of iHO solution was added to 1.5 mL Matrigel and pipetted briefly to mix, then the resulting solution plated out into a 24 well plate and overlaid with BGM containing growth factors as described above. To prepare for an invasion assay experiment, iHO were passaged 4-5 days prior to an experiment as described above, but 120µl droplets of Matrigel/iHO solution were placed into 5mm glass bottomed microinjection dishes. Rather than leaving the iHO suspension in a droplet as with routine passaging, the solution was spread over the bottom of the dish to create a thin layer of Matrigel and overlaid with 2.5 mL base growth medium plus growth factors. If antibiotics had been used in BGM, these were removed and replaced with non-antibiotic supplemented media prior to microinjection experiments.

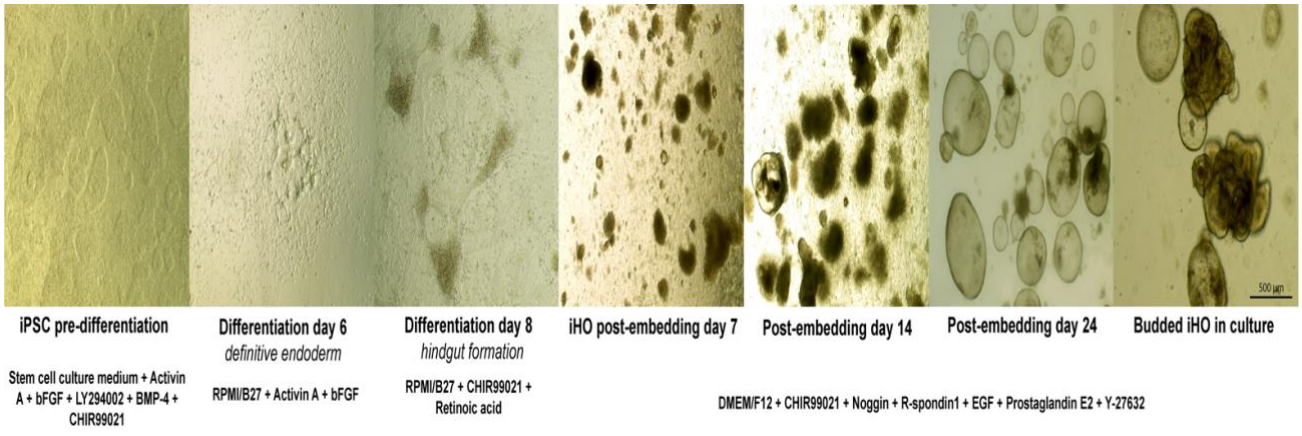

Figure 2.1: Sequential imaging of differentiation process from iPSC to iHO (Images taken on Thermo-Fisher EVOS XL imaging system at 4x / 10x magnification).

Table 2.3: Components of iHO base growth medium

Component:	Manufacturer:	Amount:
Advanced DMEM/F12	Invitrogen	500 mL
B27 serum-free supplement 50x	Life Technologies	10 mL
N2 serum-free supplement 100x	Life Technologies	5 mL
HEPES 1 M	Life Technologies	5 mL
L-glutamine 200 mM	Life Technologies	5 mL
Optional: Penicillin-streptomycin (10,000 U/mL)	Life Technologies	5ml

Table 2.4: Components of collagenase solution

Component:	Manufacturer:	Amount:
Collagenase IV powder	Life Technologies	500 mg
Advanced DMEM/F12	Gibco	400 mL
KnockOut Serum Replacement	Gibco	100 mL
L-glutamine 200 mM	Life Technologies	5 mL
2-Mercaptoethanol	Sigma-Aldrich	3.5 μL

Table 2.5: Growth factors for iHO base growth medium

Component:	Manufacturer:	Amount:
Recombinant human R-spondin 1	R&D	500 ng/mL
Recombinant human Noggin	R&D	100 ng/mL
Epidermal growth factor (EGF)	R&D	100 ng/mL
Prostaglandin E_2	Sigma	2.5 μM
CHIR99021	Abcam	3 μM
Y-27632 dihydrochloride monohydrate	Sigma-Aldrich	10 μM

2.1.5 Phenotyping of iHO

After 4 weeks in culture, iHO underwent phenotyping by means of RT-qPCR, immunostaining for cell types and fixation for transmission electron microscopy (TEM).

RT-qPCR for markers of cell types

RNA was extracted from iHO using RNeasy Mini Kit (Qiagen), and reverse transcribed using Qiagen QuantiTect reverse transcription kit as per the manufacturer's instructions.

Resultant cDNA was used to perform RT-qPCR using TaqMan gene expression assays and gene expression mastermix (Applied Biosystems) on the Applied Biosystems StepOne real-time PCR system. The aim here was to confirm phenotyping by monitoring the upregulation of transcripts for markers of intestinal tissue in comparison to iPSC.

Quantitative PCR (qPCR) was used to perform a comparison of selected gene expression between iPSC and iHO. This approach revealed that markers of pluripotency such as POU5F and NANOG are highly expressed in iPSC, whereas Vil1 (protein coding gene for villin), Lys (lysozyme, secreted by Paneth cells), Muc2 (mucin 2, secreted by goblet cells) and Chga (chromogranin A – produced by enteroendocrine cells) genes were more highly expressed in iHO, indicating differentiation into these cell types (**Figure 2.2**).

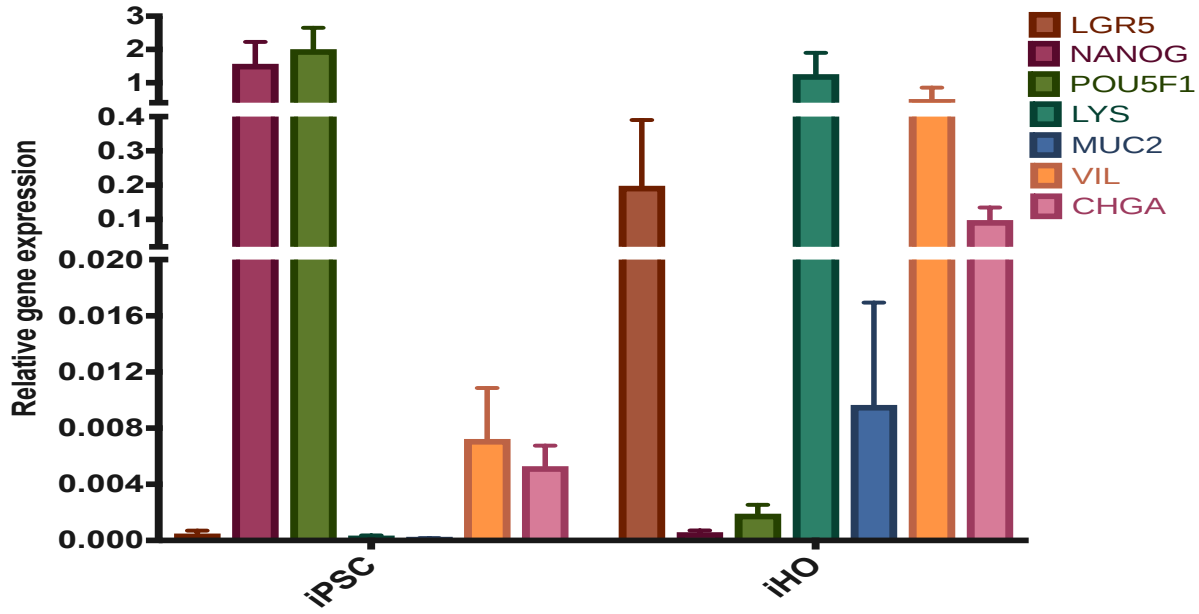

Figure 2.2: Differences in relative gene expression between iPSC and iHO in Kolf2 cell line. Data presented are from 4 technical replicates, with assays repeated 3 times using paired iPSC/iHO of different batches. Data were analysed using the comparative cycle threshold (C_T) method, with GAPDH as an endogenous control.

Immunostaining for markers of constituent cell types in iHO

Organoids were grown in 40µl Matrigel on Millicell EZ slide 4-well slides (Merck) for 5-6 days, then fixed in 4% paraformaldehyde (Sigma) in DPBS (no Ca^{2+} or Mg^{2+}) for 1 hour at r.t. Samples were rinsed x3 in DPBS; then blocked and permeabilised in 2% Triton X-100 (Sigma) with 5% foetal bovine serum (FBS; Sigma-Aldrich) diluted in DPBS for 2 hours. Primary antibodies diluted in 0.25% Triton X-100 / 5% FBS in DPBS were applied overnight at 15°C

(see **Table 2.6** for antibody concentrations and suppliers). Samples were rinsed x3 in DPBS and secondary antibodies applied then incubated for 3-4 hours at r.t. Samples were again rinsed x 3 in DPBS and nuclei counterstained with 10nM DAPI dilactate (Sigma-Aldrich) diluted in DPBS for 30 minutes at r.t. Samples were rinsed x6 in DPBS, immersed in FocusClear™ (2B Scientific) and covered for 2-4 hours to enhance sample transparency. FocusClear™ was removed and the plastic cage taken off samples, which were mounted directly in Prolong Gold with DAPI (Invitrogen), and analysed on the Zeiss LSM 510 Meta or Leica SP8 confocal microscopes. **Figure 2.3** demonstrates representative images of the phenotyping process for iHO from the Kolf2 cell line.

This protocol was also used to investigate protein expression and demonstrate presence of bacteria interacting with the epithelium following microinjection of the organoids with pathogens of interest.

Table 2.6: Antibodies used for immunostaining

Target	Host	Clonality	Isotype	Source	Dilution
Primary antibodies					
MUC2	Mouse	Monoclonal	IgG1	Abcam	1:200
LYZ	Rabbit	Polyclonal	Unknown	Abcam	1:50
VIL1	Mouse	Monoclonal	IgG1	Abcam	1:50
CHGA	Mouse	Monoclonal	IgG2b / IgG1	Abcam / Bio-Techne	1:50 / 1:100
IL-10R2	Rabbit	Polyclonal	IgG	Abcam	1:50
IL-22R1	Rabbit	Polyclonal	IgG	Abcam	1:100
S100A9	Rabbit	Polyclonal	IgG	Abcam	1:200
Rab7	Mouse	Monoclonal	IgG	Abcam	1:50
CARD8	Rabbit	Polyclonal	IgG	Abcam	1:100
Integrin alpha 6	Mouse	Monoclonal	IgG2b	Abcam	1:400
Goat anti-salmonella CSA-1 (FITC)	Goat	Polyclonal	Unknown	Insight Biotechnology	1:20
Secondary antibodies					
Goat anti-rabbit IgG Alexa fluor 456	Goat	Polyclonal	IgG	Life Technologies	1:100
Goat anti-mouse IgG FITC	Goat	Polyclonal	IgG	Abcam	1:100
Goat anti-mouse IgG TRITC	Goat	Polyclonal	IgG	Thermo-Fisher	1:200
Donkey anti-rabbit IgG Alexa fluor 647	Donkey	Polyclonal	IgG	Abcam	1:100
Other compounds used for staining					
Alexa fluor 647 phalloidin	N/A	N/A	N/A	Thermo-Fisher	1:1000
Lectin UEA-I (FITC conjugated)	N/A	N/A	N/A	Sigma-Aldrich	1:100
DiD (4-chlorobenzene sulfonate salt)	N/A	N/A	N/A	Biotium	2µg/ml
DAPI dilactate	N/A	N/A	N/A	Sigma-Aldrich	10nM

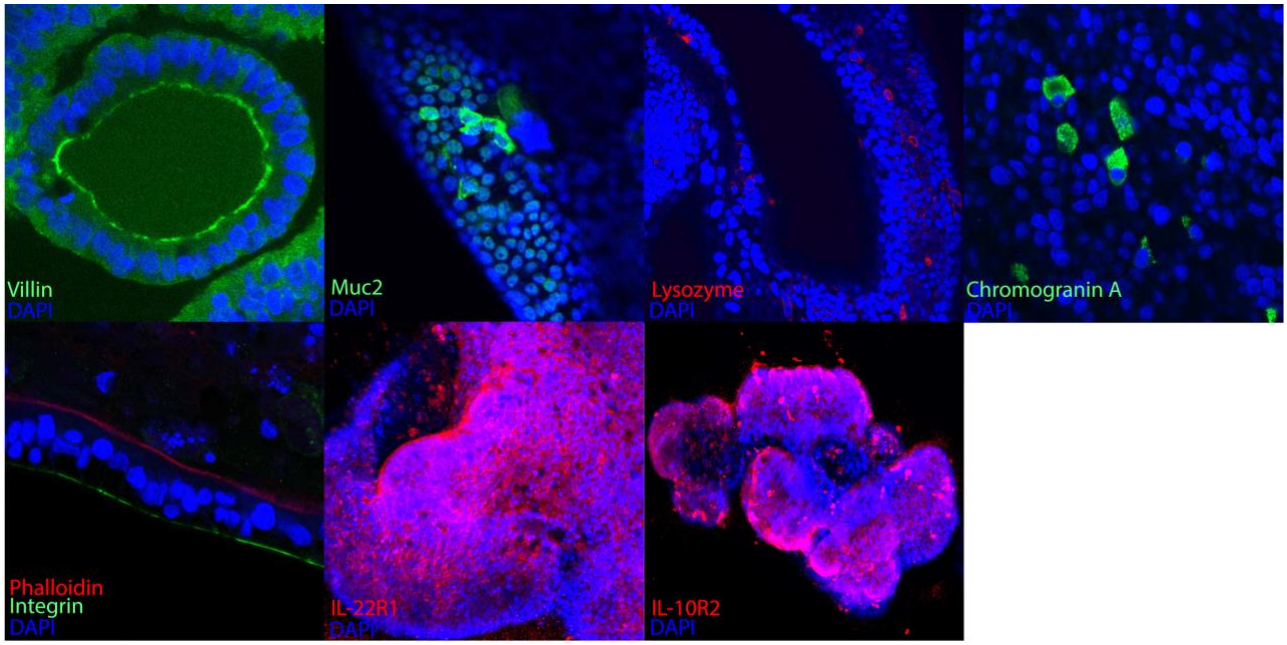

Figure 2.3: Immunostaining with specific antibodies for presence of constituent intestinal cell types in Kolf2 iHO. Imaged are iHO with nuclei stained blue with DAPI. Villin is a cytoskeletal protein of microvilli of the epithelial brush border in the intestine, and therefore a marker of the presence of enterocytes. Secretory cell types are marked by staining of the proteins they produce; lysozyme is an antimicrobial enzyme produced by Paneth cells, chromogranin A is a neuroendocrine secretory protein produced by enteroendocrine cells and mucin 2 is a protein secreted by intestinal goblet cells. Staining for integrin alpha 6 and phalloidin demonstrates an organised, polarised epithelium with an apparently continuous luminal surface. Images taken on Zeiss LSM 510 Meta confocal microscope (villin and phalloidin at 40x magnification, all other markers at 20x magnification).

TEM for constituent cell types in iHO

iHO were grown for 5-6 days on 50mm glass bottomed wells (MatTek corporation). BGM was aspirated and iHO fixed in 2.5% glutaraldehyde and 2% paraformaldehyde in 0.1 M sodium cacodylate buffer (see **Table 2.7** for components) for 1 hour at r.t. Specimens were washed x 3 in sodium cacodylate buffer, then incubated in 1% osmium tetroxide in sodium cacodylate buffer at r.t. for 1 hour. Samples were washed x 3 in sodium cacodylate buffer, transferred to glass vials and stained with 1% tannic acid in sodium cacodylate for 30 minutes at r.t. Samples were then washed with 1% sodium sulphate in distilled water for 10 minutes. Samples were dehydrated through suspension in ethanol in series of concentrations: 30%, 30% with uranyl acetate (also at 30%), 50%, 70%, 90% and then 3 X 100%, for 20 minutes each. A rotator was used to aid infiltration in these and the following steps. Samples were incubated for 2 x 15 minutes in propylene oxide (Sigma-Aldrich), then changed for a 1:1 mix of propylene oxide and Epon resin (Epoxy Embedding Medium kit, Sigma-Aldrich) for 1 hour. This was changed for neat Epon resin overnight, then samples

were embedded in fresh Epon resin in a flat moulded tray and cured at 65°C for 48 hours. 500nm semi-thin sections were cut on a Leica UCT ultramicrotome and stained with toluidine blue on a microscope slide. Images were recorded on the Zeiss Axiovert CCD camera and areas selected for ultrathin 50nm sectioning. Ultrathin sections were collected onto copper grids and contrasted with uranyl acetate and lead citrate before viewing on a FEI 120kV Spirit BioTWIN TEM and recording CCD images on an F4.15 Tietz charge-coupled device camera. **Figure 2.4** displays representative TEM images for iHO from the Kolf2 cell line.

Table 2.7: Components of sodium cacodylate buffer

Component:	**Manufacturer:**	**Amount:**
Distilled H_2O	MilliQ	1 litre
Sodium cacodylate trihydrate	Sigma-Aldrich	21.4 g
Magnesium chloride	Sigma-Aldrich	1 g
Calcium chloride	Sigma-Aldrich	0.5g
Hydrochloric acid	Fisher Scientific	Use to adjust to pH 7.42

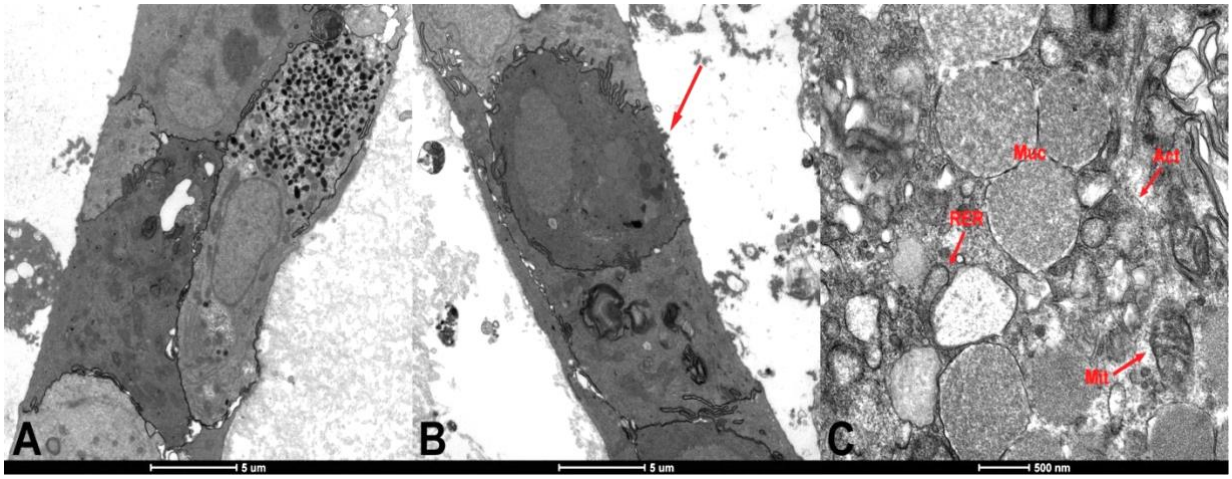

Figure 2.4: TEM images of iHO generated from Kolf2 cell line: (**A**) Enteroendocrine cell (identifiable by presence of secretory products stored in cytoplasmic granules) and (**B**) Goblet cell (recognisable by pale-staining mucin granules visible to right of nucleus). Also visible in this image are microvilli on the luminal aspect of the cell (arrow). (**C**) Magnified goblet cell (labelled are mucin granules (Muc), presence of mitochondria (Mit), actin (Act) and rough endoplasmic reticulum (RER)). Images taken on FEI 120kV Spirit BioTWIN TEM by D Goulding.

2.2 Pre-stimulation of iHO with rhIL-22

18 hours prior to invasion assays, media was aspirated from iHO, replaced with fresh BGM and rhIL-22 (R&D) then added to this culture media to a final concentration of 100 ng/mL.

2.3 Microinjection of iHO and intracellular invasion / intracellular survival / luminal killing assays

Cultures of bacteria of interest in 10 mL Luria-Bertani broth were incubated at 37 °C overnight with shaking, then diluted in DPBS (containing Ca^{2+} and Mg^{2+}) to an optical density of 2 at 600 nm (OD_{600}). Following this, cultures were mixed 1:1 with phenol red. The environmental chamber on the microscope was heated to 37 °C prior to starting the assay. A 6 μm microinjection drill tip (Eppendorf) was loaded with the bacterial culture, attached to the microinjection arm of the Eppendorf TransferMan NK2-FemtoJet express system (see **Figure 2.5**) and injection pressure set to 600kPa, with an injection time of 0.5 secs. The microscope was focused on the iHO plate and a target iHO selected for injection. Each iHO was injected 3 times, and a set number of iHO injected per experiment (30 for invasion assays, 60 for RNA-Seq assays). Due to heterogeneity in iHO size and structure within a culture, it is necessary to inject a large number of iHO to control for variation. The use of phenol red allowed injected iHO to be identified for downstream processing and avoid duplicate injections. Following injections, iHO plates were incubated at 37 °C / 5% CO_2 for 90 minutes (or 3 hours for RNA-Seq / imaging assays), following which, BGM was aspirated, replaced with 3 mL Cell Recovery Solution and incubated at 4°C for 45 minutes. iHO / Cell Recovery Solution was then moved into a 15 mL falcon containing 5 mL DPBS, centrifuged at 1500 rpm for 3 minutes and supernatant removed. For intracellular invasion assays, a modified gentamicin protection assay was performed.[5] iHO were disaggregated by vigorous pipetting and resuspended in 5 mL BGM containing gentamicin (Sigma-Aldrich) at 0.1 mg/mL. This suspension was incubated at 37 °C for 1 hour to kill extracellular bacteria, then centrifuged at 1500 rpm for 3 minutes and washed x 1 with DPBS. iHO were resuspended in 500 μL Triton X-100 1% in DPBS (Sigma-Aldrich) and manually dissociated by pipetting ~50x. This mixture was incubated for 5 minutes at r.t. then serially diluted in DPBS 10-fold to generate 10^{-1}, 10^{-2} and 10^{-3} concentrations. 3 x 20 μL droplets of the neat and diluted solutions were pipetted onto pre-warmed LB agar plates and incubated overnight at 37 °C. Colony counting was performed the following day.

Assays to investigate intracellular invasion versus survival were completed using the technique above, with harvesting at 30 minutes to assay initial invasion or incubation for an

additional 90 minutes following gentamicin treatment, to allow assessment of intracellular survival.

Luminal killing assays were used to assess the survival of *S.* Typhimurium inside the iHO lumen. Here, untreated or rhIL-22 pre-treated iHO were microinjected and incubated for 90 min at 37°C with 5% CO_2. iHO were isolated from Matrigel as described above and care was taken not to disrupt the general structure of phenol red marked organoids. iHO were gently washed in DPBS, centrifuged at 1500 rpm, supernatant removed, re-suspended in 500 μL DPBS and then broken open by vigorous pipetting. The resulting solution containing bacteria, iHO and DPBS was centrifuged at 1500 rpm to pellet cellular material whilst leaving bacteria in suspension. Supernatants were serially diluted and 20 μl spots were plated onto pre-warmed LB agar plates for CFU counting. An alternative method for this assay was used for assays requiring iHO harvest over longer time periods. In these assays, 3 single iHO were isolated from Matrigel at each time point using a disposable scalpel (Swann Morton) and manually disrupted into 100 μL DPBS. This solution was then centrifuged at 1500 rpm, serially diluted and plated as described above. Results for both methods gave comparable bacterial counts when directly compared.

Gentamicin protection assays and luminal killing assays were performed with at least three biological replicates per condition. For statistical comparisons of bacterial counts, unpaired, two-tailed *t* tests or Mann-Whitney tests were carried out, using the Prism 7 software (GraphPad).

Time course assays of both intracellular and luminal contents were performed, with iHO harvested at varying timepoints over the 6 hour period post-injection. Competition assays between different strains of *S*. Typhimurium were carried out by co-infecting iHO with 2 bacterial strains simultaneously, one of which was the TIMER^{bac}-*Salmonella*, as described by Claudi et al,[6] which produces fluorescent orange colonies, thus allowing discrimination between the strains when recovered from the intracellular compartment and plated.

For assays investigating inhibition of phagolysosomal fusion, iHO that had been pre-treated with rhIL-22 were either treated with 50μM W7 phagolysosomal fusion inhibitor (*N*-(6-Aminohexyl)-5-chloro-1-naphthalenesulfonamide hydrochloride, Sigma-Aldrich) for 6 hours

prior to injection, 100nM Concanamycin A (Insight Biotechnology) for 4 hours prior to injection, or left untreated. Microinjections and gentamicin protection assays were then completed as described above. **Table 2.8** lists all bacterial strains used for infection assays.

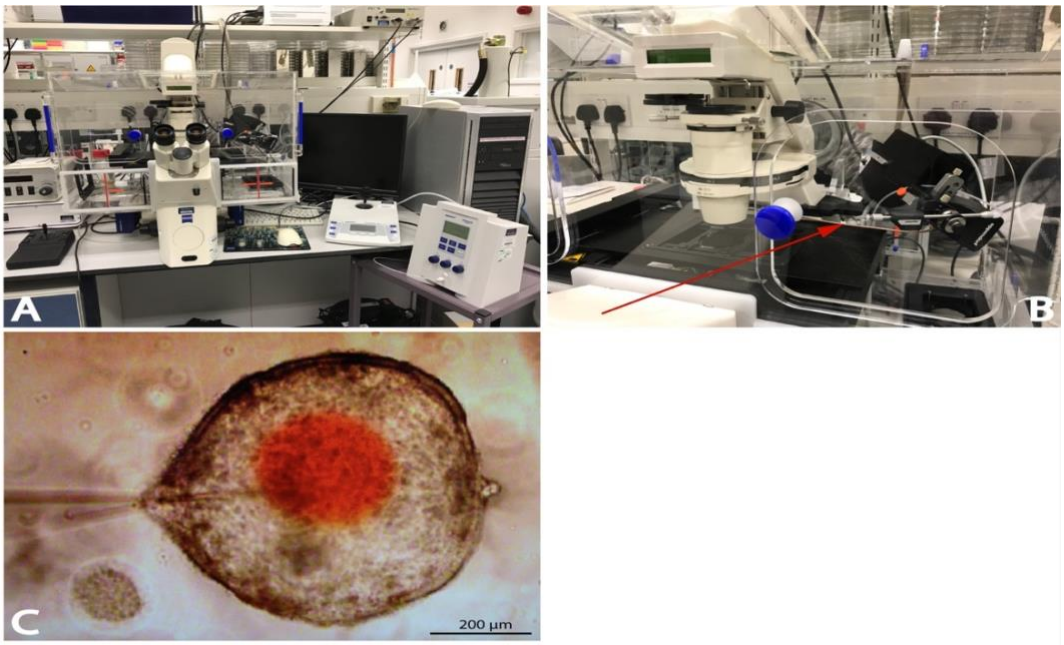

Figure 2.5 Microinjection of iHO with *S*. Typhimurium SL1344. Image (**A)** shows the setup of the microinjection system with environmental chamber, allowing for injection of the iHO at 37 °C. The Eppendorf TransferMan NK2-FemtoJet express system fitted with microcapillary (**B**) allows bacterial inoculum to be delivered directly into the luminal cavity of the iHO. By mixing bacterial inoculums with phenol red, infected iHO can be marked for downstream processing (**C**). Images were taken at ×100 magnification.

Table 2.8: Bacterial strains used for infection assays

Strain name and number:	**Source:**
S. Typhimurium SL1344 WT	Derek Pickard, WTSI
S. Typhimurium ST4/74 WT	Derek Pickard, WTSI
S. Typhimurium ST4/74 Δ*PhoPQ*	Derek Pickard, WTSI
S. Typhimurium SL1344 Δ*invA*	Derek Pickard, WTSI
S. Typhimurium TIMER^{bac}-*Salmonella* SL1344	Dirk Bumann, University of Basel
Enteropathogenic *Escherichia Coli* (EPEC) E2348/69	Derek Pickard, WTSI
TIMER^{bac}- EPEC E2348/69	Produced in collaboration with Derek Pickard
S. Enteritidis 6206	Rafal Kolenda, University of Wroklaw
S. Enteritidis 6174	Rafal Kolenda, University of Wroklaw
S. Enteritidis P125109 (PT4)	Derek Pickard, WTSI
S. Typhi Ty2 BRD948 Δ*aroC, aroD, htrA*	Derek Pickard, WTSI
S. Typhimurium ST313 D23580	Derek Pickard, WTSI
S. I:4,[5],12:i:− *(S*. Typhimurium variant) ST34 VNB1779	Stephen Baker, OUCRU (clinical isolate, Vietnam)
S. I:4,[5],12:i:− *(S*. Typhimurium variant) ST34 VNB2140	Stephen Baker, OUCRU (clinical isolate, Vietnam)
S. I:4,[5],12:i:− *(S*. Typhimurium variant) ST34 VNB2315	Stephen Baker, OUCRU (clinical isolate, Vietnam)
S. I:4,[5],12:i:− *(S*. Typhimurium variant) ST34 VNS20081	Stephen Baker, OUCRU (clinical isolate, Vietnam)
S. I:4,[5],12:i:− *(S*. Typhimurium variant) ST34 VNS20101	Stephen Baker, OUCRU (clinical isolate, Vietnam)
S. Typhi Quailes strain	Oxford Vaccine Group (challenge strain)
S. Paratyphi A NVGH308	Oxford Vaccine Group (challenge strain)
S. Typhi E02-1180 SGB90	Derek Pickard, WTSI (clinical isolate, India)
S. Typhi 2010K-0515 101TY	Derek Pickard, WTSI (clinical isolate, Kenya)
S. Typhi 2010K-0517 116TY	Derek Pickard, WTSI (clinical isolate, Kenya)

2.4 Electroporation of TIMER^{bac} plasmid into alternative bacteria

The TIMER^{bac} plasmid was electroporated into Enteropathogenic *Escherichia Coli* (EPEC) to provide fluorescent bacteria for imaging of bacterial-epithelial interactions in the iHO lumen. To obtain plasmid DNA, TIMER^{bac} Salmonella were incubated overnight at 37°C in 10 mL LB broth with shaking, then a Qiagen plasmid midi prep kit was used as per manufacturer's instructions to extract the TIMER^{bac} plasmid, which was stored at 4°C until use. Cultures of EPEC strain E2348/69 (serotype O127:H6) in 10 mL LB broth were incubated at 37°C with shaking. 1 mL of overnight culture was added to a conical flask containing 100 mL of LB broth and re-incubated at 37°C with shaking for 2-3 hours until an OD_{600} of 0.3 was reached. This solution was split into 4 x 25 mL aliquots and centrifuged at 4000 rpm at 4°C for 10 mins. Supernatant was discarded and bacteria resuspended in 30 mL ice-cold glycerol 10% (Sigma-Aldrich) before again being centrifuged at 4000 rpm at 4°C for 10 mins. This glycerol washing step was repeated, supernatant discarded and bacterial pellet re-suspended in 130 µL glycerol. 60 µL of this suspension and 3-5 µg of PCR product was added to pre-cooled 2mm electroporation cuvettes (Cell Projects Ltd). The extracted plasmid RNA was electroporated into bacterial cells at 2.4 kV using the Bio-Rad Micropulser. 500 µL of S.O.C. medium (Invitrogen) was added to the cuvette, which was incubated at 37°C for 2 hours to allow cells to recover. 3 x 100 µL bacterial solution was plated onto LB plates containing ampicillin (for maintenance of plasmid) and incubated overnight at 37°C. 20 colonies from these plates were placed onto fresh agar plates and again incubated overnight at 37 °C. Colonies fluoresced orange, indicating the successful transfer of the TIMER^{bac} plasmid.

2.5 Production and culture of murine organoids (iMO)

Mucosal tissue was harvested from 2 wild type C57/B6 mice and 2 equivalent mice harbouring the IL-22RA1$^{-/-}$ mutation and seeded into Matrigel in order to generate small intestinal iMO as described by Sato *et al*.[7] Organoids were overlaid with media comprising 90% base growth media (see **Table 2.9** for composition) and 10% R-Spondin 1 conditioned media. Growth factors were added to media in the concentrations described in **Table 2.10**.

In addition, 1 µM Y-27632 was added to media for initial seeding, but was not required for subsequent passages. iMO were passaged every 3-4 days by dissolving Matrigel using Cell Recovery Solution, then centrifugation at 2000 rpm for 2 minutes. Supernatant was removed, iMO were resuspended in BGM and manually disrupted via vigorous pipetting. Disrupted iMO were resuspended in Matrigel at a ratio of 1:3 – 1:5 depending on desired density, re-plated into 6 well plates and overlaid with BGM, which was changed every 2-3 days.

Table 2.9: Base growth media for iMO

Component:	**Manufacturer:**	**Amount:**
Advanced DMEM/F12	Invitrogen	500 mL
GlutaMax	Life Technologies	5 mL
HEPES 1M	Life Technologies	5 mL
N2 serum-free supplement 100x	Life Technologies	5 mL
B27 serum-free supplement 50x	Life Technologies	10 mL

Table 2.10: Growth factors for iMO media

Component:	**Manufacturer:**	**Amount:**
Recombinant murine Noggin	Peprotech	100 ng/mL
N-acetyl-cysteine	Sigma	1 mM
Murine epidermal growth factor (EGF)	Invitrogen	50 ng/mL

iMO produced in this way underwent phenotyping via light microscopy and immunostaining for cell-specific markers, with methods as for these assays done in iHO (**Figure 2.6 & 2.7**).

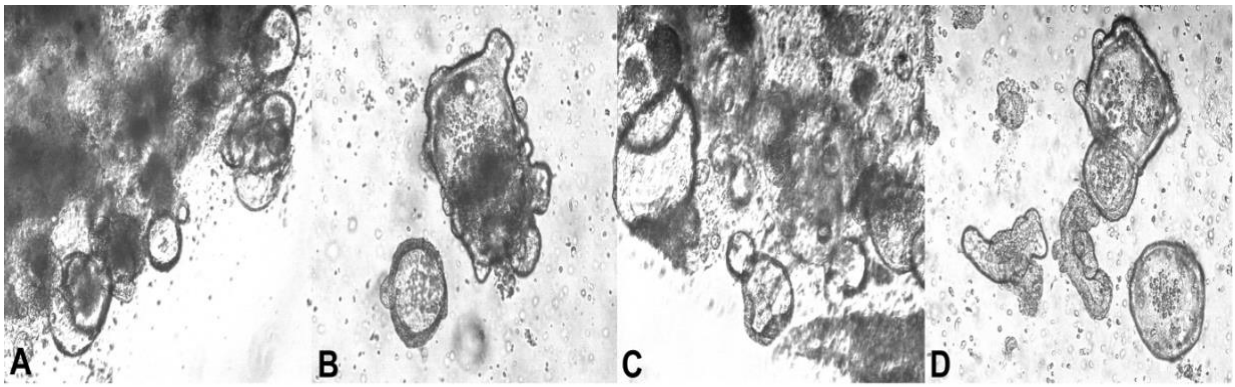

Figure 2.6: Light microscopy of iMO development. Panels A & C show WT and IL-22RA1$^{-/-}$ iMO respectively at day 3 post-embedding, and panels B & D at passage 13. Clearing of non-organoid tissue and development of budded structure is noted in both WT and IL-22RA1$^{-/-}$ lines.

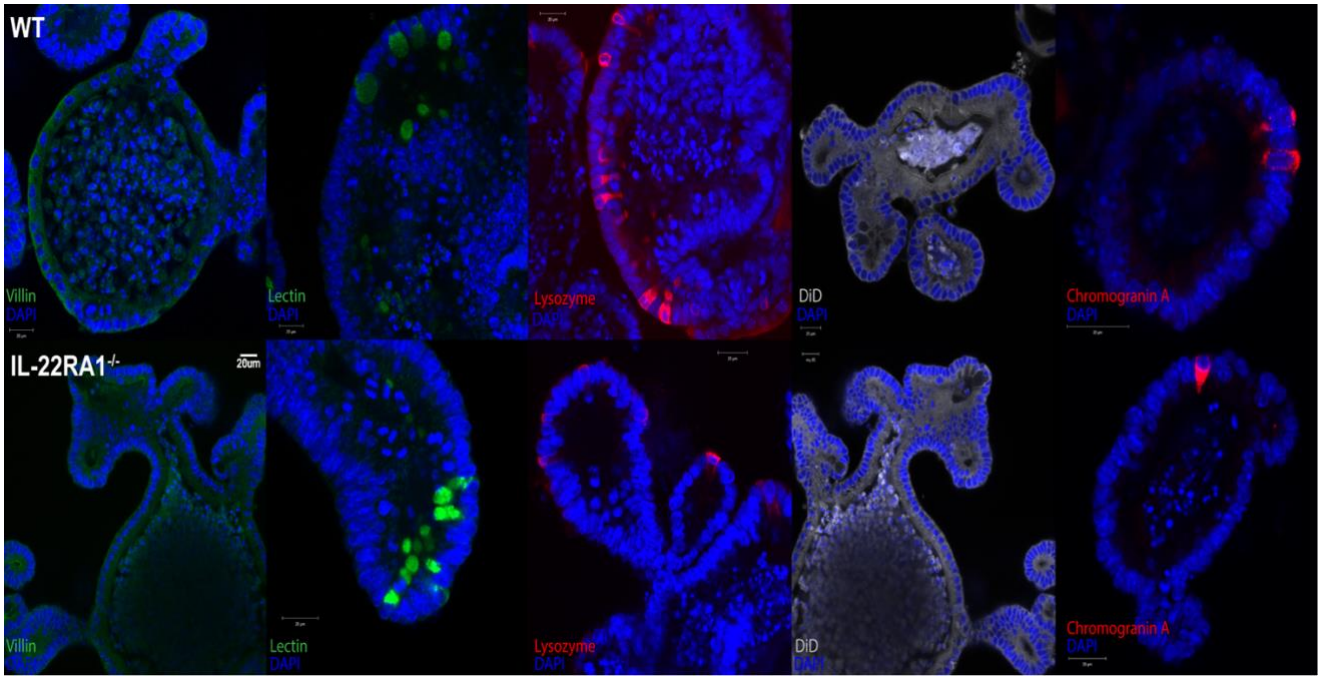

Figure 2.7: Immunostaining of iMO with specific antibodies for presence of constituent intestinal cell types. Imaged are iMO from WT and IL-22RA1$^{-/-}$ mice with nuclei stained blue with DAPI. iMO epithelial cells are stained with villin, Paneth cells with lysozyme and enteroendocrine cells with Chromogranin A. Goblet cells are stained with Lectin, and membrane staining is done with DiD . Images taken on Zeiss LSM 510 Meta confocal microscope at 20x magnification (scale bars indicate 20μm in each panel).

2.6 Microinjection of iMO and intracellular invasion assays

The set up for these assays was similar to that outlined for microinjection of iHO in 2.3. Differences with the iMO injection protocol were that iMO were microinjected at a pressure of 400 kPa and injection time 0.1 secs, with one injection per iMO, reflecting the smaller internal volume of these organoids. Because of difficulties manually disaggregating iMO related to their small size; following injection, incubation and washing in DPBS, iMO were re-suspended in 1 mL TrypLE (Gibco), incubated at 37°C for 3 minutes, then gently pipetted to dissociate cells to a single cell solution. 2 mL BGM was added to the solution to stop the dissociation reaction, samples were centrifuged at 2000 rpm for 3 minutes and re-suspended in BGM containing gentamicin at 0.1 mg/mL. The remainder of the protocol was identical to that described in 2.3.

2.7 Single cell sequencing of iHO following rhIL-22 stimulation

The detailed single cell sequencing and data analysis protocol is provided in **Appendix 1.** Briefly, iHO were grown for 5 days, stimulated with rhIL-22 100ng / mL for 18 hours or left unstimulated. iHO were dissociated to single cells and FACS sorted onto 96 well plates. Cells were lysed and mRNA extracted and polyadenylated then reverse transcribed with SmartSeq-2 PCR. Nextera libraries were produced from resultant cDNA and were further amplified, pooled and submitted to the WTSI sequencing pipeline.

2.8 Western blotting for proteins of interest in iHO

Western blots were used to demonstrate the presence / absence of caspase-1 in iHO produced from hiPSC lines with a mutation in the CARD8 gene versus a healthy control. iHO were harvested using Cell Recovery Solution and washed once with ice-cold DPBS (No Ca^{2+} or Mg^{2+}). This was replaced with 200-300 μL chilled Radio Immunoprecipitation Assay (RIPA) buffer (see **Table 2.11** for contents) and samples were agitated for 30 minutes at 4°C, followed by centrifuging at 4°C for 20 minutes at 12,000 rpm. Supernatants were aspirated, placed into chilled microcentrifuge tubes and underwent bicinchoninic acid assays (Pierce BCA Protein Assay Kit, Thermo-Fisher), run on the FLUOstar Omega microplate reader (BMG Labtech) to determine protein concentration. Samples were diluted in RIPA buffer and denatured by addition of Laemmli buffer (see **Table 2.12** for composition) and heating to 95°C for 5 mins.

Table 2.11: Components of RIPA buffer

Component:	**Manufacturer:**	**Amount:**
Distilled H_2O	MilliQ	9 mL
Sodium chloride	VWR	150 mM
Triton X-100	Sigma-Aldrich	100 μL
Sodium deoxycholate	Sigma-Aldrich	0.05 g
Sodium dodecyl sulphate 10%	Sigma-Aldrich	100 μL
TRIS hydrochloride (pH 8)	Invitrogen	50nM
cOmplete Protease Inhibitor Cocktail	Roche	1 tablet

Table 2.12: Components of Laemmli buffer

Component:	Manufacturer:	Amount:
TRIS hydrochloride (pH 6.8)	Invitrogen	3.6 mL
Sodium dodecyl sulphate 20%	Invitrogen	4.5 mL
Glycerol 100%	Invitrogen	4.5 mL
β-mercaptoethanol	Sigma-Aldrich	2.4 mL
Bromophenol blue	Honeywell Fluka	0.74 μg

Samples were cooled to room temperature and electrophoresed by SDS-PAGE. 1 μL /mL of each sample was loaded onto Mini-PROTEAN TGX 12% gels (Bio-Rad), with All Blue Precision Plus Protein Standards (Bio-Rad) for comparison, and run at 175 V for 45 mins, with TRIS/glycine running buffer (National Diagnostics). Semi-dry transfer was completed onto ethanol-activated polyvinylidene difluoride (PDVF) membranes (Thermo-Fisher) at 70 mA for 75 mins in transfer buffer (see **Table 2.13** for components). Membranes were blocked in 5% milk in DPBS and 0.1% Tween-20 (PBS-T) (Bio-Rad), before incubating in primary antibody in 2% milk in PBS-T. Membranes were washed x 3 in PBS-T and incubated for 45 minutes with HRP-conjugated secondary antibody. Membranes were washed x 3 in PBS-T, developed using Clarity ECL blotting substrates (Bio-Rad) and imaged on the ImageQuant LAS 4000 (GE Healthcare). All membrane incubations were completed on a rocking platform at r.t. β-actin was used as an internal control for protein loading (see **Table 2.14** for antibodies used for Western blotting).

Table 2.13: Components of transfer buffer (1 L)

Component:	Manufacturer:	Amount:
TRIS hydrochloride	Invitrogen	5.62 g
Sodium dodecyl sulphate 10%	Invitrogen	3.7 mL
Glycine	Sigma-Aldrich	2.93 g
Methanol	Fisher Scientific	200 mL
Distilled H_2O	MilliQ	800 mL

Table 2.14: Antibodies used for Western blotting

Target	Host	Clonality	Isotype	Source	Dilution
Primary antibodies					
β-actin	Rabbit	Polyclonal	IgG	Abcam	1:2500
Caspase-1	Mouse	Monoclonal	IgG2a	R&D	1:1000
Secondary antibodies					
Goat anti-rabbit immunoglobulins/HRP	Goat	Polyclonal	IgG	Dako	1:2000
Goat anti-mouse immunoglobulins/HRP	Goat	Polyclonal	IgG	Dako	1:2000

2.9 FACS for expression of proteins in iHO after stimulation / infection

iHO were stimulated with rhIL-22, and/or microinjected with bacteria of interest and incubated for 90 minutes. iHO were recovered from Matrigel using Cell Recovery Solution, washed in DPBS and incubated with TrypLE for 5-10 minutes at 37°C until they had dissociated into a single cell solution. Samples were washed with BGM to de-activate TrypLE and then in DPBS, before splitting into the requisite amount of tubes to stain for proteins of interest. Samples were incubated with viability staining compounds for 15 mins at r.t. in the dark. Cells were fixed in 4% paraformaldehyde at 4°C for 20 mins (optional). Cells were blocked with 3% BSA in PBS for 30min at 4°C, centrifuged at 4000 rpm and re-suspended in Perm/Wash buffer (BD) for 15 mins at r.t. in the dark. Samples were then stained with required antibodies diluted in Perm/Wash, washed x 2, re-suspended in FACS buffer and transferred to Fortessa FACS tubes, and run on the Becton Dickinson 8 FACSAria IIIu using FACS Diva software (v8). **Table 2.15** lists antibodies used for FACS assays.

Table 2.15: Antibodies / stains used for FACS assays

Target	Host	Clonality	Isotype	Source	Dilution
Primary antibodies					
S100A9	Rabbit	Polyclonal	IgG	Abcam	1:1000
S100A9 (isotype control)	Rabbit	Polyclonal	IgG	Abcam	1:1000
Other compounds used for staining					
DAPI dilactate	N/A	N/A	N/A	Sigma-Aldrich	10 µM
Zombie aqua fixable viability kit	N/A	N/A	N/A	BioLegend	1:100
Fixable viability dye eFluor 780	N/A	N/A	N/A	eBioscience	1:2000
Calcein blue, AM	N/A	N/A	N/A	GeneCopoeia	0.5 µg/mL

2.10 Production of hiPSC lines with isogenic mutations

For studies on the mechanism of rhIL-22-related enhancement of phagolysosomal fusion, an S100A9 knockout hiPSC line was produced by the Cellular Generation and Phenotyping (CGaP) facility at the WTSI as outlined in **Appendix 2**.

2.11 Growth and differentiation of hiPSC into macrophages

Embryoid body formation

hiPSCs from the Kolf2 cell line were cultured on mouse embryonic feeder (MEF) plates (gelatinised plates coated with mouse embryonic fibroblasts (Amsbio)), in Hu iPS base medium (BM) (see **Table 2.16** for components) containing hFGF basic (R&D) at a concentration of 4 ng/mL, as per the method by Hale et al.[8]

Table 2.16: Components of Hu iPS base medium (BM)

Component:	**Manufacturer:**	**Amount:**
Advanced DMEM F12	Invitrogen	400 mL
Knockout serum (KOSR)	Invitrogen	100 mL
L-glutamine 200 mM	Invitrogen	5.5 mL
Mercaptoethanol	Sigma-Aldrich	3.5 µL
Optional: Penicillin-streptomycin (10,000 U/mL)	Invitrogen	5 mL

Cells were harvested from plates using collagenase / dispase mix (Becton Dickinson), and the suspension centrifuged at 1200 rpm for 7 mins. Supernatant was aspirated and replaced with 5 mL BM, cells counted and re-suspended at 1 x 10^6 cells/ mL. 2 mL of this suspension was aliquoted into tissue culture treated 10 cm plates (Corning) with 8 mL BM. Plates were incubated at 37 °C / 5% CO_2 for 3-4 days to allow formation of embryoid bodies (EBs).

Embryoid bodies to monocytes

EBs were harvested into a 50 mL Falcon tube and allowed to settle, before removal of supernatant and resuspension in monocyte differentiation base medium (see **Table 2.17** for composition) with rhM-CSF at 50 ng/mL (R&D) and rhIL-3 at 25 ng/mL. 10 mL of this suspension was plated onto gelatinised tissue culture treated 10 cm plates and incubated at 37 °C / 5% CO_2. Medium was changed every 7-8 days, until day 21, at which point it was possible to harvest floating monocyte precursors and refill plates still containing adherent EBs with fresh medium, in order to repeat this harvest on a weekly basis.

Table 2.17: Components of monocyte differentiation base medium

Component:	**Manufacturer:**	**Amount:**
X-Vivo 15 with gentamicin	Lonza	500 mL
L-glutamine 200 mM	Invitrogen	5.5 mL
Mercapto-ethanol	Sigma-Aldrich	3.5 µL
Optional: Penicillin-streptomycin (10,000 U/mL)	Invitrogen	5 mL

Monocytes to macrophages

Monocyte precursors were counted and resuspended at the concentration required for each assay in macrophage differentiation base medium (MDBM; see **Table 2.18** for composition) containing hM-CSF (R&D) at 100 ng/mL, then plated onto appropriately-sized tissue culture treated dishes. Cells were incubated at 37 °C / 5% CO_2 for 6-7 days prior to use in assays. The first batch of macrophages from a differentiation were checked for human CD14 and CD34 expression by flow cytometry. Phenotyping of these macrophages via TEM has been previously reported.[8]

Table 2.18: Components of macrophage differentiation base medium (MDBM)

Component:	**Manufacturer:**	**Amount:**
RPMI 1640	Sigma	500 mL
Foetal bovine serum (heat-inactivated)	Sigma	50 mL
L-glutamine 200 mM	Invitrogen	5.5 mL
Optional: Penicillin-streptomycin (10,000 U/mL)	Invitrogen	5 mL

2.12 Intracellular infection assays using hiPSC-derived macrophages

Macrophages were plated at a density of $1x10^5$ cells / well and incubated for 7 days prior to infection. Cultures of bacteria of interest were set up in 10 mL LB broth and incubated overnight at 37°C with shaking. Medium overlaying cells was replaced with fresh MDBM immediately prior to assay. Bacterial cultures were diluted to an OD_{600} of 1 and appropriate volume of bacteria added to each well to give a multiplicity of infection (MOI) of 10:1. Cells were incubated for 1 hour at 37 °C / 5% CO_2, infection medium removed and cells washed with DPBS. This was replaced with MDBM containing gentamicin at 0.1 mg/mL for 1 hour to kill extracellular bacteria. Cells were washed again in DPBS and incubated in MDBM for a further 4 hours.

To establish intracellular bacterial counts at 6 hours, macrophages were washed with DPBS and lysed with 500 µL 1% Triton X-100 in DPBS. This mixture was serially diluted in DPBS 10-fold to generate 10^{-1}, 10^{-2} and 10^{-3} concentrations. 3 x 10 µL droplets of the neat and diluted solutions were pipetted onto pre-warmed LB agar plates and incubated overnight at 37 °C. Colony counting was performed the following day.

2.13 Immunostaining of infected hiPSC-derived macrophages

Macrophages were grown on glass coverslips inside tissue culture treated 24-well plates (Corning) at a concentration of $1x10^5$ cells / well. Gentamicin protection assay was carried out as described above following infection of macrophages with *S*. Typhimurium SL1344, *S*. Typhi (Quailes strain) or *S*. Paratyphi A (NVGH308). At the 6 hour timepoint, macrophages were fixed with 4% paraformaldehyde in DPBS (no Ca^{2+} or Mg^{2+}) for 20 minutes, then washed in DPBS and covered in 0.1% Triton X-100 in DPBS for 10 mins at r.t. to permeabilise cells. Cells were washed with DPBS and covered with 1% BSA (Fisher Scientific) in DPBS for 15 mins at r.t. (blocking buffer). Antibodies were diluted in 1% BSA, and CSA-1 applied at 1:50 for 1 hour at r.t. in the dark. Cells were washed x 3 in DPBS and incubated with Alexa fluor 647 Phalloidin (Thermo-Fisher) at 1:1000 for 1 hour at r.t. in the dark. Cells were again washed x 3 with DPBS and coverslips mounted onto 20 µL aliquots of Prolong Gold with

DAPI placed onto Superfrost glass slides (VWR). Slides were stored overnight at 4 °C in the dark and images taken on the Leica SP8 confocal microscope. Number of bacteria per macrophage were recorded for the first 150 macrophages imaged from each condition, using fields chosen at random and compared across groups. Three biological replicates were completed for this assay. Antibodies used for this assay are listed in **Table 2.6**.

2.14 TEM of infected hiPSC-derived macrophages

Macrophages were grown on tissue culture treated 6-well plates (Corning) at a concentration of $2.5x10^5$ cells / well. Gentamicin protection assay was carried out as described above following infection of macrophages with *S*. Typhimurium SL1344, *S*. Typhi (Quailes strain) or *S*. Paratyphi A (NVGH308). MDBM was aspirated and macrophages fixed in 2.5% glutaraldehyde and 2% paraformaldehyde in 0.1 M sodium cacodylate buffer (see **Table 2.7** for components) for 1 hour at r.t. Specimens were washed x 3 in sodium cacodylate buffer, then incubated in 1% osmium tetroxide in sodium cacodylate buffer at r.t. for 1 hour. Samples were washed x 3 in sodium cacodylate buffer. Adherent macrophages were then shaved off the plate using a Teflon strip and transferred to a 1.5 mL Eppendorf tube, centrifuged and the supernatant removed. Macrophages were dehydrated by suspension in ethanol in the series of concentrations: 30%, 30% with uranyl acetate (also at 30%), 50%, 70%, 90% and then 3 X 100%. Samples were incubated for 2 x 15 minutes in propylene oxide and embedded in araldite resin (Sigma-Aldrich). Ultrathin sectioning was then completed, with sections collected onto copper grids and contrasted with uranyl acetate and lead citrate before viewing on a FEI 120kV Spirit BioTWIN TEM and recording CCD images on an F4.15 Tietz charge-coupled device camera.

2.15 Luminex assays for cytokines post-infection in iHO and macrophages

These assays were completed on iHO from Kolf2, Sojd2 and Rayr2 cell lines and macrophages from Kolf2 line infected with CL3 pathogens (*S*. Typhi, *S*. Paratyphi A), therefore supernatants were filtered prior to removal from the CL3 facility and analysis. 200 µL supernatant was removed from all iHO and macrophage samples prior to infection, then at 6 hours post-infection for macrophages, or 1.5 hours and 3 hours post-infection for iHO.

Supernatants were passed through Costar Spin-X centrifuge tube 0.22 μm filters (Corning) and stored in sterile Eppendorf tubes at -80°C prior to analysis.

Once defrosted, a custom Luminex panel (MILLIPLEX MAP kit, Millipore) was used as per manufacturer's instructions to assay levels of: EGF, TGF-α, GROa, CD40L, IL-1RA, IL-1, IL-6, IL-8 and TNF-α in each sample. Samples were run in duplicate on the Luminex MAGPIX instrument and results collected using the xPONENT software. Data analysis was performed in R Version 3.6.0 and Prism version 7.0 software (GraphPad). LOG_2 fold change in median fluorescence intensity versus baseline was calculated for each sample and results compared using unpaired Student's t-test.

2.16 Bulk RNA-Seq for infected iHO and macrophages

Macrophages were cultured at concentration of $2.5x10^5$ cells/well and gentamicin protection assays were performed as described in 2.12. Cells were harvested at the 6 hour time point by washing in DPBS (no Ca^{2+} or Mg^{2+}), followed by addition of 250 μL RLT buffer (RNeasy mini kit, Qiagen), agitation of cells and transfer into 15 mL Falcon tube.

60 iHO per plate were microinjected with bacteria of interest and incubated for 3 hours. iHO were harvested using Cell Recovery Solution, placed into 15 mL Falcon tubes, washed in DPBS (no Ca^{2+} or Mg^{2+}) and 350 μL RLT buffer added to samples.

RNA extractions were performed using the RNeasy mini kit, as per manufacturer's instructions, and RNA was eluted into 40 μL RNase-free water and frozen at -80°C prior to submission to the WTSI's RNA sequencing pipeline. Samples were sequenced on the HiSeq 4000 in dual indexed pools, generating 75bp paired-end reads for both iHO and macrophage infection assays. Subsequent QC and alignment steps are detailed separately for iHO and macrophage samples in **Appendix 3**.

References:

1. Forbester JL, Hannan N, Vallier L, Dougan G. Derivation of Intestinal Organoids from Human Induced Pluripotent Stem Cells for Use as an Infection System. *Methods Mol Biol.* 2016.
2. Leha A, Moens N, Meleckyte R, et al. A high-content platform to characterise human induced pluripotent stem cell lines. *Methods.* 2016;96:85-96.
3. Forbester JL, Lees EA, Goulding D, et al. Interleukin-22 promotes phagolysosomal fusion to induce protection against Salmonella enterica Typhimurium in human epithelial cells. *Proc Natl Acad Sci U S A.* 2018;115(40):10118-10123.
4. Yeung ATY, Hale C, Lee AH, et al. Exploiting induced pluripotent stem cell-derived macrophages to unravel host factors influencing Chlamydia trachomatis pathogenesis. *Nat Commun.* 2017;8:15013.
5. Raffatellu M, Wilson RP, Chessa D, et al. SipA, SopA, SopB, SopD, and SopE2 contribute to Salmonella enterica serotype typhimurium invasion of epithelial cells. *Infect Immun.* 2005;73(1):146-154.
6. Claudi B, Sprote P, Chirkova A, et al. Phenotypic variation of Salmonella in host tissues delays eradication by antimicrobial chemotherapy. *Cell.* 2014;158(4):722-733.
7. Sato T, Stange DE, Ferrante M, et al. Long-term expansion of epithelial organoids from human colon, adenoma, adenocarcinoma, and Barrett's epithelium. *Gastroenterology.* 2011;141(5):1762-1772.
8. Hale C, Yeung A, Goulding D, et al. Induced pluripotent stem cell derived macrophages as a cellular system to study salmonella and other pathogens. *PLoS One.* 2015;10(5):e0124307.

treatment of iHO with rhIL-22 and microinjection with SL1344. These findings were demonstrated via RT-qPCR and immunostaining (**Figure 4.14**).

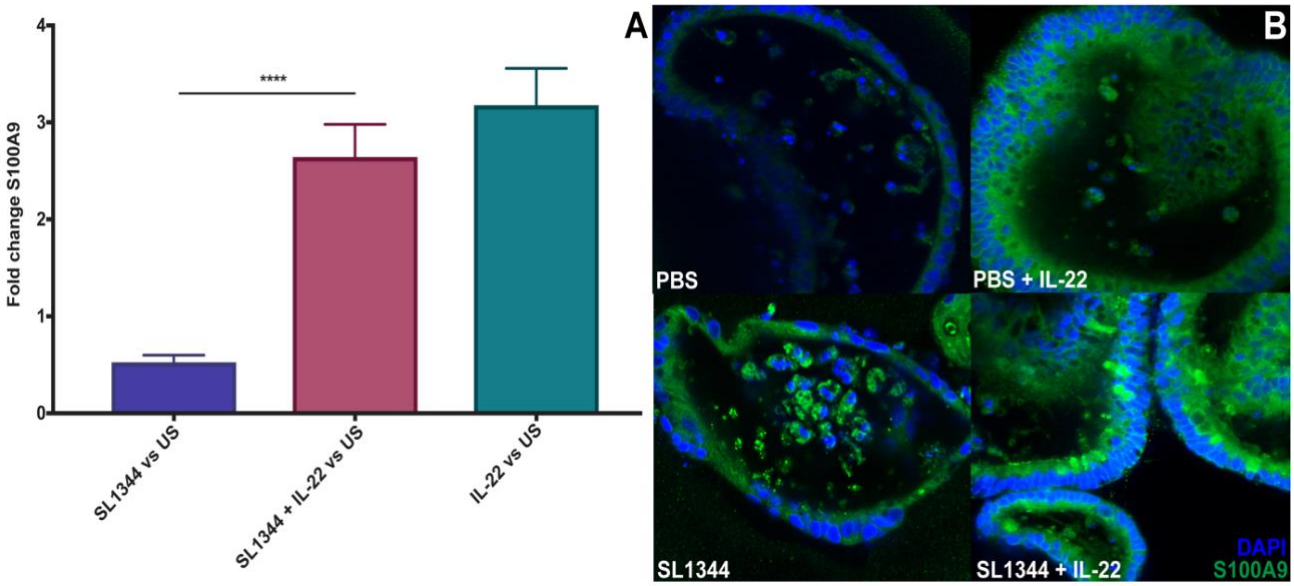

Figure 4.14: Increased expression of S100A9 in iHO pre-treated with rhIL-22. (**A**) iHO were either left unstimulated, or treated for 18 hours with rhIL-22 at 100 ng/mL. iHO were then left uninfected or injected with SL1344 and incubated for 3 hours, followed by harvesting and RNA extraction. RT-qPCR with TaqMan gene expression assay for S100A9 was then completed to compare S100A9 expression between treatment groups and unstimulated iHO. Data presented are fold change in expression of S100A9, averaged from 4 technical replicates, with assays repeated 3 times. Data were analysed using the comparative cycle threshold (C_T) method, with GAPDH as an endogenous control. Unpaired student's t-test was used to compare results (****$p < 0.0001$). A significant difference in S100A9 expression was noted in SL1344-infected iHO pre-treated with rhIL-22 versus those left untreated. (**B**) Kolf2 iHO pre-treated with rhIL-22 for 18 hours at 100 ng/mL, or left unstimulated, were microinjected with PBS (control) or SL1344 and incubated for 3 hours, before fixing and immunostaining for nuclei with DAPI (blue) and S100A9 expression (green). Increased intensity of S100A9 staining was demonstrated in samples treated with rhIL-22 and exposed to bacteria, with maximal staining seen in iHO both pre-treated with rhIL-22 and infected. Images taken on Zeiss LSM 510 Meta confocal microscope at 20x magnification.

IL-22 has been shown to upregulate S100A9 production in fibroblast-like synoviocytes, via induction of STAT3 phosphorylation,[25] therefore, given the findings on qPCR / immunostaining, the role of S100A9 in phagolysosomal fusion was further investigated by the use of hiPSC with a biallelic mutation in the S100A9 gene ($S100A9^{-/-}$). This cell line was produced by the Cellular Generation and Phenotyping (CGaP) facility at the Wellcome Trust Sanger Institute, via CRISPR/Cas9 engineering, as outlined in 2.10/Appendix 2. Organoids were differentiated from hiPSC as previously described and phenotyped via immunostaining and RT-qPCR, with no morphological differences noted between iHO generated from $S100A9^{-/-}$ and Kolf2 cell lines (**Figure 4.15**).

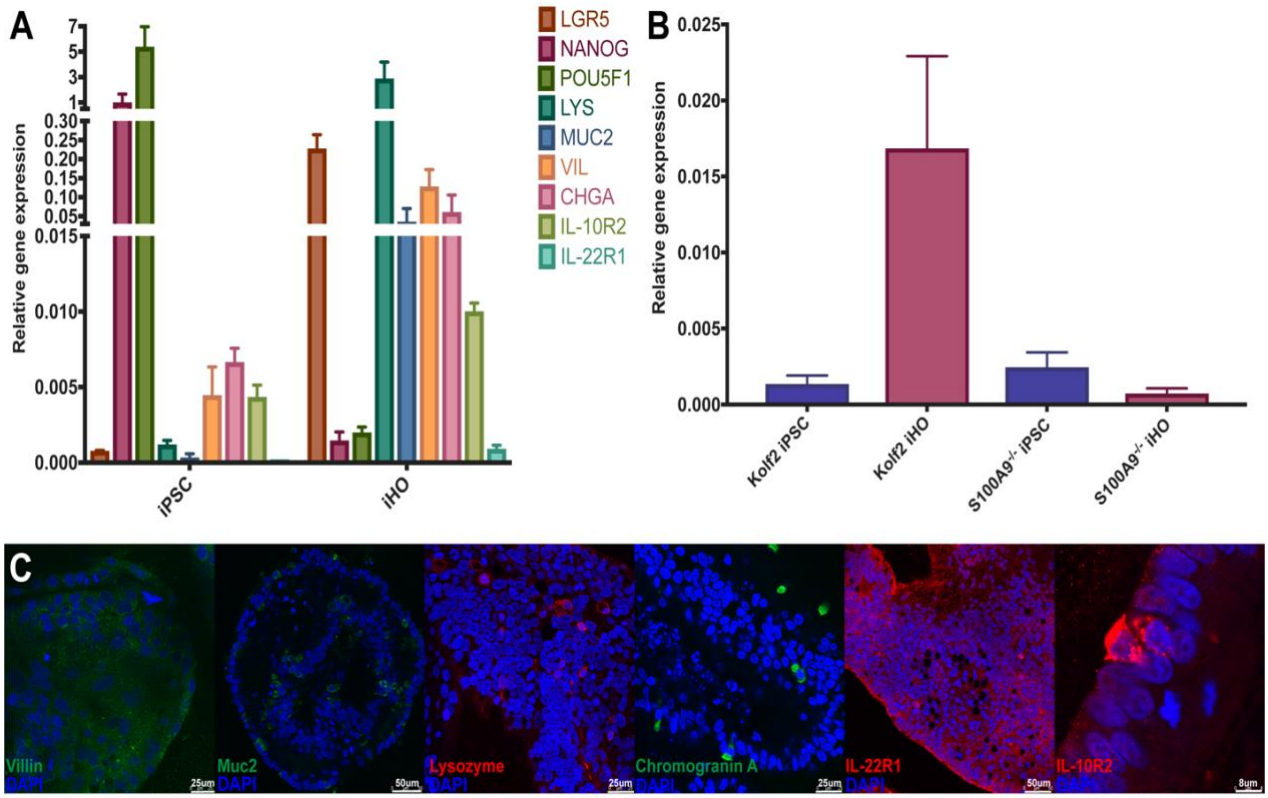

Figure 4.15: Phenotyping of iHO generated from S100A9$^{-/-}$ cell line. (**A**) Relative expression of genes in S100A9$^{-/-}$ iPSC versus iHO, demonstrating that markers of pluripotency (NANOG, POU5F) are highly expressed in iPSC, whereas genes coding for specific cell types (Vil1, Lys, Muc2, ChgA) and stem cells (LGR5) are highly expressed in iHO, denoting differentiation. Data presented are from 4 technical replicates, with assays repeated 3 times using paired iPSC/iHO of different batches. Data were analysed using the comparative cycle threshold (C_T) method, with GAPDH as an endogenous control. (**B**) Expression of S100A9 in Kolf2 iPSC/iHO versus S100A9$^{-/-}$ iPSC/iHO, demonstrating expression of S100A9 in Kolf2 iHO, but minimal expression in S100A9$^{-/-}$ iHO. (**C**) Immunostaining of S100A9$^{-/-}$ iHO to demonstrate presence of constituent intestinal cell types. Imaged are iHO with nuclei stained with DAPI (blue) and for the presence of: Villin, Mucin2, Chromogranin A (green), Lysozyme, IL-22R1 and IL10R2 (red). Images taken on the Leica SP8 confocal microscope at 20x (Villin, Muc2, Lysozyme, Chromogranin A, IL-22R1) or 40x (IL-10R2) magnification.

No expression of S100A9 protein or Rab7 expression was detected using immunostaining following IL-22 stimulation and infection with SL1344 in S100A9$^{-/-}$ iHO (**Figure 4.16 A&B**). iHO from both cell lines were stimulated with rhIL-22 and dissociated, then stained with S100A9 antibody and FACS sorted. Increased S100A9 expression was seen in Kolf2 iHO versus S100A9$^{-/-}$ iHO (**Figure 4.16 C**). Gentamicin protection assays in S100A9$^{-/-}$ iHO demonstrated no significant difference in intracellular bacterial counts of SL1344 in rhIL-22 treated versus untreated S100A9$^{-/-}$ iHO (**Figure 4.16 D**). These data suggest that S100A9, induced by IL-22, inhibits SL1344 infection in the intestinal epithelium.

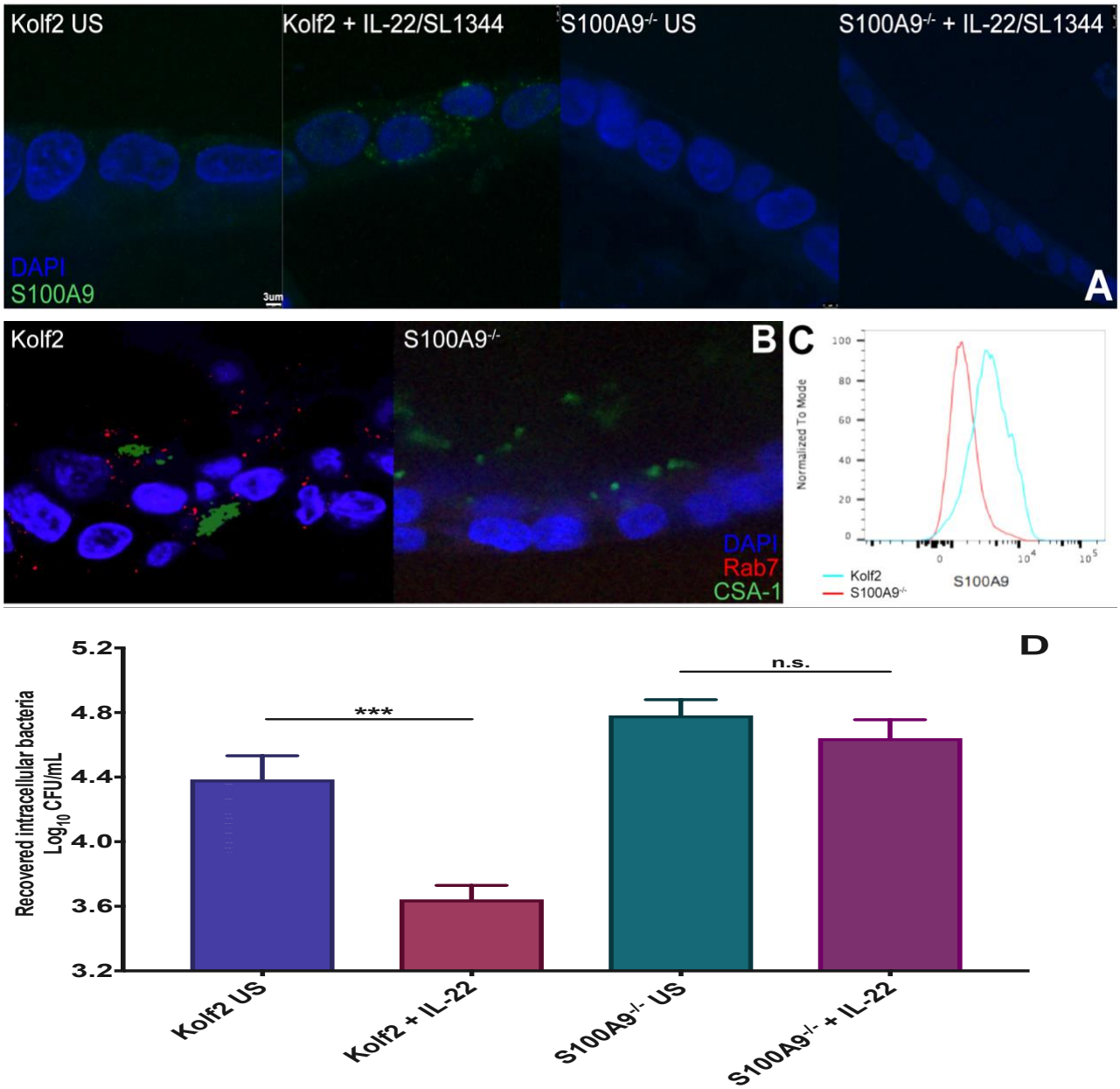

Figure 4.16: IL-22 induces S100A9-mediated protection from SL1344 infection. (**A**) Kolf2 and S100A9$^{-/-}$ iHO were pre-treated with rhIL-22 for 18 hours at 100 ng/mL or left unstimulated, then injected with SL1344, followed by incubation for 3 hours, fixing and immunostaining. (**A**) S100A9 protein (green) expression is demonstrated in Kolf2, but not S100A9$^{-/-}$ iHO. (**B**) Kolf2 and S100A9$^{-/-}$ iHO were pre-treated with rhIL-22 at 100 ng/mL for 18 hours and injected with SL1344, followed by fixing and immunostaining for DAPI (blue), CSA-1 (green) and RAB7 (red). RAB7 was expressed in Kolf2 iHO but not in S100A9$^{-/-}$ iHO. Images for **A** & **B** were taken on the Leica SP8 confocal microscope at 40x magnification. (**C**) Kolf2 and S100A9$^{-/-}$ iHO were pre-stimulated with rhIL-22 at 100 ng/mL for 18 hours, dissociated into single cells, stained and FACS sorted. Histogram showing expression of S100A9 demonstrates increased S100A9 expression in Kolf2 iHO. (**D**) Kolf2 and S100A9$^{-/-}$ iHO were pre-treated with rhIL-22 for 18 hours at 100 ng/mL or left unstimulated, then injected with SL1344 and incubated for 1.5 hours, before undergoing modified gentamicin protection assays for recovery of intracellular bacteria. Data presented are for 3 biological replicates (each averaged from 3 technical replicates), with 30 iHO injected per replicate +/- SEM. Unpaired Mann-Whitney tests were used to compare results (**n.s.** not significant, *** p<0.001). Significantly fewer bacteria were recovered intracellularly in Kolf2 iHO pre-treated with rhIL-22 before SL1344 infection. No significant difference is seen between treated and untreated S100A9$^{-/-}$ iHO.

To confirm that S100A9$^{-/-}$ iHO were able to produce a response to IL-22 in aspects other than S100A9 secretion, iHO were stimulated with rhIL-22 for 18 hours and RT-qPCR completed to measure expression of IL-22 regulated genes DUOX2 and LCN2. There was a significant increase in expression of both genes following IL-22 treatment (**Figure 4.17**).

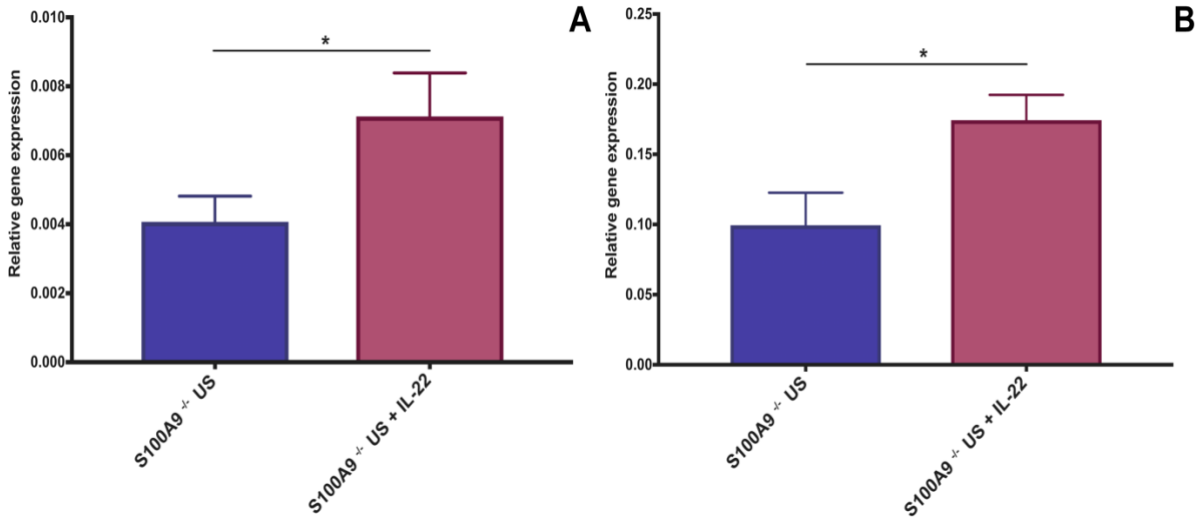

Figure 4.17: Relative gene expression of IL-22 regulated genes DUOX2 and LCN2 in S100A9$^{-/-}$ iHO. S100A9$^{-/-}$ iHO were treated with rhIL-22 at 100 ng/mL for 18 hours or left unstimulated. RNA was harvested and RT-qPCR completed to compare expression of IL-22 regulated genes DUOX2 (Panel **A**) and LCN2 (Panel **B**). Data presented are from 4 technical replicates, with assays repeated 3 times. Data were analysed using the comparative cycle threshold (C_T) method, with GAPDH as an endogenous control. Unpaired Mann-Whitney test was used to compare results (*$p < 0.05$). Expression of DUOX2 (**A**) and LCN2 (**B**) is significantly upregulated in response to rhIL-22 treatment in S100A9$^{-/-}$ iHO, demonstrating that S100A9$^{-/-}$ iHO retain the ability to respond to IL-22.

4.8 Single cell responses after IL-22 stimulation

Although the mechanism for the restrictive effect of IL-22 on *S*. Typhimurium SL1344 by phagolysosomal fusion has been demonstrated via a number of methods, the specific cell types responding to IL-22 and the transcriptional changes that occur within these cells have yet to be elucidated. A small-scale trial of single cell sequencing of unstimulated Kolf2 iHO and those pre-treated with rhIL-22 was completed to begin to address this. Methods for cell sorting, barcoding, sequencing and data analysis are described in 2.7/Appendix 1. For the remaining figures in this chapter, 'Unstimulated' refers to single cells from iHO not pre-treated and 'IL-22 stimulated' refers to single cells from iHO treated for 18 hours at 100 ng/mL. As an initial method of quality control and responsiveness to IL-22 in the cells sequenced, remaining RNA following sample submission for RNA-Seq was transcribed and RT-qPCR completed. Both LCN2 and IFITM3 were significantly upregulated in rhIL-22 treated

cells, but interestingly there was a large degree of variation between cells in terms of levels of relative gene expression (**Figure 4.18**).

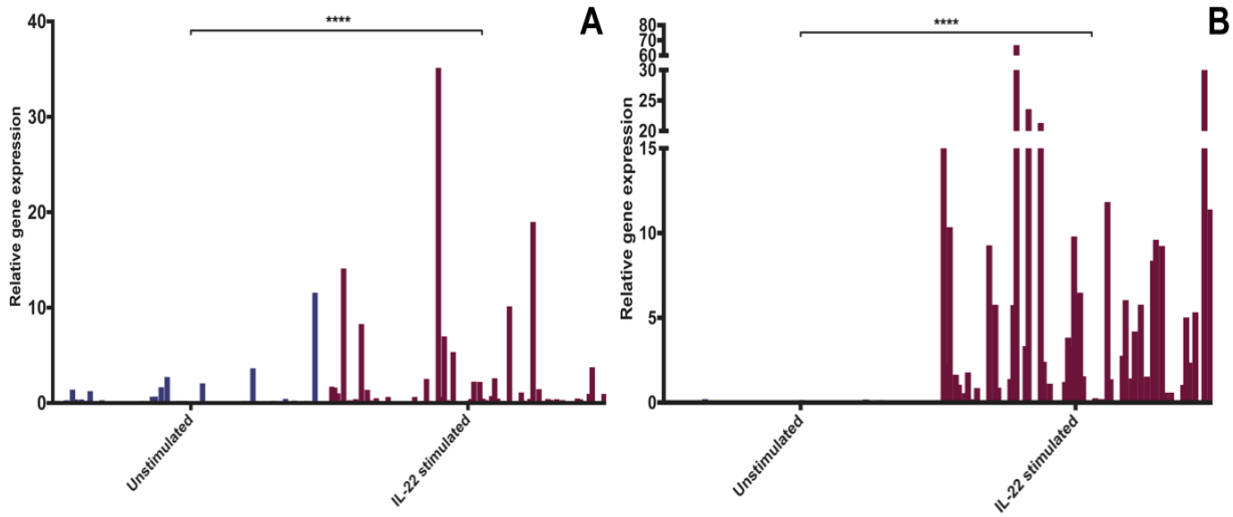

Figure 4.18: Relative gene expression of IL-22 regulated genes LCN2 and IFITM3 in rhIL-22 stimulated and unstimulated single cells. RT-qPCR was completed to compare expression of LCN2 and IFITM3 between single cells from IL-22 stimulated and unstimulated iHO. Data presented are from 1 technical replicate, with assays repeated once. Each bar represents a single cell. Data were analysed using the comparative cycle threshold (C_T) method, with GAPDH as an endogenous control. Unpaired Mann-Whitney test was used to compare results (****$p < 0.0001$). (**A**) LCN2 and (**B**) IFITM3 are significantly upregulated in response to rhIL-22 treatment.

The Single Cell Consensus Clustering (SC3) programme[26] and Seurat package[27] were used to examine the data, and G:Profiler (https://biit.cs.ut.ee/gprofiler/gost) to look at differential enrichment data. SC3 is an unsupervised clustering approach which uses parallelisation to simultaneously analyse multiple clustering solutions, which are then combined into a consensus matrix summarising how frequently each pair of cells is placed in the same cluster and thus similarity between cells. The results of the consensus matrix then undergo complete-linkage hierarchical clustering into *k* groups. The program is also able to identify differentially expressed genes, which are genes that vary between two or more clusters, and identify marker genes, which are genes highly expressed in one particular cell cluster and able to distinguish this cluster from the remaining ones. In order to identify marker genes, a binary classifier for each gene is produced from mean cluster-expression values, and the area under ROC curve is used to quantify how accurate these predictions are. Each gene receives a p-value using the Wilcoxon signed-rank test, which allows comparison of gene ranks in the cluster with the highest mean expression with all others. Marker genes are defined as those with an area under the ROC curve of >0.85 and $p<0.01$.

Firstly, PCA plots were used to look at clustering by IL-22 status (cohort). Interestingly, there did not appear to be a distinct separation between cells based on cohort, which demonstrates a lack of plate effect, but also that an alternative factor was the primary driver of differences between cell groups. This was confirmed on clustering analysis, which suggested 4 primary clusters of cells, but that cells from each cohort were to be found in each cluster (**Figure 4.19**).

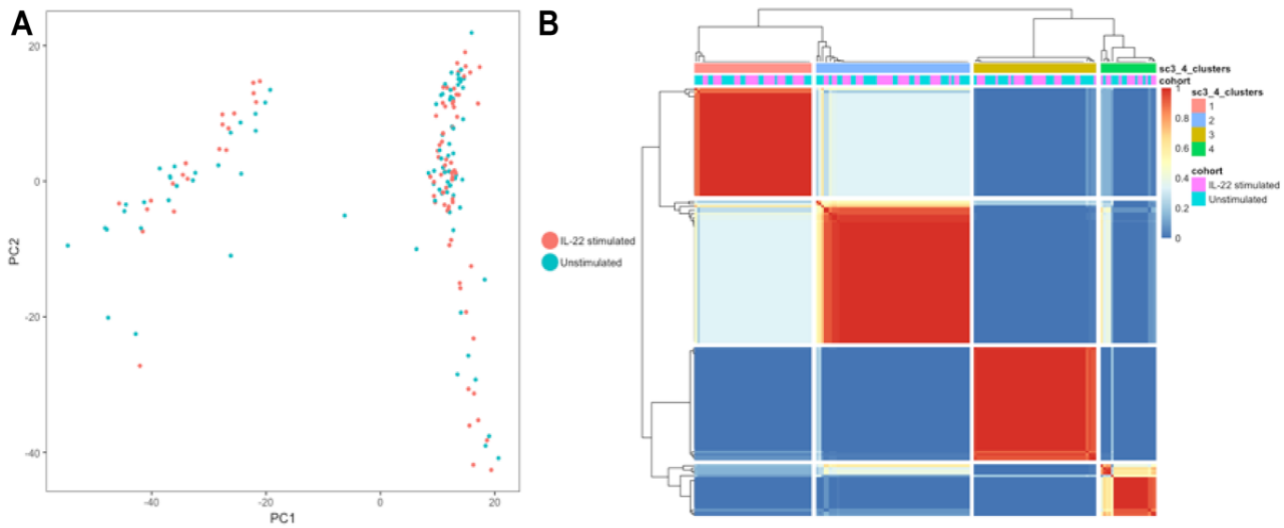

Figure 4.19: PCA and clustering analysis for all cells using SC3. (**A**) PCA of all cells by cohort, with mixing of IL-22 stimulated and unstimulated cells. (**B**) Clustering analysis; similarity of 1 (red) indicates that the two cells are always assigned to the same cluster and suggests robustness of clustering strategy. Four clusters were suggested by the analysis, each containing a mix of unstimulated and IL-22 stimulated cells. Images generated using SC3 package.

Using Seurat to interrogate PCAs, (following scaling for UMIs and mitochondrial gene content) suggested that for all cells, PC1 was primarily defined by MAP1B – microtubule related protein important for maintaining cell structure; other elements of this PC included genes related to epithelial cell differentiation and cell-cell adhesion. PC2 was defined by a number of cell cycle related genes, including CKS1B, MAD2L1, HMGN2, HMGB2, CKS2, MKI67 and TOP2A (**Figure 4.20**). PCAs were also run for cells by cohort, with PC1 for the unstimulated group being made up of genes responsible for cell-cell adhesion, and protein localisation to the plasma membrane and PC2 cell development and differentiation. For IL-22 stimulated cells, PC1 was dominated by genes responsible for extracellular and phagocytic vesicle membrane production and PC2 regulation of cytokine production, platelet derived growth factor signalling and negative regulation of cell differentiation. The

upregulation of these genes in the IL-22 stimulated group makes biological sense, given the mechanism established in this thesis for the role of IL-22 in increased phagolysosomal fusion, and in response to infection / inflammation wherein it is known to increase cell proliferation, decrease differentiation and induce a secretory response for defence of the epithelium.[2,28]

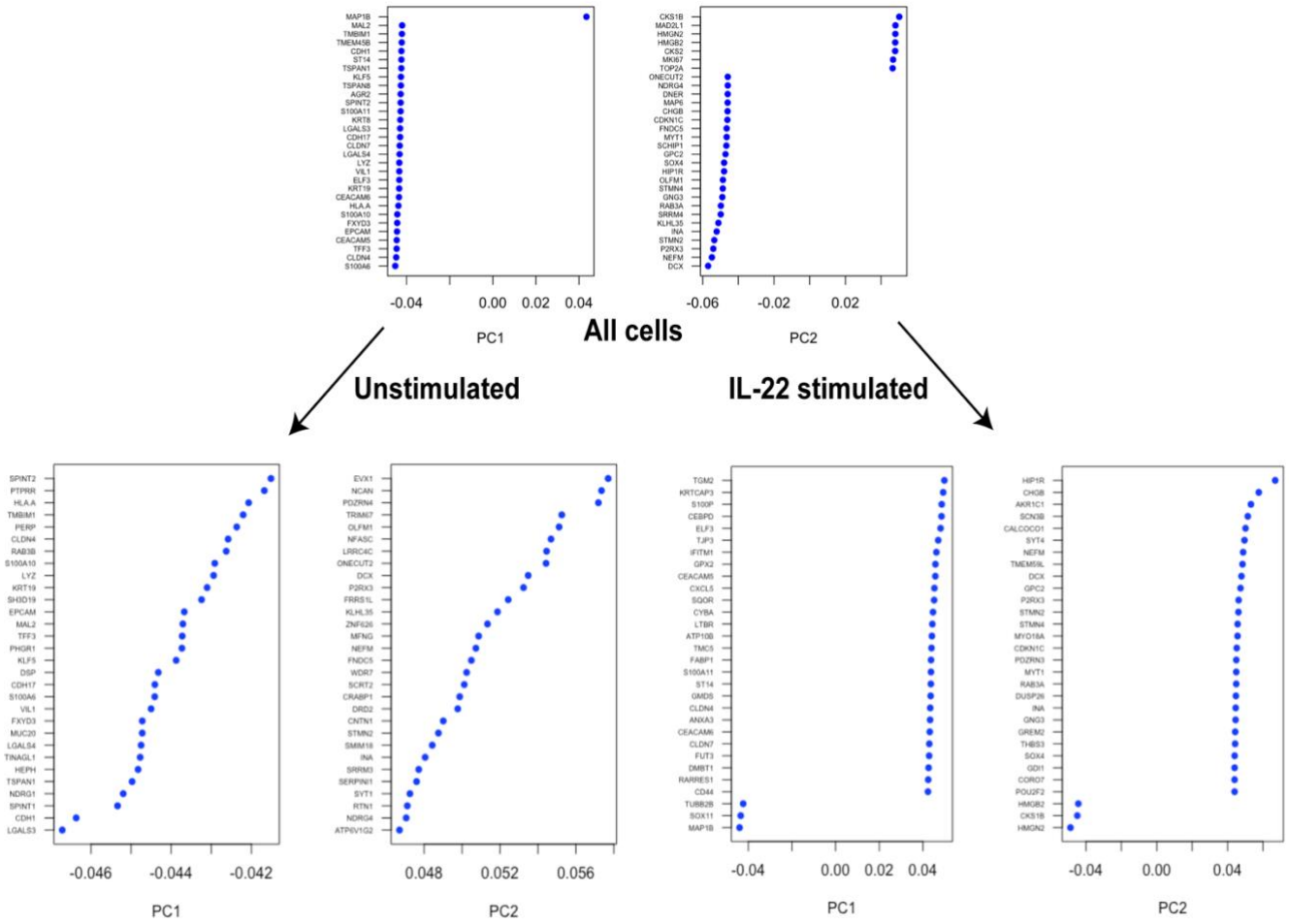

Figure 4.20: PCA for all cells and subsets using Seurat. PC1 and PC2 for all cells, with subdivision into PCs for unstimulated and IL-22 stimulated cells. Plotted are the top 30 genes influencing PC for each group. Images generated using Seurat package.

Differential expression (DE) and clustering analysis was performed using SC3. DE was calculated using the Kruskal-Wallis test. A significant p value demonstrates that gene expression in at least 1 cluster dominates 1 other cluster. For unstimulated cells, SC3 denoted 4 clusters, identifying 880 differentially expressed genes based on this clustering. The top 10 marker genes for each cluster are represented in the plots in **Figure 4.21**. Cluster 1 contains genes responsible for cell-cell adhesion and production of extracellular organelles, cluster 2 - cell cycle, cluster 3 – cell signalling / amino acid transport and cluster

4 - neurogenesis. For IL-22 stimulated cells, SC3 denoted 5 clusters, with 894 differentially expressed genes based on this clustering. Marker genes for clusters suggested the following functions: cluster 1 - extracellular exosome and vesicle production / prostaglandin synthesis, cluster 2 - cell cycle, cluster 3 – (Vimentin); a cytoskeletal protein involved in cell migration and signalling (bacterial and viral pathogen attachment), cluster 4 - cell-cell signalling and neurogenesis, cluster 5 - (C8orf46) neurogenesis.

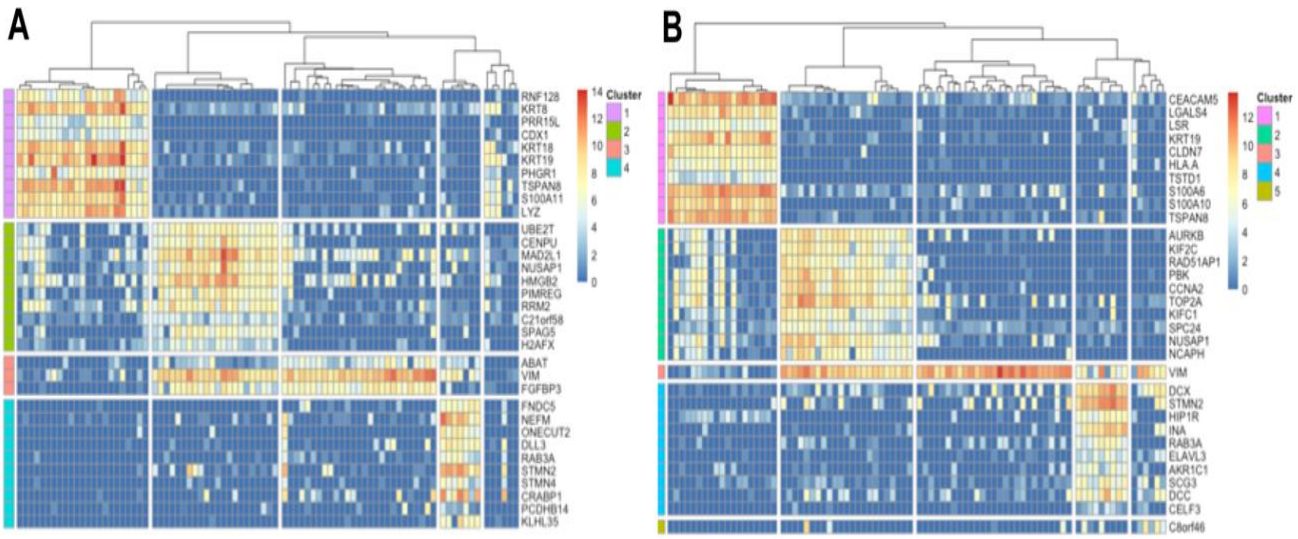

Figure 4.21: Differential expression and marker gene analysis for cohorts using SC3. Differential expression matrix (cells in columns, genes in rows) for unstimulated (**A**) and IL-22 stimulated (**B**) cells, delineating the cell clusters, and listing up to the top 10 marker genes for each cluster. Images generated using SC3 package.

In comparison to the clustering done using SC3, T-SNE plotting using Seurat suggested 3 clusters when using all cohorts. These clusters were interrogated by using known cell type markers to assess whether it was possible to discern whether particular cell types (e.g. secretory cells) clustered together. Markers for cell types searched included: enterocytes, goblet cells, stem cells, enteroendocrine cells, Paneth cells and cell cycle related genes. Plots for each cohort separately did not differ to those produced for all cells, therefore plots for all cells are represented below (**Figure 4.22**). Importantly, IL-10R2 appeared to be expressed by multiple cell clusters, suggesting that whilst it may be expressed strongly on enteroendocrine cells (as noted on immunostaining in **Figure 4.3**), it also appears to be expressed on other IEC types.

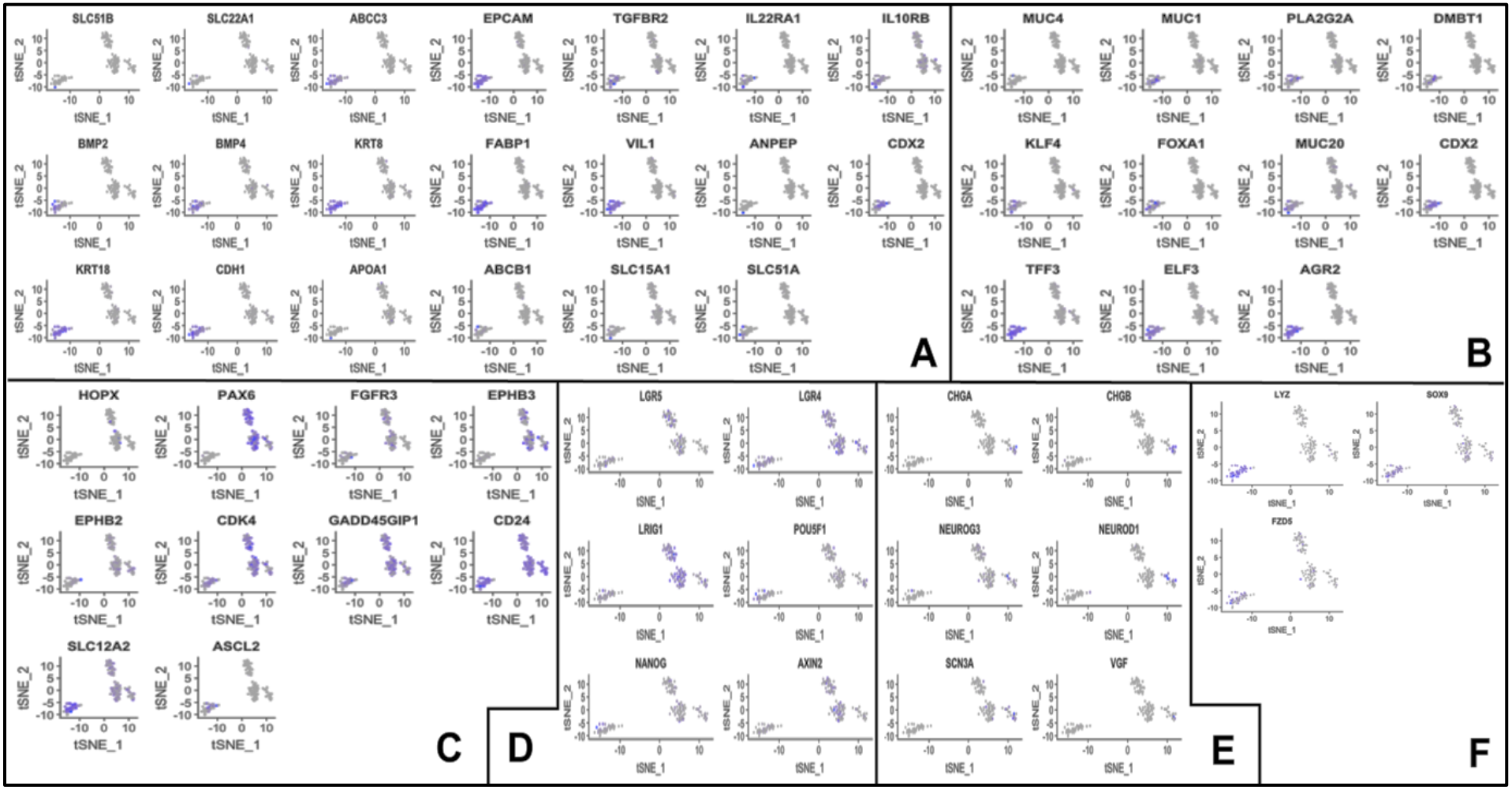

Figure 4.22 – Investigating cell types using known gene markers. Data are t-SNE plots representing all cells, with cells positive for the listed gene highlighted in purple. Data represent cells from iHO both unstimulated and IL-22 stimulated. (**A**) are genes expected on enterocytes, (**B**) goblet cells, (**C**) cell cycle genes, (**D**) stem cells, (**E**) enteroendocrine cells and (**F**) Paneth cells. Plots constructed using Seurat package.

Based on t-SNE clustering (**Figure 4.23**) and interrogation of gene markers, there is a clearly delineated cluster of cells (cluster 1) which look to be differentiated enterocytes / secretory cells, whereas clusters 0 and 2 are marked by cell cycle and stem cell related genes. This fits with clustering run by this programme, which denoted a combination of cytoskeletal and cell cycle genes in cluster 0, extracellular vesicle/organelle related genes in cluster 1 and cell cycle genes in cluster 2. Interestingly, (as seen in **Figure 4.22**) enteroendocrine cells appeared to cluster in the outer part of cluster 0, rather than with the other secretory cells.

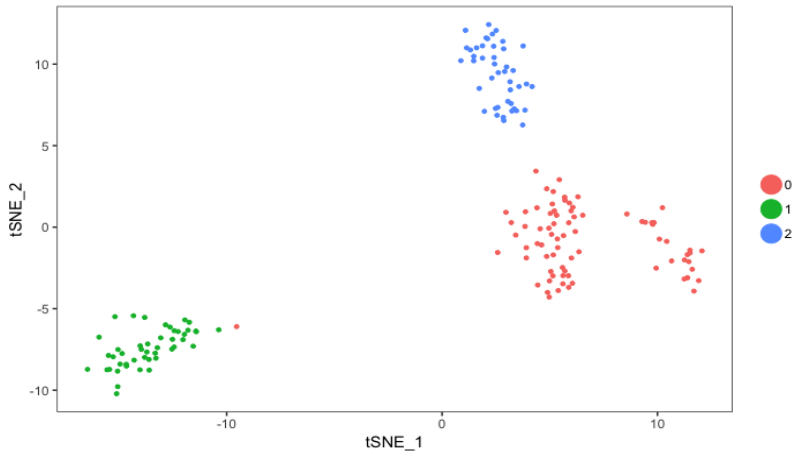

Figure 4.23 – t-SNE plot for all cells using Seurat. This plot includes both unstimulated and IL-22 stimulated cells. Cells are divided into 3 clusters. Based on interrogation with gene markers, cluster 1 are likely enterocytes / secretory cells, clusters 0 and 2 contain high proportions of cell cycling / stem cell gene markers.

Plots were made of the top 30 IL-22 upregulated genes in all cells, and demonstrated that these genes were located within all cell clusters, reinforcing what was seen on imaging about the ubiquity of the IL-22 receptor on all cell types (**Figure 4.24**). The genes upregulated were those expected as part of the epithelial defensive response to pathogens, (IFITM1, IFITM2, IFITM3, LCN2, DUOX2, DMBT1, MUC1 and MUC4), those which are a part of the phagolysosomal fusion pathway (RAB7A, LAMP1, S100A9), the JAK/STAT pathway (JAK1, STAT3, IL-23A) and those responsible for antimicrobial peptide production (PLA2G2A) and the innate immune response (TIFA, CEACAM1, SERPINA3). Given the limited number of cells in the cohort and the dominance of cell cycle genes in most cells sequenced, it is difficult to draw further conclusions about the effect of IL-22 on single cells.

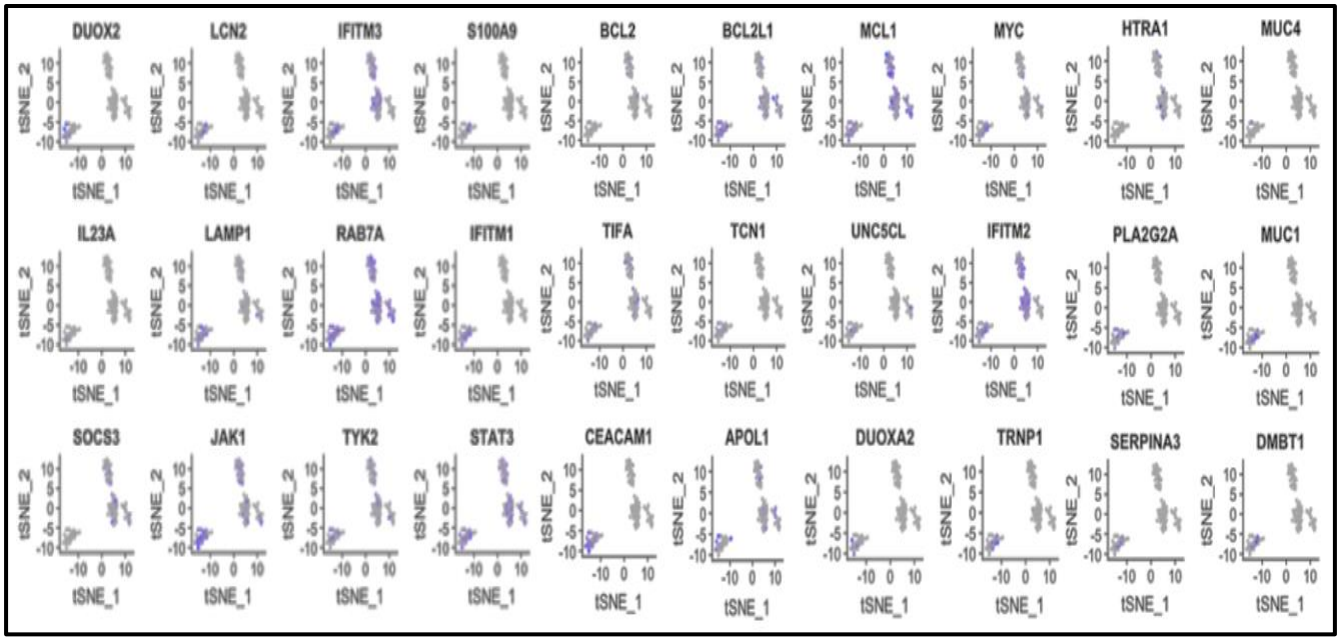

Figure 4.24 – Top 30 IL-22 upregulated genes. Plots represent all cells (both unstimulated and IL-22 stimulated), with cells expressing the gene of interest highlighted in purple. Plots produced using Seurat.

4.9 Discussion

This chapter demonstrates a defensive role for IL-22 in the intestinal epithelial response to *S*. Typhimurium infection and outlines a major mechanism by which this is occurring. Restriction of intracellular *M. tuberculosis* growth secondary to IL-22-enhanced phagolysosomal fusion has been demonstrated previously in macrophages[18], but this is the first demonstration of this process with a Gram-negative pathogen, and we show that calgranulin B (S100A9) is required for this process, rather than solely calgranulin A as previously thought.[24] Both calgranulin A and B consist of 2 helix-loop-helix EF binding motifs, which are connected by a hinge region. They can exist as heterodimers or homodimers. After binding with Ca^{2+}, the molecule opens up, exposing a hydrophobic cleft in the hinge region, which binds with the molecule's target protein of interest.[29] It is proposed that IL-22 enhances phagolysosomal fusion by increasing intracellular levels of Ca^{2+}, causing movement of calgranulin A (or in this case, B) to the phagosomal membrane. Following conformational change of the molecule on binding with Ca^{2+}, calgranulin A / B is able to bind with a currently unidentified molecule to increase Rab7 expression and increase phagosomal maturation / bacterial killing.[24] In humans, S100A8 and S100A9 are known to be associated with both immune-related inflammatory disorders such as psoriasis and in infection-related inflammation.[30] Murine studies have demonstrated decreased

phagocytosis of *Klebsiella pneumoniae* by S100A9$^{-/-}$ murine macrophages with increased dissemination of infection,[31] and impaired leukocyte migration in S100A9$^{-/-}$ mice, as well as an important role for S100A8/9 in regulation of cytoskeletal modulation (essential for successful phagocytosis).[32] There is little data on the role of S100A9 in either the murine or human intestinal epithelium; further study would be required to establish the relevance of this pathway for phagolysosomal fusion and bacterial defence in the intact immune system *in vivo*, and to determine what the specific interactions are between S100A9, RAB7 and the phagolysosome.

Data on the IL-22 response in the intact intestinal immune system would be of particular interest, given that in contrast to our findings that IECs appear to be less susceptible to *S*. Typhimurium invasion with a functional IL-22 pathway, IL-22$^{-/-}$ mice were not demonstrated to have any significant difference in susceptibility to *S*. Typhimurium infection.[15] In this case, it may be that antimicrobial peptides whose secretion is induced by IL-22 favoured the growth of non-protective elements of the microbiota, allowing increased colonisation and thus infection with *S*. Typhimurium in wild type mice, whereas although the immune response in IL-22$^{-/-}$ mice may be diminished, their microbiota were less favourable for *S*. Typhimurium colonisation. Additionally it is possible that *Salmonella* were using different methods of crossing the epithelial barrier, such as direct capture from the lumen by phagocytes/dendritic cells, or transfer via M cells; pathways which are not possible in the iHO model.[33]

Our data demonstrate differences in IEC susceptibility to infection after pre-incubation with IL-22, suggesting that this response may be more relevant to later stages of infection, rather than the very early stages whilst the IL-22 pathway is activated. However, constitutive epithelial expression of factors such as IL-17A have been demonstrated in some models to provide initial protection and delay invasion of *S*. Typhimurium,[34] and both IL-22 and IL-22-regulated genes have been demonstrated to be upregulated at early timepoints post-infection,[35,36] suggesting that there could be a role for the defensive mechanism of IL-22 we have outlined in the initial stages of infection.

With regards to the attempt to identify populations of cell subsets and better understand the transcriptional response of each cell type to IL-22, it is clear that despite providing a very

high depth of sequencing, the SmartSeq2 method is too time-consuming and allows limited batches of cells to be processed on a particular occasion. The pipeline is long (2 days to process a plate), and difficulties with cell sorting or either clean up step can lead to plates not being processable at the barcoding stage. In addition, barcoding incurs a large expense per cell, which limited the ability to do this on a large scale during this project. Since the sequencing for this project was done, new methods have come to the fore for this type of work, such as microfluidic techniques, including droplet-based single cell RNA-Seq,[37] which can provide large amounts of data very rapidly. A relevant example would be its use to profile cell populations in the mouse intestine, profiling over 50,000 cells during one experiment.[38] This method allowed not only identification of rare populations such as enteroendocrine cells (thought to represent around 1% of cells in iHO), but their division into specific subpopulations and was also able to demonstrate changes in cell population in response to infection.

The clustering and data analysis techniques used here would similarly work better on larger scale data; as gene filtering in the SC3 programme removes both very rare and ubiquitous transcripts, as analysis has previously demonstrated that these factors do not affect clustering.[26] However, this would make the method less sensitive to picking up rare cell types. It is possible to alter these parameters to provide increased sensitivity but the fact that clustering done with Seurat, which filters only for high mitochondrial reads and specifically searches for genes which display high cell-cell variability (as would have been expected between IL-22 stimulated and unstimulated cells) provided the same types of cell clusters suggests that both were valid tools, but the limitation lay in the number of cells sequenced.

Using a microfluidic-based approach to perform larger-scale single cell sequencing would be an ideal next step to definitively identify cell populations in an *in vitro* human intestinal epithelial model such as the iHO, and study cellular responses to IL-22 treatment and *S*. Typhimurium infection.

References:

1. Schreiber F, Arasteh JM, Lawley TD. Pathogen Resistance Mediated by IL-22 Signaling at the Epithelial-Microbiota Interface. *J Mol Biol.* 2015;427(23):3676-3682.
2. Sabat R, Ouyang W, Wolk K. Therapeutic opportunities of the IL-22-IL-22R1 system. *Nat Rev Drug Discov.* 2014;13(1):21-38.
3. Kotenko SV, Izotova LS, Mirochnitchenko OV, et al. Identification of the functional interleukin-22 (IL-22) receptor complex: the IL-10R2 chain (IL-10Rbeta) is a common chain of both the IL-10 and IL-22 (IL-10-related T cell-derived inducible factor, IL-TIF) receptor complexes. *J Biol Chem.* 2001;276(4):2725-2732.
4. Ranjbar S, Haridas V, Jasenosky LD, Falvo JV, Goldfeld AE. A Role for IFITM Proteins in Restriction of Mycobacterium tuberculosis Infection. *Cell Rep.* 2015;13(5):874-883.
5. Grasberger H, El-Zaatari M, Dang DT, Merchant JL. Dual oxidases control release of hydrogen peroxide by the gastric epithelium to prevent Helicobacter felis infection and inflammation in mice. *Gastroenterology.* 2013;145(5):1045-1054.
6. Flores MV, Crawford KC, Pullin LM, Hall CJ, Crosier KE, Crosier PS. Dual oxidase in the intestinal epithelium of zebrafish larvae has anti-bacterial properties. *Biochem Biophys Res Commun.* 2010;400(1):164-168.
7. Forbester JL, Lees EA, Goulding D, et al. Interleukin-22 promotes phagolysosomal fusion to induce protection against Salmonella enterica Typhimurium in human epithelial cells. *Proc Natl Acad Sci U S A.* 2018;115(40):10118-10123.
8. Sabat R. IL-10 family of cytokines. *Cytokine Growth Factor Rev.* 2010;21(5):315-324.
9. Commins S, Steinke JW, Borish L. The extended IL-10 superfamily: IL-10, IL-19, IL-20, IL-22, IL-24, IL-26, IL-28, and IL-29. *J Allergy Clin Immunol.* 2008;121(5):1108-1111.
10. Glocker EO, Kotlarz D, Boztug K, et al. Inflammatory bowel disease and mutations affecting the interleukin-10 receptor. *N Engl J Med.* 2009;361(21):2033-2045.
11. Spencer SD, Di Marco F, Hooley J, et al. The orphan receptor CRF2-4 is an essential subunit of the interleukin 10 receptor. *J Exp Med.* 1998;187(4):571-578.
12. Pham TA, Clare S, Goulding D, et al. Epithelial IL-22RA1-mediated fucosylation promotes intestinal colonization resistance to an opportunistic pathogen. *Cell Host Microbe.* 2014;16(4):504-516.

13. Zheng Y, Valdez PA, Danilenko DM, et al. Interleukin-22 mediates early host defense against attaching and effacing bacterial pathogens. *Nat Med.* 2008;14(3):282-289.
14. Engelhardt KR, Shah N, Faizura-Yeop I, et al. Clinical outcome in IL-10- and IL-10 receptor-deficient patients with or without hematopoietic stem cell transplantation. *J Allergy Clin Immunol.* 2013;131(3):825-830.
15. Behnsen J, Jellbauer S, Wong CP, et al. The cytokine IL-22 promotes pathogen colonization by suppressing related commensal bacteria. *Immunity.* 2014;40(2):262-273.
16. Muller AJ, Kaiser P, Dittmar KE, et al. Salmonella gut invasion involves TTSS-2-dependent epithelial traversal, basolateral exit, and uptake by epithelium-sampling lamina propria phagocytes. *Cell Host Microbe.* 2012;11(1):19-32.
17. Friedrich N, Hagedorn M, Soldati-Favre D, Soldati T. Prison break: pathogens' strategies to egress from host cells. *Microbiol Mol Biol Rev.* 2012;76(4):707-720.
18. Dhiman R, Indramohan M, Barnes PF, et al. IL-22 produced by human NK cells inhibits growth of Mycobacterium tuberculosis by enhancing phagolysosomal fusion. *J Immunol.* 2009;183(10):6639-6645.
19. Vergne I, Chua J, Deretic V. Tuberculosis toxin blocking phagosome maturation inhibits a novel Ca2+/calmodulin-PI3K hVPS34 cascade. *J Exp Med.* 2003;198(4):653-659.
20. Drose S, Altendorf K. Bafilomycins and concanamycins as inhibitors of V-ATPases and P-ATPases. *J Exp Biol.* 1997;200(Pt 1):1-8.
21. Yates RM, Hermetter A, Russell DG. The kinetics of phagosome maturation as a function of phagosome/lysosome fusion and acquisition of hydrolytic activity. *Traffic.* 2005;6(5):413-420.
22. Mottola G. The complexity of Rab5 to Rab7 transition guarantees specificity of pathogen subversion mechanisms. *Front Cell Infect Microbiol.* 2014;4:180.
23. Via LE, Deretic D, Ulmer RJ, Hibler NS, Huber LA, Deretic V. Arrest of mycobacterial phagosome maturation is caused by a block in vesicle fusion between stages controlled by rab5 and rab7. *J Biol Chem.* 1997;272(20):13326-13331.
24. Dhiman R, Venkatasubramanian S, Paidipally P, Barnes PF, Tvinnereim A, Vankayalapati R. Interleukin 22 inhibits intracellular growth of Mycobacterium

tuberculosis by enhancing calgranulin A expression. *J Infect Dis.* 2014;209(4):578-587.

25. Carrion M, Juarranz Y, Martinez C, et al. IL-22/IL-22R1 axis and S100A8/A9 alarmins in human osteoarthritic and rheumatoid arthritis synovial fibroblasts. *Rheumatology (Oxford).* 2013;52(12):2177-2186.
26. Kiselev VY, Kirschner K, Schaub MT, et al. SC3: consensus clustering of single-cell RNA-seq data. *Nat Methods.* 2017;14(5):483-486.
27. Butler A, Hoffman P, Smibert P, Papalexi E, Satija R. Integrating single-cell transcriptomic data across different conditions, technologies, and species. *Nat Biotechnol.* 2018;36(5):411-420.
28. Hernandez P, Gronke K, Diefenbach A. A catch-22: Interleukin-22 and cancer. *Eur J Immunol.* 2018;48(1):15-31.
29. Marenholz I, Heizmann CW, Fritz G. S100 proteins in mouse and man: from evolution to function and pathology (including an update of the nomenclature). *Biochem Biophys Res Commun.* 2004;322(4):1111-1122.
30. Wang S, Song R, Wang Z, Jing Z, Wang S, Ma J. S100A8/A9 in Inflammation. *Front Immunol.* 2018;9:1298.
31. Achouiti A, Vogl T, Urban CF, et al. Myeloid-related protein-14 contributes to protective immunity in gram-negative pneumonia derived sepsis. *PLoS Pathog.* 2012;8(10):e1002987.
32. Vogl T, Ludwig S, Goebeler M, et al. MRP8 and MRP14 control microtubule reorganization during transendothelial migration of phagocytes. *Blood.* 2004;104(13):4260-4268.
33. Velge P, Wiedemann A, Rosselin M, et al. Multiplicity of Salmonella entry mechanisms, a new paradigm for Salmonella pathogenesis. *Microbiologyopen.* 2012;1(3):243-258.
34. Mayuzumi H, Inagaki-Ohara K, Uyttenhove C, Okamoto Y, Matsuzaki G. Interleukin-17A is required to suppress invasion of Salmonella enterica serovar Typhimurium to enteric mucosa. *Immunology.* 2010;131(3):377-385.
35. Aujla SJ, Chan YR, Zheng M, et al. IL-22 mediates mucosal host defense against Gram-negative bacterial pneumonia. *Nat Med.* 2008;14(3):275-281.

36. Raffatellu M, Santos RL, Verhoeven DE, et al. Simian immunodeficiency virus-induced mucosal interleukin-17 deficiency promotes Salmonella dissemination from the gut. *Nat Med.* 2008;14(4):421-428.
37. Macosko EZ, Basu A, Satija R, et al. Highly Parallel Genome-wide Expression Profiling of Individual Cells Using Nanoliter Droplets. *Cell.* 2015;161(5):1202-1214.
38. Haber AL, Biton M, Rogel N, et al. A single-cell survey of the small intestinal epithelium. *Nature.* 2017;551(7680):333-339.

3: Methods modification

Collaboration note:

I am very grateful to David Goulding for his help in developing and trialling the EM methods for imaging of the CL3 pathogens.

Some of the methods described in this chapter have been published as: “Using Human Induced Pluripotent Stem Cell-derived Intestinal Organoids to Study and Modify Epithelial Cell Protection Against Salmonella and Other Pathogens” (Lees et al. 2019).

A number of methods used in this study were modified from existing procedures in order to increase efficiency, or to attempt new methods of investigating infections in the iHO system. New methods employed in this study are outlined below.

3.1 Growth and differentiation of iHO

The method outlined in 2.1.2 streamlines the differentiation process of hiPSCs compared to previously published work.[1] Previously used methods required the transfer of hiPSCs from other hiPSC culture systems (e.g., feeder-dependent hiPSC culture) to chemically-defined medium–polyvinyl alcohol (CDM-PVA). This transfer to CDM-PVA typically took 2–3 weeks and required daily feeding of the hiPSCs. This protocol was also not consistently effective, with some differentiations failing; therefore, this study trialed differentiation using the same growth factors but starting with hiPSCs grown in Essential 8 Flex medium (Gibco) on Vitronectin XF (Stem Cell Technologies) coated plates, rather than in CDM-PVA on gelatin/MEF-coated plates, as well as replacement of CDM-PVA with Essential 8 Flex medium during differentiation days 0–3. This was successful for the five independent hiPSC lines trialed thus far, making the differentiation process much more rapid and efficient. This also allowed weekend-free culturing of hiPSCs prior to differentiation, allowing more flexibility with the hiPSC culture. iHO lines produced by this method were phenotyped via light microscopy (**Figure 3.1**), qPCR for cell markers (**Figure 3.2**), immunostaining (**Figure 3.3**) and

TEM as described in 2.1.5 and appeared phenotypically indistinguishable from iHO produced using the previous protocol, with markers for differentiated IECs being clearly demonstrable via RT-qPCR and imaging following embedding and passage of iHO.

In addition, following seeding, iHO usually require at least 4 weeks of routine passaging, with splitting every 4–7 days to facilitate maturation and clearing of contaminating cells from the culture. There is always a degree of variation in the speed of iHO development depending on the iPSC line used and the density of the initial culture. During the first few passages, there were visibly contaminating cells which were not iHO, which eventually died, leaving a clean culture of spherical and, after approximately 4-6 weeks, budded iHO. For recent differentiations, the use of an in-hood imaging system (EVOS XL; Thermo-Fisher) allowed acceleration of the cleaning of the culture, as it was possible to select iHO with the desired morphology and remove them from the contaminating material. These combined modifications have reduced the time required to differentiate and mature iHO from 3 months to 4-6 weeks in total.

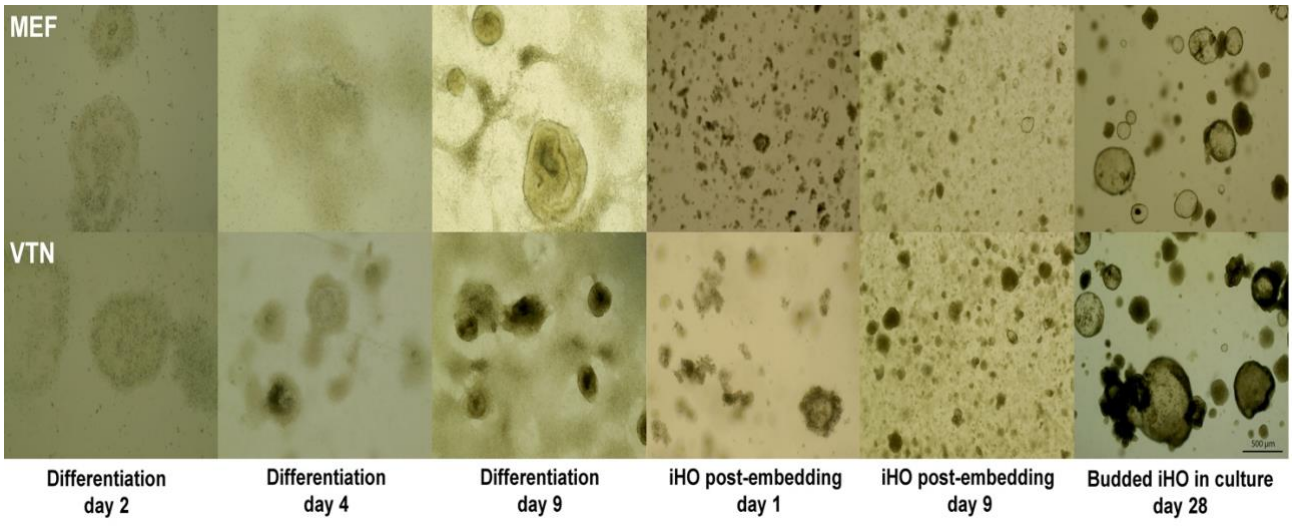

Figure 3.1 - Comparative differentiation and embedding of iHO lines using new method (Sojd2 hiPSC line as example). Cytokine supplementation during differentiation was as described in 2.1.2, however Essential 8 Flex medium (Gibco) was used as a base on days 0-3 rather than CDM-PVA. Plates were coated either in Vitronectin XF (VTN), or gelatin/MEF media (MEF). For gelatin/MEF coating, plates were incubated at 37°C for 30 minutes in gelatin (1mg/ mL gelatin in water for embryo transfer; Sigma-Aldrich), followed by 24 hours incubation with MEF media (Dulbecco's Modified Eagle Medium (DMEM; Invitrogen), 10% foetal bovine serum (Biosera), 1% 200 mM L-glutamine (Invitrogen), and 1% penicillin-streptomycin (10,000 U ml^{-1} ; Invitrogen). No macroscopic differences between iHO were seen with use of alternative media / plate coating. Images taken on Thermo-Fisher EVOS XL imaging system at 4x / 10x magnification.

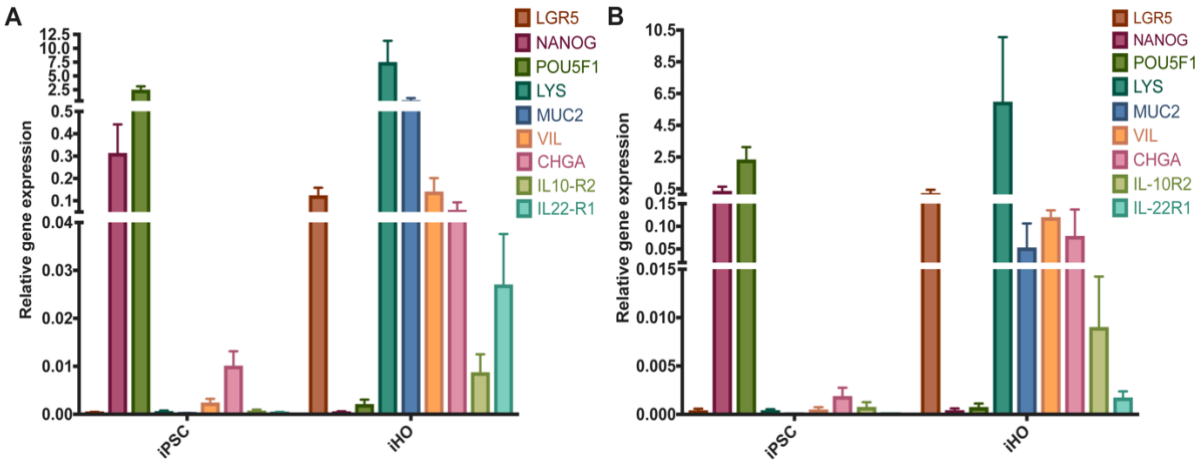

Figure 3.2: Differences in relative gene expression between iPSC and iHO from Rayr2 and Sojd2 cell lines. Data presented are from 4 technical replicates, using cDNA at 1:100 concentration, with assays repeated 3 times using paired iPSC/iHO of different batches for Rayr2 (**A**) and Sojd2 (**B**) cell lines. Data were analysed using the comparative cycle threshold (C_T) method, with GAPDH as an endogenous control.

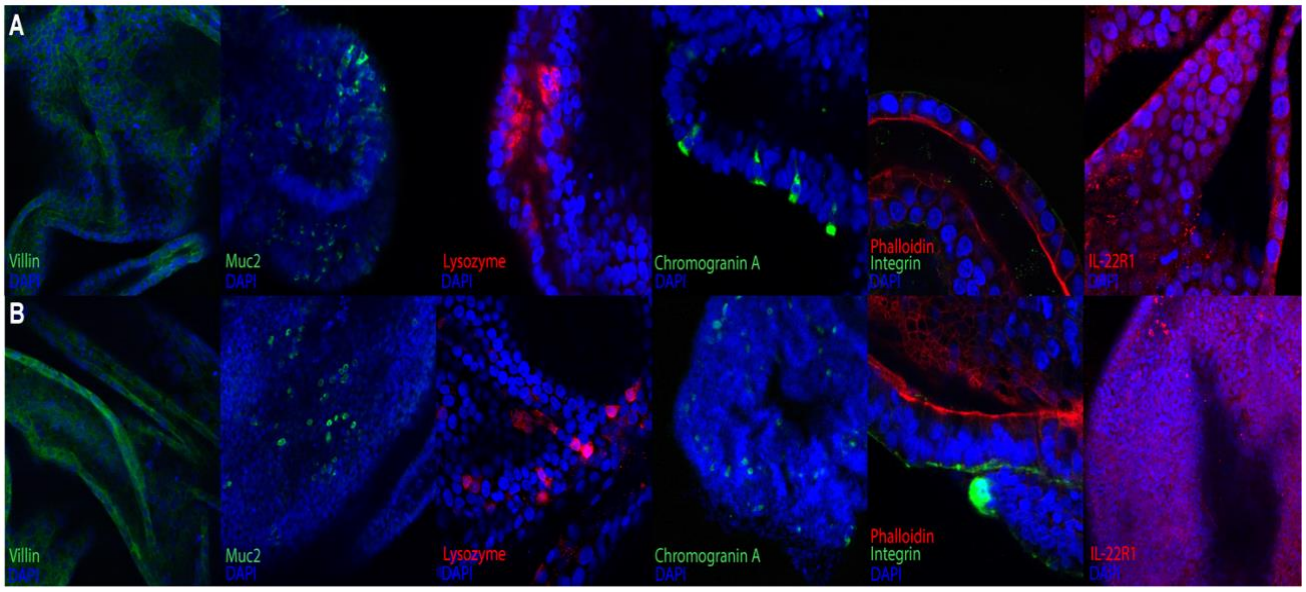

Figure 3.3: Immunohistochemistry of iHO lines generated with new method. Presence of constituent intestinal cell types demonstrated in iHO from Rayr2 (**A**) and Sojd2 (**B**) cell lines; namely goblet, Paneth, enteroendocrine cells and enterocytes, with a polarised epithelium and widespread presence of IL-22R1 on the basal surface of iHO generated using the modified method. Images taken on Zeiss LSM 510 Meta confocal microscope at 20x (Villin, Muc2, Lysozyme, Chromogranin A and IL-22R1 panels) or 40x (Phalloidin panel) magnification.

3.2 Establishing multiplicity of infection (MOI) in the iHO model

Establishing MOI in the iHO model is not as simple as in the macrophage model of infection, wherein it is possible to know how many cells are in a given well based on counting cells and seeding at specific densities. There is heterogeneity of iHO size and maturity within iHO cultures, which is why it is important to inject a relatively large number of iHO for

experiments, in order to reduce the impact of this variable. During routine splitting, attempts were made to establish the average number of cells in an iHO as follows.

iHO were released from Matrigel using Cell Recovery Solution. Five iHO were selected and transferred into a Falcon tube containing DPBS. iHO were washed, supernatant was removed and iHO resuspended in 1 mL of TrypLE, then incubated at 37 °C for 5 minutes to produce a single cell solution. 10 µL of cells were mixed with 10 µL Trypan Blue (Sigma Aldrich), and 10 µL of the resulting solution was added to a disposable C-Chip haemocytometer (NanoEnTek). Cells were counted, averaged and the number of cells per organoid determined. This was repeated 3 times on 3 separate occasions. The mean number of cells per iHO was 46,000 (SEM = 8413 cells).

It was also important to determine the inoculum of bacteria being injected into the closed lumen of the iHO. Two methods were trialled to achieve this. Luminal assays using microinjection (as described in 2.3) were set up, and 25 iHO per plate injected, but instead of incubating prior to harvesting, iHO were released from Matrigel immediately after injection, and their contents diluted and plated to give CFU injected per plate. This was repeated 3 times on 3 separate occasions to obtain an average CFU injected per plate (**Figure 3.4**).

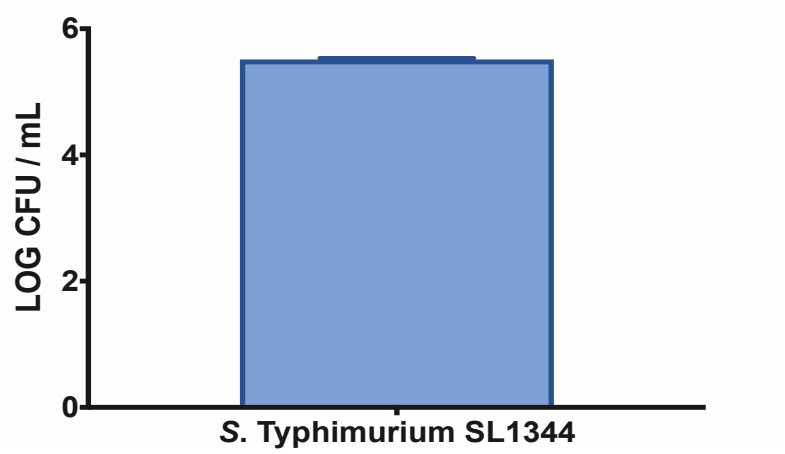

Figure 3.4 - Luminal contents at Time 0 after microinjection. LOG CFU/mL shown for microinjections with 25 x iHO per plate which were harvested immediately post-injection. Results plotted are for 3 biological replicates, each comprising 3 technical replicates. Mean LOG CFU/mL was 5.51; error bar indicates SEM.

This was compared with the expected CFU injected per iHO, by injecting the bacterial / Phenol red solution into a droplet of oil, and using a stage micrometer to measure the diameter (and therefore calculate the volume) of the injection. This was repeated 3 times on 3 separate occasions to obtain an average volume of inoculum.

At an OD_{600} of 1, counts of *S*. Typhimurium would be 1.6×10^9 CFU/mL, therefore:

Volume of inoculum: 3.59×10^{-6} mL
CFU per injection: $3.59 \times 10^{-6} \times 1.6 \times 10^9 = 5744$ CFU per injection
CFU per iHO (3 injections per iHO): 5744 x 3 = 17,232 (LOG 4.23)
CFU per plate (25 iHO per plate): 430,800 (LOG 5.63)

Having established cell counts in iHO and bacterial counts at injection, it is therefore possible to work out that MOI for experiments at the above settings was ~0.4.

3.2 Alternative antibiotic protection assays, to study gentamicin-resistant bacteria

It was of interest to study clinically relevant strains of *S*. Typhimurium to establish how different serovars interact with the epithelium. We consequently used a collection of Vietnamese ST34*, S*. I:4,[5],12:i:− (*S.* Typhimurium variant) clinical isolates, all from the same BAPS (Bayesian Analysis of Population Structure) cluster, which had been found in the blood or stool of patients presenting with salmonelloses (**Table 3.1**):[2]

Strain number:	Flagellar status:	Isolated from:	Presenting feature:	Gentamicin MIC:
VNB1779	Biphasic	Blood	Bloodstream infection	5
VNB2140	Biphasic	Blood	Bloodstream infection	7
VNB2315	Monophasic	Blood	Bloodstream infection	0.094
VNS20081	Biphasic	Stool	Diarrhoea	4
VNS20101	Monophasic	Stool	Diarrhoea	0.25

Table 3.1: Vietnamese clinical strains used in iHO, with flagellar status, location of isolation and minimum inhibitory concentration (MIC) for gentamicin highlighted.

Given that a number of these strains were gentamicin-resistant, results of antibiotic sensitivity assays run on the Vitek 2 system (Biomérieux) were examined to establish whether there was an alternative antibiotic that could be used to replace this in the modified gentamicin protection assay used for intracellular invasion assays in the iHO. There were only 3 antibiotics which all strains were sensitive to: Cefepime, Meropenem and Ertapenem. Cefepime is a 4th generation cephalosporin with particular action against Enterobacteriaceae. Cephalosporins disrupt the synthesis of the peptidoglycan layer of the bacterial cell wall, and are able to accumulate in the cytoplasm to a degree (far less in epithelial cells than phagocytic cells), but do not efficiently penetrate lysosomes.[3] Variable concentrations of Cefepime over the MIC were used until bacterial growth was inhibited. This concentration was then trialled as the antibiotic agent in the intracellular invasion competition assay in the iHO (for full protocol, see 2.1.7), allowing these assays to be performed with gentamicin-resistant bacteria.

3.3 Use of IncuCyte for observation of progress of infection in iHO

In order to help establish the fate of bacteria in the lumen of the organoids, it was beneficial to image them at regular time points during infection assays. This process was automated by use of the IncuCyte S3 Live-Cell Analysis system (Sartorius). Use of the TIMER^{bac}-*Salmonella* SL1344, which contains a DsRed S197T variant called TIMER that acts as a growth rate reporter by fluorescing at different wavelengths depending on replication stage,[4] allowed observation of bacterial replication and changes to the structure of the organoid in the hours following microinjection. In bacterial cells which are not growing, both green (rapidly maturing) and orange (slowly maturing) TIMER particles accumulate, with the predominant fluorescence being orange. In contrast, in dividing cells, rapidly maturing green particles are the predominant source of fluorescence, since whilst both molecules are diluted by cell division before they have matured, this disparately affects the orange molecules as they are slower to accumulate. Images were taken every 10 minutes, using the 10 x objective. Videos were produced from the collation of images, and red versus green fluorescence intensity over time plotted using the Incucyte S3 software.

3.4 Development of CryoEM methods for CL3 pathogens

Having reviewed TEM images from iHO injected with *S*. Typhi, and seen that a number were remaining in the lumen of the organoid at 3 hours post-injection, we wished to better visualise what was happening in the lumen and obtain better definition of the luminal contents, namely the mucus layer lining the epithelium. We therefore decided to trial high pressure freezing of the iHO to facilitate this.

iHO were microinjected with the pathogen of interest as described in 2.1.7 and incubated at 37 °C for 3 hours. The bottom of an aluminium planchette was lined with 1-Hexadecen 92% (Sigma-Aldrich), and a single iHO placed into the planchette using a 20 μL pipette. The planchette was placed into the sample holder and the sample holder was then placed directly into a 250 mL conical flask, which was sealed with Parafilm M (Bemis), sprayed with 70 % ethanol and removed from the CL3 laboratory as rapidly as possible.

Once in the CL2 facility, the sample holder was placed directly into the high pressure freezer (Bal-Tec HP010), and the HPF programme engaged and completed. Following this, the sample holder containing the planchette was held under liquid nitrogen, then the planchette removed, opened and placed into a 2 mL cryovial (Corning) and stored under liquid nitrogen. After freezing, the planchette was opened and placed in an automated Leica FS100 freeze-substitution unit at -200 °C, then gently warmed to -90 °C in 0.1% tannic acid with 0.5% glutaraldehyde in acetone for 6 hours, followed by 0.2% uranyl acetate (Sigma-Aldrich) and 1% osmium tetroxide (Acros Organics) in acetone (Sigma-Aldrich) for 72 hours. The samples were then rinsed in acetone and the temperature raised slowly to 4 °C. Acetone was then replaced with an epon resin/acetone mix overnight, followed by neat epon resin (Epoxy Embedding Medium kit, Sigma-Aldrich) for 24 hours. The sample was removed from the planchette, embedded in epon resin and cured at 65 °C for 48 hours. 500nm semi-thin sections were cut on a Leica UCT ultramicrotome and stained with toluidine blue on a microscope slide. Images were recorded on the Zeiss Axiovert CCD camera and areas selected for ultrathin 50nm sectioning. Ultrathin sections were collected onto copper grids and contrasted with uranyl acetate and lead citrate before viewing on a FEI 120kV Spirit BioTWIN TEM and recording CCD images on an F4.15 Tietz charge-coupled device camera.

References:

1. Forbester JL, Hannan N, Vallier L, Dougan G. Derivation of Intestinal Organoids from Human Induced Pluripotent Stem Cells for Use as an Infection System. *Methods Mol Biol.* 2016.
2. Mather AE, Phuong TLT, Gao Y, et al. New Variant of Multidrug-Resistant Salmonella enterica Serovar Typhimurium Associated with Invasive Disease in Immunocompromised Patients in Vietnam. *MBio.* 2018;9(5).
3. Hof H. Listeriosis: therapeutic options. *FEMS Immunol Med Microbiol.* 2003;35(3):203-205.
4. Claudi B, Sprote P, Chirkova A, et al. Phenotypic variation of Salmonella in host tissues delays eradication by antimicrobial chemotherapy. *Cell.* 2014;158(4):722-733.

5: Investigation of the iHO luminal response to infection, iHO as a model for alternative pathogens, competition between bacterial strains and interactions of *Salmonella* with iHO derived from cell lines with isogenic mutations

Collaboration note:

The data in this chapter on *Salmonella enterica* serovar Enteritidis (*S*. Enteritidis) were generated jointly with Rafal Kolenda, a PhD student from the University of Wrocław whom I taught how to generate iHO and complete intracellular and luminal infection assays.

5.1 Introduction

As detailed in Chapter 4, it was possible to demonstrate an enhanced barrier phenotype associated with iHO in response to IL-22. Additionally, whilst we identified a mechanism for intracellular protection following IL-22 stimulation, further questions can potentially be answered using this system. Compared to 2-D cell culture, the iHO model incorporates more components of the intestinal luminal environment found *in vivo*. The use of microinjection, allows the introduction of pathogens into a closed system, which reproduces aspects of the intestinal luminal environment and allows controlled observations to be made. For example, studies on *Helicobacter pylori* in gastric organoids were able to demonstrate that bacteria were attracted to the urea being produced by the gastric organoid epithelial cells, and the bacteria were able to use this signal to locate the epithelium for binding and subsequent colonisation.[1] Similarly, other studies using gastric organoids were able to demonstrate that parietal cells (which are difficult to maintain in monolayer culture but viable within the organoid structure), were responsible for Sonic hedgehog (Shh) production, which is a factor that induces macrophage infiltration post-infection.[2] More specifically to the small intestinal organoid model, studies have attempted to look at α-defensin concentrations following secretion by Paneth cells into the organoid lumen, and whether these exist at high enough

concentrations to have a directly antimicrobial effect.[3] These types of question are more difficult to answer *in vivo*, given the multiple interactions with the mucosal immune system and intestinal microbiota.[4] A study in murine intestinal organoids, demonstrated the ability of alpha defensins to restrict growth of strains of *S*. Typhimurium for up to 20 hours after microinjection, with a 3.9-log reduction in bacterial counts versus those seen in organoids derived from $Mmp7^{-/-}$ mice, which lack matrix metalloproteinase 7 and are unable to produce functional α-defensins.[3] Organoids as vessels for infection modeling are growing in use, with pathogens such as *H. pylori*,[5] norovirus,[6] rotavirus,[7] Shiga toxin-producing *Escherichia coli*,[8] Cryptosporidium,[9] and Zika virus[10] having been shown to survive and replicate within these systems.

Having investigated how well *S*. Typhimurium SL1344 invades intracellularly and survives in the lumen of the iHO system, it was of interest to expand this line of enquiry to other serovars of *Salmonella*, such as *S*. *enterica* serovar Enteritidis, which causes both gastrointestinal disease and invasive non-typhoidal salmonellosis (iNTS).[11] Additionally, with the hypothesis that bacteria may be killed by antimicrobial peptides in the iHO lumen, assays were performed to assess this with an attaching and effacing pathogen, Enteropathogenic *E. coli* (EPEC), which would not be expected to extensively reside within cells.[12] We also wished to investigate how drug-resistant isolates of *Salmonella* that cause invasive disease in humans would behave in the iHO model. This is particularly relevant when considering that these isolates have the potential to outcompete other sensitive strains in the microbiota *in vivo*, either within or across species, as suggested by a recent study.[13] A number of Vietnamese clinical strains were therefore put directly in competition with the laboratory reference strain (*S*. Typhimurium SL1344) with the hypothesis that strains causing severe disease in humans may be better able to invade the iHO epithelium. The clinical strains used were a mixture of those expressing monophasic and biphasic flagellae. Flagellar protein (fliC or fljB) is the main structural subunit of the flagellar filament in most *Salmonella* strains,[14] with fliC coding phase 1 flagellins and fljB phase 2 flagellins. FliC is antigenic and is expressed in multiple *Salmonella* serotypes, as well as having a homolog in other pathogens such as *E*. *coli*.[15] FljB is only expressed in *S. enterica* subspecies I, II, IIIb and Vi, and the *fljB* gene is located on a different part of the chromosome to the *fliC* gene.[16] Both flagellin genes are not normally expressed at the same time as biphasic

bacteria display phase variation, switching between the two phases, with the switch controlled by an invertible element called *hin.*[17] (**Figure 5.1**)

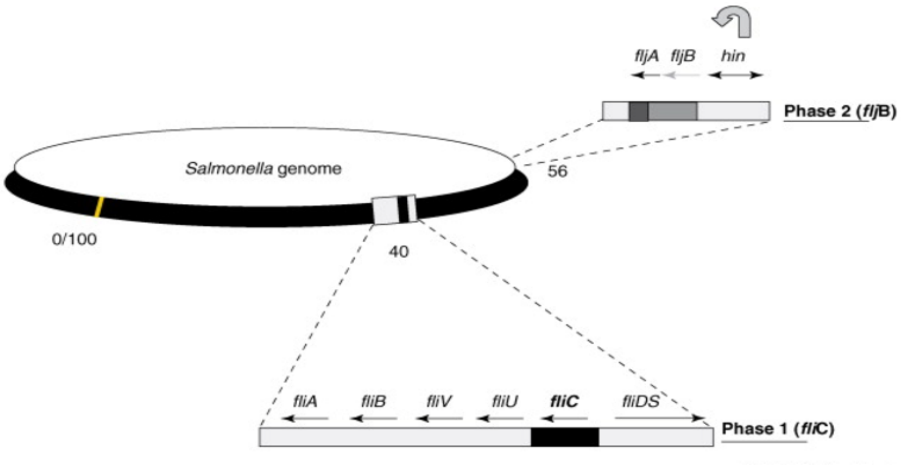

Figure 5.1: Interactions of *fliC* and *fljB* loci. This figure demonstrates the locations on the *Salmonella* genome of the *fliC* and *fljB* loci, as well as the location of the reversible *hin* element which facilitates phase variation. In one orientation, *hin* promotes expression of both *fljB* and the post-transcriptional repressor *fljA,* leading to lack of expression of *fliC*. The converse is true when the orientation of *hin* is reversed. (Figure taken from McQuiston et al, 2008[16])

It is unclear what exactly leads to the phase switch. Some *Salmonella* strains are monophasic, through the loss or deletion of *fljB.* Possible advantages from the biphasic lifestyle could include limited antigenic diversity and temporary evasion of the immune response, or improved adaptation to a particular environmental niche.[16]

Finally, we hypothesised that it would be possible to expand the clinical utility of iHO by deriving them from individuals with mutations in genes involved in the immune response to directly investigate the effect of these mutations on IEC response to infection. To this end, we generated iHO from an individual with a mutation in the caspase recruitment domain-containing protein 8 (CARD8) gene as described below and conducted infection assays in this model using *S*. Typhimurium SL1344.

5.2 Assessing whether luminal bacterial killing occurs in the iHO model

As described in Chapter 4, initial invasion of *S*. Typhimurium SL1344 was restricted in rhIL-22 treated iHO and there was uncertainty about the location of killing of the less invasive strain ST4/74 ΔPhoPQ. Therefore, the question arose of whether there was any luminal killing effect

induced by IL-22 treatment, perhaps mediated by an increased antimicrobial peptide release into the iHO lumen. This was investigated by microinjecting bacteria and harvesting the luminal contents of the iHO at 90 minutes post-infection, as described in 2.3. Initial assays performed with ST4/74 and ST4/74 ΔPhoPQ bacteria at a starting OD_{600} of 1 (1.6 x 10^9 CFU/mL) did not show any significant difference in bacterial counts recovered from the lumen with or without rhIL-22 treatment. To assess whether this could be due to the bacterial inoculum overloading the defensive capacity of the iHO, the assay was expanded by inoculating iHO with *S*. Typhimurium SL1344 at a series of 10-fold dilutions. In these assays, significantly fewer bacteria were recovered from the lumen of rhIL-22 treated iHO compared to unstimulated equivalents at bacterial concentrations of 1.6 x 10^8 CFU/mL and 1.6 x 10^7 CFU/mL (**Figure 5.2**).

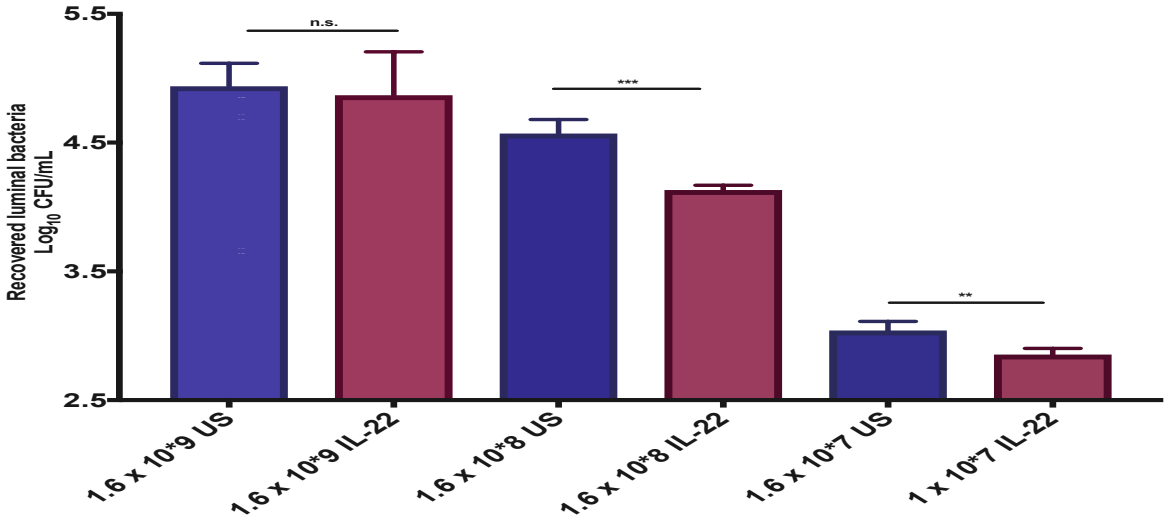

Figure 5.2: Luminal bacterial counts using decreasing SL1344 inoculums in Kolf2 iHO pre-treated with rhIL-22 vs unstimulated (US). iHO were either pre-treated with rhIL-22 at 100 ng/mL for 18 hours or left unstimulated. iHO were injected with a series of 10-fold dilutions of SL1344 and incubated for 1.5 hours prior recovery of intraluminal bacteria. Data presented are for 3 biological replicates (each averaged from 3 technical replicates), with 30 iHO injected per replicate +/- SEM. Unpaired Mann-Whitney tests were used for all assays (n.s. – not significant, ** p< 0.01, *** p < 0.001). There were significantly fewer bacteria recovered from the lumen in iHO pre-treated with rhIL-22 at both of the lower concentrations of bacteria injected.

Luminal killing assays were additionally performed using an *S*. Typhimurium SL1344 *invA* mutant, which has a deletion in the *invA* gene of *Salmonella* pathogenicity island 1. This derivative has been demonstrated to be less invasive in the iHO system,[18] and therefore may remain in the iHO lumen for a longer time before entering the epithelial cells. These assays were performed over a time course with iHO harvested directly after injection and then

hourly for 4 hours. Having observed luminal survival differences at the lower inoculums, the concentration of the bacterial solution used for these assays was 1.6 x 10^8 CFU/mL. For SL1344, there appeared to be some luminal killing effect, with significantly fewer bacteria recovered from the lumen at 1, 2 and 3 hours post injection for those iHO pre-treated with rhIL-22. For SL1344 Δ*invA*, there were significantly fewer bacteria recovered at the 1 hour timepoint following rhIL-22 treatment, but this effect was not obvious from the 2 hour timepoint onwards. It is possible that with increased numbers of bacteria remaining in the lumen, rather than invading, the bacterial load in the lumen was high enough to exceed any killing effect related to IL-22 treatment. Interestingly, for both groups treated with rhIL-22, there were significantly increased counts of bacteria recovered from the lumen at 4 hours, suggesting that the protective effect of IL-22 on luminal bacteria is limited to the early stages of infection (**Figure 5.3**). Perhaps the increased mucus release stimulated by IL-22, whilst preventing entry into cells, provides a niche in which bacteria can replicate. This is discussed further later in the chapter.

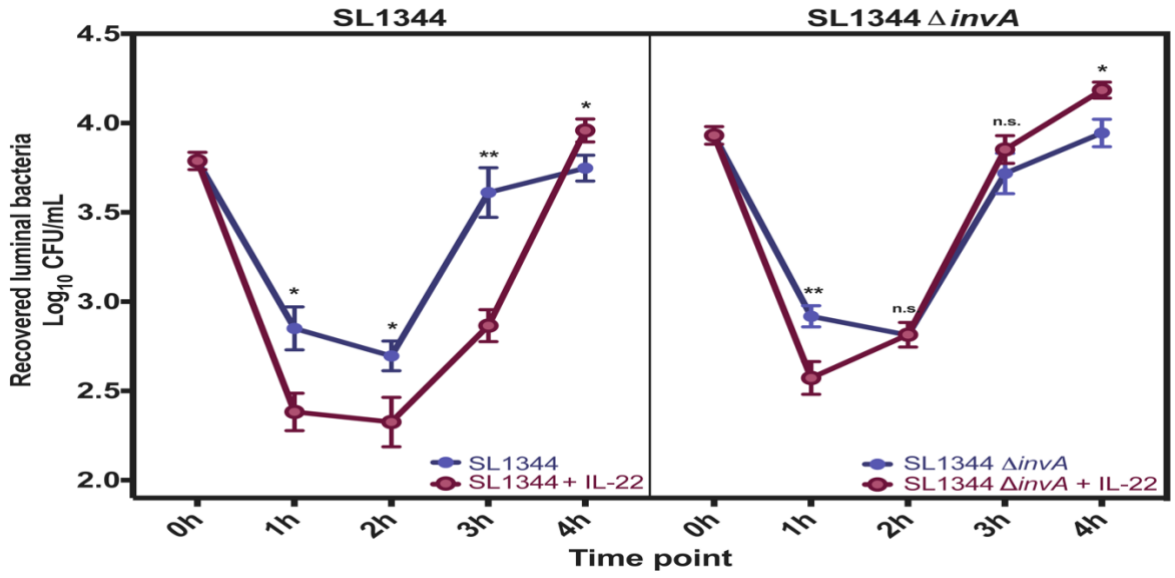

Figure 5.3: Luminal bacterial counts at timepoints following injection of Kolf2 iHO with SL1344 or SL1344 Δ*invA*. iHO were either pre-treated with rhIL-22 at 100 ng/mL for 18 hours or left unstimulated. iHO were injected with SL1344 or SL1344 Δ*invA* at 1.6 x 10^8 CFU/mL and incubated for 0, 1, 2, 3 or 4 hours prior to recovery of intraluminal bacteria. Data presented are for 3 biological replicates (each averaged from 3 technical replicates), with 30 iHO injected per replicate, +/- SEM. Unpaired Mann-Whitney tests were used for all assays (n.s. – not significant, * < p<0.05, ** p< 0.01). There were significantly fewer bacteria recovered from the lumen in rhIL-22-treated iHO for the first 3 hours after injection with SL1344. This effect was only detected for the first hour for SL1344 Δ*invA*-infected iHO.

From these assays it was clear that initially, killing of bacteria in the lumen was occurring, but eventually, significant numbers of bacteria were able to survive and replicate in the lumen, enabling them to invade and damage the iHO epithelium. Imaging of iHO using the Incucyte S3 live cell analysis system (Sartorius) at 3-4 hours post-injection demonstrated clear destruction of iHO tissue (**Figure 5.4**). Bacteria used for imaging in the Incucyte system were TIMER^{bac}-*Salmonella* SL1344,[19] which produce differently coloured fluorophores depending on their growth rate, therefore via measurement of colour change, it was possible to witness bacterial survival and replication in the lumen over time. Green fluorophores are initially produced, which later mature into orange fluorophores. Thus, rapidly dividing cells will fluoresce predominantly green, since the slower maturing orange fluorophores will be diluted by cell division. On sequential imaging, it was possible to view areas where TIMER^{bac}-*Salmonella* SL1344 had been injected into the iHO and observe these infected spots fluorescing green over time as exponential growth phase is reached.

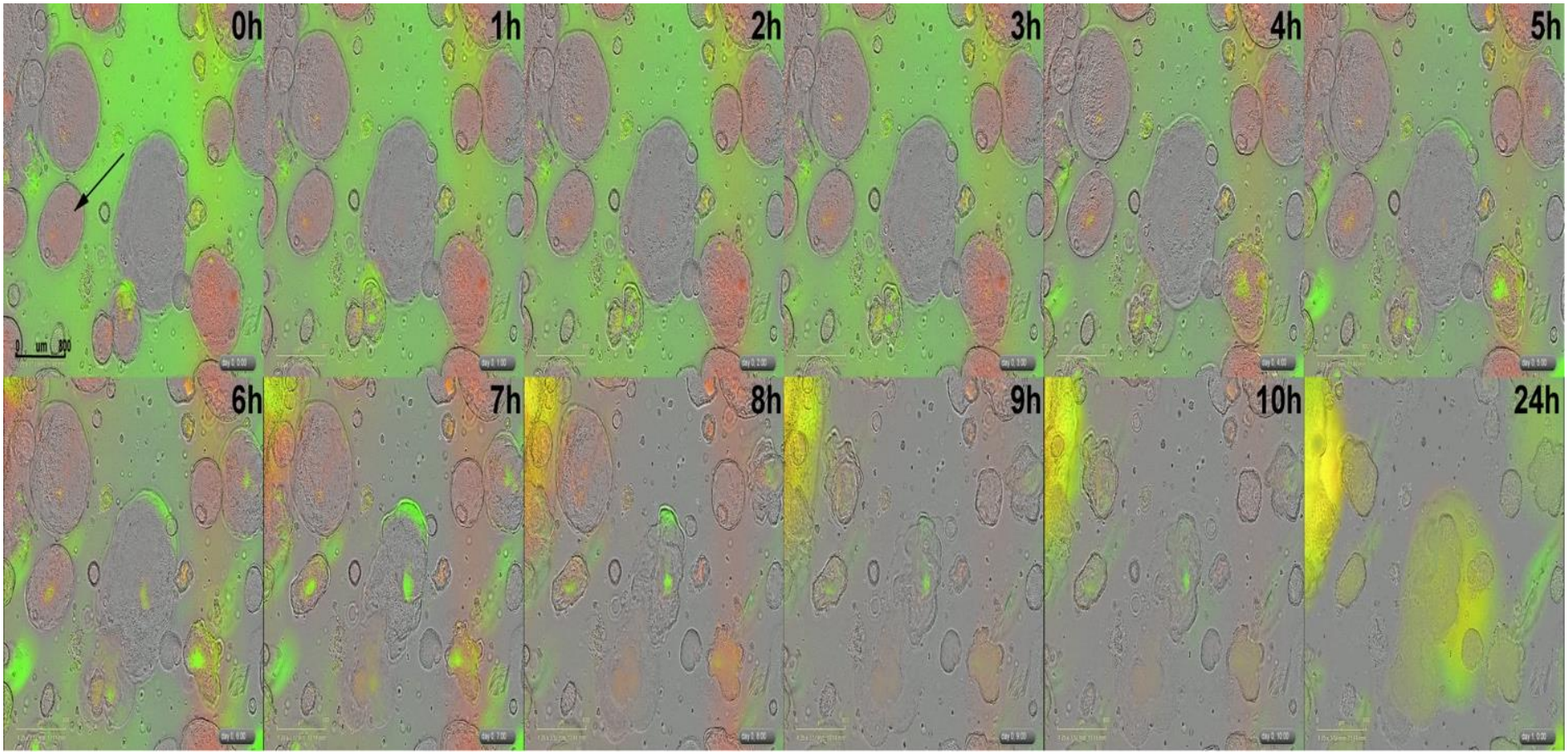

Figure 5.4: Sequential imaging of Kolf2 iHO infected with TIMER^{bac}-*Salmonella* SL1344. Organoids were imaged every 10 minutes for 24 hours following infection with TIMER^{bac}-*Salmonella* SL1344. Injection sites on iHO are visible as green/orange dots (arrow) which initially appear static in terms of growth, but later fluoresce green as bacteria overtake iHO defences and start to replicate rapidly. Visible destruction of the iHO architecture is witnessed between 3 and 4 hours after injection. By 24 hours after infection, iHO are destroyed and bacteria are dividing rapidly in the culture media. Artefactual green background staining in initial images is generated by Matrigel embedding scaffold and red staining by phenol red injected with bacteria. Images taken using the Incucyte S3 system at 4x magnification; scale bar = 800μm.

It was also possible to use these images to measure green and red fluorescence of TIMER^{bac}-*Salmonella* SL1344 over time, for infected unstimulated and rh-IL22-treated iHO. There was no significant difference in groups between green fluorescence, although some initial growth advantage was suggested in the unstimulated group (**Figure 5.5**). Total red fluorescence was significantly higher in the unstimulated group, particularly in the first 8 hours following infection, suggesting a non-replicating cohort of bacteria surviving either in the lumen or intracellularly within unstimulated iHO and bacterial death in the IL-22 stimulated group. Studies of *S*. Typhimurium in human and mouse macrophages have demonstrated a non-replicating subset of bacteria existing intracellularly following infection.[20,21]

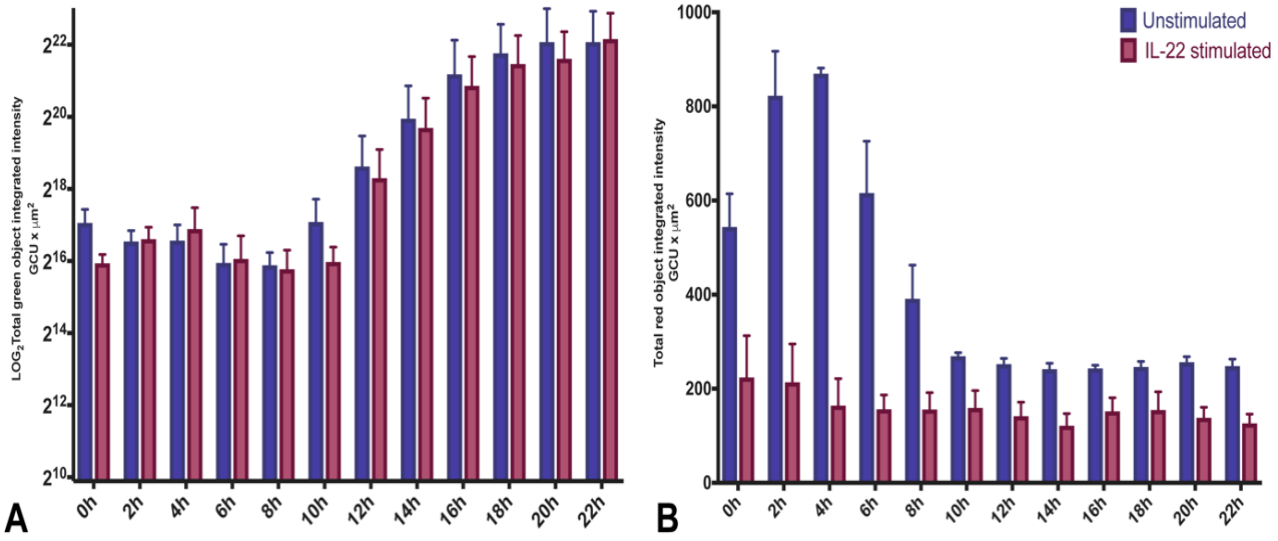

Figure 5.5: Total green / red fluorescence over time for TIMER^{bac}-*Salmonella* SL1344 following Kolf2 iHO infection. iHO were either pre-treated with rhIL-22 at 100 ng/mL for 18 hours or left unstimulated, then injected with TIMER^{bac}-*Salmonella* SL1344 and incubated for 22 hours, and red/green fluorescence recorded over time. Wilcoxon matched pairs signed rank test was used for statistical analysis. There was no significant difference in green fluorescence over time between the two groups (**A**), but significantly higher total red fluorescence in the unstimulated group (**B**) ($p = 0.0005$).

5.3 Reviewing the luminal contents of the iHO and their effects on other bacterial strains

Ideally, study of the intra-luminal AMP contents of the iHO would involve being able to directly extract the luminal contents and run proteomic analysis on them. In lieu of the ability to do this, transcripts for antimicrobial peptides of interest were measured as a proxy. RT-qPCR assays using Taqman reagents were completed for REGIIIα, Lysozyme C

(LYZ), Alpha defensin 5 (DEFA5), Defensin beta 4B (DEFB4B) and Phospholipase A2 group IIA (PLA2G2A). These genes were chosen as they represent a combination of alpha and beta defensins and C-type lectins and would be expected to be upregulated in response to *Salmonella*[22], or *E*. coli infections in iHO.[23] It was not possible to consistently detect transcripts for REGIIIα, even at an increased starting concentration of cDNA (1:50 vs 1:100), therefore these data were excluded from the analysis. iHO were either harvested uninfected (time 0), or infected with SL1344 and harvested at 1, 2 or 3 hours post-infection and RNA extracted (**Figure 5.6**). Transcripts for DEFB4B were significantly upregulated from 1 hour post infection, and DEFA5 from 2 hours post-infection. Basal levels of Lysozyme C were very high (partly to be expected as this AMP should be found in all Paneth cells), therefore no significant difference in its expression across timepoints was observed.

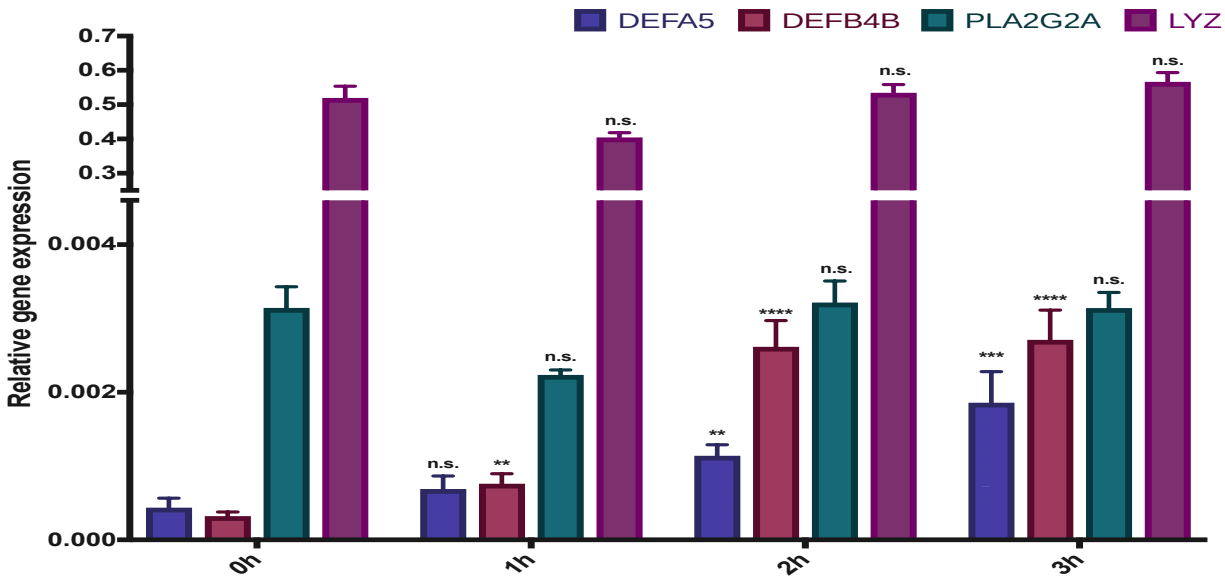

Figure 5.6: Expression of antimicrobial peptides over time following Kolf2 iHO infection with SL1344. iHO were injected with SL1344 and harvested at 0, 1, 2 or 3 hours post-infection, RNA extracted and RT-qPCR completed for AMP transcripts of interest. Data presented are for 3 biological replicates, each averaged from 4 technical replicates. Data were analysed using the comparative cycle threshold (C_T) method, with GAPDH as an endogenous control. Unpaired Mann-Whitney test was used to compare results (**n.s.** not significant, **p <0.01, ***p <0.001, ****p <0.0001). Transcripts for DEFB4B were significantly upregulated from 1 hour post infection, and DEFA5 from 2 hours post-infection.

Having studied a number of strains of *S*. Typhimurium, and witnessed initial drops in luminal bacterial counts before a recovery period, the question arose of whether this pattern would be repeated for other serovars of *Salmonella*. Assays were completed using *S*. Enteritidis strains 6206 and 6174. These were isolates from stool; 6174 from a human sample and 6206

from a poultry sample. *S*. Enteritidis 6174 has a mutation in the gene coding the outer membrane porin protein *ompD*. Previously, *Salmonella* with *ompD* mutations have been shown to have increased ability to survive and replicate within murine organs,[24] and have an increased resistance to beta-lactam antibiotics.[25] *S*. Enteritidis 6206 has a SNP in the N-acetylmuramyl-L-alanine amidase (*amiA*) promoter. *amiA* has a role in cell wall hydrolysis during cell division. *E. coli* with these mutations have been shown to be more susceptible to human neutrophil peptide 1 (HNP-1; a type of alpha-defensin).[26] *S*. Typhimurium SL1344 was used as a control, given that its behaviour in the iHO model had been previously established. In addition, P125109 (PT4); a reference isolate of *S*. Enteritidis[27] frequently used for laboratory work was trialled in the model as a comparator. Single iHO were harvested immediately following infection (time 0), and at hourly timepoints thereafter. SL1344 demonstrated intraluminal survival following an initial drop in viable bacteria as seen previously. Significantly fewer P125109 survived in the lumen, and the luminal bacterial population appeared to be at an equilibrium between rates of replication and death from 2-4 hours. Counts for 6174 and 6206 consistently decreased over time, suggesting intraluminal killing; particularly relevant to 6206 given its increased susceptibility to alpha-defensins. Modified gentamicin protection assays were completed to assess the ability of these strains to invade the iHO epithelium. Strains 6206 and 6174 were also consistently less able to invade and survive within the iHO epithelial cells, with only 6206 being recoverable at 3 hours post-infection. Whilst P125109 was significantly more invasive than the other *S*. Enteritidis strains, intracellular counts at 3 hours remained lower than those for SL1344, suggesting that these *S*. Enteritidis are less able to adapt to the iHO environment than *S*. Typhimurium (**Figure 5.7**).

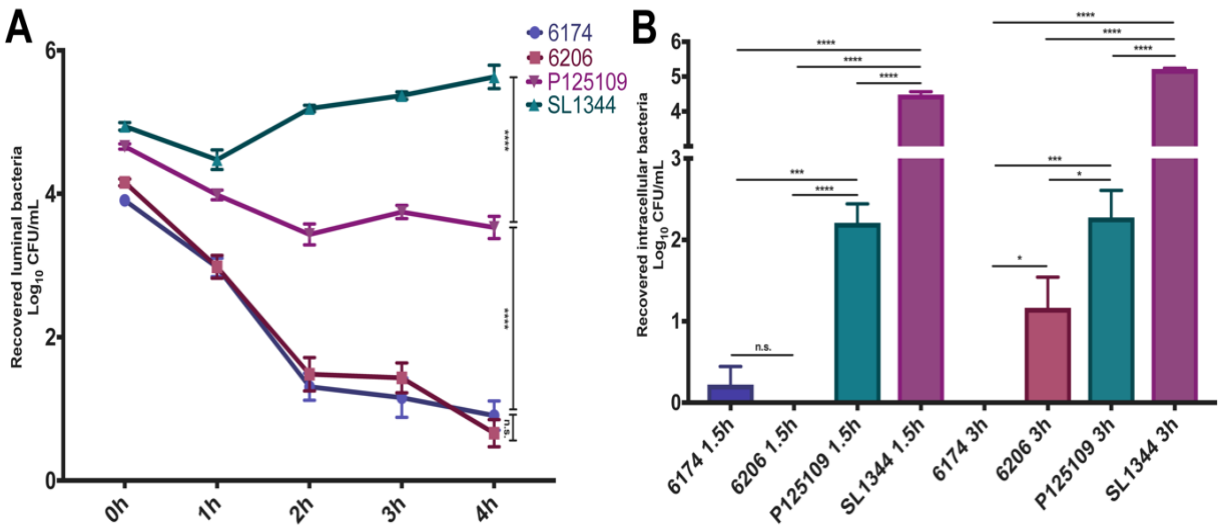

Figure 5.7: Recovered intraluminal and intracellular counts for *S.* Enteritidis in Kolf2 iHO. iHO were injected with S. Enteritidis 6174, 6206, P125109 or S. Typhimurium SL1344 and either incubated for 0, 1, 2, 3 or 4 hours, and luminal contents recovered (**A**), or incubated for 1.5 or 3 hours and modified gentamicin assays completed to recover intracellular bacteria (**B**). Data are presented for 3 biological replicates, (each averaged from 3 technical replicates) per condition +/- SEM. Multiple single iHO were used for luminal assays and 30 iHO injected per replicate for intracellular assays. Unpaired Mann-Whitney test was used to compare results (**n.s.** not significant, * p<0.05, ***p <0.001, ****p <0.0001). (**A**) Intraluminal counts from 0-4 hours post-infection. An initial decrease in recovered counts was observed for all strains, followed by recovery in SL1344, static counts in P125109 and continuous decrease in 6174 and 6206. (**B**) Intracellular counts show significantly more invasion in SL1344 and P125109, with no bacteria from strain 6174 invading and surviving until 3 hours post infection.

Given the large difference in luminal survival between the serovars of *Salmonella*, these assays were repeated using BRD948, an attenuated derivative of *S.* Typhi Ty2, with mutations in the *aroC* and *aroD* genes (responsible for aromatic amino acid biosynthesis[28]) and *htrA* (a serine protease required for virulence[29]). It was anticipated that this attenuated *S*. Typhi derivative would be less invasive than the virulent isolates previously tested, and should be present for longer in the iHO lumen. Luminal infection assays and modified gentamicin protection assays were carried out as previously described, with the exception that BRD948 required growth in LB broth supplemented with aromatic amino acids (Aro mix: phenylalanine 0.04 g/L, tryptophan 0.04 g/L, para-aminobenzoic acid 0.01 g/L and dihydro-oxbenzoic acid 0.01 g/L) and tyrosine 0.04 g/L. As predicted, numbers of recovered intracellular BRD948 were markedly lower; in this case ~3-log lower than those observed in previous assays with SL1344. Similarly, when harvesting iHO at the usual luminal timepoint of 1.5 hours, no viable bacteria remained, therefore assays were shortened and iHO harvested at 0, 20 and 40 minutes post-infection to check whether viable bacteria were present immediately following infection. By 40 minutes post-infection, intraluminal BRD948 counts were only 20% of those recovered at 0h (**Figure 5.8**). As an additional comparator,

these assays were completed for *S*. Typhimurium D23580, a multi-drug resistant ST313 isolate, known to cause invasive salmonellosis in sub-Saharan Africa,[30] in order to assess whether this isolate survived in the iHO prior to its use in experiments discussed later in the chapter. D23580 survived both intracellularly and in the lumen at higher counts than BRD948.

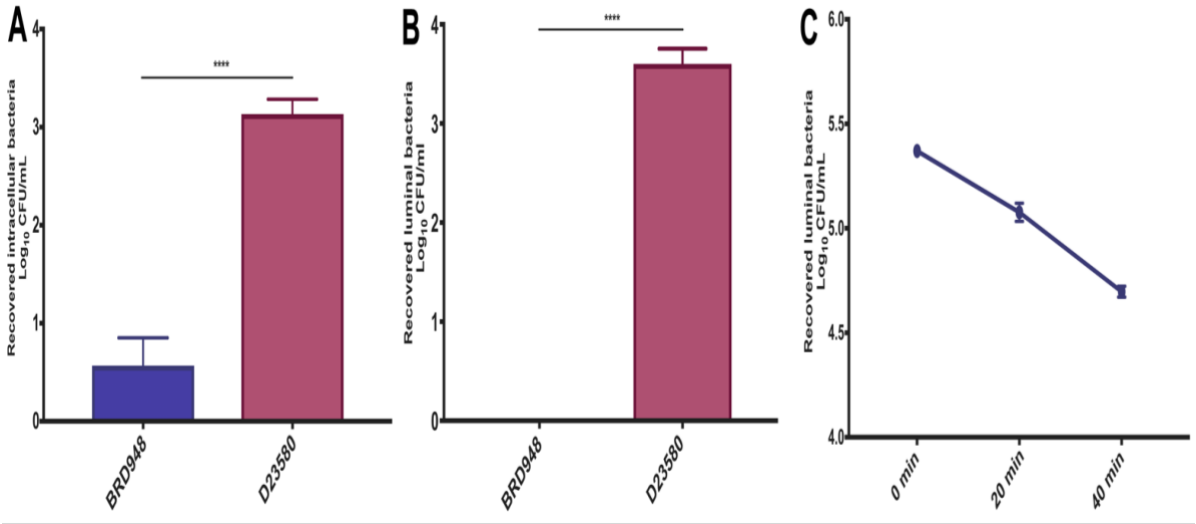

Figure 5.8: Recovered intraluminal and intracellular counts for *S*. Typhimurium D23580 and *S*. Typhi BRD948 in Kolf2 iHO. iHO were injected with S. Typhi BRD942 or S. Typhimurium D23580 and incubated for 1.5 hours, following which they underwent either modified gentamicin assay to recover intracellular bacteria (**A**) or recovery of luminal contents (**B**). Data presented are for 3 biological replicates (each averaged from 3 technical replicates), with 30 iHO injected per replicate, +/- SEM. Unpaired Mann-Whitney test was used to compare results (****p <0.0001). (**A**) Significantly more D23580 were recovered from inside enterocytes at 1.5 hours post-infection. (**B**) Intraluminal counts showed no recovery of BRD948 at 1.5 hours post-infection. Therefore, iHO were harvested at 0, 20 and 40 minutes following infection (**C**), which demonstrated a rapid drop in numbers of bacteria recovered by 40 minutes post-infection.

Given that intraluminal killing of bacteria was taking place with these 'less invasive' isolates, the question arose as to what would happen in the lumen to diarrhoeagenic bacterial strains which are non-invasive; preferentially existing in the lumen, such as Enteropathogenic *E. coli* (EPEC). In order to image these interactions, EPEC wild type isolate E2348/69 was transformed using electroporation with the TIMER^{bac} plasmid as described in 2.4. Intraluminal assays using single iHO and immunostaining following microinjection into iHO demonstrated a significant initial decrease in viable bacterial numbers retrieved from the iHO lumen, followed by some stabilisation of bacterial counts (**Figure 5.9**). Immunostaining was performed in order to try and determine whether the TIMER^{bac}-EPEC were producing attaching and effacing lesions on the iHO epithelium. It was not possible to clearly demonstrate these lesions, but immunostaining did reveal close interaction and apparent attachment of TIMER^{bac}-EPEC to the apical surface of the enterocytes.

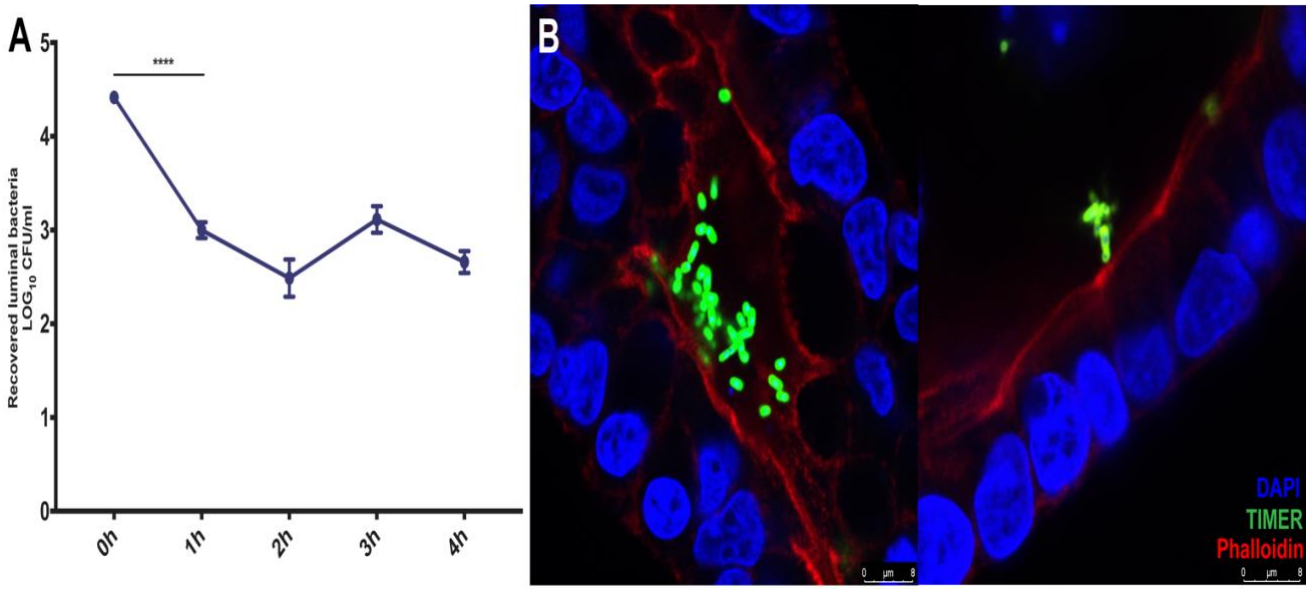

Figure 5.9: Recovered intraluminal counts for TIMER^{bac}-EPEC and immunostaining of interactions with the Kolf2 iHO epithelium. (**A**) iHO were injected with TIMER^{bac}-EPEC and luminal contents recovered at 0, 1, 2, 3 or 4 hours post-infection. Data presented are for 3 biological replicates (each averaged from 3 technical replicates) +/- SEM. Unpaired Mann-Whitney test was used to compare results (****p <0.0001). Intraluminal counts of recovered bacteria displayed a significant drop in initial viable counts followed by some stabilisation. (**B**) iHO were injected with TIMER^{bac}-EPEC and incubated for 3 hours prior to fixing and immunostaining for nuclei (DAPI) and epithelial brush border (phalloidin), which demonstrated TIMER^{bac}-EPEC interacting with the iHO epithelium. Images taken on the Leica SP8 confocal microscope at 63x magnification.

5.4 Other applications for the iHO model – study of competition between bacterial strains

There are a wide range of *Salmonella* capable of causing different types of disease in different hosts. *S*. Typhi are discussed in Chapter 6, but having assessed the survival of an invasive salmonellosis (iNTS) isolate in the iHO model, it was investigated as to how other 'invasive' *Salmonella* would behave in comparison to the *S*. Typhimurium reference isolate SL1344 if iHO were simultaneously infected by multiple isolates. Would the isolates causing the more severe disease picture outcompete those causing milder disease *in vitro*? To this end, as an initial comparator, TIMER^{bac}-*Salmonella* SL1344 were assayed in competition with *S*. Typhimurium D23580. As described in 2.3, modified gentamicin protection assays were completed, with results recorded for intracellular counts when each isolate was injected alone into the iHO, followed by both isolates in combination. The fluorescence demonstrated by the TIMER^{bac}-SL1344 colonies made it possible to distinguish easily between the two bacterial strains when colonies were counted at the end of the experiment. There was no significant difference in recovered counts of each isolate when injected separately into the iHO, but D23580 outcompeted the TIMER^{bac}- SL1344, with

significantly more D23580 being located intracellularly when both isolates were injected in equal ratios into the iHO (**Figure 5.10**). Mean competition index was 2.05 (SEM 0.31).

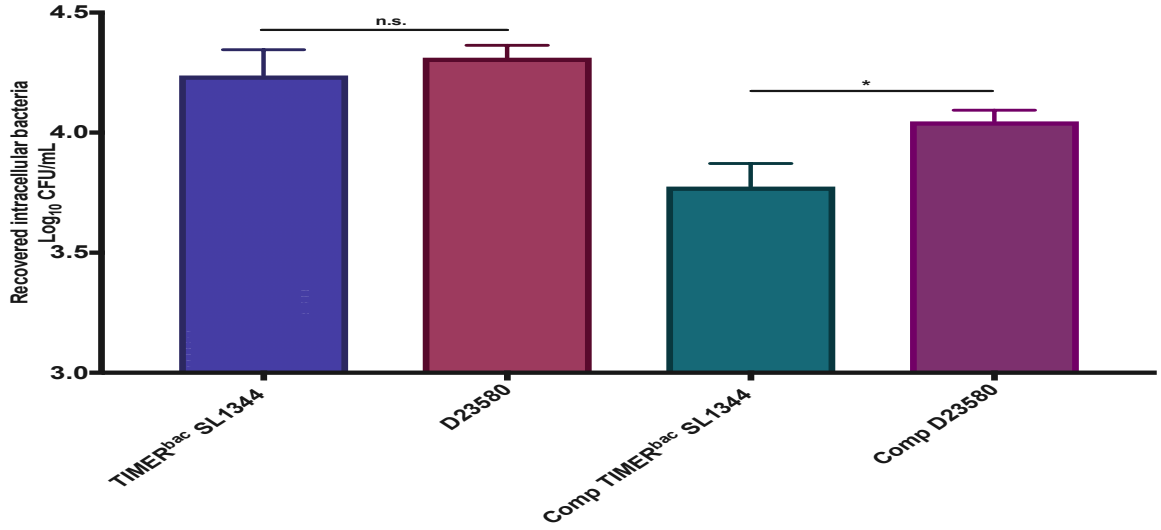

Figure 5.10: Recovered intracellular counts for TIMER^{bac}-*Salmonella* SL1344 and D23580 alone and in competition. iHO were either injected with TIMER^{bac}-SL1344 or D23580 at 1.6 x 10^9 alone, or in competition at a 50:50 ratio and incubated for 1.5 hours, prior to undergoing modified gentamicin assay to recover intracellular bacteria. Data are presented for 3 biological replicates (each averaged from 3 technical replicates) +/- SEM. Unpaired Mann-Whitney test was used to compare results (**n.s.** not significant, *p <0.05). There was no significant difference between recovered intracellular counts of each strain when injected alone into Kolf2 iHO, however when injected together in competition, (Comp TIMER^{bac} / Comp D23580), significantly more D23580 were recovered from within cells.

This investigation into iNTS-causing isolates was continued by undertaking assays with 5 Vietnamese ST34 clinical isolates from the same BAPS (Bayesian analysis of population structure) cluster, which had been isolated from blood or stool of patients presenting with salmonelloses.[31] Full details of the isolates are provided in Table 3.1. Briefly, the collection comprised 3 bloodstream isolates, 2 of which had biphasic flagellae (VNB1779, VNB2140) and 1 monophasic (VNB2315), and 2 stool isolates; 1 biphasic (VNS20081) and 1 monophasic (VNS20101). Cefepime protection competition assays were completed for these isolates as outlined in 3.2, given their high levels of gentamicin resistance. The three biphasic isolates VNB1779, VNB2140 and VNS20081 were able to successfully outcompete TIMER^{bac}-SL1344, with mean competition indices (CI) ranging from 6.35-16.34. Of the monophasic *Salmonella*, the bloodstream isolate VNB2315 was less invasive than TIMER^{bac}-SL1344, with a CI of 0.64 and the stool isolate VNS20101 was similarly invasive with a CI of 1.15 (**Figure 5.11**). These assays demonstrate the utility of the iHO model for examining interactions between different bacteria within the iHO system, and could pave the way for

work looking at the interactions and competition between commensals and pathogenic bacteria.

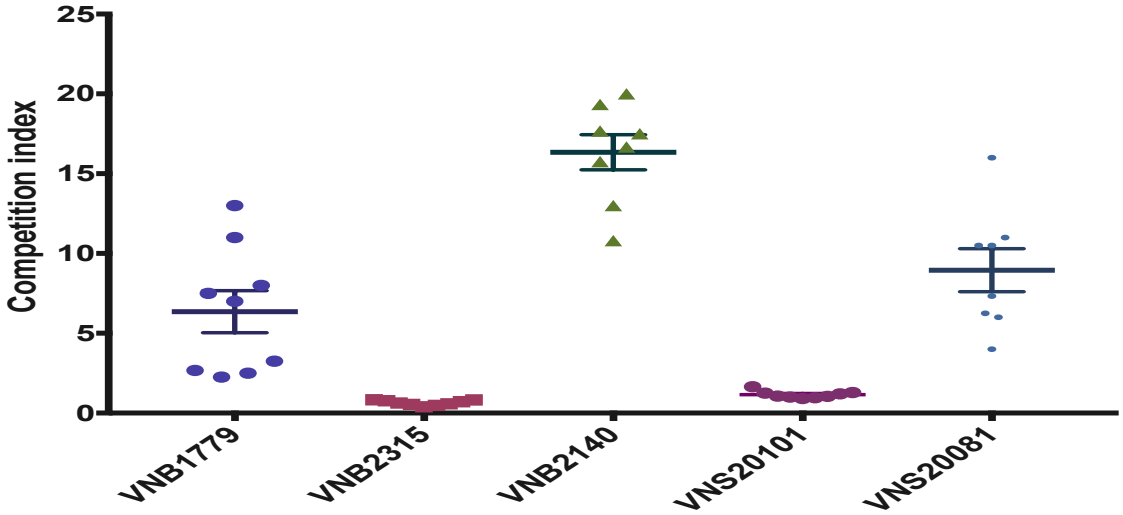

Figure 5.11: Competition indices for ST34 Salmonella versus TIMER^{bac}-*Salmonella* SL1344. Kolf2 iHO were injected with equal ratios of TIMER^{bac}-SL1344 and an ST34 strain and incubated for 1.5 hours prior to undergoing modified Cefepime protection assay and recovery of intracellular bacteria. Data are presented for 3 biological replicates (each averaged from 3 technical replicates) +/- SEM. ST34 isolates expressing biphasic flagellae were much more invasive than their monophasic counterparts; outcompeting TIMER^{bac}-SL1344 with 6 to 16-fold higher intracellular counts of recovered bacteria.

5.5 Other applications for the iHO model – investigating mutations of interest

One of the major advantages of hiPSC-derived iHO is the ability to produce models of the gut epithelium from individuals with disease-causing mutations without requiring an invasive biopsy. This approach facilitates studies on the function of the epithelium in diseased individuals compared to healthy controls. As an example, this project utilised hiPSC from an individual with a mutation in the CARD8 gene, a host gene with a role in the immune response to infection. CARD8 is an inhibitor of the pro-inflammatory protein, caspase-1. CARD8 and other CARD-containing proteins regulate apoptosis via interaction with caspases and control activation of the NF-κB pathway, modulating expression of genes involved in inflammation.[32] CARD8 has no murine homolog. Mutations in CARD8 can lead to loss of inhibition of NF-κB mediated signalling and a clinical phenotype of auto-inflammation and immune dysregulation, including an association with systemic inflammatory response syndrome in human studies.[33] There is debate about where exactly CARD8 fits in with the inflammasome, with some studies suggesting that CARD8 directly

interacts with capsase-1 through a CARD-CARD homophilic interaction, negatively regulating the activation of caspase-1.[32] Others have suggested a model where the nucleotide binding oligomerization domain-like receptor 3 (NLRP3) inflammasome is made up of a complex of NLRP3, apoptosis-associated speck-like protein (ASC), caspase-1 and CARD8; having witnessed interactions between the FIIND domain of CARD8 and the NOD domain of NLRP3.[34] More recent studies have demonstrated that NLRP3 interacts with CARD8 in the resting state, but following stimulation with LPS, NLRP3 instead interacts with ASC, suggesting that CARD8 may hold NLRP3 in an inactive form until a certain stimulation threshold is reached.[35] It may well be that elements of both of these hypotheses are true, with CARD8 having been shown to interact with the NOD domain of NOD2 (an NLR protein), decreasing NOD2-mediated defence from *Listeria*, via inhibition of construction of the nodosome.[36] The outcome of these mechanisms is that CARD8 causes caspase-1 inhibition; resulting in decreased IL-1β levels, in addition to decreasing NF-κB signalling.[36] NF-κB-mediated signalling is also responsible for levels of IFNγ, IL-2, IL-6, IL-8 and β-interferon. Loss of function alleles in CARD8 have been reported to lead to increased cell death during *in vitro Salmonella* infections in lymphoblastoid cells.[33]

To investigate this potential phenotype of attenuated response to infection, hiPSC reprogrammed from a skin biopsy from a child with a mutation in the CARD8 gene were differentiated into iHO. This child had presented to paediatricians with unexplained multisystem inflammation and cirrhosis (medical history disclosed by T Kuijpers, Academic Medical Centre, Amsterdam). There was also evidence of 'immune dysregulation'; although the patient's primary humoral responses were normal, they had suboptimal immunologic memory function for Epstein-Barr virus and varicella-zoster virus and the presence of a number of autoantibodies. None of the child's direct relatives were similarly affected. Whole genome sequencing revealed a SNP causing a homologous missense mutation in an amino acid of the CARD8 gene (p.His280Tyr c.838C>T exon 7).

iHO generated from this individual were embedded and cultured as outlined in 2.1.2-2.1.4 (and are referred to henceforth as 'CARD8 cell line'). Light microscopy images taken during the differentiation process did not demonstrate any obvious differences between the CARD8 mutant line and the healthy control lines previously differentiated (**Figure 5.12**).

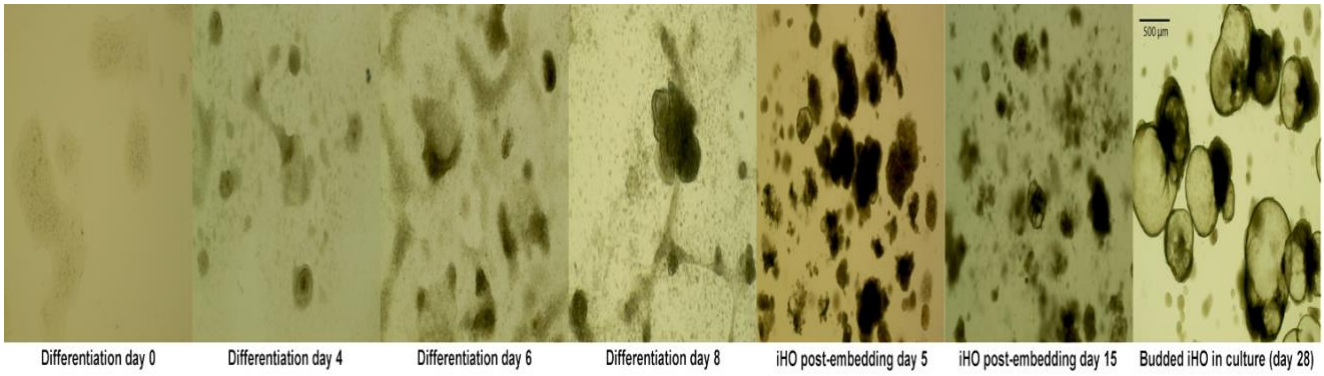

Figure 5.12: Sequential imaging of differentiation process for CARD8 cell line from hiPSC to iHO. Images taken on Thermo-Fisher EVOS XL imaging system at 4x (Differentiation and embedding panels) / 10x (iHO in culture) magnification.

CARD8 RNA and protein were previously shown to be expressed in haematopoietic cells and some gut tissue, including the small intestine.[37] On interrogation of the RNA-Seq data generated previously by Jessica Forbester on Kolf2 iHO, transcripts for CARD8 in intestinal epithelial cells were detected at a relatively low level. RNA was extracted from Kolf2 and CARD8 iPSC and iHO and RT-qPCR completed for genes of interest. There was no significant difference between the relative expression of the cell markers for iPSC or iHO from each cell line, although there was a trend towards higher lysozyme expression in CARD8 iHO versus Kolf2 iHO. Transcripts for CARD8 were expressed at low levels in all 4 conditions, suggesting that the commercial primers used were able to detect the transcript in both normal and mutant lines (**Figure 5.13**).

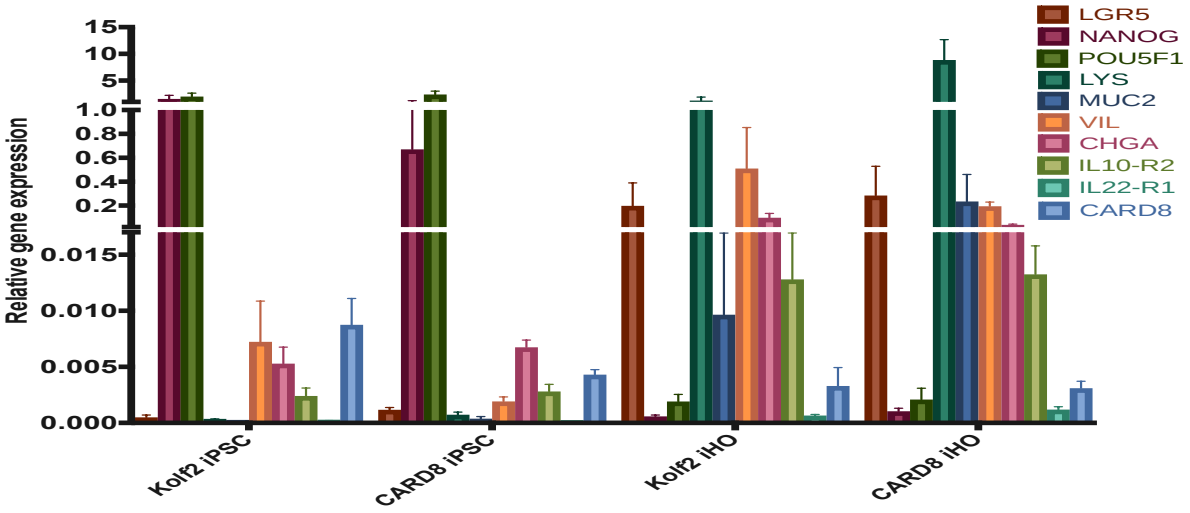

Figure 5.13: Expression of cell type markers in Kolf2 vs CARD8 iPSC and iHO. CARD8 transcripts appear to be expressed at low levels in both Kolf2 and CARD8 lines, with highest expression in Kolf2 iPSC. There are no significant differences in relative gene expression between the cell lines, although markers for Paneth cells appear to be more highly expressed in CARD8 iHO. Data presented are from 4 technical replicates, with assays repeated 3 times using paired iPSC/iHO of different batches. Data were analysed using the comparative cycle threshold (C_T) method, with GAPDH as an endogenous control. Unpaired Mann-Whitney test was used to compare results.

All expected cell type markers were visible on immunostaining, however the markers for secretory cell types (goblet cells, Paneth cells, enteroendocrine cells) appeared to be expressed at a relatively higher level in the CARD8 line (**Figure 5.14**).

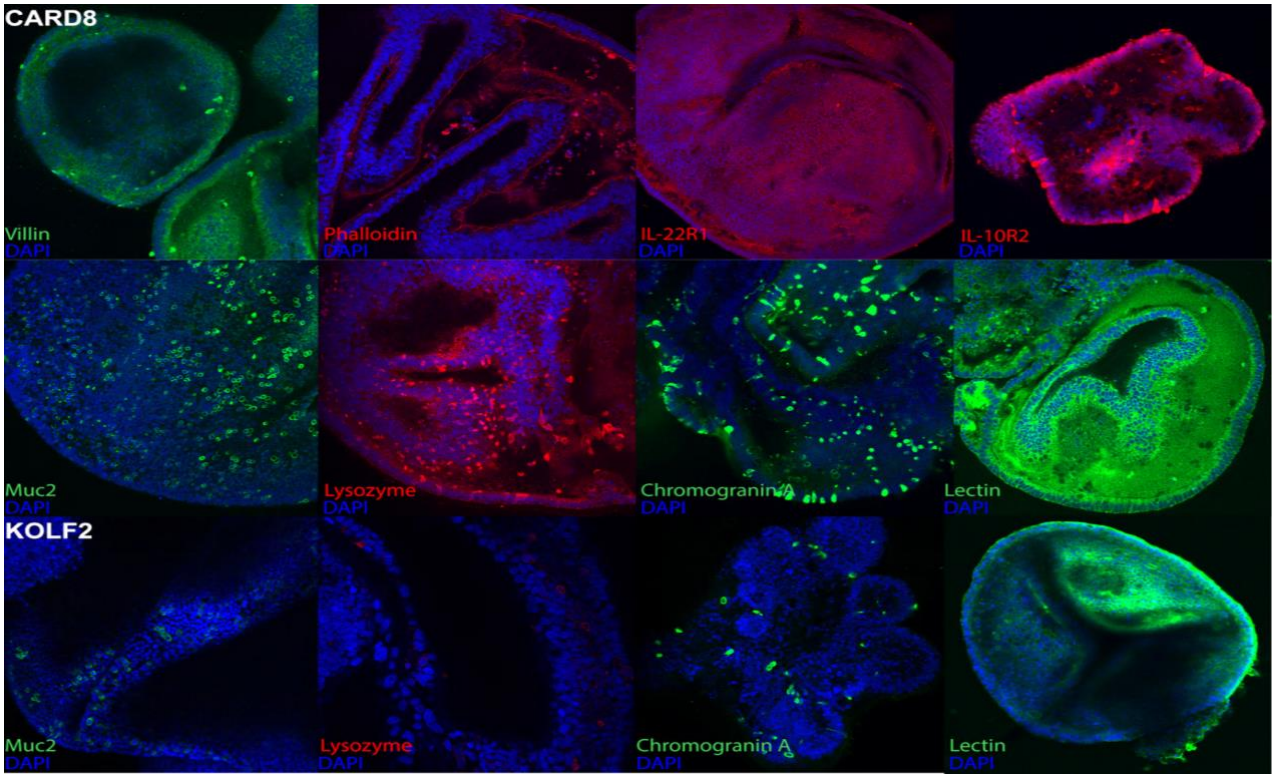

Figure 5.14: **Cell marker expression in iHO generated from CARD8 versus Kolf2 cell lines.** CARD8 iHO immunostaining demonstrates the presence of enterocytes (Villin), a polarised epithelium (Phalloidin) and components of the IL-22 receptor complex (IL-22R1, IL-10R2). Comparative to the Kolf2 iHO imaged in the lower panels, there are a relative abundance of goblet, Paneth and enteroendocrine cells in iHO from the CARD8 lineage (Muc2, Lysozyme, Chromogranin A respectively) and a well-formed mucus layer (Lectin). Images taken on Zeiss LSM 510 Meta confocal microscope at 20x magnification.

iHO from both lineages were then stained for the presence of the CARD8 protein, known to be expressed in both the nucleus and cytoplasm of cells.[37] Immunostaining again demonstrated the presence of the protein in iHO from both cell lines (**Figure 5.15**). The antibody used binds to the last 50 amino acids in the C-terminus of the CARD8 protein. Given the nature of the mutation (a mis-sense mutation, with single aa replacement), this portion of CARD8 protein may still be transcribed and translated.

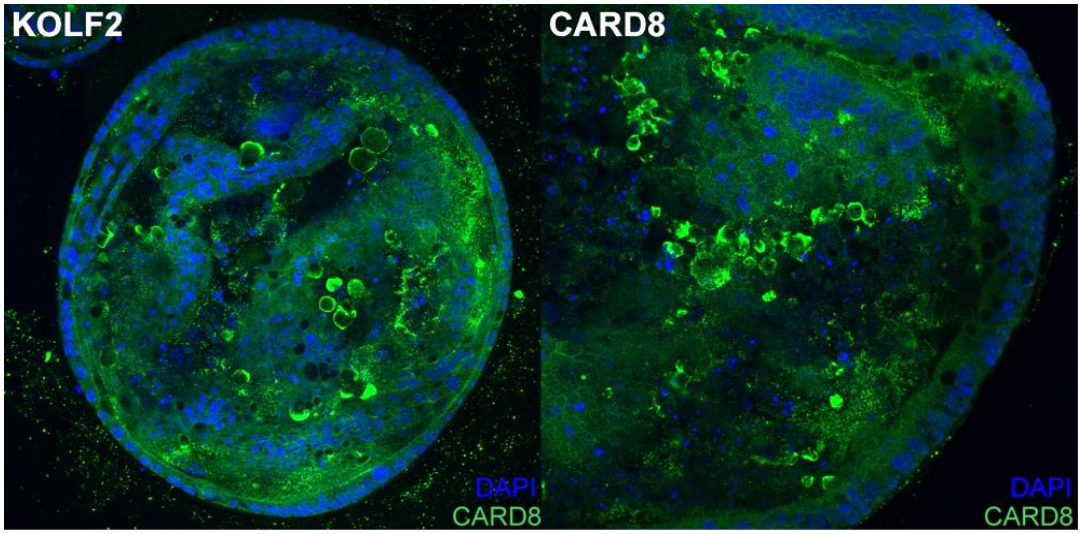

Figure 5.15: **CARD8 protein expression in CARD8 versus Kolf2 cell lines.** CARD8 immunostaining demonstrates the presence of CARD8 protein in iHO from both cell lines. Images taken on Zeiss LSM 510 Meta confocal microscope at 20x magnification.

Supernatants were taken from iHO of both Kolf2 and CARD8 lines microinjected with SL1344 and assayed for a number of cytokines. Previous data have shown decreased levels of circulating monocyte chemoattractant protein (MCP-1) associated with those with CARD8 polymorphisms and atherosclerotic disease[38]; our data showed an increased expression over time post-infection of MCP-1 in Kolf2 versus CARD8 iHO, but this was not significant (data not shown). Similarly, increase in IL-8 levels over time was greater in Kolf2 iHO, but this was again not significant due to lack of data points (data not shown). Western blots were completed for caspase-1 both pre-infection and after 1.5 and 3 hours post-infection with SL1344. Caspase-1 levels increased over time in the Kolf2 iHO, whereas in the CARD8 iHO caspase-1 levels decreased over time (**Figure 5.16**). This suggests that in the Kolf2 line, functional CARD8 protein may be binding to caspase-1 and inhibiting its activation and cleavage into active form.[32] Levels of caspase-1 thus increase, as production continues as part of the positive feedback loop in response to infection/inflammatory stimulus.[39] Whereas, in the CARD8 line, the lack of CARD8 allows processing and cleavage of caspase-1, and its autoprocessing, hence the decrease in levels over time.[32]

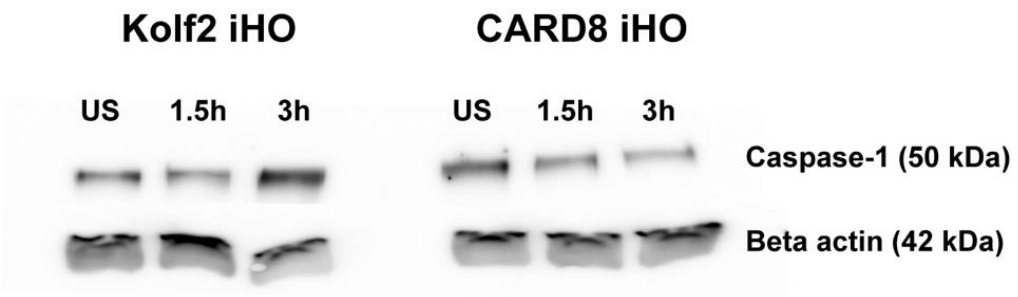

Figure 5.16: Western blot for caspase-1 using protein from unstimulated and infected iHO from Kolf2 and CARD8 lines. CARD8 and Kolf2 iHO were injected with SL1344, and harvested either prior to infection (US) or at 1.5 or 3 hours post-infection and protein extracted for western blotting for the presence of Caspase-1. Samples were also stained with anti-beta actin antibody to ensure equal protein loading across conditions. Images taken using ImageQuant LAS 4000. Increasing concentrations of caspase-1 are seen over time in Kolf2 iHO following infection, whereas the converse is seen in CARD8 iHO.

Given the interesting phenotypical differences seen using immunostaining and Western blotting, CARD8 iHO were microinjected with *S*. Typhimurium SL1344 to assess their susceptibility to infection versus their Kolf2 counterparts (**Figure 5.17**). These assays demonstrated significantly fewer bacteria invading intracellularly in the CARD8 iHO. Counts were lower at both 1.5 and 3 hours after infection, suggesting a decreased ability to invade and replicate intracellularly. It was hypothesised that bacteria may be being killed in the lumen by an increased concentration of antimicrobial peptides, given the higher proportion of Paneth cells suggested by staining in the CARD8 line. Therefore, luminal infection assays were done both in bulk and on sequentially harvested single iHO (**Figure 5.17**). Initial counts of SL1344 surviving in the lumen were similar for both cell lines, however at 3 hours, significantly more SL1344 were surviving and replicating in the lumen of the CARD8 iHO than the Kolf2 iHO. This was contrary to the expectation that more bacteria would be killed in the lumen by AMPs in the CARD8 iHO. However, it is worth noting that alongside the increased amount of Paneth cells in CARD8 iHO, there were also increased numbers of goblet cells and a more robust mucous layer, which may provide a protective environment for SL1344 to survive and replicate within in the lumen of the iHO (**Figure 5.18**). In addition, it is possible that the thicker mucus layer formed a physical barrier to prevent invasion, or that decreased intracellular invasion could be due to there being relatively fewer enterocytes versus secretory cells for the bacteria to invade through; given that epithelial invasion would be expected to occur via enterocytes (**Figure 5.17**).

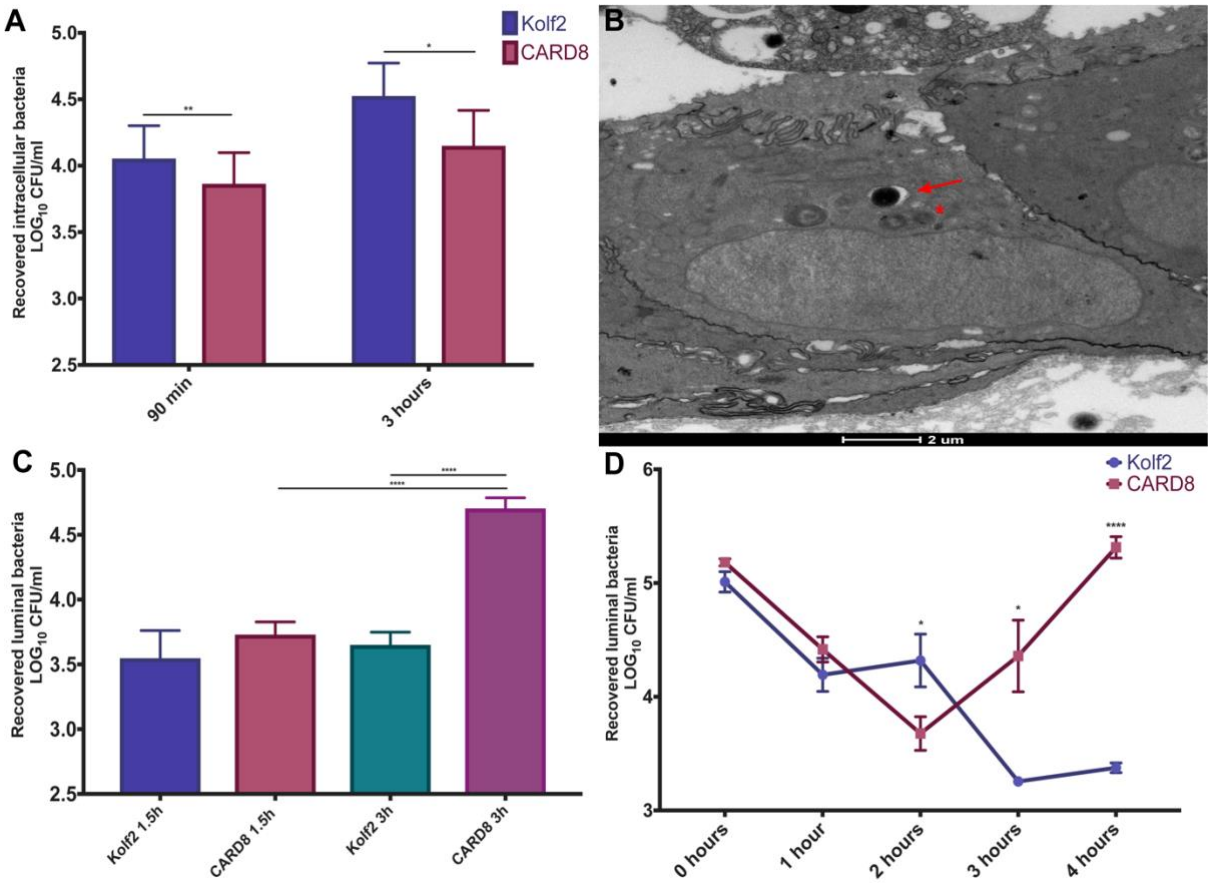

Figure 5.17: Intracellular and luminal bacterial counts in SL1344-infected Kolf2 and CARD8 iHO. (**A**) Kolf2 and CARD8 iHO were injected with SL1344 and incubated for 1.5 or 3 hours post-infection, followed by modified gentamicin protection assay to recover intracellular bacteria. Intracellular bacterial counts were lower in CARD8 iHO at both 1.5 and 3 hours. (**B**) TEM imaging of SL1344 bacteria inside of an enterocyte from CARD8 iHO at 1.5 hours post-infection, with bacteria located in SCV (arrow) and phagolysosome (asterisk). (**C**) Significantly more bacteria were recovered from the lumen of CARD8 versus Kolf2 iHO at 3 hours post-infection, with significant increase in the amount of bacteria between 1.5h and 3 hours in the CARD8 lumen. (**D**) Similar results were seen when single iHO were harvested at hourly intervals, with significantly more intraluminal bacteria being recovered from CARD8 iHO at 4 hours post infection. Data are presented for 3 biological replicates, (each averaged from 3 technical replicates) per condition +/- SEM. Multiple single iHO were used for luminal assays in **D** and 30 iHO injected per replicate for intracellular assays in **A** and luminal assays in **C**. Unpaired Mann-Whitney test was used to compare results (*p <0.05, **p<0.01, ****p<0.0001).

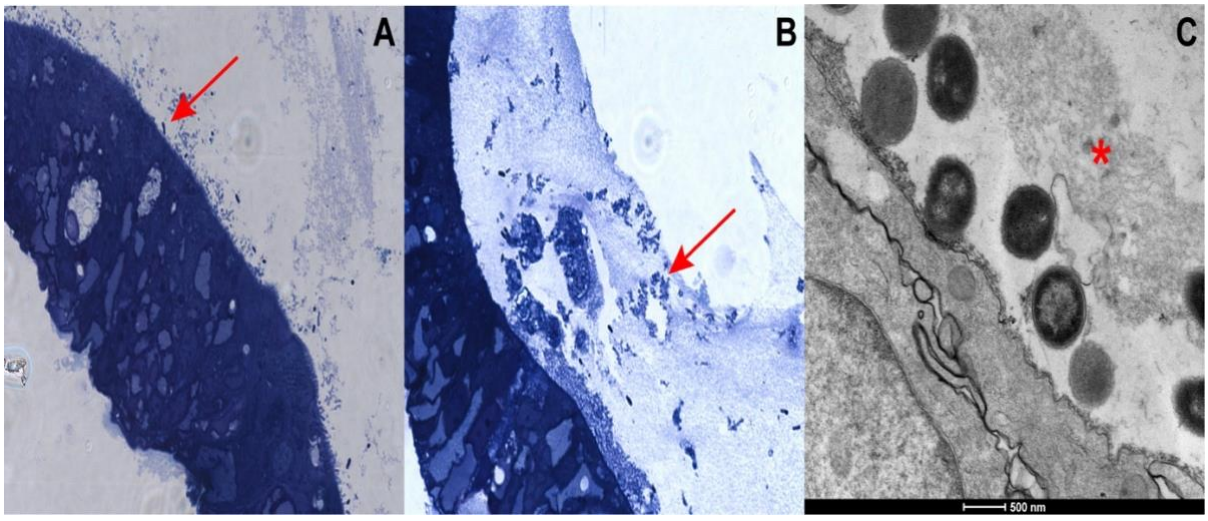

Figure 5.18: Bacterial interactions with the mucus layer following infection. Kolf2 and CARD8 iHO were injected with SL1344 and incubated for 1.5 hours prior to fixing and undergoing preparations for TEM. Toluidine blue staining demonstrates a thinner mucus layer in the Kolf2 iHO lumen (**A**), with more direct interaction between bacteria and epithelium (arrow), versus a thick mucus layer containing bacteria, seen in CARD8 iHO lumen (arrow) (**B**). Images taken at 63x magnification. (**C**) TEM imaging of SL1344 having breached the mucus layer (asterisk) and damaged microvilli on the apical surface of the epithelium in Kolf2 iHO.

5.6 Discussion

This chapter addresses a number of questions about the intraluminal environment of the iHO system, which is challenging to study. Ideally, obtaining material from the iHO lumen would involve a reverse microinjection system, and direct removal of luminal contents, since even breaking up iHO and releasing their luminal contents into small amounts of PBS will markedly dilute any peptides held within the lumen. Harvesting of cells and transcriptional analysis seemed an initial logical proxy as a method of making this measurement, but this would rely upon harvesting at the correct moment that each cytokine is being transcribed. The timing may, of course, differ amongst cytokines, which could explain why limited response was recorded amongst some of the AMPs studied in this chapter. Perhaps a later harvesting point and blotting for protein would have yielded additional data, as attempted in the mouse model described by Wilson et al.[3] This study notes restriction of *S.* Typhimurium LT2 strain growth in the lumen of murine organoids for up to 20 hours post infection due to alpha-defensin production, however, results presented at 9 hours post infection showed killing / growth restriction in some replicates and replication over the initial inoculum in others. In addition, the infective dose administered in these experiments was between 50 and 5000 CFU per organoid, versus ~17,000 CFU per iHO in this study, suggesting that there are sufficient defensin concentrations in the lumen to restrict growth of a small inoculum, but that this system can become overwhelmed with a larger infective dose, as seen in the current study.

It was curious to note that strains of *S*. Enteritidis, despite their ability to cause a similar clinical picture to *S*. Typhimurium of gastrointestinal disease and iNTS (even being recorded as a more common cause of invasive disease in some studies[11,40,41]), were much less successful at invading the epithelium. Both serovars harbour SPI-1 and SPI-2, so would be expected to have similar machinery for invading and replicating within cells.[40] None of the *S*. Enteritidis strains trialled in this study were known to have mutations in SPI-1 or SPI-2 genes. *S*. Enteritidis are known to have monophasic flagellae, as compared to *S.* Typhimurium SL1344 which is biphasic. The monophasic ST34 *S*. Typhimurium variants used in the competition model did however invade to a greater extent than *S.* Enteritidis, so it is unlikely that this is the sole cause of their limited invasion potential. Other outcomes of

genetic differences between *S*. Enteritidis and *S*. Typhimurium such as differing O antigens may have played a role in their ability to be recognised by an inflammatory response induced by the iHO epithelium. *S*. Enteritidis with outer membrane instabilities (such as antimicrobial peptide resistance gene mutations) were demonstrably less effective at colonising the avian intestine.[42] In this study, both *S*. Enteritidis 6206 and 6174 harboured membrane-related mutations, in addition to which, the *amiA* mutation in 6206 may have rendered it more sensitive to luminal AMP killing.

It was satisfying to witness the survival of EPEC within the iHO lumen. If time allowed, it would have been useful to obtain more detailed imaging, via TEM, of the interactions between the bacteria and the epithelial surface. This could clarify whether A/E lesions are being formed, and allow study of survival of mutant strains of this bacteria, such as those with mutations in adhesins such as bundle forming pili and EspA filaments, which have been demonstrated to be key in brush border attachment.[43]

The results generated when clinical isolates of *Salmonella* were placed into competition with a reference strain produced evidence of the potential of the iHO model for investigating differences between native and invasive bacteria in the gut. They also demonstrated a possible role for biphasic flagellae in success at invading the epithelium and evading the antibacterial response in the iHO system. Assays performed using these strains in murine bone marrow-derived macrophages demonstrated the same pattern of increased invasiveness of the biphasic versus monophasic strains, greater release of IL-1β in supernatants and pyroptosis of macrophages following infection with biphasic strains (S. Baker, unpublished data). The isolates used here were all multiply drug-resistant, so it may be that the plasmids encoding AMR are partly responsible for their increased invasiveness. It would be useful to generate mutants of these strains lacking their MDR plasmids and observe whether there is still a difference between monophasic and biphasic serovars. High resolution TEM imaging may also provide information as to the nature of flagellin expression during interactions with the epithelium.

The CARD8 work outlined in this chapter demonstrates the potential of the iHO model for the non-invasive investigation of response to infection in patients with genetic mutations

causing immune dysregulation. There were some interesting phenotypical differences in iHO generated from the patient cell line, which correlated with a differing response to *S*. Typhimurium infection than that seen in the healthy volunteer cell lines used elsewhere in this project. It would be of interest to look at responses in macrophages generated from this stem cell line too, as their response to infection will likely differ; one would expect to see a caspase-1 dependent inflammatory pyroptosis in *Salmonella*-infected macrophages (also witnessed in dendritic cells) versus the caspase-1 independent apoptosis seen in epithelial cells.[44] Given their lack of inhibition of caspase-1, one may expect CARD8-deficient macrophages to undergo pyroptosis more quickly following infection. Caspase-1 deficient mice demonstrated increased susceptibility to invasive salmonellosis, suggesting that in vivo, controlled pyroptosis is a protective mechanism to prevent disseminated infection.[45,46] In the pilot experiments with the CARD8 cell line outlined in this chapter, the patient line was being compared to a healthy control line with a different genetic background, meaning that there is the possibility of other genetic sources of variance causing the unusual CARD8 iHO phenotype and response to infection. It was therefore planned to construct an isogenic control line with which to repeat these experiments; using CRISPR/Cas9 to reproduce the point mutation seen in the patient line in the Kolf2 hiPSC background. This however proved more challenging than expected and at the time of writing, only heterozygous mutants have been produced, with one allele edited to have the CARD8 mutation and one remaining wild type. Once a homozygous mutant is produced, this work could be taken forwards by repeating the assays outlined above, completing experiments to assess relative proportions of iHO epithelial cell death following infection and investigating more closely the luminal environment produced during infection in iHO from a cell line deficient in CARD8. It would also be interesting to produce macrophages from this cell line with which to perform invasion assays and imaging, transcriptomics and supernatant analysis to study differences in inflammatory response between cells expressing CARD8 versus those that do not.

References:

1. Huang JY, Sweeney EG, Sigal M, et al. Chemodetection and Destruction of Host Urea Allows Helicobacter pylori to Locate the Epithelium. *Cell Host Microbe.* 2015;18(2):147-156.
2. Schumacher MA, Feng R, Aihara E, et al. Helicobacter pylori-induced Sonic Hedgehog expression is regulated by NFkappaB pathway activation: the use of a novel in vitro model to study epithelial response to infection. *Helicobacter.* 2015;20(1):19-28.
3. Wilson SS, Tocchi A, Holly MK, Parks WC, Smith JG. A small intestinal organoid model of non-invasive enteric pathogen-epithelial cell interactions. *Mucosal Immunol.* 2015;8(2):352-361.
4. Bevins CL, Salzman NH. Paneth cells, antimicrobial peptides and maintenance of intestinal homeostasis. *Nat Rev Microbiol.* 2011;9(5):356-368.
5. Schlaermann P, Toelle B, Berger H, et al. A novel human gastric primary cell culture system for modelling Helicobacter pylori infection in vitro. *Gut.* 2016;65(2):202-213.
6. Ettayebi K, Crawford SE, Murakami K, et al. Replication of human noroviruses in stem cell-derived human enteroids. *Science.* 2016;353(6306):1387-1393.
7. Saxena K, Blutt SE, Ettayebi K, et al. Human Intestinal Enteroids: a New Model To Study Human Rotavirus Infection, Host Restriction, and Pathophysiology. *J Virol.* 2016;90(1):43-56.
8. Karve SS, Pradhan S, Ward DV, Weiss AA. Intestinal organoids model human responses to infection by commensal and Shiga toxin producing Escherichia coli. *PLoS One.* 2017;12(6):e0178966.
9. Heo I, Dutta D, Schaefer DA, et al. Modelling Cryptosporidium infection in human small intestinal and lung organoids. *Nat Microbiol.* 2018;3(7):814-823.
10. Garcez PP, Loiola EC, Madeiro da Costa R, et al. Zika virus impairs growth in human neurospheres and brain organoids. *Science.* 2016;352(6287):816-818.
11. Galanis E, Lo Fo Wong DM, Patrick ME, et al. Web-based surveillance and global Salmonella distribution, 2000-2002. *Emerg Infect Dis.* 2006;12(3):381-388.
12. Cepeda-Molero M, Berger CN, Walsham ADS, et al. Attaching and effacing (A/E) lesion formation by enteropathogenic E. coli on human intestinal mucosa is dependent on non-LEE effectors. *PLoS Pathog.* 2017;13(10):e1006706.

13. Hafza N, Challita C, Dandachi I, Bousaab M, Dahdouh E, Daoud Z. Competition assays between ESBL-producing E. coli and K. pneumoniae isolates collected from Lebanese elderly: An additional cost on fitness. *J Infect Public Health.* 2018;11(3):393-397.
14. Haiko J, Westerlund-Wikstrom B. The role of the bacterial flagellum in adhesion and virulence. *Biology (Basel).* 2013;2(4):1242-1267.
15. Macnab RM. Genetics and biogenesis of bacterial flagella. *Annu Rev Genet.* 1992;26:131-158.
16. McQuiston JR, Parrenas R, Ortiz-Rivera M, Gheesling L, Brenner F, Fields PI. Sequencing and comparative analysis of flagellin genes fliC, fljB, and flpA from Salmonella. *J Clin Microbiol.* 2004;42(5):1923-1932.
17. Silverman M, Simon M. Phase variation: genetic analysis of switching mutants. *Cell.* 1980;19(4):845-854.
18. Forbester JL, Goulding D, Vallier L, et al. Interaction of Salmonella enterica Serovar Typhimurium with Intestinal Organoids Derived from Human Induced Pluripotent Stem Cells. *Infect Immun.* 2015;83(7):2926-2934.
19. Claudi B, Sprote P, Chirkova A, et al. Phenotypic variation of Salmonella in host tissues delays eradication by antimicrobial chemotherapy. *Cell.* 2014;158(4):722-733.
20. Helaine S, Thompson JA, Watson KG, Liu M, Boyle C, Holden DW. Dynamics of intracellular bacterial replication at the single cell level. *Proc Natl Acad Sci U S A.* 2010;107(8):3746-3751.
21. Abshire KZ, Neidhardt FC. Growth rate paradox of Salmonella typhimurium within host macrophages. *J Bacteriol.* 1993;175(12):3744-3748.
22. Salzman NH, Ghosh D, Huttner KM, Paterson Y, Bevins CL. Protection against enteric salmonellosis in transgenic mice expressing a human intestinal defensin. *Nature.* 2003;422(6931):522-526.
23. Hill DR, Huang S, Nagy MS, et al. Bacterial colonization stimulates a complex physiological response in the immature human intestinal epithelium. *Elife.* 2017;6.
24. Ipinza F, Collao B, Monsalva D, et al. Participation of the Salmonella OmpD porin in the infection of RAW264.7 macrophages and BALB/c mice. *PLoS One.* 2014;9(10):e111062.

25. Sun S, Berg OG, Roth JR, Andersson DI. Contribution of gene amplification to evolution of increased antibiotic resistance in Salmonella typhimurium. *Genetics.* 2009;182(4):1183-1195.
26. Oguri T, Yeo WS, Bae T, Lee H. Identification of EnvC and Its Cognate Amidases as Novel Determinants of Intrinsic Resistance to Cationic Antimicrobial Peptides. *Antimicrob Agents Chemother.* 2016;60(4):2222-2231.
27. Thomson NR, Clayton DJ, Windhorst D, et al. Comparative genome analysis of Salmonella Enteritidis PT4 and Salmonella Gallinarum 287/91 provides insights into evolutionary and host adaptation pathways. *Genome Res.* 2008;18(10):1624-1637.
28. Tacket CO, Hone DM, Curtiss R, 3rd, et al. Comparison of the safety and immunogenicity of delta aroC delta aroD and delta cya delta crp Salmonella typhi strains in adult volunteers. *Infect Immun.* 1992;60(2):536-541.
29. Lewis C, Skovierova H, Rowley G, et al. Salmonella enterica Serovar Typhimurium HtrA: regulation of expression and role of the chaperone and protease activities during infection. *Microbiology.* 2009;155(Pt 3):873-881.
30. Kingsley RA, Msefula CL, Thomson NR, et al. Epidemic multiple drug resistant Salmonella Typhimurium causing invasive disease in sub-Saharan Africa have a distinct genotype. *Genome Res.* 2009;19(12):2279-2287.
31. Mather AE, Phuong TLT, Gao Y, et al. New Variant of Multidrug-Resistant Salmonella enterica Serovar Typhimurium Associated with Invasive Disease in Immunocompromised Patients in Vietnam. *MBio.* 2018;9(5).
32. Razmara M, Srinivasula SM, Wang L, et al. CARD-8 protein, a new CARD family member that regulates caspase-1 activation and apoptosis. *J Biol Chem.* 2002;277(16):13952-13958.
33. Ko DC, Shukla KP, Fong C, et al. A genome-wide in vitro bacterial-infection screen reveals human variation in the host response associated with inflammatory disease. *Am J Hum Genet.* 2009;85(2):214-227.
34. Agostini L, Martinon F, Burns K, McDermott MF, Hawkins PN, Tschopp J. NALP3 forms an IL-1beta-processing inflammasome with increased activity in Muckle-Wells autoinflammatory disorder. *Immunity.* 2004;20(3):319-325.

35. Ito S, Hara Y, Kubota T. CARD8 is a negative regulator for NLRP3 inflammasome, but mutant NLRP3 in cryopyrin-associated periodic syndromes escapes the restriction. *Arthritis Res Ther.* 2014;16(1):R52.
36. von Kampen O, Lipinski S, Till A, et al. Caspase recruitment domain-containing protein 8 (CARD8) negatively regulates NOD2-mediated signaling. *J Biol Chem.* 2010;285(26):19921-19926.
37. Atlas HP. CARD8 - available from the Human Protein Atlas. 2019; https://www.proteinatlas.org/ENSG00000105483-CARD8/tissue. Accessed 24th June 2019.
38. Paramel GV, Folkersen L, Strawbridge RJ, et al. CARD8 gene encoding a protein of innate immunity is expressed in human atherosclerosis and associated with markers of inflammation. *Clin Sci (Lond).* 2013;125(8):401-407.
39. Lee DJ, Du F, Chen SW, et al. Regulation and Function of the Caspase-1 in an Inflammatory Microenvironment. *J Invest Dermatol.* 2015;135(8):2012-2020.
40. Alghoribi MF, Doumith M, Alrodayyan M, et al. S. Enteritidis and S. Typhimurium Harboring SPI-1 and SPI-2 Are the Predominant Serotypes Associated With Human Salmonellosis in Saudi Arabia. *Front Cell Infect Microbiol.* 2019;9:187.
41. Marder EP, Cieslak PR, Cronquist AB, et al. Incidence and Trends of Infections with Pathogens Transmitted Commonly Through Food and the Effect of Increasing Use of Culture-Independent Diagnostic Tests on Surveillance - Foodborne Diseases Active Surveillance Network, 10 U.S. Sites, 2013-2016. *MMWR Morb Mortal Wkly Rep.* 2017;66(15):397-403.
42. McKelvey JA, Yang M, Jiang Y, Zhang S. Salmonella enterica serovar enteritidis antimicrobial peptide resistance genes aid in defense against chicken innate immunity, fecal shedding, and egg deposition. *Infect Immun.* 2014;82(12):5185-5202.
43. Cleary J, Lai LC, Shaw RK, et al. Enteropathogenic Escherichia coli (EPEC) adhesion to intestinal epithelial cells: role of bundle-forming pili (BFP), EspA filaments and intimin. *Microbiology.* 2004;150(Pt 3):527-538.
44. Paesold G, Guiney DG, Eckmann L, Kagnoff MF. Genes in the Salmonella pathogenicity island 2 and the Salmonella virulence plasmid are essential for

Salmonella-induced apoptosis in intestinal epithelial cells. *Cell Microbiol.* 2002;4(11):771-781.

45. Fink SL, Cookson BT. Pyroptosis and host cell death responses during Salmonella infection. *Cell Microbiol.* 2007;9(11):2562-2570.

46. Lara-Tejero M, Sutterwala FS, Ogura Y, et al. Role of the caspase-1 inflammasome in Salmonella typhimurium pathogenesis. *J Exp Med.* 2006;203(6):1407-1412.

7: Future directions

The work presented in this thesis generates some interesting observations on the interactions between enteric pathogens and the intestinal epithelium in the form of the hiPSC-derived iHO model. This work does however lead to additional questions and highlights aspects of this area which would benefit from further investigation or use of alternative techniques.

7.1 More detailed transcriptional profiling of the iHO model

Firstly, the data presented in Chapter 4 on the single cell sequencing of IL-22 stimulated iHO using Smartseq2 proved that sample size is key if one wishes to be able to make meaningful observations about the differences between single cell responses on the transcriptional level. Whilst Smartseq2 allows a great depth of sequencing, the work intensity and cost of the protocol meant that the size of any effect seen between IL-22 stimulated and unstimulated groups was masked by technical noise from the data. However, given the now widespread use of droplet-based single cell RNA-Seq,[1] a repeat experiment with a much larger sample size would likely facilitate the identification of any differences between the two groups, identify with confidence the different cell types contained within the epithelium and define their individual reactions to IL-22 treatment.

For example, a recent paper by Fujii *et al* (2018),[2] (authors of this paper produced the first report on production of organoids derived from murine intestinal crypts) suggested trial of a new combination of growth factors for primary iHO which may favour the emergence of secretory cells whilst maintaining the pluripotency of the intestinal stem cells; something which has been a difficult balance for those producing primary and hiPSC-derived iHO via standard methods. To demonstrate the utility of this protocol, the group reported the enhancement in secretory cell types via the use of droplet-based single cell RNAseq, examining >2500 cells per condition. They were able to discern four different subtypes of enteroendocrine cells, alongside goblet and Paneth cells. They were also able to denote tuft cells, M cells and transit amplifying cells, demonstrating the power of large data sets in this context. Similarly, researchers looking at mouse small intestine and organoids profiled

>50,000 single cells, allowing them to characterise novel subsets of cells which hadn't been defined at this resolution previously.[3]

In addition, single cell RNA-Seq was carried out on murine small intestinal cells after infection with *S.* Typhimurium SL1344 or the helminth *Heligmosomoides polygyrus.* It was possible to discern cell-intrinsic changes to the transcriptome displaying an inflammatory response to infection, and excitingly, altered cellular functions, such as induction of RegIIIα and RegIIIγ in all cell types, rather than just enterocytes during *Salmonella* infection. In addition, both organisms were able to change the cellular composition in the intestine, with *H. polygyrus* inducing an expansion of goblet and tuft cell populations, and *S*. Typhimurium causing increased abundance of mature Paneth cells (1.1% to 2.3%) and enterocytes (13.1% to 21.7%), but a marked decrease in transit-amplifying (52.9% to 18.3%) and intestinal stem cells (20.7% to 6.4%). Being able to study cell populations in this level of detail goes some way to resolving the question on the mechanism of increased proliferation of enterocytes when markers of ISC had been noted to be downregulated in murine organoids during infection.[4]

It would be attractive to complete these types of assay in human organoids to determine whether this picture is recapitulated in a model of human infection. In addition to using this model to establish the response of individual cell types to *Salmonella*, it would be fascinating to study infected cells in the context of IL-22 stimulation, both to learn more about the individual cellular response to stimulation and to seek further confirmation for our hypothesis of enhanced phagolysosomal fusion. This type of experiment would also provide more information on the antimicrobial peptides which are upregulated, and perhaps define these changes at various timepoints following infection.

In particular, detailed single cell response data from *S*. Typhi and *S*. Paratyphi A infected organoid-derived cells would be valuable for comparison with non-typhoidal *Salmonella* data, in order to define differences in cellular response to each pathogen and perhaps help guide the search for alternative treatment methods for drug-resistant infections. To undertake this type of work would require a FACS sorter in a CL3 facility, which is difficult to organise but will potentially be available to my group soon.

Another application of transcriptomic technology would be the use of dual RNA-Seq to assay both infected organoids and *Salmonella* to interrogate bacterial transcriptomic response during early interactions with the epithelium or macrophage. It would be fascinating to learn which pathogenicity factors are being upregulated in particular by the H58 *S*. Typhi used in this study which appear to have increased invasion and replication capacities within the macrophage and an undefined ability to subvert the immune response without reliance on AMR genes to make them treatment resistant. Further data could be gathered on the genes activated during events we witnessed on TEM images of infection, such as the novel finding of production of pili by *S*. Paratyphi A. This type of data could also help in the identification of targets for future vaccines. This would be especially valuable if commonalities between key clades of *Salmonella* were identified and efforts could be directed towards a multivalent vaccine.

It would be sensible to trial these types of assays at a range of different multiplicities of infection (MOIs), along with concurrent TEM imaging and RNA-Seq, in order to investigate whether MOI alters the behaviour or transcriptome of the bacteria and the factors it expresses when interacting with the epithelium. These findings could be relevant for clinical infections, as MOI will frequently differ here. Further data on genes employed by *Salmonella* to evade phagolysosomal fusion could be obtained by studies over different timepoints following infection. Selection of these timepoints could perhaps be guided by assays such as live confocal imaging during infection (requiring confocal facilities within a CL3 laboratory) with labelling of bacteria and relevant host proteins such as Rab7 or Lamp1. Use of the Perkin Elmer Opera Phenix™ system could provide this. In addition, the high throughput capabilities of such a system could allow study of aspects such as bacterial invasion and replication under stress conditions, such as the presence of a range of antibiotic concentrations in the cell media, to discover more about what is happening in individuals treated with inappropriate antibiotics.

7.2 Luminal studies

As described above, information on AMPs released into the lumen at timepoints following infection could be garnered from transcriptional data. In addition, proteomic data on the AMP concentrations within the organoid lumen and factors such as the luminal pH and

osmotic gradient would be fascinating, in order to build a picture of the environment that bacteria are exposed to during infection assays. This may prove tricky given the difficulties with accessing the luminal compartment of the organoids, but perhaps harvesting post-infection and extracting protein may be a method of achieving some measure of this, with trial of a more rapid dissolution of Matrigel with ice cold PBS rather than the 45 minutes usually required when using Cell Recovery Solution. This would however provide information on whole iHO protein expression rather than just luminal content. Another option would be development of a system whereby microinjection needles could be used to extract rather than inject contents into the lumen. One study reported directly aspirating iHO from their extracellular matrix (e.g. Matrigel) using a 30 gauge needle to disrupt the iHO and extract luminal bacterial contents, but this would again lead to the likelihood of some iHO material rather than just luminal contents being harvested, which would not be optimal.[5]

Another luminal issue requiring further investigation is the question of whether gentamicin is penetrating the mucus layer lining the iHO lumen and killing bacteria contained within, or whether less invasive bacteria such as *S*. Typhi are surviving in the mucus and being erroneously considered to be intracellular once harvested. Recent commercial release of fluorescently tagged antibiotics such as gentamicin could help to resolve this; using live imaging with fluorescent antibiotics and live/dead staining of bacteria could clarify whether antibiotics are co-localising with bacteria within the mucus and the outcome of these interactions.[6]

7.3 Alteration of iHO to closer resemble *in vivo* scenarios

Whilst one advantage of the iHO system is its reductionist nature, this is also a potential drawback to replicating conditions experienced by *Salmonella* in the intestinal lumen *in vivo*. Having shown that iHO can successfully be colonised by commensal *E. coli* [7] and more recently that murine intestinal organoids supported growth of human transplanted intestinal microbiota for up to 4 days,[5] the next step would be to trial microinjection of pathogens into iHO that harbour an established commensal community. This would more closely recapitulate the colonisation resistance conditions experienced by *Salmonella* in the

intestine, and would introduce infection into an epithelium primed for contact with microbes.

Another manner in which iHO cultures could be adapted to closer replicate innate immune response *in vivo* would be the growth of iHO on a monolayer (using the Transwell® support system for example), or perhaps released from Matrigel and grown freely in media for a brief period. In this way, bacteria could be added to the apical aspect of the epithelium, and macrophages to the basal aspect, in order to observe whether the iHO epithelial response to infection is enhanced by communication with and response to cytokines secreted by macrophages. Simultaneously, phagocytosis and microbial killing by macrophages may also take place.[8] Previous research has demonstrated that cell surface protein expression is altered when cells are co-cultured with macrophages in 2-D[9] and 3-D[10] cellular models; another factor which ought to be considered when translating findings from *in vitro* assays to *in vivo* infection.

Typhoid, paratyphoid disease and iNTS predominantly occur in populations experiencing additional factors which may alter their intestinal environment. Malnutrition is a risk factor for iNTS, and can effect structural changes on the gut epithelium such as decreased villus height and reduced proliferation of enterocytes.[11] In addition, there can be decreased bile secretion, meaning loss of another protective factor against infections with enteric pathogens.[12] Alongside *Salmonella* disease, prevalence of environmental enteropathy (EE) is also potentially increased in areas with limited access to clean water and sanitation facilities. EE can be a driver of malnutrition, and its clinical features include: malabsorption, growth restriction, increased intestinal permeability and impaired gut immune function.[13] The increased permeability of the gut epithelium seen in individuals with this condition can lead to increased translocation of bacteria into the lamina propria and local and systemic inflammation.[14] Importantly, EE has been linked to failure of oral vaccines against polio, cholera and rotavirus.[15] There is also some evidence that environmental insults can be inherited epigenetically,[16,17] suggesting that there would be value in producing either hiPSC-derived or primary organoids from individuals with EE, in order to recreate a gut architecture and environment, which may more closely resemble that seen in children experiencing *Salmonella* infection in endemic areas.

7.4 Neglected pathogens

Finally, whilst the burden of typhoid disease worldwide remains high and treatment becomes more complicated by the emergence of AMR, it is promising that interventions such as effective vaccines are starting to become more widely available to prevent cases of the disease. It has become clear during the course of this project that this is not the case for paratyphoid disease. Our understanding of this pathogen is very limited in comparison to what we have established about *S*. Typhi and NTS, largely due (until now) to the lack of an animal proxy or representative human disease model. Although it causes a similar clinical picture to typhoid disease, clearly *S*. Paratyphi A does not behave in the same way at an epithelial level, therefore efforts ought to be focused on learning more about this pathogen in order to advance attempts to create vaccines and contingencies for the likely continued increase in its prevalence worldwide if we do not intervene.

It should also be noted that I have suggested experiments specific to *Salmonella* in these ideas on future directions for iHO technology, but these techniques could equally be used with other human restricted or neglected pathogens in order to generate a cohesive understanding of disease and guide drug or vaccine development for these pathogens too. If *in vitro* disease modelling using organoids progresses as rapidly over the next 5 years as it has over the past 5, these ambitions are eminently achievable.

References:

1. Macosko EZ, Basu A, Satija R, et al. Highly Parallel Genome-wide Expression Profiling of Individual Cells Using Nanoliter Droplets. *Cell.* 2015;161(5):1202-1214.
2. Fujii M, Matano M, Toshimitsu K, et al. Human Intestinal Organoids Maintain Self-Renewal Capacity and Cellular Diversity in Niche-Inspired Culture Condition. *Cell Stem Cell.* 2018;23(6):787-793 e786.
3. Haber AL, Biton M, Rogel N, et al. A single-cell survey of the small intestinal epithelium. *Nature.* 2017;551(7680):333-339.
4. Zhang YG, Wu S, Xia Y, Sun J. Salmonella-infected crypt-derived intestinal organoid culture system for host-bacterial interactions. *Physiol Rep.* 2014;2(9).
5. Williamson IA, Arnold JW, Samsa LA, et al. A High-Throughput Organoid Microinjection Platform to Study Gastrointestinal Microbiota and Luminal Physiology. *Cell Mol Gastroenterol Hepatol.* 2018;6(3):301-319.
6. Escobedo JO, Chu YH, Wang Q, Steyger PS, Strongin RM. Live cell imaging of a fluorescent gentamicin conjugate. *Nat Prod Commun.* 2012;7(3):317-320.
7. Karve SS, Pradhan S, Ward DV, Weiss AA. Intestinal organoids model human responses to infection by commensal and Shiga toxin producing Escherichia coli. *PLoS One.* 2017;12(6):e0178966.
8. Barrila J, Yang J, Crabbe A, et al. Three-dimensional organotypic co-culture model of intestinal epithelial cells and macrophages to study Salmonella enterica colonization patterns. *NPJ Microgravity.* 2017;3:10.
9. Striz I, Slavcev A, Kalanin J, Jaresova M, Rennard SI. Cell-cell contacts with epithelial cells modulate the phenotype of human macrophages. *Inflammation.* 2001;25(4):241-246.
10. Crabbe A, Sarker SF, Van Houdt R, et al. Alveolar epithelium protects macrophages from quorum sensing-induced cytotoxicity in a three-dimensional co-culture model. *Cell Microbiol.* 2011;13(3):469-481.
11. Guiraldes E, Hamilton JR. Effect of chronic malnutrition on intestinal structure, epithelial renewal, and enzymes in suckling rats. *Pediatr Res.* 1981;15(6):930-934.
12. Opleta K, Butzner JD, Shaffer EA, Gall DG. The effect of protein-calorie malnutrition on the developing liver. *Pediatr Res.* 1988;23(5):505-508.

13. Korpe PS, Petri WA, Jr. Environmental enteropathy: critical implications of a poorly understood condition. *Trends Mol Med.* 2012;18(6):328-336.
14. Harper KM, Mutasa M, Prendergast AJ, Humphrey J, Manges AR. Environmental enteric dysfunction pathways and child stunting: A systematic review. *PLoS Negl Trop Dis.* 2018;12(1):e0006205.
15. Gilmartin AA, Petri WA, Jr. Exploring the role of environmental enteropathy in malnutrition, infant development and oral vaccine response. *Philos Trans R Soc Lond B Biol Sci.* 2015;370(1671).
16. Burdge GC, Lillycrop KA. Nutrition, epigenetics, and developmental plasticity: implications for understanding human disease. *Annu Rev Nutr.* 2010;30:315-339.
17. Hochberg Z, Feil R, Constancia M, et al. Child health, developmental plasticity, and epigenetic programming. *Endocr Rev.* 2011;32(2):159-224.

Appendix 1: Single cell sequencing methods

(Adapted from protocol by Hayley Bennett / Maria Duque)

The full method for single cell sequencing is outlined below, but as a brief overview of the process; iHO were grown in two 24 well plates for 5 days, one plate was stimulated with rhIL-22 100ng / mL 18 hours prior to commencement of the assay. iHO were isolated from Matrigel with Cell Recovery Solution, pelleted via centrifugation at 750rpm and washed with DPBS (No Ca^{2+} or Mg^{2+}). iHO were treated for 15 minutes with TrypLE to dissociate cells, washed with DPBS, transferred to Eppendorf tubes and stained with Calcein blue AM (0.5μg /mL, GeneCopoeia) and fixable viability dye eFluor 780 (1:2000; eBioscience). Cells were then washed with FACS buffer and samples run on the Becton Dickinson FACsAria11 using FACS Diva software. Three 100 cell and 3 zero cell well controls were sorted on each plate (see plate design below); the remaining 90 wells received a single cell during the sort. Once sorted, cells were lysed in 0.8% Triton-X, and mRNA was polyadenylated using OligoDT anchored 30 (Sigma-Aldrich), then reverse transcribed and amplified by SmartSeq-2 PCR. Resultant cDNA was cleaned up using Agencourt Ampure XP beads (Beckman Coulter). Quality control of selected wells was performed using Agilent High Sensitivity DNA kit. Nextera libraries were prepared using Nextera XT DNA Library Prep Kit (Illumina) and then underwent a further PCR amplification step. Plates were split into 3 pools, which were again cleaned up with Agencourt Ampure beads, and QC of pools was undertaken with Agilent High Sensitivity DNA kits. Pools were submitted to the WTSI sequencing pipeline.
Pools were sequenced on the Illumina-C HiSeq V4, generating 125bp paired-end reads. Read outputs were quality assessed using numerous parameters in an automatic standard pipeline managed by the DNA Pipeline Informatics team at WTSI. Reads were aligned to the human (hg19) reference genome. Quality control (QC) metrics of >100,000 reads per cell, <20% mitochondrial (MT) content and >2000 genes detected per cell were used to select cells for further analysis. 89% of cells sequenced passed QC. Data were processed using the Seurat[1] and Single Cell Consensus Clustering (SC3)[2] packages, and principal components analyses run after scaling data for mitochondrial content and number of unique molecular identifiers (UMIs). Identification of cell types was attempted by clustering of cells by marker genes and enrichment analysis was done using the G:Profiler

(https://biit.cs.ut.ee/gprofiler/gost) resource to identify differences between unstimulated and rhIL-22 stimulated cells.

1. Plate preparation for sorting

- Eighteen hours prior to commencing sort, pre-stimulate half of plates to be sorted with rhIL-22 100 ng/mL (R&D).
- In addition, make up 10% stock of Triton X-100 (Sigma-Aldrich), diluting in Ambion nuclease-free water (Thermo-Fisher) and place on rotator to mix overnight. Dilute 800 µL of 10% stock in 9.2 mL Ambion nuclease-free water (Thermo-Fisher) in a 50 mL falcon tube to produce a final concentration of 0.8%.
- Put the tube under UV light in the UV Stratalinker 2400 (Stratagene) at 2000 joules/cm for 30 minutes.
- Prepare a master mix of the following in a 1.5 mL DNA LoBind Eppendorf tube in a clean microbiological safety cabinet (MSC):

Reagents	**For 1 Reaction (µL)**	**For 100 reactions (µL)**
0.8% Triton X-100	2	200
dNTP mixes (Thermo Scientific™)	1	100
OligoDT anchored 30. HPLC purified, 100 µM. 5”-AAGCAGTGGTATCAACGCAGAGTACTTTTTTTTTTTTTTTTTTTTTTTTTTTTVN-3” (Sigma-Aldrich)	0.1	10
SUPERase In™ RNase inhibitor (Thermo-Fisher)	0.1	10
Ambion nuclease-free water (Thermo-Fisher)	0.8	80

- Using the Eppendorf Multipette Xstream dispenser with 0.2 mL Combitip advanced®, distribute 4 µL of the above mix per well of a nuclease-free non-skirted 96 well plate (Thermo Scientific™) and cover plate with a sterile film (AlumaSeal® CS Films for cold storage, Sigma-Aldrich).
- Spin briefly at 1000 rpm and keep the plate on wet ice until cell sort.
- Repeat for number of plates required for sort.

2. Cell preparation for sorting

- Remove media from iHO and dissolve Matrigel using Corning® Cell Recovery Solution (Sigma-Aldrich) for 1 hour.
- Pellet cells via centrifugation at 750 rpm, remove overlying media and wash x1 in PBS (No calcium or Magnesium – Gibco)
- Treat iHO for approximately 15 minutes with 5 mL TrypLE™ Express (Gibco) to dissociate cells, then add 5 mL base growth media to inactivate.
- Centrifuge cells at 750 rpm and wash x1 with PBS
- Split suspended cells into 1.5 mL Eppendorf tubes and label for the following conditions:
    1. Unstimulated - Unstained
    2. Unstimulated - Calcein blue
    3. Unstimulated - Fixable viability dye
    4. Unstimulated - Calcein blue + Fixable viability dye (experimental sample for sort)
    5. IL-22 stimulated - Unstained
    6. IL-22 stimulated - Calcein blue
    7. IL-22 stimulated - Fixable viability dye
    8. IL-22 stimulated - Calcein blue + Fixable viability dye (experimental sample for sort)
- Spin down cells in Eppendorf tubes and incubate in 100 μL of 0.5μg/mL Calcein blue AM (GeneCopoeia) or Fixable viability dye eFluor 780 (1:2000; eBioscience) in PBS under conditions outlined above, for 15 minutes at room temperature, protected from light.
- Add 1 mL FACS buffer (containing 2mM EDTA (Sigma) in DPBS and Trustain FcX block (5 μL/ 100μL buffer; BioLegend)), spin and wash again with 1 mL FACS buffer and re-suspend in 0.5 mL FACS buffer for sorting.

3. Cell sorting

- Decontaminate surfaces in FACS hood with RNaseZap (Thermo-Fisher).
- Complete sorting using Becton Dickinson FACsAria11 and FACS Diva software; plate plan as outlined in **Figure A1** (100 cell and 0 cell wells used as controls).

- Once sort is complete, seal each plate in the hood (MicroAmp™ Clear Adhesive Film, Thermo-Fisher), spin briefly at 1000 rpm in Star Lab plate centrifuge and transfer immediately to a bed of dry ice.

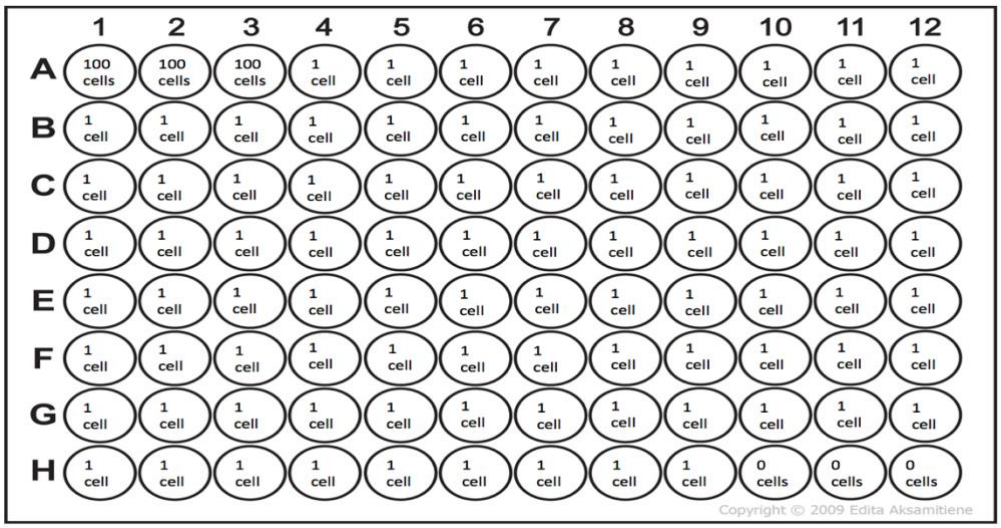

Figure A1: Plate plan for single cell sequencing

4. Reverse transcription and PCR

- Transport samples on dry ice to a clean PCR hood which has not been used for generating post-PCR NexteraXT libraries and has been cleaned thoroughly with RNaseZap and DNA Away (Fisher Scientific).
- Prepare reverse transcription (RT) mastermix for Smart-seq2 (adding reagents in order below) in 1.5 mL DNA LoBind Eppendorf tube, invert tube, spin briefly then store on ice until use:

Reagents	**For 1 Reaction (µL)**	**For 100 reactions (µL)**
Pre-RT Ambion nuclease-free water (Thermo-Fisher)	0.29	29
TSO, HPLC purified, stock 100 µM (Exiqon) 5'AAGCAGTGGTATCAACGCAGAGTACATrGrG+G-3'	0.1	10
1M $MgCl_2$ (nuclease-free, Ambion)	0.06	6
5M ultrapure Betaine solution (VWR International)	2	200
SMARTScribe™ 5x RT Buffer (Clontech)	2	200
20mM DTT (dithiothreitol; part of SMARTScribe™ kit, Clontech)	0.5	50
SUPERase In™ RNase inhibitor (Thermo-Fisher)	0.25	25
SMARTScribe™ Reverse Transcriptase (Clontech)	0.5	50

- Place first plate on thermocycler and run the denaturing step at 72 ^{o}C for 3 min. Immediately afterwards, spin down plate for 10 seconds at 1000 rpm and place on CoolRack® XT PCR 96 (BioCision®). (If working with more than one plate, place the ones not in use on dry ice).
- Dispense 5.5 µL of RT mastermix into each well using the Eppendorf Multipette Xstream dispenser with 0.5 mL Combitip advanced®, seal plate using MicroAmp™ Clear Adhesive Film using a plate roller to ensure tight seal.
- Spin down plate at 1000 rpm and run the following programme on the Tetrad 2 thermal cycler (Bio-Rad) to reverse transcribe:

  Step 1: 42 ^{o}C 1.5hr

  Step 2: 42 ^{o}C 2 min

  Step 3: 50 ^{o}C 2 min

  Step 4: Go to Step 2 x9

  Step 5: 70 ^{o}C 15 min

  Step 6: 4 ^{o}C forever

- Following RT, proceed to Smart-seq-2 PCR step. Spin down plate at 1000 rpm and place on CoolRack® XT PCR 96.
- Prepare PCR mastermix in 1.5 mL DNA LoBind Eppendorf tube, invert tube, spin briefly then store on ice until use:

Reagents	**For 1 Reaction (µL)**	**For 100 reactions (µL)**
KAPA Hotstart HiFi 2X ReadyMix (Kapa Biosystems)	12.5	1250
ISO SMART primer (100 µM), HPLC purified 5'-AAGCAGTGGTATCAACGCAGAGT-3 (Sigma Genosys)	0.25	25
Post-RT Ambion nuclease-free water (Thermo-Fisher)*	2.25	225

*__NB__: This must be a different bottle of nuclease-free water from that used in RT step

- Add 15 µL of PCR mastermix per well to each plate, using Rainer multichannel pipette and fresh individual 20 µL tip for each well. Seal plate with MicroAmp™ Clear Adhesive Film, spin down at 1000 rpm and run the following programme on the Tetrad 2 thermal cycler for PCR:

Step 1: 98 °C 3 min

Step 2: 98 °C 20 sec

Step 3: 67 °C 15 sec

Step 4: 72 °C 6 min

Step 5: Go to Step 2 x 22

Step 6: 72 °C 5 min

Step 7: 4 °C forever

- Plates can be frozen at -20 °C at this point prior to completing next steps.

5. Bead clean-up 1

- Warm Agencourt AMPure XP beads (Beckman Coulter) for 20 min until at room temperature. Ensure beads are well mixed in suspension.
- Make up 40 mL of 80% ethanol (add 32 mL 100% molecular biology grade ethanol (Fisher Scientific) to 8 mL Ambion nuclease-free water (Thermo-Fisher)) per plate.

    - Use beads at 1x ratio for clean-up; therefore, add 25 µL beads per well, using multi-channel pipette and reagent boat and allow to bind at room temperature for 6 minutes
    - Place plate on 96 well plate magnet and allow beads to settle for 5 minutes
    - Remove supernatant using multichannel pipette
    - Without removing the plate from the magnet, add 200 µL 80% ethanol, then remove. Do not attempt to resuspend beads.
    - Repeat ethanol wash and carefully remove any remaining ethanol from wells.
    - Allow the beads to dry for 8 minutes.
    - Remove plate from magnet and using a multi-channel pipette, resuspend beads in 10 µL Ambion nuclease-free water per well.
    - Place on magnet and leave for at least 5 minutes for beads to settle. Remove eluted amplified cDNA (being careful to not transfer beads) to a new plate (skirted

SuperPlate 96 well plate, Thermo-Fisher) and seal with AlumaSeal® CS Film for cold storage.

Quality control:

Run an Agilent High-sensitivity DNA chip on the Agilent 2100 Bioanalyzer, following the manufacturer's instructions, for one 0-cell well, one 100-cell well and 9 single cell wells to check for presence of cDNA in each well.

- Store all plates at -20 °C prior to library preparation.
- At this point 1 µL of PCR product can be used to prepare a 1:100 dilution for qRT-PCR.

6. Nextera XT Library preparation

- Using Nextera XT index kit v2 (Illumina), make up index plate as per manufacturer's instructions. Depending on number of plates being processed, may need up to 4 different index kits (A, B, C and D). Seal with AlumaSeal® CS Film for cold storage; indexes can be stored at -20 °C prior to use.

- Prepare first mix using reagents contained in Nextera XT DNA Library Prep Kit in a 1.5 mL DNA LoBind Eppendorf tube (due to viscosity of reagents, prepare an excess of 125x reactions):

Reagents	**For 1 Reaction (µL)**	**For 125 reactions (µL)**
Tagment DNA buffer	2.5	312.5
Amplification tagment mix	1.25	156.25

- Add 3.75 µL of first mix per well of a new SuperPlate 96 well plate, using a multi-channel pipette, seal the plate with MicroAmp™ Clear Adhesive Film and spin briefly at 1000 rpm.
- Spin down the cDNA-containing plate at 1000 rpm and prepare a 1:50 dilution (in Ambion nuclease-free water) of the 100 cell controls. Add 1.25 µL of cDNA per well of the plate containing the first mix, pipetting onto the side of the well.

- Seal the first mix plate, briefly spin at 1000 rpm and incubate at 55 °C for 10 min in thermocycler. Let the block reach 10 °C, remove the plate and spin briefly again. During incubation step, thaw and spin down index plate at 1000 rpm.
- Add 1.25 µL NT buffer per well to the first mix plate, using a multichannel pipette and fresh tip for each well, seal and briefly spin at 1000 rpm.
- Add 3.75 µL NPM per well to the first mix plate, using a multichannel pipette and fresh tip for each well, seal and briefly spin at 1000 rpm.
- Add 2.5 µL index mix per well to the first mix plate, seal and briefly spin at 1000 rpm. Ensure index kit used for each plate is recorded.
- Run the following PCR programme on thermocycler:

  Step 1: 72 ^{o}C 3 min

  Step 2: 95 ^{o}C 30 sec

  Step 3: 95 ^{o}C 10 sec

  Step 4: 55 ^{o}C 30 sec

  Step 5: 72 ^{o}C 1 min

  Step 6: Go to Step 3 x 11

  Step 7: 72 ^{o}C 5 min

  Step 8: 10 ^{o}C forever

7. Bead clean-up 2

- Warm Agencourt AMPure XP beads (Beckman Coulter) for 20 min until at room temperature. Ensure beads are well mixed in suspension.
- In each of two 2 mL DNA LoBind Eppendorf tubes, pool half of the single cell and 0 cell wells (i.e. wells A4-D12 and E1-H12). Pool the 100 cell wells (A1-A3) in a 1.5 mL DNA LoBind Eppendorf tube.
- Use beads at 0.8x ratio for clean-up, therefore 12 µL of beads per sample. Add 36 µL beads to the tube containing A1-A3, 526 µL to tube containing A4-D12 and 540 µL to tube containing E1-H12. Pipette up and down 6 times, vortex tubes and spin down in benchtop centrifuge.

- Incubate at room temperature for 6-10 minutes, periodically mixing tubes by hand. During this time, prepare 5ml 80% ethanol as described above.
- Briefly spin down tubes, place onto magnetic tube rack and allow beads to settle for 5 minutes.
- Discard supernatant, then without removing tubes from the magnet, add 1 mL 80% ethanol to both of the 2 mL Eppendorf tubes and 200 µL to the 1.5 mL tube. Do not attempt to resuspend beads.
- Remove and discard the ethanol and repeat ethanol wash.
- Spin down tubes and replace on the magnetic rack. Carefully remove any remaining ethanol.
- Allow beads to dry for approximately 8 minutes, or until beads appear dull.
- Remove tubes from magnetic rack and resuspend beads in Ambion nuclease-free water. Use 10 µL per 100 cell well (therefore 30 µL for tube containing wells A1-A3), and 5 µL per single cell well (therefore 225 µL for tube containing A4-D12 and 240 µL for tube containing E1-H12).
- Replace tubes onto magnetic rack and leave for at least 5 minutes, then transfer eluted amplified cDNA (being careful not to transfer beads) to fresh DNA LoBind 1.5 mL Eppendorf tubes.

Quality control:

- Run an Agilent High-sensitivity DNA chip on the Agilent 2100 Bioanalyzer, following the manufacturer's instructions for each pool to check for presence of cDNA.
- Store pools at -20 ^{o}C prior to submission to pipeline.

References:

1. Butler A, Hoffman P, Smibert P, Papalexi E, Satija R. Integrating single-cell transcriptomic data across different conditions, technologies, and species. *Nat Biotechnol.* 2018;36(5):411-420.
2. Kiselev VY, Kirschner K, Schaub MT, et al. SC3: consensus clustering of single-cell RNA-seq data. *Nat Methods.* 2017;14(5):483-486.

Appendix 2: Generation of S100A9$^{-/-}$ hiPSC line

S100A9 knockout was generated by WTSI CGaP facility, by a single T base insertion in the third exon containing the EF-hand motif at cDNA position 228 using CRISPR/Cas9 in the Kolf2 human iPSC line. This was achieved by nucleofection of 10^6 cells with Cas9-crRNA-tracrRNA ribonucleoprotein (RNP) complexes. Synthetic RNA oligonucleotides (target site: 5'- AGACAAGCAGCTGAGCTTCG -3', WGE CRISPR ID: 915082321, 225 pmol crRNA/tracrRNA) were annealed by heating to 95°C for 2 min in duplex buffer (IDT) and cooling slowly, followed by addition of 122 pmol recombinant eSpCas9_1.1 protein (in 10 mM Tris-HCl, pH 7.4, 300 mM NaCl, 0.1 mM EDTA, 1 mM DTT). Complexes were incubated at r.t. for 20 minutes before electroporation. After recovery, cells were plated at single cell density and colony were picked into 96 well plates. 96 clones were screened for heterozygous and homozygous mutations by high throughput sequencing of amplicons spanning the target site using an Illumina MiSeq instrument. Final cell lines were further validated by Illumina MiSeq. The homozygous targeted clone was used in downstream differentiation assays. Additional supporting data:

S100A9 WT sequence: GCAGCTGAGCTTCGAGGAGTTCA
S100A9 MUT sequence: GCAGCTGAGCTTTCGAGGAGTTCA
Insertion of T at position 228

PCR amplification primers:
F: TTTGGTATGTGCTCAGTGTCTG
R: GAAGAGGTGGAAGAAGCACAC

WT Protein
MTCKMSQLERNIETIINTFHQYSVKLGHPDTLNQGEFKELVRKDLQNFLKKENKNEKVIEHIMEDLDTNA
DKQLSFEEFIMLMARLTWASHEKMHEGDEGPGHHHKPGLGEGTP

MUT Protein

MTCKMSQLERNIETIINTFHQYSVKLGHPDTLNQGEFKELVRKDLQNFLKKENKNEKVIEHIMEDLDTNA

DKQLSFRGVHHADGEANLGLPREDARG.RGPWPPP.ARPRGGHPL

Appendix 3 - Bulk RNA-Seq data analysis methods

RNA-Seq analysis of hiPSC-derived macrophages infected with different Salmonella enterica serovars

For all 12 samples, the mean sequencing depth was approximately 19.30 million reads. FASTQC was run on all samples to assess data quality. The 75bp paired-end sequencing reads were aligned to the human (hg19) reference genome, downloaded and indexed from the UCSC Genome Browser, using STAR RNA-Seq aligner version *2.5.3a*.[1] Only the reads that mapped uniquely as pairs were retained for downstream analysis. The resulting BAM files containing the aligned reads were provided to *featureCounts version 1.6.2*[2] *to obtain gene-level read counts* using the reference annotation file (GTF format downloaded from the UCSC browser). Lowly expressed genes, defined as having less than 5 counts per million (CPM) reads in at least three samples, were removed. A total of 11,473 genes were retained for downstream analyses. Raw count data was then subjected to Trimmed Mean of M values (TMM) normalisation,[3] followed by voom transformation[4] that estimates the mean-variance relationship in the data. To identify differentially expressed genes between each stimulation condition and PBS control samples, a linear model was fitted to each gene using the *lmFit* function in the Limma R package.[5] The technical differences between the three replicate groups (batch effects) were modelled as covariates in the analysis. Contrasts were defined for three pairwise comparisons (*S.* Typhi *vs.* PBS control; *S.* Typhimurium *vs*. PBS control; *S.* Paratyphi A *vs.* PBS control), and empirical Bayes moderated t-statistics, *log2-fold*-change, and *P*-values were computed for each comparison using the eBayes function in Limma. *P*-values were adjusted using the Benjamini and Hochberg FDR correction procedure.[6] To obtain a list of biologically meaningful genes, in each comparison, differential analysis was further assessed for genes that achieved an absolute *log2-fold*-change greater than 0.58 and FDR < 0.05 using the TREAT method in Limma.[7] Principal component analysis (PCA) was performed on log2-transformed FPKM Fragments Per Kilobase of transcript per Million mapped reads (FPKM) values using the prcomp function in R software. Volcano plots for each pairwise comparison was produced using the ggplot2 R package.

RNA-Seq analysis of hiPSC-derived intestinal organoids infected with different Salmonella enterica serovars

iHO samples were multiplexed across three sequencing lanes, generating 75bp paired-end reads, with each lane achieving a depth of approximately 5.84 – 8.06 million reads. Since the read depth was consistent across the lanes, lane-level FASTQ files for each sample were merged into a single file. FASTQC was run on all the 36 samples to assess data quality. The sequencing reads were aligned to the human (hg19) reference genome, downloaded and indexed from the UCSC Genome Browser, using STAR RNA-Seq aligner version *2.5.3a*. Only the reads that mapped uniquely as pairs were retained for downstream analysis. The resulting BAM files containing the aligned reads were provided to *featureCounts version 1.6.2 to obtain gene-level read counts* using the reference annotation file (GTF format downloaded from the UCSC browser). To separate the known transcriptional heterogeneity that exists between hiPSC cell lines[8] from the stimulation-specific transcriptional differences, differential analysis in each of the three cell lines was performed separately. First, lowly expressed genes, defined as having less than 5 counts per million (CPM) reads in at least three samples, were removed. Approximately 12,000 genes were retained for downstream analyses in each cell line. Then, the raw count data was subjected to Trimmed Mean of M values (TMM) normalisation, followed by voom transformation. To identify differentially expressed genes between each stimulation condition and PBS control samples, a linear model was fitted to each gene using the *lmFit* function in the Limma R package. Contrasts were defined for three pairwise comparisons (*S.* Typhi *vs.* PBS control; *S.* Typhimurium *vs*. PBS control; *S.* Paratyphi *vs.* PBS control), and empirical Bayes moderated t-statistics, *log2-fold*-change, and *P*-values were computed for each comparison using the eBayes function in Limma. *P*-values were adjusted using the Benjamini and Hochberg FDR correction procedure. Principal component analysis (PCA) was performed on log2-transformed FPKM Fragments Per Kilobase of transcript per Million mapped reads (FPKM) values using the prcomp function in R software. Volcano plots for each pairwise comparison were produced using the ggplot2 R package.

References:

1. Dobin A, Davis CA, Schlesinger F, et al. STAR: ultrafast universal RNA-seq aligner. *Bioinformatics.* 2013;29(1):15-21.
2. Liao Y, Smyth GK, Shi W. featureCounts: an efficient general purpose program for assigning sequence reads to genomic features. *Bioinformatics.* 2014;30(7):923-930.
3. Robinson MD, Oshlack A. A scaling normalization method for differential expression analysis of RNA-seq data. *Genome Biol.* 2010;11(3):R25.
4. Law CW, Chen Y, Shi W, Smyth GK. voom: Precision weights unlock linear model analysis tools for RNA-seq read counts. *Genome Biol.* 2014;15(2):R29.
5. Ritchie ME, Phipson B, Wu D, et al. limma powers differential expression analyses for RNA-sequencing and microarray studies. *Nucleic Acids Res.* 2015;43(7):e47.
6. Benjamini Y, Hochberg Y. Controlling the false discovery rate: a practical and powerful approach to multiple testing. . *J R Stat Soc Ser B* 1995;57(1):289-300.
7. McCarthy DJ, Smyth GK. Testing significance relative to a fold-change threshold is a TREAT. *Bioinformatics.* 2009;25(6):765-771.
8. Carcamo-Orive I, Hoffman GE, Cundiff P, et al. Analysis of Transcriptional Variability in a Large Human iPSC Library Reveals Genetic and Non-genetic Determinants of Heterogeneity. *Cell Stem Cell.* 2017;20(4):518-532 e519.